Universitatea *Transilvania* din Braşov

HABILITATION THESIS

MODELS FOR THE STUDY OF MECHANICAL RESPONSE OF THE SOLIDS AND SYSTEMS OF SOLIDS

Domain: MECHANICAL ENGINEERING

Author: Associate Professor SCUTARU Maria Luminița

Transilvania University of Brașov

BRASOV, 2015

CONTENT

(A) Rezumat

Teza de abilitare " Modele pentru analiza statică şi dinamică a sistemelor mecanice" reflectă o activitate de cercetare de un deceniu, desfăşurată în domeniul Ingineriei Mecanice cu un accent special pe metodele de analiză dinamică a sistemelor şi mecanica materialelor compozite.

Teza este bazată pe contribuţiile originale, publicate prin articole în jurnale cotate ISI Thomson, rezultate ca urmare a activităţilor de cercetare ştiinţifică desfăşurate în cadrul Universităţii "Transilvania" din Braşov, după conferirea titlului de doctor în anul 2006.

Capitolul 1 se referă la cercetările întreprinse în ultimii ani în domeniul dinamicii sistemelor multicorp cu elemente rigide sau elastice. Cercetarea a pornit de la nevoile practice apărute în domeniul turbinelor eoliene, de mică putere, folosite în gospodăriile agricole, o temă de foarte mare actualitate. Cercetările au condus la o propunere de transmisie formată dintr-un mecanism cu două grade de libertate, pendular, care răspunde foarte bine necesităților practice.

A fost făcut un studiu numeric al sistemului propus și s-au integrat ecuațiile de mișcare obținute. Rezultatele teoretice au fost verificate prin verificari experimentale ale înregistrării mișcării mecanismului studiat. S-a executat un stand la o scară redusă pe care s-au făcut înregistrările necesare. Studiul acestei probleme a condus la implicarea în analiza sistemelor mecanice cu două grade de libertate și la rezolvarea unor probleme dificile de modelare și analiză numerică.

Capitolul 2 al prezentei teze prezintă într-o primă etapă rezultatele cunoscute în analiza dinamică a sistemelor multicorp cu elemente elastice, dar și cercetările întreprinse de autoare în acest domeniu. Problema este de mare interes practic întrucât, ipoteza elementelor rigide, care se face la studiul unor sisteme mecanice, de multe ori nu corespunde datorită vitezelor mari implicate și a forțelor considerabile care apar în funcționare. Pentru acest studiu se folosește Metoda Elementelor Finite, dar care ține seama de mișcarea relativă a elementelor elastice față de sisteme de referință mobile, legate de elementele în mișcare. Primul pas în analiza dinamică a unui astfel de sistem este scrierea ecuațiilor de mișcare, tipul elementelor finite alese determinând forma finală a acestor ecuații. Se consideră că deformațiile elastice mici ale elementelor deformabile nu vor afecta mișcarea generală, de rigid, a întregului sistem.

Dificultatea majoră în studiul unei astfel de probleme este neliniaritatea puternică a ecuațiilor de mișcare obținute. Pentru a putea face integrarea, se consideră mișcarea "înghețată" pe intervale scurte de timp, pe care sistemul de ecuații poate fi considerat un sistem de ecuații diferențiale cu coeficienți constanți. Am demonstrat proprietăți remarcabile ale ecuațiilor de mișcare obținute, proprietăți care permit o analiză calitativă a sistemelor de ecuații studiate. Pentru scrierea ecuațiilor de mișcare am folosite ecuațiile lui Lagrange. Efectele de tip Coriolis determină apariția unor termeni suplimentari în cadrul ecuațiilor care pot duce la fenomene de instabilitate ale mișcării.

Capitolul 3 al tezei abordează o altă direcţie de cercetare referitoare la studiul proprietăților mecanice a materialelor compozite. Deoarece domeniul materialelor compozite este un domeniu interdisciplinar şi mai mult decât o conexiune între disciplinele stabile, cum ar fi chimia, fizică sau inginerie, experienţa din acestea este esenţială pentru dezvoltarea unor materiale noi cu aplicaţii bine definite. Triunghiul: sinteză şi fabricare – compoziţie precum şi structură – proprietăţi şi performanţă reprezintă relaţiile esenţiale în domeniul materialelor

compozite. Proprietăţile unui material de compoziţie dată depind, într-o foarte mare măsură, de metoda după care a fost realizat, acestea fiind o consecinţă a structurilor diferite. Invers, aplicaţiile speciale necesită proprietăţi structurale concrete, prin urmare şi o compoziţie exactă, care implică procedee de sinteză şi fabricare corespunzătoare.

Ideea utilizării materialelor compozite nu se reduce numai la înlocuirea pur şi simplu a metalelor sau a altor materiale cu compozite ci şi la utilizarea în mod constructiv al acestor materiale, ţinând seama de proprietăţile deosebite şi posibilităţile de obţinere pentru a crea structuri inovative, de forme noi, care să fie utilizabile pentru construcţii particulare

Continuând în domeniul materialelor compozite, capitolul 4 prezintă aspecte legate de îmbinarea unor tehnici experimentale şi metode teoretice pentru a înţelege efectele pe care le au radiaţiile ionizante asupra materialelor compozite. Practic s-au expus diferite materiale compozite la doze controlate de radiații, folosind instalaţia IRASM din cadrul IFIN-HH, urmărind atingerea unor performanţe structurale ridicate, statice şi dinamice.

Radiaţiile X şi gamma sunt radiaţii electromagnetice penetrante şi se află la limita superioară a spectrului de energie. Ele au proprietatea de a produce, prin interacţie cu atomii substanţei străbătute (iradiate), fenomenul de ionizare. Radiaţiile X cu o energie mai mică de 100 keV sunt puternic absorbite de substanţă, în timp ce radiaţiile X dure (energie mai mare de 200 keV) şi radiaţiile gamma pot să străbată grosimi considerabile din substanţă, absorbţia în cazul acestora fiind mult mai mică.

Sub acţiunea radiaţiilor ionizante, polimerii suferă profunde transformări chimice şi structurale, se modifică compoziţia lor chimică, structura şi toate proprietăţile fizico-chimice şi mecanice. Iradierea poate afecta însuşirile materialelor atât în mod negativ, caz în care vorbim despre o distrugere prin iradiere, cât şi pozitiv, ceea ce conduce la o îmbunătăţire a unor proprietăţi.

(B) Scientific and professional achievements and the evolution and development plans for career development

(B-i) Scientific and professional achievements

Introduction

The research presented in the following covers a period of about 10 years, the author was concerned mainly with the study of mechanical systems, both in terms of the study of the new materials and composite's mechanics and the dynamics of multibody systems.

Studies in both directions in the Mechanical Engineering field covered were generated by practical applications, imposed by the current development of the industry.

Thus the study of modern pumping systems driven by wind energy led to dynamic analysis of mechanical transmission of power from the wind turbine to pumping unit, where they reported operational problems. The study of such system is too imposed by the necessity to obtain a better efficiency of the transmission. In this direction we have proposed a mechanism with two degrees of freedom, closed by inertia. Such type of systems were rarely studied in the dynamic analysis and involves special problems related on the one hand to the mechanical modelling of the system and secondly by solving mathematical equations of motion obtained. From a theoretical standpoint, the problem is very interesting and involves the use of concepts and results of the systems of dynamic theory. Apart from theoretical modelling, which leaves room for further developments, we have experimentally verify these results. To realise this, a small-scale experimental model was made and optical recordings of the motion were performed. This has combined theoretical study of such problems with the experimental study, in order to make a validation of the results. Based on research undertaken results have been published in the literature, the work being cited in the paper.

Also in the field of the dynamic analysis of mechanical systems were studied, in a group of Mechanical Engineering Department, the behaviour of mechanical systems with liaisons having a "rigid" body motion. To conduct this study was applied Finite Element Method. The author has contributed, along with other researchers, to obtain results in the elasto-dynamic of linear elastic bodies participating to rigid three-dimensional motion. Coriolis forces and inertial effects have major influence on the equations of motion that can qualitatively alter the dynamic response of such system. The results of these researches were published in the Thomson ISI listed in the References.

The results obtain in the domain of the dynamics analysis of mechanical systems with rigid or/and deformable elements constituted therefore a major concern in the last decade of my research work, conducted within the department. Within habilitation thesis I presented those results where my contribution was significant or exclusive.

The second major area of research was constituted of composite material mechanics, an area where we began research under demand pressure of the economic environment. If at first the researches were limited to the study of materials whose mechanical properties were generally known, slowly were conducted researches in field of new materials with new structures and specific properties, required by the economic environment. High demand for study of new materials has led several colleagues from the department to engage in this kind of work, which is

why at the moment there is a group dealing with these issues. The mentor this group was Mr. Assoc. Prof. Dr. Eng. Teodorescu Horatiu-Drăghicescu that led many researches in this interesting and exciting field. Some of the research we conducted in this team and the results are obtained in common. Among the numerous works published in this group in the paper I presented only those works that my contribution has been significant.

An original path followed was that of irradiated composite materials research. Irradiation, which can occur in human nature or in technical systems, greatly influences the properties of a composite material. The author has dealt with this type of material and studied mechanics of such composites, after being irradiated.

The irradiation process revealed structural and morphological changes that affected the mechanical properties of new hybrid carbon-hemp composite however, the improvement of mechanical properties in case of a small irradiation dosis recommends this type of material for a wide range of applications.

The purpose of this chapter is the presentation of an from the mechanical and micro-structural point of view of this new biocomposite subjected to radiations, with applications in both nuclear industry and the accomplishment of parts in aerospace industry and automotive engineering to reduce their weight and manufacturing costs. This new biocomposite improves the recycling degree meeting at the same time the structural and passive protection performances.

The presented results, published in journals Thomson ISI indexed, offers exceptional opportunities in the development of future research.

Chapter 1

Dynamical Analysis of the Mechanical System with Two Degree of Freedeom Applied to the Transmission of the Wind Turbine

1.1. State of the art in the field of the wind turbines

This chapter covers the researches of the author, in recent years, in the field of the dynamics of multibody systems with rigid or elastic elements. These researches have results many articles published by the author in recent years. Other ongoing researches and partial results are presented first time in this paper. The research started from practical needs that led to the problems raised by industry. The author tries to give an answer to these problems. One of problem studied was that of transmitting motion in small wind pumps, highly topical theme and with interesting potential practical developments. The study of this problem has led to involvement in the study of mechanical systems with two degrees of freedom and leads to difficult problems of modeling and numerical analysis. After some numerical analysis of such systems were performed measurements and recordings and have revealed the properties that we have identified and validated by experiment.

1.1.1. The background research

Wind power represented for ancient a power source and was used in various applications, but insufficient empirical knowledge of the laws of aerodynamics and low mechanical knowledge, applied in the design, implementation and operation of this free energy sources made the technology used remain in a rudimentary stage until mid last century (although over time were conducted numerous applications that make use of wind energy).

The wind has the advantage of being a virtually inexhaustible energy source, free, is found in almost all places on the planet and can be converted directly into electricity, giving it the status of a quality source of energy. There is a major drawback: the parameters that define the wind are characterized by strong spatial and temporal fluctuations, showing irregularity that direction, intensity and duration.

Currently there are many producing wind energy turbines: wind turbines are almost entirely horizontal axis, vertical axis models are exceptions (the Savonius and Darrieus rotor are still used but are endangered). Latest innovations allow variable speed operation of wind turbines or wind turbine speed control depending on wind speeds.

1.1.2. The recent situation in wind turbines

As regards the exploitation of wind energy potential, today we can say that technology has almost reached maturity, the modern era of wind energy exploitation and production starting in the late 70s of XX century in Denmark. There are many countries, especially in Europe, where wind turbines are widely used, this being favored by specific geographic conditions. At present, in the world there are thousands of wind turbines functional, with a total installed capacity of 94,123 MW, of which 60.70% are located in Europe.

Although the modern era of wind energy exploitation opened by Denmark, currently the first place is occupied by Germany with an installed capacity of 22,247 MW, representing 23.6% of total electricity production resulting from the conversion of wind energy. The following places are filled in the order of US, Spain, India and China [AMA96].

The recent wind turbines are designed to work efficiently from a wind velocity of 10 m/s. On the other hand, current turbines require a large initial investment, in order to generate profit, from the operation of the unit without interruption.

Also, to the unit cost are added additional initial costs that are related to geotechnical, foundation and execution costs for support pillars, transport etc. These costs can be extremely important and they are to grow exponentially if the location of a wind aggregated is in a mountainous area, with is difficult to access or where, although the captured energy is high, in terms of financial investment is not profitable.

1.1.3. Wind turbine

Wind turbines used currently works on the same principle as the ancient windmills. Thus, the blades of a propeller gathers kinetic energy of the wind and a generator turns the power in electricity. The biggest disadvantage of wind energy is that it does not get electricity when the wind does not blow all or beat too weak, so they must be provided an alternative source of electricity. Other disadvantages of wind are the impact on the birds, the visual impact, impact on the environment and costs.

Wind energy is a renewable energyes. Aero-generator uses kinetic energy of wind to drive its rotor shaft, so rotation is transmitted to an electric generator.

The wind turbine is a device that transforms the propeller blade movement into mechanical energy. If the mechanical energy is then converted into electricity we are dealing with a generator driven by wind - wind energy converter, but the term that has become established as "wind turbine".

1.1.4. Types of wind turbines

1.1.4.1. Horizontal axis wind turbines

Wind turbines can be divided into two main categories, depending on the orientation of the rotor axis: vertical axis and horizontal axis. On the market, greater popularity have the horizontal axis, the overall picture of such a wind turbine with a rotor being that having three

blades, with a particular airfoil; This results in a good trade-off between the coefficient of power, cost and speed of rotation of the sensor wind, but also an improvement in terms of aesthetics. These wind shaft is disposed along the air flow.

Horizontal axis wind turbines are mostly used because of their aerodynamic efficiency is superior to the vertical axis, being less subject to significant mechanical stress and having a lower cost. Currently, the horizontal axis wind turbines with rotor propeller, has the highest interest for the production of electricity on an industrial scale.

1.1.4.2. Vertical axis wind turbines

Vertical axis wind turbines are characterized by a vertically arranged rotor, the pillars of this wind is small, with a height of 0.1 to 0.5 of the height of the rotor. This allows placement of the entire energy conversion equipment (multiplier generator) wind leg, thus facilitating maintenance. In addition, it is not necessary to use a device for the orientation of the rotor, as in the case of horizontal axis wind turbines.

However, the wind is mild to the ground, resulting in a reduced efficiency of turbine, which is subject to wind and turbulence. More, the turbine must be started, pillar being subjected to significant mechanical stress. This type of turbine, although having the advantage of the independence on the direction of the wind, are used especially in areas with lower wind potential, with very low operating speed, placed around 2.7 m/s, which they makes it extremely feasible.

There are two main types of vertical axis wind turbines according to the principle of operation: Savonius turbine and the Darrieus turbine. The rest of the solutions are, or combinations of these two main types, or solutions which are based on the principle of the concentrator and guiding the airflow to the turbine.

1.1.5. Advantages and disadvantages of wind turbines

Advantages. In the current context, characterized by an alarming increase of pollution caused by energy production from fossil fuels, is becoming increasingly important to reduce dependence on these fuels.

Wind energy has already proven to be a very good solution to the problem of global energy. Using renewable resources is addressed not only produce energy, but the particular way of generating reformulated the model development, through decentralization sources. Wind energy in particular is among renewable energy forms that are suitable in small-scale applications. [COS06], [DOR14]

The main advantage of wind energy is zero emissions of pollutants and greenhouse gases, because it does not burn fuel. Other advantages are:

- *Does not produce waste;*
- *Reduced costs per unit of energy produced;*

- *The cost of electricity produced in modern wind power plants has decreased substantially in recent years, reaching US even smaller than in the case of generation using the fuel;*
- *Reduced costs when the turbine is out of service. Unlike nuclear power plants, for example, where the costs of shutdown can be several times higher than the costs of the plant.*

Disadvantages. The main disadvantages are relatively limited energy resource, wind speed variation and the reduced number of possible locations. Few places on earth offer the possibility to obtain enough electricity through wind energy [COS06], [DOR14].

Initially, an important disadvantage of wind energy production was rather high price of energy production and relatively low reliability of the turbines. In the last 25 years, energy efficiency has doubled, the cost of a kWh produced decreased from EUR 0.7 to about 0.32 euro today.

Another disadvantage is the "visual pollution" - that is, their appearance is unpleasant - and also produce "noise" (too loud). It also states that the turbines affect the environment and the surrounding ecosystems, killing birds and requiring large vacant land for their installation.

Arguments against them are that wind turbines have a modern stylized appearance attractive http://ro.wikipedia.org/wiki/Energie_eolian%C4%83 - cite_note-24 that cars kill more birds than wind turbines per year and that other sources of energy, electricity generation using coal, are more harmful to the environment because it creates pollution and lead to the greenhouse effect.

Another major disadvantage is the high risk of destruction during the storms, when wind speeds exceed permissible limits considered in design. No matter how great big is this limit, there is always the possibility that it will be exceeded.

1.2. Water pumping, a particular application of wind energy use

Because of Romania's hydro potential allowing the use of hydropower, windmills were not very common in Romania. Only in Dobrogea lack of water and high wind speed caused the inhabitants to build windmills. Some saved from destruction and extinction are now in the museum in the village of Sibiu and Bucharest.

In Fig. 1.1 is shown the sketch of a water pump used in a wind turbine, where the rotational movement is converted, by means of a quadrilateral mechanism and a slider-crank mechanism connected in series, to the intermittent translational movement of the pump piston.

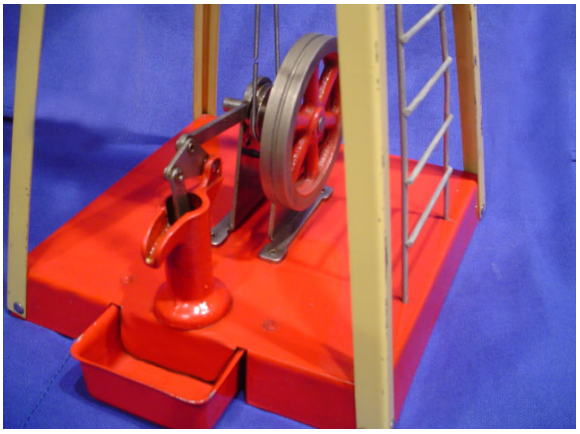

Figure 1.1. Model of a wind driven water pumps. The system of transmission of motion

1.2.1. Wind driven pumps for watering animals

The main practical application of the wind energy, worldwide, in addition to producing electricity, is to the pumps for watering animals. This is due to the following reasons:

a. Historical

In the largest farm in the American plains, during the 1920s were in use about 3 million wind farm pumps. Currently it is estimated that globally the number of pumps which are in use reaches about 1 million; 150,000 of them are still active in the US and another 600,000 in Australia.

Most of the pumps in operation are used to drinking (and / or the supply of drinking water to livestock farms). For this reason, while an entire industry has developed to manufacture wind turbines and associated plants: drinking, culverts, storage tanks and other equipment needed.

b. Economic

Drinking water quantity used in farms is large and, therefore, its value. Let's see a concrete case: the wind speed being v = 3.8 m / s (14km / h), a 3.65 m standard rotor of a wind farm pumps can maintain a herd of 70 steers and 500 sheep (a pessimistic estimate) if deemed a pumping height of 35 m. A wind of this size pump attached to a pole 10 feet high cost, usually $ 1500-3000 and has a normal lifetime of 20 years and maintenance once a year. The value of 70 steers of average quality is normally over $ 10,000.

Thus investment in a wind pump extremely useful, which will provide the absolutely necessary water is a realistic investment. Investing is accessible to farmers in financial terms, as the amount of capital required is normally greater than the gain from the sale of cattle annually (if considered four years sales cycle).

c. Opportuneness

Reasons for wind pumps are well suited to feed water livestock farms are: a) require minimal maintenance; b) reliable; c) have long working life; d) can not be easily stolen; e) are

sufficiently robust, enduring occasional physical demands of the animals. It follows that farmers will have to pay only little attention and financial resources to maintain the operation and maintenance of wind pumps and escape the complicated logistical issues such as procurement, storage and handling of fuel.

In developing countries, where resources are extremely scarce, the ultimate goal seems to be of vital importance. In these countries, with arid cat, is the most reasonable method to exploit the land. Has already been demonstrated in these places, that both in terms of social, but also organizational possibilities, livestock is the best solution.

Thus local communities get to grow cattle on surfaces which, objectively, could provide better crop. There is a trend of pasture degradation through over-exploitation. This is why some scholars oppose drinking water supply in arid areas such as the Sahel in Africa. It was found, however, that the problem of over-exploitation is the effect of a massive concentration of animals in one area. The main reason leading to the development of these concentrations is actually complete lack of water in other neighborhoods.

Wind pumps is the easiest way to solve this problem as resulting from decades of industry experience in this area, in US and Australia.

1.2.2. Wind driven pumps for water supply

Many of the requirements that make wind pumps are suitable for watering it applies to drinking water. In lowland farms use water remains the most widespread use in livestock farms, the same technology used for watering animals can be used to supply water. This presents a great advantage because farmers are familiar with this type of installation.

In the developing countries are currently, little wind pumps to be used for the production of drinking water. Some were installed by religious missions in communities and schools in Africa, as motor fuel is difficult to transport in isolated areas lacking infrastructure. In Morocco has installed a pump “Aeromotor” through the 70’ in a village in the Rif mountains.

Also have installed more wind pumps in the 50 and 60 in Algeria and Mali. The main problem is their lack of spare parts.

At the moment there is intense international concerns for water, having as promoters UN and World Bank in the "UN International Decade of Water and Sanitation (1981-1990)" however achievements in this area are relatively modest. In developing countries, although in the past several wells were drilled, many of which were then sealed for lack of minimal pumping equipment.

Wind pumps are profitable plants when the wind speed is greater than v> 3.5 m/s, so they cover large areas in developing countries. If the purchaser water supply is often the government, which allows finding practical solutions easier. It may be pointed out that because drilling can involve significant costs (eg over $ 100 / m in parts of Africa) is warranted to investment in a facility able to optimize the use of the well. It is possible to conduct a calculus of wind pumps for isolated location. It can be appreciated that it is necessary 10-15l consumption/day/person.

Water should be transported to a distance of 100-500 m. A classic wind pump will remove 500,000 liters at a height of 1 m/day in a wind of v = 14 km/h (3,8 m/s) that is could feed a community of about 600 people if deemed necessary 15 l/day man delivered a head of 50m or 1200 people if pumping is at 25m. If you are making a calculation shows that capital investment required for installation of a pump will be about 3.5 $ /person for pumping water at 25 m. The lifetime of such a system can be at least 20 years with a appropriate annual maintenance.

1.2.3. Wind pumps for irrigation

Current practice has shown that conventional wind pumps used on farms, industrially manufactured, are not suitable for irrigation works, they are rarely used for this purpose, since the technical and economic requirements are different from those of irrigation water supply.

As a result, wind pumps for irrigation will be more oversized for the needs, most part of the year. In some months they will not be used at all, as in the rainy season or during the sowing and harvesting. It therefore requires an investment in a plant with a low utilization efficiency to maintain an investment cost irrigation pump as low as possible.

Therefore, generally, there are not many results in this area and most pumps used today in irrigation works are traditional and rudimentary (China, Thailand, Crete). Generally there is a tendency for them to be replaced with fuel pumps. With extra attention, wind pumps for irrigation can be simple and cheap

The basic requirements for a wind pump for irrigation will be:

- Existence of the automatic protection in case of storm damage;
- Ability to perform maintenance and repair operations with minimal effort.

Compliance with these requirements will result in a considerable decrease in the cost of investment. Simple and inexpensive pumps usually indigenous, used in irrigation usually have a piston pump undersized. They are a low-cost but they have low efficiency and low flow. In China and Thailand are used hydraulic elevators but can only be used for small heights pumping and flow rates. The high flow rates of pumping traditional to small heights was obtained in the Netherlands, by means of a wheels mill (traditional windmill for Dutch) or a screw pumps (hydraulic conveyor). In practice, however, there are not a wind turbine with a reasonable price and are relatively efficient for high flow rates and low pumping heights, despite numerous experiments in this regard.

In the case of small heights pumping, for an irrigation system corresponding to the necessities of poor countries in the developing world, expecting is a rapid return on investment, which will increase the competitiveness of wind power system as against to the electric or fuel, obviously more expensive. The technological level of a current wind turbine, 50kW, has advanced rapidly in recent years and, are the most used, especially in wind farms built in the US.

With a large series in production, their profitability has become excellent. It also appears that the use of large turbines for driving pumps high flow rates and low pressure is more cost efficient for a group of farms than for one.

1.2.4. The drive pumps

For use and maintenance of the pumps, which have shown that they are very simple mechanical systems, it is necessary that the transmission of the motion from wind driven pump impeller to the pump will be made usin a system as simple as possible. The most common pump drive system is by the use of the crank mechanism which converts the rotation of the pump impeller into a periodical movement in the direction of an axis. Transmission mechanism can be placed horizontally or vertically in mechanically approach is similar in both cases.

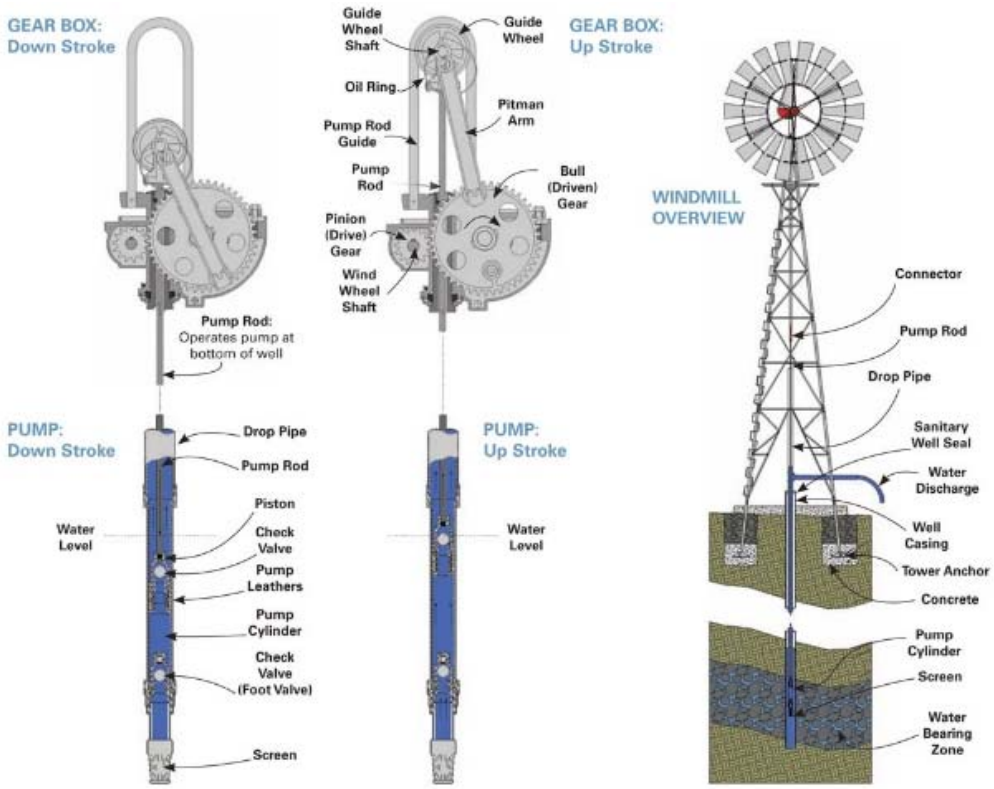

Figure 1.2. Rotor assembly, structure, pump. Adapted from [***13]

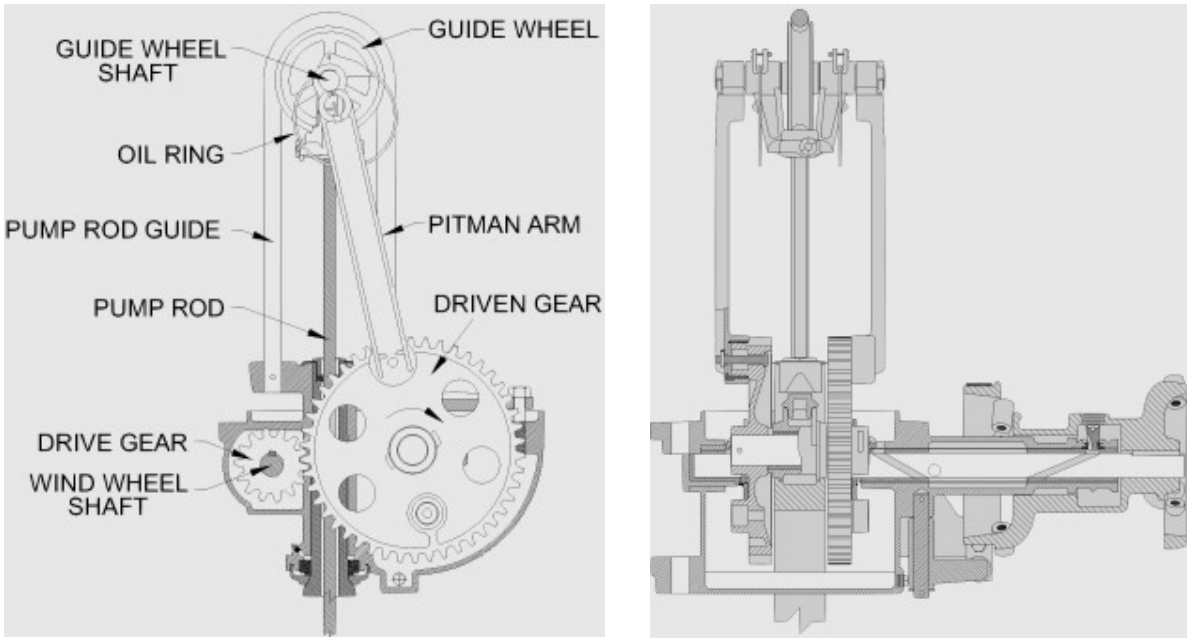

Front view Side view

Figure 1.3. Sketch of mechanism that transform the blade rotation in translation (after [***13])

Figure 1.4. Pumps discarded, used as teaching material (after [DUY80],[LAT05])

1.2.5. Conclusions

The following is an overview of the main issues of wind turbines and the problems generated of the use of wind power to pump water. Also, in this chapter, is presented an analysis of wind-driven pumps, specifically to drive the pump.

Following this analysis have emerged following conclusions:

- literature are treated an impressive number of small wind turbines with horizontal shaft power, which differ in the design of the rotor, the number of blades, material and form, the complexity of the designs, rated power, startup speed, size and working speed, cost price;

- in areas with low wind potential, implementation of small wind turbines operating at wind speeds less than 3 m / s, is a feasible alternative;
- choosing the type and capacity of wind power involves prior analysis of wind potential in the local area installation;
- use and maintenance of pumps and transmitting motion implies that the rotor pump driven by wind itself be achieved by simple systems as the most used system pump drive is a crank type mechanism that converts rotation pump impeller in a periodic translation motion along an axis.

1.3. The objectives of the chapter

The objectives of the researches presents in the chapter are:

1. *Critical analysis of the current state in the construction of wind-driven low-power pumps used to pump water.* This analysis is necessary because the field has a great practical applicability, currently estimated that there are a large number of pumps in operation. Therefore both the study and research of such systems has greatly expanded, yielding numerous results and a high volume of publications dealing with the issue. For developing countries there are solutions that can be applied easily and having minimal maintenance.

2. *Analysis of the problems that occurs in the study of power transmission from the turbine to the pump.* There are practical solutions for mechanical transmissions using wind turbine pumps. However the progress made by the appearance of new materials with superior properties and the possibility of making careful calculations of the transmission make it possible and desirable new solutions showing wind turbine pumps reliable, easy to maintain and install and with a low price of manufacturing.

3. *Proposal of a type of mechanism with two degrees of freedom to provide adaptability to various wind conditions.* To eliminate the inconvenience of a mechanism with constant transmission ratio (hard starting to small wind and overspeed to strong) is proposed a mechanism with automatic variable transmission ratio depending on input conditions (wind speed).

4. *Dynamic analysis of a transmission mechanism with two degrees of freedom (closing driveline by inertia).* To achieve this objective were integrated the equations of motion. For it will use the models proposed in the paper on which were written in Matlab softwares. Mixed system of differential equations, where algebraic and differential unknowns occur (DAE - differential algebraic equations) will be reduced to a system of second order differential equations (DOE - ordinary differential equations). It was made numerical integration of the equations of motion and it is possible to compute, with simple relations the liaison forces.

5. *Experimental verification of the results obtained in different phases of the work.* To verify the results will be designed an experimental stand for studying motion of a mechanism with two degrees of freedom. Was realized a physical model of the

mechanism, in order to confirm its usefulness as an automatic speed regulator. The records shall be made using the method of video recording using a high-speed cameras.

Based on the results expected to be obtained, we intend to establish a set of conclusions derived from numerical analysis of the systems studied and from the experimental verifications performed. Will be provided a dissemination of results through publication in specialized publications and participation in national and international conferences.

1.4. Analysis of wind generator pumping

1.4.1. Piston pump

The piston pump included in the category of volumetric pumps is a suction phenomenon of constructive solution which is based on the principle of volume variation. This is obtained by the periodic movement of a mobile body, the piston, inside the fix corresponding profile of the pump. The piston pump has an important practical significance due to its simplicity and as a result has long been used with good results.

The motion of the piston can be linear or circular, most commonly used being the models where is considerating the piston performin regular race in both directions of motuion. Such a pump is composed by a piston, two valves, a suction pipe and a discharge pipe. More elaborate solutions using tubes to achieve uniform flow and reduce shock. In a conventional piston pump, the discharge valve is located in the piston, the suction valve in the lower part of the pump, usually above the suction head (Fig. 1.5).

If the piston and the discharge valve are separate, we have a plunger pump. In this pump the piston moves down, the discharge valve is opened, the suction valve is closed, the flow rate is zero and the piston comes down freely through the water column. If the piston moves up, the outlet valve will close, the vacuum valve will open and the water is rised (above the piston) and aspirated (as the pump piston is situated above the water level) until the plunger moves down again.

This will result in a pulsating sinusoidal water flow. This type of pump is called simple pump effect. There is also a double-acting pump: the two pistons moving in opposite directions, with two piston and suction and exhaust valves and the differential pump. The pumps have a double effect can provide more uniform water flow.

.

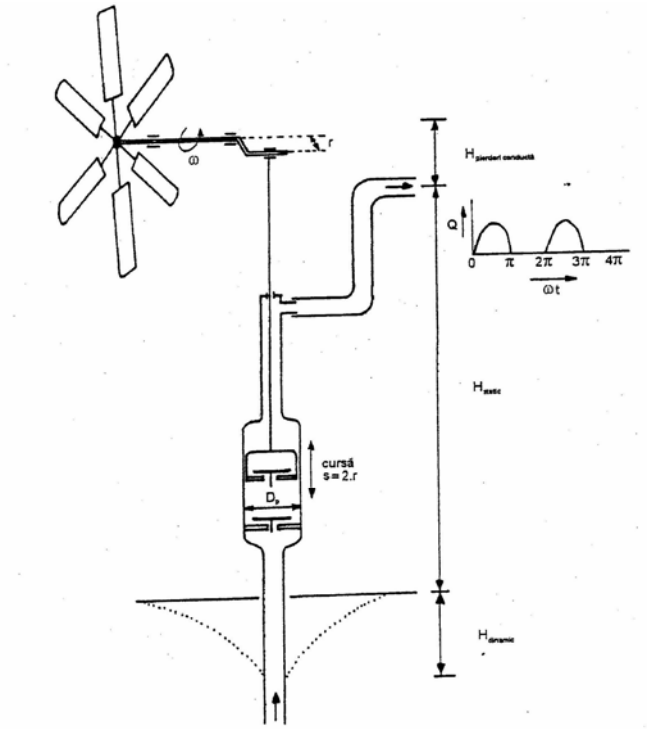

Figure 1.5. Schematic representation of a piston pump driven by an wind rotor [ION04], [LAT05]

1.4.2. The behavior of an ideal pump

The following describes the behavior of an ideal pump at low speeds and low accelerations compared to the gravitational acceleration. We neglect friction forces and dynamic forces. The force which presses the piston is equal to the weight of the column of water (from water level to water discharge - operating the pump immersed in the water).

$$F_p = \rho_h \cdot g \cdot H \cdot \frac{\pi}{4} \cdot D_p^2 \tag{1.1}$$

where: ρ_h - water density;

H - height of water column (which gives static pressure);

F_p - force transmitted to the the crank (with radius r) of the wind rotor pump through the rod r = s / 2 (s stroke).

The resistance torque has a sinusoidal variation during lifting and become zero during the lowering race.

$$\begin{aligned} M_p &= \rho_h \cdot g \cdot H \cdot \frac{\pi}{4} \cdot D_p^2 \cdot \frac{1}{2} \cdot s \cdot \sin \omega t \quad , && 0 \le \omega t \le \pi \\ M_p &= 0 && \pi \le \omega t \le 2\pi \end{aligned} \tag{1.2}$$

Obtaining average torque (torque resistance) involves integrating this expression over a complete cycle:

$$\frac{1}{2\pi}\cdot\int_0^{\pi}\sin\omega t\cdot d\omega t=\frac{1}{\pi} \tag{1.3}$$

and it results the average torque expression

$$\overline{M_p}=\frac{1}{\pi}\cdot\rho_h\cdot g\cdot H\cdot\frac{\pi}{4}D_p^2\cdot\frac{s}{2} \tag{1.4}$$

or $\overline{M_p}=\frac{1}{2\pi}\cdot\rho_h\cdot g\cdot H\cdot\overline{V_s}$

where is denoted: $\overline{V_S}=\frac{\pi D_p^2}{4}\cdot s$ - stroke volume.

It notes that the average torque does not depend on the rotation speed. The average power required can be calculated using the relationship:

$$\overline{P_p}=\overline{M_p}\cdot\omega=\frac{\omega}{2\pi}\rho_p g\cdot H\cdot\overline{V_s} \tag{1.5}$$

If we represent the rel. (1.3.5), we can observe in Fig. 1.6 the relation power- rotation is a straight line passing through origin.

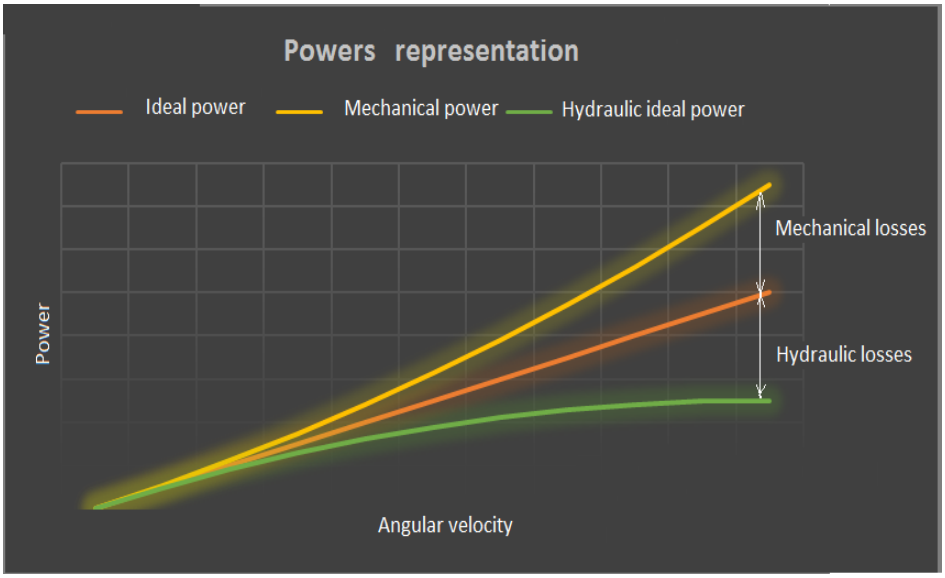

Figure 1.6. The relation speed-power showing the lost of the mechanical and volumic power

1.4.3. Real pump

Ideal pump will require virtually mechanical power equal to the net power to lift water, so its yield would be 100%. Realistically, however, the necessary mechanical strength will be greater than the net lifting power because of water loss occurring in the system, loss of mechanical, hydraulic and volume.

In order to perform a calculus will include mechanical losses, losses of friction between piston and cylinder and hydraulic losses mainly due to friction hydraulic valves.

Also we introduce the concept of yield volume, denoted and defined by the ratio between the real and theoretical volume of the race. However it also notes:

P_{mec} – the mechanical power of the rotor;

$P_{id} = \overline{\upsilon_s} \cdot \frac{\omega}{2\pi} \rho_h g H = \overline{P_p}$ – ideal pump power required;

$P_h = Q \rho_h g H$ – net hydraulic power for lifting water,

The efficiencies are:

$$\eta_{vol} = \frac{Q}{\overline{\upsilon_s} \cdot \frac{\omega}{2\pi}} = \frac{P_h}{P_{id}} \tag{1.6}$$

$$\eta_{mec} = \frac{P_{id}}{P_{mec}} \tag{1.7}$$

and the total efficiency of the pump is

$$\eta_p = \eta_{vol} \cdot \eta_{mec} = \frac{P_h}{P_{mec}} \tag{1.8}$$

The characteristics for power, torque and mechanical efficiency are presented in the Figs. 1.7-1.8. The functional characteristics (conventional) for a SWD pump are: diameter – 0.131m; slider displacement – 0.080m; valve stroke 0.005 m; pumping height – 11.300m.

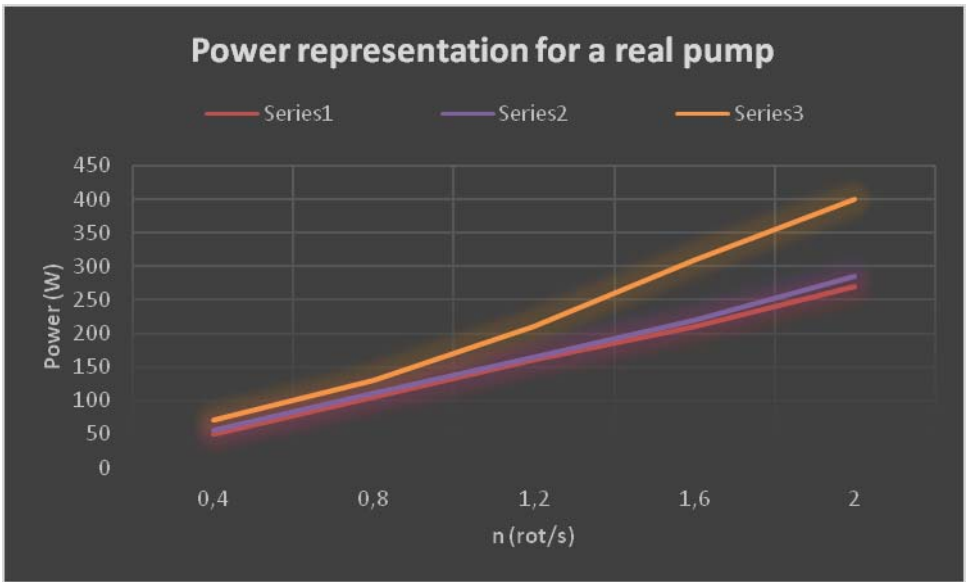

Figure 1.7. Powers graph for a real pump

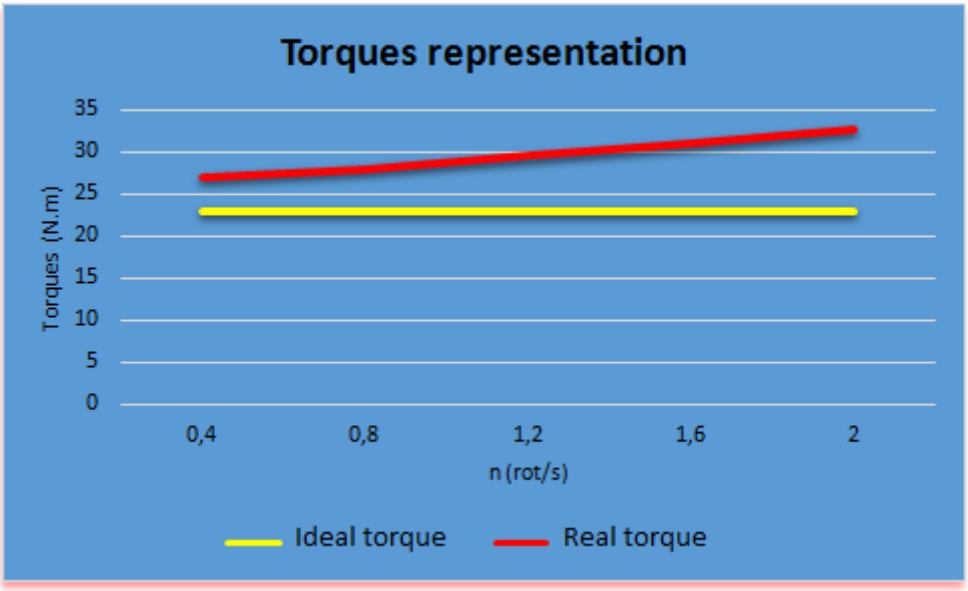

Figure 1.8. Graph of the necessary torque

1.5. Dynamic analysis of pumps used in small wind power systems

1.5.1 Methods used in the analysis of the dynamic systems

If a multibody mechanical system (consisting of several rigid bodies in connection) may be used, to determine the motion equations (and also to obtain solutions), one of the following methods [VOI84], [VÂL63], [IAC77], [DEL08]:

a) theorems of the linear and angular momentum;

b) Lagrange's form of the d` Alembert principle;

c) Lagrange's equations;

d) method of the Lagrange multipliers;

e) Hamilton's equations;

f) theorem of kinetic energy;

g) principle of virtual work,

that in time they take different forms in different author's presentation.

In an analysis of a multibody dynamic system the equations of motion seeks to determine the motion using integration. If the equations of motion are necessary only are advantageous methods b), c), e), f) and g) because they will contain unknown liaison forces. If it is desired to determine the liaison forces (for example, it is necessary to determine the reactions occurring in the links of the mechanism to make a strength calculus) then requires the use of methods a) and d).

If the method a) is applied the equations which are obtained will be a system of second order differential equations (DAE - differential algebraic equations) where, along with independent coordinates appear unknowns and uncertainties related forces. Liaison forces in the

links between elements of the system interfere linear in the motion equations. This leads to solving a system of equations mixed differential and algebraic, which implies a certain difficulty in solving.

In practice are eliminated, in the first phase, the unknown liaison forces and are solved the system of equations, obviously more complicated system. After solving the system of differential equations, the movement is determined and can proceed to the second stage, determining liaison forces by solving a linear algebraic system. Removal of the reactions suppose the use of a matrix inversion techniques.

In the following will be shown a natural method to eliminate the liaison forces, replacing the method of removal the linear liaison forces using an inversion of a matrix with a simple matrix multiplication and thus will ease remarkable numerical approach.

1.5.2. Kinematic conditions in a multibody system

We summarize known results to express the kinematic conditions that will be used in the paper.

Coordinate systems located in the centers of mass of bodies are very useful for writing equations of motion. For this reason we will calculate velocities and accelerations of each element in the mass center.

We will denote with $\{\dot{x}_i\}$ the 6 x 1 vector containing on the first three positions the linear velocity components of the center of mass and on the last three positions the angular velocity vector components of the item *i*. It will be noted with $\{\ddot{x}_i\}$ the vector containing the sequence of linear acceleration components of the center of mass and angular acceleration of the element *i*. If *s* is the number of relationships that exist between the coordinates (the number of kinematic conditions), than the vectors $\{\dot{x}_i\}$, *i = 1,2, ..., n* where *n* is the number of bodies in liaison, can be expressed linearly on q_j , *j = 1,2, ..., s*. (the independent coordinates):

$$\{\dot{x}\} = \begin{Bmatrix} \dot{x}_1 \\ \dot{x}_2 \\ \vdots \\ \dot{x}_n \end{Bmatrix} = [A] \begin{Bmatrix} \dot{q}_1 \\ \dot{q}_2 \\ \vdots \\ \dot{q}_s \end{Bmatrix} = [A]\{\dot{q}\} \tag{1.9}$$

In the following is noted:

$$\{\dot{q}_2\} = [\ \dot{q}_1^2 \quad \dot{q}_1\dot{q}_2 \quad \dot{q}_1\dot{q}_3 \ \dots \ \dot{q}_s^2 \quad]^T \tag{1.10}$$

Vectors $\{\ddot{x}_i\}$, *i = 1,2, ..., n* can be expressed by a linear function of $\ddot{q}_j$ and a quadratic function of $\dot{q}_j$, *j = 1,2, ..,* and finally we have:

$$\{\ddot{x}\} = [A]\{\ddot{q}\} + [B]\{\dot{q}_2\} \tag{1.11}$$

obtained by differentiating rel. (1.9).

1.5.4. Motion equations for a multibody system

In the following is denoted by m_i the mass of the element *i* of the system, with $[J]_i$ the inertia matrix calculated in the center of mass, with $\{Q\}_i^{ext}$ the screw of the external forces in the center of mass and with $\{Q\}_i^{leg}$ the screw of the liaison forcess in the center of mass. The equations of motion for the element numbered with *i* are written in the center of mass of the body in the form:

$$[M]_i\{\ddot{x}\}_i + [M']_i\{\dot{x}\}_i = \{Q\}_i^{ext} + \{Q\}_i^{leg}$$

For the whole system, grouping the equations written for the every element, is possibile to obtain:

$$[M]\{\ddot{x}\} + [M']\{\dot{x}\} = \{Q\}^{ext} + \{Q\}^{leg} \tag{1.12}$$

If we consider the relation (1.12) can be written:

$$[M][A]\{\ddot{q}\} + ([M][B] + [M'][A])\{\dot{q}_2\} = \{Q\}^{ext} + \{Q\}^{leg} \tag{1.13}$$

which is a system of second order nonlinear differential equations having the unknown coordinates $\{q\}$. In general, if *n* is the number of bodies, and *s* is the number of constraints appear *6n - s* constraints equations. If we denote by *i = 1,2, .., 6n-s* liaison forces we can write:

$$\{Q\}^{leg} = [T]\{F\} \tag{1.14}$$

where in the matrix $[T]$ depends on the geometry of the system. If the number of the liaisons forces is greater than *6n*-s, we are dealing with a statically indeterminate structure. To determine the liaison forces must use the elastic properties of the constitutive elements.

1.5.5. Liaison forces elimination

If we denote with $\{v_C\}_i$ the mass center of the *i* element of the system, the velocity of the point A will be:

$$\{v_A\}_i = \{v_C\}_i + [\omega]_i\{r_A\}_i \tag{1.15}$$

where $[\omega]_i$ is the angular velocity operator of the *i* element. We denote with $\{R\}_i$ a liaison force and A the acting point of $\{R\}_i$ (Fig.1.9).

In this case the work of the force $\{R\}_i$ to an infinitesimal displacement with respect the liaisons is:

$$dL_i = \{R\}_i^T\{v_A\}_i dt = \{R\}_i^T(\{v_C\}_i + [\omega]_i\{r_A\}_i)dt =$$

$$= (\{v_C\}_i^T \{R\}_i + \{\omega\}_i^T [r_A]_i \{R\}_i)dt = \{\dot{x}\}_i^T \begin{Bmatrix} \{R\}_i \\ [r_A]_i \{R\}_i \end{Bmatrix} \tag{1.16}$$

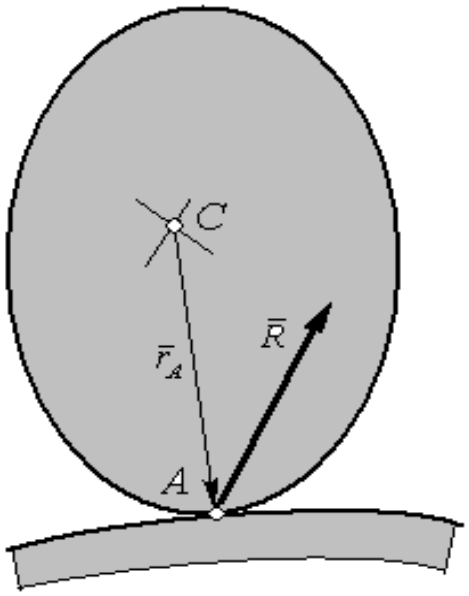

Figure 1.9. Body subjected to liaisons

But expression (1.16) represents the screw of the force $\{R\}_i$ on C . If we take into account all the liaison forces and it is computed the work of the liaison forces it obtains:

$$dL_i^e = \{\dot{x}\}_i^T \begin{Bmatrix} \{R\} \\ \{M_A\} \end{Bmatrix} = \{\dot{x}\}_i^T \{Q\}_i^{leg} \tag{1.16'}$$

where $\{Q\}_i^{leg}$ represents the screw of the liaison forces on mass center C . For the whole system is possible to write:

$$dL = dL_{1e} + dL_{2e} + \ldots + dL_{ne} = \{\dot{x}\}_1^T \{Q\}_1^{leg} + \ldots + \{\dot{x}\}_n^T \{Q\}_n^{leg} = \{\dot{x}\}^T \{Q\}^{leg}.$$

The work of the internal liaison forces is null if the liaison are frictionless, it results:

$$\{\dot{x}\}^T \{Q\}^{leg} = 0 \tag{1.17}$$

If we consider rel. (1.9), the equation (1.17) become:

$$\{\dot{q}\}^T [A]^T \{Q\}^{leg} = 0 \tag{1.18}$$

The coordinates $\{q\}$ beeing independents, it results:

$$[A]^T \{Q\}^{leg} = 0 \tag{1.19}$$

The result will be used to eliminate the liaison forces in (1.11). So, premultiplying (1.11) with $[A]^T$, it obtains:

$$[A]^T [M][A]\{\ddot{q}\} + [A]^T ([M][B] + [M'][A])\{\dot{q}_2\} = [A]^T \{Q\}^{leg} + [A]^T \{Q\}^{ext} \tag{1.20}$$

and, using (1.19), it results:

$$[A]^T[M][A]\{\ddot{q}\}+[A]^T([M][B]+[M'][A])\{\dot{q}_2\}=[A]^T\{Q\}^{ext} \quad (1.20')$$

that there will be a system of *s* differential equations of the second order where the liaisons forces missing. If this system integrates [ARN73], [ARN80] can then easily get the liaisons forces solving a linear system. It follows that, essentially, to eliminate the liaisons forces in the differential equations reduces to multiplying the system with the matrix $[A]^T$.

1.5.5 Writing equations of motion for a classic pump with single or double effect

The equations of motion are the same for a single or a double acting pumps. What is changing in the two cases are expressions of the rotor drive torque and force pump. The mechanism used for transmission in such a pump is a crank mechanism [MAN72], [PEL67].

We will apply the methods described above for the equation of motion writing, the mechanism beeing horizontally or vertically oriented. Writing equations of motion is made in the same way in both cases and therefore we will study initially a slide with horizontal movement, acting pump without considering the technical solution with a little impact on the phenomenon itself.

It will considered, therefore, a crank and connecting rod mechanism where *r* is the length of the crank AB, BC connecting rod length is *L*, the crank mass is m_1, m_2 is the mass of the connecting rod, the slide mass is m_3, the moment of inertia of the crank J_1.

At the same time will make the following notations:

- C_1 and C_2 are the mass center position of the crank and rod;
- a is the length of AC_1;
- b is the length of BC_2;
- ω_1 is denoted the angular speed of the crank ;
- ω_2 is denoted the angular speed of the rod;
- v_C represent the point *C* velocity;
- ε_1 is the angular acceleration of the crank;
- ε_2 is the angular acceleration of the rod;
- a_C is acceleration of point *C*;
- α represent the angular position of the crank;
- β represent the angle between the rod and the horizontal axis.

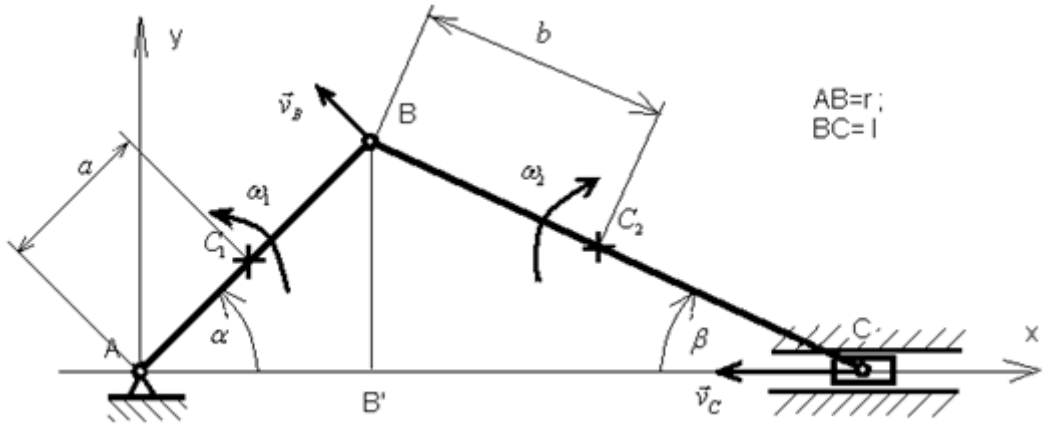

Figure 1.10. Scheme of crank and connecting rod mechanism used for the kinematic analysis

It will write kinematic conditions for simple mechanism presented.

We can write:

$$\begin{aligned} &x_{C1} = a\cos\alpha\ ; \quad y_{C1} = a\sin\alpha\ ; \\ &x_{C2} = r\cos\alpha + b\cos\beta\ ; \quad y_{C2} = r\sin\alpha - b\sin\beta\ ; \\ &x_C = r\cos\alpha + l\cos\beta\ ; \\ &r\sin\alpha = l\sin\beta\ ; \end{aligned} \tag{1.21}$$

If we differentiate the last relation from (1.4.14) it can be obtained:

$$r\dot{\alpha}\cos\alpha = l\dot{\beta}\cos\beta \tag{1.22}$$

or, if we take into account the previous relations:

$$\dot{\alpha} = \omega_1 \quad ; \quad \dot{\beta} = -\omega_2 \quad ; \quad \dot{\omega}_1 = \varepsilon_1 \quad ; \quad \dot{\omega}_2 = \varepsilon_2 \tag{1.23}$$

It results, from (1.4.15):

$$r\omega_1 \cos\alpha = -l\omega_2 \cos\beta \tag{1.23'}$$

or: $$\omega_2 = -\frac{r\cos\alpha}{l\cos\beta}\omega_1 = t\omega_1 \tag{1.24}$$

where the notation:

$$t = -\frac{r\cos\alpha}{l\cos\beta} \tag{1.25}$$

was used. By differentiating (1.4.15') we obtain:

$$r\varepsilon_1 \cos\alpha - r\omega_1^2 \sin\alpha = -l\varepsilon_2 \cos\beta - l\omega_2^2 \sin\beta \tag{1.26}$$

from where: $\varepsilon_2 = -\frac{r\cos\alpha}{l\cos\beta}\varepsilon_1 + \left(\frac{r\sin\alpha}{l\cos\beta} - t^2\frac{\sin\beta}{\cos\beta}\right)\omega_1^2 = t\varepsilon_1 + u\omega_1^2$. (1.27)

We denoted:

$$u = \frac{r\sin\alpha}{l\cos\beta} - t^2\frac{\sin\beta}{\cos\beta}. \tag{1.28}$$

By differentiating the remaining relations from (1.21) it results:

$\dot{x}_{C1} = -a\omega_1 \sin\alpha$;

$\dot{y}_{C1} = a\omega_1 \cos\alpha$;

$\dot{x}_{C2} = -r\omega_1\sin\alpha + b\omega_2\sin\beta = \omega_1(-r\sin\alpha + bt\sin\beta)$;

$\dot{y}_{C2} = r\omega_1\cos\alpha + b\omega_2\cos\beta = \omega_1(r\cos\alpha + bt\cos\beta)$;

$\dot{x}_C = -r\omega_1\sin\alpha + l\omega_2\sin\beta = \omega_1(-r\sin\alpha + lt\sin\beta)$ (1.29)

We put togheter all these relations in a matrix form:

$$\begin{Bmatrix} \dot{x}_{C1} \\ \dot{y}_{C1} \\ \omega_1 \\ \dot{x}_{C2} \\ \dot{y}_{C2} \\ \omega_2 \\ \dot{x}_C \end{Bmatrix} = \begin{Bmatrix} -a\omega_1\sin\alpha \\ a\omega_1\cos\alpha \\ 1 \\ -r\sin\alpha + bt\sin\beta \\ r\cos\alpha + bt\cos\beta \\ t \\ -r\sin\alpha + lt\sin\beta \end{Bmatrix}\omega_1 = \{A_1\}\omega_1 \tag{1.30}$$

By a second differentiation we can obtained the kinematic conditions for accelarations:

$\ddot{x}_{C1} = -a\varepsilon_1\sin\alpha - a\omega_1^2\cos\alpha$;

$\ddot{y}_{C1} = a\varepsilon_1 \cos\alpha - a\omega_1^2 \sin\alpha$;

$$\ddot{x}_{C2} = -r\varepsilon_1\sin\alpha - r\omega_1^2\cos\alpha + b\varepsilon_2\sin\beta - b\omega_2^2\cos\beta =$$
$$= (-r\sin\alpha + bt\sin\beta)\varepsilon_1 + (-r\cos\alpha - bt^2\cos\beta + bu\sin\beta)\omega_1^2;$$

$$\ddot{y}_{C2} = r\varepsilon_1 \cos\alpha - r\omega_1^2 \sin\alpha + b\varepsilon_2 \cos\beta + b\omega_2^2 \sin\beta =$$
$$= (r\cos\alpha + bt\cos\beta)\varepsilon_1 + (-r\sin\alpha + bt^2\sin\beta + bu\cos\beta)\omega_1^2 ;$$

$$\ddot{x}_C = r\varepsilon_1\cos\alpha - r\omega_1^2\sin\alpha + l\varepsilon_2\cos\beta + l\omega_2^2\sin\beta =$$
$$= (r\cos\alpha + lt\cos\beta)\varepsilon_1 + (-r\sin\alpha + lt^2\sin\beta + lu\cos\beta)\omega_1^2 ; \tag{1.31}$$

or:

$$\begin{Bmatrix} \ddot{x}_{C1} \\ \ddot{y}_{C1} \\ \varepsilon_1 \\ \ddot{x}_{C2} \\ \ddot{y}_{C2} \\ \varepsilon_2 \\ \ddot{x}_C \end{Bmatrix} = \begin{Bmatrix} -a\sin\alpha \\ a\cos\alpha \\ 1 \\ -r\sin\alpha + bt\sin\beta \\ r\cos\alpha + bt\cos\beta \\ t \\ -r\sin\alpha + lt\sin\beta \end{Bmatrix} \varepsilon_1 + \begin{Bmatrix} -a\cos\alpha \\ -a\sin\alpha \\ 0 \\ -r\cos\alpha - bt^2\sin\beta + bu\sin\beta \\ -r\sin\alpha + bt^2\sin\beta + bu\cos\beta \\ u \\ -r\sin\alpha + lt^2\sin\beta + lu\cos\beta \end{Bmatrix} \omega_1^2 \qquad (1.32)$$

or, in a compact form:

$$\{a\} = \{A_1\}\varepsilon_1 + \{A_2\}\omega_1^2, \qquad (1.32')$$

where the notations for A_1 and A_2 are obvious.

In the following we will write the equations of motion for the every body of the slider-crank system, considered in order to obtain the equations of motion for the whole mechanism.

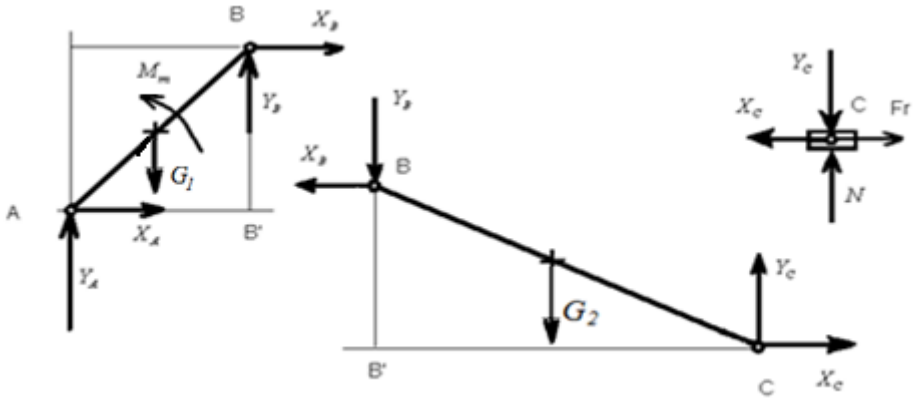

Figure 1.11. Free body diagram

Determination of the equations of motion for each element of the system involves the use of fundamental theorems of mechanics. It is therefore considered that the mechanism is composed of three rigid and should be written at a time for each body:

- crank AB is loaded by a moment Mm representing the wind pump impeller. For bar AB will write three equations of motion:

$$m_1\ddot{x}_{C1} = X_A + X_B$$
$$m_1\ddot{y}_{C1} = Y_A + Y_B - G_1$$

$$J_{C1}\varepsilon_1 = M_m + X_A\frac{r}{2}\sin\alpha - Y_A\frac{r}{2}\cos\alpha - X_B\frac{r}{2}\sin\alpha + Y_B\frac{r}{2}\cos\alpha \qquad (1.33)$$

- To rod BC are obtained analogously relations:

$$m_2\ddot{x}_{C2} = -X_B + X_C$$
$$m_2\ddot{y}_{C2} = -Y_B + Y_C - G_2$$

$$J_{C2}\varepsilon_2 = X_C\frac{l}{2}sin\beta + Y_C\frac{l}{2}cos\beta + X_B\frac{l}{2}sin\beta + Y_B\frac{l}{2}cos\beta \tag{1.34}$$

- The slider C will have a rectilinear translation motion, so it can write:

$$m_3\ddot{x}_C = F_r - X_C \ . \tag{1.35}$$

where with Fr is denoted the weight of the water column to be raised by Fg pump (pumping force developed by the pump) and resistance forces occurring in the pump and in the entire mechanism, denoted with Ff:

$$F_r = F_g + F_f \ .$$

$$\begin{bmatrix} m_1 & 0 & 0 & 0 & 0 & 0 & 0 \\ 0 & m_1 & 0 & 0 & 0 & 0 & 0 \\ 0 & 0 & J_{C1} & 0 & 0 & 0 & 0 \\ 0 & 0 & 0 & m_2 & 0 & 0 & 0 \\ 0 & 0 & 0 & 0 & m_2 & 0 & 0 \\ 0 & 0 & 0 & 0 & 0 & J_{C2} & 0 \\ 0 & 0 & 0 & 0 & 0 & 0 & m_3 \end{bmatrix} \begin{Bmatrix} \ddot{x}_{C1} \\ \ddot{y}_{C1} \\ \varepsilon_1 \\ \ddot{x}_{C2} \\ \ddot{y}_{C2} \\ \varepsilon_2 \\ \ddot{x}_C \end{Bmatrix} = \begin{Bmatrix} X_A + X_B \\ Y_A + Y_B - G_1 \\ [M_m + X_A a\sin\alpha - Y_A a\cos\alpha - \\ \quad - X_B(r-a)\sin\alpha + Y_B(r-a)\cos\alpha] \\ -X_B + X_C \\ -Y_B + Y_C - G_2 \\ X_C(l-b)\sin\beta + Y_C(l-b)\cos\beta + X_B b\sin\beta + Y_B b\cos\beta \\ F_r - X_C \end{Bmatrix} \tag{1.36}$$

or, if one takes account the kinematic and separate the liaison forces we have:

$$\begin{bmatrix} m_1 & 0 & 0 & 0 & 0 & 0 & 0 \\ 0 & m_1 & 0 & 0 & 0 & 0 & 0 \\ 0 & 0 & J_{C1} & 0 & 0 & 0 & 0 \\ 0 & 0 & 0 & m_2 & 0 & 0 & 0 \\ 0 & 0 & 0 & 0 & m_2 & 0 & 0 \\ 0 & 0 & 0 & 0 & 0 & J_{C2} & 0 \\ 0 & 0 & 0 & 0 & 0 & 0 & m_3 \end{bmatrix} \left(\begin{Bmatrix} -a\sin\alpha \\ a\cos\alpha \\ 1 \\ -r\sin\alpha + bt\sin\beta \\ r\cos\alpha + bt\cos\beta \\ t \\ -r\sin\alpha + lt\sin\beta \end{Bmatrix} \varepsilon_1 + \begin{Bmatrix} -a\cos\alpha \\ -a\sin\alpha \\ 0 \\ -r\cos\alpha - bt^2\sin\beta + bu\sin\beta \\ -r\sin\alpha + bt^2\sin\beta + bu\cos\beta \\ u \\ -r\sin\alpha + lt^2\sin\beta + lu\cos\beta \end{Bmatrix} \omega_1^2 \right) =$$

(1.37)

If you take into account the previous notation, we obtain the equations of motion in the form:

$$[m]\left(\{A_1\}\varepsilon_1 + \{A_2\}\omega_1^2\right) = \{Q^{ext}\} + \{Q^{leg}\} = \{Q^{ext}\} + [N]\{R\} \tag{1.37'}$$

the other notations beeing obvious.

The following shows how to remove the liaison forces ([VLA87], [BLA08]. In the first stage we compute the work of the liaison forces with the relation:

$$dL = \{\delta\Delta\}^T\{Q\}^{leg} = \{\dot{\Delta}\}^T\{Q\}^{leg}dt = \{\dot{q}\}^T[A_1]^T\{Q\}^{leg}dt = \omega_1\{A_1\}\{Q\}^{leg}dt \tag{1.38}$$

where $\{\delta\Delta\}$ represents the infinitesimal displacements of the acting points of the liaisons forces $\{Q\}^{leg}$.

The forces of liaison are orthogonal with the possible displacements of the acting points and it is possible to write:

$$\{A_1\}^T \{Q\}^{leg} =$$

$$= \begin{bmatrix} -a\sin\alpha & a\cos\alpha & 1 & -r\sin\alpha + bt\sin\beta & r\cos\alpha + bt\cos\beta & t & -r\sin\alpha + lt\sin\beta \end{bmatrix} x$$

$$x \begin{bmatrix} 1 & 0 & 1 & 0 & 0 & 0 \\ 0 & 1 & 0 & 1 & 0 & 0 \\ a\sin\alpha & -a\cos\alpha & -(r-a)\sin\alpha & (r-a)\cos\alpha & 0 & 0 \\ 0 & 0 & -1 & 0 & 1 & 0 \\ 0 & 0 & 0 & -1 & 0 & 1 \\ 0 & 0 & b\sin\beta & b\cos\beta & (l-b)\sin\beta & (l-b)\cos\beta \\ 0 & 0 & 0 & 0 & -1 & 0 \end{bmatrix} \begin{Bmatrix} X_A \\ Y_A \\ X_B \\ Y_B \\ X_C \\ Y_C \end{Bmatrix} =$$

$$= \begin{Bmatrix} -a\sin\alpha + a\sin\alpha \\ a\cos\alpha - a\cos\alpha \\ -a\sin\alpha - (r-a)\sin\alpha + r\sin\alpha - bt\sin\beta + bt\sin\beta \\ a\cos\alpha + (r-a)\cos\alpha - r\cos\alpha - bt\cos\beta + bt\cos\beta \\ -r\sin\alpha + bt\sin\beta + t(l-b)\sin\beta + r\sin\alpha - lt\sin\beta \\ r\cos\alpha + bt\cos\beta + t(l-b)\cos\beta \end{Bmatrix}^T \begin{Bmatrix} X_A \\ Y_A \\ X_B \\ Y_B \\ X_C \\ Y_C \end{Bmatrix} =$$

$$= \begin{Bmatrix} 0 \\ 0 \\ 0 \\ 0 \\ 0 \\ r\cos\alpha + tl\cos\beta \end{Bmatrix}^T \begin{Bmatrix} X_A \\ Y_A \\ X_B \\ Y_B \\ X_C \\ Y_C \end{Bmatrix} = \begin{bmatrix} 0 & 0 & 0 & 0 & 0 & 0 \end{bmatrix} \begin{Bmatrix} X_A \\ Y_A \\ X_B \\ Y_B \\ X_C \\ Y_C \end{Bmatrix} = 0 \qquad (1.39)$$

since $t = -\dfrac{r\cos\alpha}{l\cos\beta}$ (according rel. 1.25), then $r\cos\alpha + tl\cos\beta = 0$.

We used the notation $\{Q^{leg}\}$ for the screw of the liaison generalized forces corresponding to the generalized coordinates considered. Equation of motion follows:

$$\begin{aligned} &[m_1 a^2 \sin^2\alpha + m_1 a^2 \cos^2\alpha + J_{C1} + m_2(-r\sin\alpha + bt\sin\beta)^2 + \\ &+ m_2(r\cos\alpha + bt\cos\beta)^2 + J_{C2}t^2 + m_3(-r\sin\alpha + lt\sin\beta)^2]\varepsilon_1 + \\ &+ [m_1 a^2 \sin\alpha\cos\alpha - m_1 a^2 \sin\alpha\cos\alpha + \\ &+ m_2(-r\sin\alpha + bt\sin\beta)(-r\cos\alpha - bt^2\sin\beta + bu\sin\beta) + \\ &+ m_2(r\cos\alpha + bt\cos\beta)(-r\sin\alpha + bt^2\sin\beta + bu\cos\beta) + \\ &+ J_{C2}tu + m_3(-r\sin\alpha + lt\sin\beta)(-r\sin\alpha + lt^2\sin\beta + lu\cos\beta)]\omega_1^2 = \\ &= M_m + F_r(-r\sin\alpha + lt\sin\beta) \end{aligned} \qquad (1.40)$$

If you do the calculations, you get:

$$[m_1a^2 + J_{C1} + m_2r^2 + m_2b^2t^2 + 2m_2rbt\cos(\alpha+\beta) + J_{C2}t^2 +$$
$$+ m_3(-r\sin\alpha + lt\sin\beta)^2]\varepsilon_1 + [m_2(rbt^2\cos(\alpha-\beta) + rbu\cos(\alpha+\beta) -$$
$$- rbt\sin(\alpha+\beta) - b^2t^3\cos 2\beta + b^2tu) + J_{C2}tu +$$
$$+ m_3(-r\sin\alpha + lt\sin\beta)(-r\sin\alpha + lt^2\sin\beta + lu\cos\beta)]\omega_1^2 =$$
$$= M_m + F_r(-r\sin\alpha + lt\sin\beta) \qquad (1.40')$$

If notes

- the reduced moment of inertia of the mechanism to the axis of rotation:

$$J(\alpha) = \{A_1\}^T[m]\{A_1\} = [m_1a^2 + J_{C1} + m_2r^2 + m_2b^2t^2 +$$
$$+ 2m_2rbt\cos(\alpha+\beta) + J_{C2}t^2 + m_3(-r\sin\alpha + lt\sin\beta)^2] \quad ; \qquad (1.41)$$

$$J'(\alpha) = \{A_1\}^T[m]\{A_2\} =$$
$$= [m_2(rbt^2\cos(\alpha-\beta) + rbu\cos(\alpha+\beta) - rbt\sin(\alpha+\beta) - b^2t^3\cos 2\beta +$$
$$+ b^2tu + J_{C2}tu + m_3(-r\sin\alpha + lt\sin\beta)(-r\sin\alpha + lt^2\sin\beta + lu\cos\beta)] \qquad (1.42)$$

- the reduced torque of the external forces:

$$M(\alpha) = M_m + F_r(-r\sin\alpha + lt\sin\beta) \qquad (1.43)$$

equation of motion is obtained as:

$$J(\alpha)\ddot{\alpha} + J'(\alpha)\dot{\alpha}^2 = M(\alpha) \qquad (1.40'')$$

Reactions can be determined in this case easily. Thus, first we can write:

$$\varepsilon_1 = \ddot{\alpha} = \frac{\left[M(\alpha) - J'(\alpha)\dot{\alpha}^2\right]}{J(\alpha)} \qquad (1.44)$$

From equations (1.4.30) where rel. (1.4.37) has been used, we obtain:

$$\begin{bmatrix} m_1 & 0 & 0 & 0 & 0 & 0 \\ 0 & m_1 & 0 & 0 & 0 & 0 \\ 0 & 0 & J_{C1} & 0 & 0 & 0 \\ 0 & 0 & 0 & m_2 & 0 & 0 \\ 0 & 0 & 0 & 0 & m_2 & 0 \\ 0 & 0 & 0 & 0 & 0 & m_3 \end{bmatrix} \left(\begin{Bmatrix} -a\sin\alpha \\ a\cos\alpha \\ 1 \\ -r\sin\alpha + bt\sin\beta \\ r\cos\alpha + bt\cos\beta \\ -r\sin\alpha + lt\sin\beta \end{Bmatrix} \frac{\left[M(\alpha) - J'(\alpha)\dot{\alpha}^2\right]}{J(\alpha)} + \begin{Bmatrix} -a\cos\alpha \\ -a\sin\alpha \\ 0 \\ -r\cos\alpha - bt^2\sin\beta + bu\sin\beta \\ -r\sin\alpha + bt^2\sin\beta + bu\cos\beta \\ -r\sin\alpha + lt^2\sin\beta + lu\cos\beta \end{Bmatrix} \dot{\alpha}^2 \right) =$$

$$=\begin{Bmatrix}0\\0\\M_m\\0\\0\\F_r\end{Bmatrix}+\begin{bmatrix}1&0&1&0&0&0\\0&1&0&1&0&0\\a\sin\alpha&-a\cos\alpha&-(r-a)\sin\alpha&(r-a)\cos\alpha&0&0\\0&0&-1&0&1&0\\0&0&0&-1&0&1\\0&0&0&0&-1&0\end{bmatrix}\begin{Bmatrix}X_A\\Y_A\\X_B\\Y_B\\X_C\\Y_C\end{Bmatrix} \tag{1.45}$$

Hence, it can obtain the reactions by solving a simple linear system.

The wind turbines transfer the motion, using the connecting rod-crank systems, this is the easiest way to carry out the transformation of the rotation of the turbine rotor in the movement of translation of the piston pump. In some cases it also introduces a speed reducer as provided that the rotor angular velocity is too high for pump.

The paper will consider the following situation: *The free motion of crank pump system under the effect of inertia* Boundary conditions will determine the mechanical energy of the system. Frictionless motion will be considered so that at any time to conserve mechanical energy. As reduced moment of inertia of the system is variable will result that the crank angular velocity will vary.

1.5.6. The free motion of the slider-crank pump system, determined by the initial conditions

First will calculate the kinetic energy of multibody system under study. Using the notations of the subchapter 1.4.2 above we have for the kinetic energy (4.1.39) the relationship:

$$E_c=\frac{1}{2}\begin{Bmatrix}-a\sin\alpha\\a\cos\alpha\\1\\-r\sin\alpha+bt\sin\beta\\r\cos\alpha+bt\cos\beta\\t\\-r\sin\alpha+lt\sin\beta\end{Bmatrix}^T\begin{bmatrix}m_1&0&0&0&0&0&0\\0&m_1&0&0&0&0&0\\0&0&J_{C1}&0&0&0&0\\0&0&0&m_2&0&0&0\\0&0&0&0&m_2&0&0\\0&0&0&0&0&J_{C2}&0\\0&0&0&0&0&0&m_3\end{bmatrix}\begin{Bmatrix}-a\sin\alpha\\a\cos\alpha\\1\\-r\sin\alpha+bt\sin\beta\\r\cos\alpha+bt\cos\beta\\t\\-r\sin\alpha+lt\sin\beta\end{Bmatrix}\omega_1^2$$

or, if we make the calculus:

$$E_c=\frac{1}{2}(m_1a^2+J_{C1}+m_2r^2+m_2b^2t^2+2rbt\cos(\alpha+\beta)+$$
$$+J_{C2}t^2+m_3(-r\sin\alpha+lt\sin\beta)^2)\omega_1^2=\frac{1}{2}J(\alpha)\dot{\alpha}^2 \tag{1.46}$$

with:

$$J(\alpha)=m_1a^2+J_{C1}+m_2r^2+m_2b^2t^2+2rbt\cos(\alpha+\beta)+J_{C2}t^2+m_3(-r\sin\alpha+lt\sin\beta)^2$$

is denoted the reduced moment of inertia of the system to handle. In this first element the element weights of the mechanism will be neglect. It will calculate the initial kinetic energy of the system which in this case is the total mechanical energy, energy will be conserved in the absence of external forces and moments:

$$E_{c0} = \frac{1}{2}(m_1 a^2 + J_{C1} + m_2 r^2 + m_2 b^2 t^2 + 2rbt\cos(\alpha_0 + \beta_0) + \\ + J_{C2} t^2 + m_3(-r\sin\alpha_0 + lt\sin\beta_0)^2)\omega_{10}^2 = \frac{1}{2} J(\alpha_0)\dot{\alpha}_0^2 \tag{1.47}$$

The expression of the kinetic energy is:

$$E_c = \frac{1}{2} J(\alpha)\dot{\alpha}^2 = E_{c0} \tag{1.48}$$

The equivalent inertia momentum of the mechanism reduced to the rotation of the crank can be computed using the relation:

$$J(\alpha_0) = m_1 a^2 + J_{C1} + m_2 r^2 + m_2 b^2 t^2 + 2rbt\cos(\alpha_0 + \beta_0) + J_{C2} t^2 + m_3(-r\sin\alpha_0 + lt\sin\beta_0)^2) \tag{1.48'}$$

and is a function of the mechanism position.

From the expression of kinetic energy it results the angular velocity of the crank for any position of the crank:

$$\dot{\alpha} = \sqrt{\frac{2E_{c0}}{J(\alpha)}} \tag{1.49}$$

Calculus of the previous expression poses no problems since the denominator can never be zero. Theoretically, with the initial condition given here may be integrating the equation of motion:

$$\frac{d\alpha}{dt} = \sqrt{\frac{2E_{c0}}{J(\alpha)}}, \tag{1.50}$$

from where:

$$\int_{\alpha_0}^{\alpha} \frac{d\alpha}{\sqrt{\frac{2E_{c0}}{J(\alpha)}}} = t - t_0 \ . \tag{1.51}$$

Integral calculation can be done using a numerical method, eg Simpson method in Matlab programming environment.

Using the relation (4.1.34) $J(\alpha)$ can be represented and using rel. 4.1.46 may represent the angular velocity of the crank and can be done Runge-Kutta integration.

Consider a case in which the integration time is 2 seconds (tspan subroutine 101 has values from 0 to 2). The data set used to run programs: m_1 = 2 kg; m_2 = 4 kg; m_3 = 10 kg; J_1=0.0066 kg.m^2; J_2 = 0.053 kg.m^2 ; t0 = 0; tfinal = 2 s.

1.5.7. Dynamic analysis of the transmission mechanism with two degree of freedom

The originality of this mechanism is to use the inertia of one of its elements, continuous change gear ratio as the input speed increases. In this respect, the mechanism will have two degrees of freedom, which could be considered the input rotation angle (crank AB), and the pump stroke (coordinate of the point D), noted x_D.

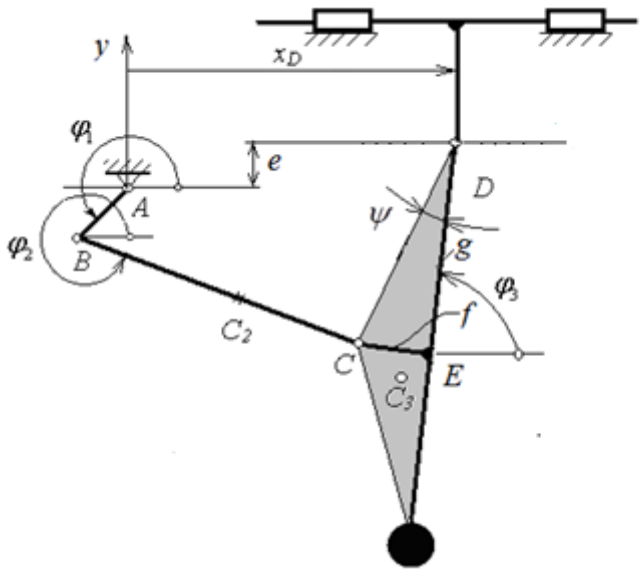

Figure 1.12. Mechanism with two degree of freedo

Closing vector equations:

$$\begin{cases} l_1 c_1 + l_2 c_2 + h c_{3-\psi} - x_D = 0 \\ l_1 s_1 + l_2 s_2 + h s_{3-\psi} - e = 0 \end{cases} \tag{1.52}$$

where: $h = \sqrt{f^2 + g^2}$

In closing vector equation will be determined the values of angles φ_2 and φ_3 depending on the angle φ_1 and the displacement x_D . In triangle ABD we know

$$AD = \sqrt{x_D^2 + e^2} \,. \tag{1.53}$$

From Fig.1.13 it results: $2\pi - \varphi_1 + \beta' + \alpha + \beta = \pi$

therefore: $\beta = \varphi_1 - \pi - \alpha - \beta'$. (1.54)

Sine theorem in the triangle ABD gives:

$$\frac{l_1}{\sin\beta} = \frac{AD}{\sin\alpha} \tag{1.56}$$

$$AD \sin\beta = l_1 \sin\alpha \quad ; \tag{1.57}$$

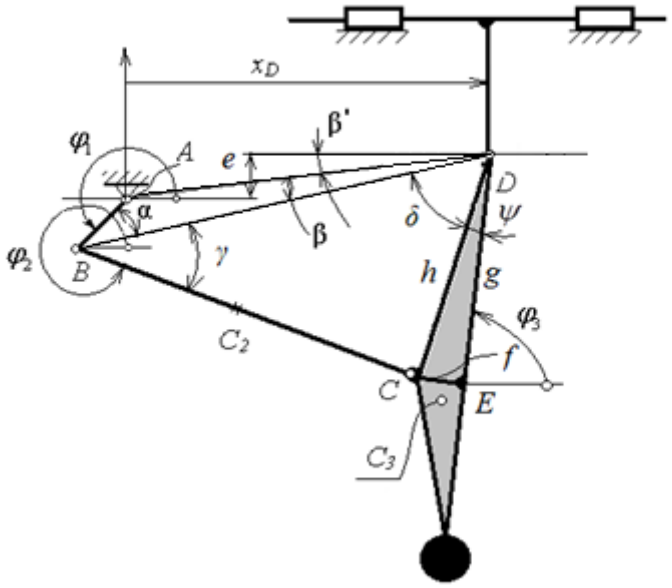

Figure 1.13. Geometry of the mechanism

Taking into account the relation:

$$\sin\beta = -\sin(\varphi_1 - \alpha - \beta') = [-\sin(\varphi_1 - \beta')\cos\alpha + \cos(\varphi_1 - \beta')\sin\alpha] \tag{1.58}$$

and substituting $\sin\beta$ in (1.5.6) into (1.5.5) we obtain:

$$l_1 \sin\alpha = AD[-\sin(\varphi_1 - \beta')\cos\alpha + \cos(\varphi_1 - \beta')\sin\alpha]$$

or: $\sin\alpha\left[l_1 - AD\cos(\varphi_1 - \beta')\right] = -AD\sin(\varphi_1 - \beta')\cos\alpha$

from where: $tg\alpha = \dfrac{-AD\sin(\varphi_1 - \beta')}{l_1 - AD\cos(\varphi_1 - \beta')}$ (1.59)

It results: $\alpha = a\tan\left[\dfrac{-AD\sin(\varphi_1 - \beta')}{l_1 - AD\cos(\varphi_1 - \beta')}\right]$. (1.59')

Now is possible to compute the angle β with the relation:

$\sin\beta = \dfrac{l_1 \sin\alpha}{AD}$ from where: $\beta = a\sin(\dfrac{l_1 \sin\alpha}{AD})$.

Further we calculate BD:

$BD^2 = l_1^2 + AD^2 - 2l_1 AD\cos(2\pi - \varphi_1 + \beta')$.

It can be applied further, in the triangle ABD, cosine theorem:

$$\cos\gamma = \frac{l_2^2 + BD^2 - h^2}{2l_2 \cdot BD} \quad ; \tag{1.60}$$

$$\gamma = a\cos\frac{l_2^2 + BD^2 - h^2}{2l_2 \cdot BD} \tag{1.60'}$$

$$\cos\delta = \frac{h^2 + BD^2 - l_2^2}{2h \cdot BD} \ ; \tag{1.61}$$

$$\delta = a\cos\frac{h^2 + BD^2 - l_2^2}{2h \cdot BD} \tag{1.61'}$$

It is possible now to compute φ_2, φ_3:

$$\varphi_2 = 2\pi - \gamma + \beta + \beta' \ ; \tag{1.62}$$

$$\varphi_3 = \beta + \beta' + \delta + \psi \ . \tag{1.63}$$

Differentiating (1.53) condition equations for velocities are obtained:

$$\begin{cases} -l_1\omega_1 s_1 - l_2\omega_2 s_2 - h\omega_3 s_{3-\psi} - \dot{x}_D = 0 \\ l_1\omega_1 c_1 + l_2\omega_2 c_2 + h\omega_3 c_{3-\psi} = 0 \end{cases} . \tag{1.64}$$

The previous system can be written as:

$$\begin{bmatrix} s_2 & s_{3-\psi} \\ c_2 & c_{3-\psi} \end{bmatrix} \begin{Bmatrix} l_2\omega_2 \\ h\omega_3 \end{Bmatrix} = \begin{bmatrix} -s_1 & -1 \\ -c_1 & 0 \end{bmatrix} \begin{Bmatrix} l_1\omega_1 \\ \dot{x}_D \end{Bmatrix} \tag{1.65}$$

with the solution:

$$\begin{Bmatrix} l_2\omega_2 \\ h\omega_3 \end{Bmatrix} = \frac{1}{s_2 c_{3-\psi} - s_{3-\psi} c_2} \begin{bmatrix} c_{3-\psi} & -s_{3-\psi} \\ -c_2 & s_2 \end{bmatrix} \begin{bmatrix} -s_1 & -1 \\ -c_1 & 0 \end{bmatrix} \begin{Bmatrix} l_1\omega_1 \\ \dot{x}_D \end{Bmatrix} =$$
$$= \frac{1}{s_2 c_{3-\psi} - s_{3-\psi} c_2} \begin{bmatrix} -c_{3-\psi} s_1 + s_{3-\psi} c_1 & -c_{3-\psi} \\ c_2 s_1 - c_1 s_2 & c_2 \end{bmatrix} \begin{Bmatrix} l_1\omega_1 \\ \dot{x}_D \end{Bmatrix} \tag{1.66}$$

We denote:

$$\begin{bmatrix} a_{11} & a_{12} \\ a_{21} & a_{22} \end{bmatrix} = \frac{1}{s_2 c_{3-\psi} - s_{3-\psi} c_2} \begin{bmatrix} -c_{3-\psi} s_1 + s_{3-\psi} c_1 & -c_{3-\psi} \\ c_2 s_1 - c_1 s_2 & c_2 \end{bmatrix}. \tag{1.67}$$

We can write:

$$\begin{Bmatrix} l_2\omega_2 \\ h\omega_3 \end{Bmatrix} = \begin{bmatrix} a_{11} & a_{12} \\ a_{21} & a_{22} \end{bmatrix} \begin{Bmatrix} l_1\omega_1 \\ \dot{x}_D \end{Bmatrix} \ . \tag{1.67'}$$

The condition equations for accelerations can be obtained differentiating (1.5.12):

$$\begin{cases} -l_1\varepsilon_1 s_1 - l_2\varepsilon_2 s_2 - h\varepsilon_3 s_{3-\psi} - l_1\omega_1^2 c_1 - l_2\omega_2^2 c_2 - h\omega_3^2 c_{3-\psi} - \ddot{x}_D = 0 \\ l_1\varepsilon_1 c_1 + l_2\varepsilon_2 c_2 + h\varepsilon_3 c_{3-\psi} - l_1\omega_1^2 s_1 - l_2\omega_2^2 s_2 - h\omega_3^2 s_{3-\psi} = 0 \end{cases} \tag{1.68}$$

From here we can to determine the two unknown angular accelerations:

$$\begin{Bmatrix} l_2\varepsilon_2 \\ h\varepsilon_3 \end{Bmatrix} = \begin{bmatrix} a_{11} & a_{12} \\ a_{21} & a_{22} \end{bmatrix} \begin{Bmatrix} l_1\varepsilon_1 \\ \ddot{x}_D \end{Bmatrix} + \frac{1}{s_2c_{3-\psi} - s_{3-\psi}c_2} \begin{bmatrix} c_{3-\psi} & -s_{3-\psi} \\ -c_2 & s_2 \end{bmatrix} \begin{Bmatrix} -\frac{(l_1\omega_1)^2 c_1}{l_1} - \frac{(l_2\omega_2)^2 c_2}{l_2} - \frac{(h\omega_3)^2 c_{3-\psi}}{h} \\ \frac{(l_1\omega_1)^2 s_1}{l_1} + \frac{(l_2\omega_2)^2 s_2}{l_2} + \frac{(h\omega_3)^2 s_{3-\psi}}{h} \end{Bmatrix} =$$

$$= \begin{bmatrix} a_{11} & a_{12} \\ a_{21} & a_{22} \end{bmatrix} \begin{Bmatrix} l_1\varepsilon_1 \\ \ddot{x}_D \end{Bmatrix} + \frac{1}{s_2c_{3-\psi} - s_{3-\psi}c_2} \begin{bmatrix} c_{3-\psi} & -s_{3-\psi} \\ -c_2 & s_2 \end{bmatrix} [\begin{Bmatrix} -\frac{c_1}{l_1} \\ \frac{s_1}{l_1} \end{Bmatrix} (l_1\omega_1)^2 + \begin{Bmatrix} -\frac{c_2}{l_2} \\ \frac{s_2}{l_2} \end{Bmatrix} (l_2\omega_2)^2 + \begin{Bmatrix} -\frac{c_{3-\psi}}{h} \\ \frac{s_{3-\psi}}{h} \end{Bmatrix} (h\omega_3)^2] =$$

$$= \begin{bmatrix} a_{11} & a_{12} \\ a_{21} & a_{22} \end{bmatrix} \begin{Bmatrix} l_1\varepsilon_1 \\ \ddot{x}_D \end{Bmatrix} + \frac{1}{s_2c_{3-\psi} - s_{3-\psi}c_2} \begin{bmatrix} c_{3-\psi} & -s_{3-\psi} \\ -c_2 & s_2 \end{bmatrix} x$$

$$x[\frac{1}{l_1} \begin{Bmatrix} -c_1 \\ s_1 \end{Bmatrix} (l_1\omega_1)^2 + \frac{1}{l_2} \begin{Bmatrix} -c_2 \\ s_2 \end{Bmatrix} (a_{11}l_1\omega_1 + a_{12}\dot{x}_D)^2 + \frac{1}{h} \begin{Bmatrix} -c_{3-\psi} \\ s_{3-\psi} \end{Bmatrix} (a_{21}l_1\omega_1 + a_{22}\dot{x}_D)^2] =$$

$$= \begin{bmatrix} a_{11} & a_{12} \\ a_{21} & a_{22} \end{bmatrix} \begin{Bmatrix} l_1\varepsilon_1 \\ \ddot{x}_D \end{Bmatrix} + \frac{1}{s_2c_{3-\psi} - s_{3-\psi}c_2} x[\frac{1}{l_1} \begin{Bmatrix} -c_{3-\psi}c_1 - s_{3-\psi}s_1 \\ c_2c_1 + s_2s_1 \end{Bmatrix} (l_1\omega_1)^2 +$$

$$+ \frac{1}{l_2} \begin{Bmatrix} -c_{3-\psi}c_2 - s_{3-\psi}s_2 \\ 1 \end{Bmatrix} (a_{11}l_1\omega_1 + a_{12}\dot{x}_D)^2 + \frac{1}{h} \begin{Bmatrix} -1 \\ c_{3-\psi}c_2 + s_{3-\psi}s_2 \end{Bmatrix} (a_{21}l_1\omega_1 + a_{22}\dot{x}_D)^2] =$$

$$= \begin{bmatrix} a_{11} & a_{12} \\ a_{21} & a_{22} \end{bmatrix} \begin{Bmatrix} l_1\varepsilon_1 \\ \ddot{x}_D \end{Bmatrix} + \frac{1}{s_2c_{3-\psi} - s_{3-\psi}c_2} x[\begin{Bmatrix} \frac{-c_{3-\psi}c_1 - s_{3-\psi}s_1}{l_1} + a_{11}^2 \frac{-c_{3-\psi}c_2 - s_{3-\psi}s_2}{l_2} - \frac{a_{21}^2}{h} \\ \frac{c_2c_1 + s_2s_1}{l_1} + \frac{a_{11}^2}{l_2} + a_{21}^2 \frac{c_{3-\psi}c_2 + s_{3-\psi}s_2}{h} \end{Bmatrix} (l_1\omega_1)^2 +$$

$$+ \begin{Bmatrix} 2a_{11}a_{12} \frac{-c_{3-\psi}c_2 - s_{3-\psi}s_2}{l_2} - \frac{2a_{21}a_{22}}{h} \\ \frac{2a_{11}a_{12}}{l_2} + 2a_{21}a_{22} \frac{c_{3-\psi}c_2 + s_{3-\psi}s_2}{h} \end{Bmatrix} (l_1\omega_1)\dot{x}_D + \begin{Bmatrix} a_{12}^2 \frac{-c_{3-\psi}c_2 - s_{3-\psi}s_2}{l_2} - \frac{a_{22}^2}{h} \\ \frac{a_{12}^2}{l_2} + a_{22}^2 \frac{c_{3-\psi}c_2 + s_{3-\psi}s_2}{h} \end{Bmatrix} (\dot{x}_D)^2].$$

It is denoted:

$$b_{11} = \frac{1}{s_2c_{3-\psi} - s_{3-\psi}c_2} \left(\frac{-c_{3-\psi}c_1 - s_{3-\psi}s_1}{l_1} + a_{11}^2 \frac{-c_{3-\psi}c_2 - s_{3-\psi}s_2}{l_2} - \frac{a_{21}^2}{h} \right) \quad ;$$

$$b_{12} = \frac{1}{s_2c_{3-\psi} - s_{3-\psi}c_2} \left(2a_{11}a_{12} \frac{-c_{3-\psi}c_2 - s_{3-\psi}s_2}{l_2} - \frac{2a_{21}a_{22}}{h} \right) \quad ;$$

$$b_{13} = \frac{1}{s_2c_{3-\psi} - s_{3-\psi}c_2} \left(a_{12}^2 \frac{-c_{3-\psi}c_2 - s_{3-\psi}s_2}{l_2} - \frac{a_{22}^2}{h} \right) \quad ;$$

$$b_{21} = \frac{1}{s_2c_{3-\psi} - s_{3-\psi}c_2} \left(\frac{c_2c_1 + s_2s_1}{l_1} + \frac{a_{11}^2}{l_2} + a_{21}^2 \frac{c_{3-\psi}c_2 + s_{3-\psi}s_2}{h} \right) \quad ;$$

$$b_{22}=\frac{1}{s_2c_{3-\psi}-s_{3-\psi}c_2}\left(\frac{2a_{11}a_{12}}{l_2}+2a_{21}a_{22}\frac{c_{3-\psi}c_2+s_{3-\psi}s_2}{h}\right)\quad;$$

$$b_{23}=\frac{1}{s_2c_{3-\psi}-s_{3-\psi}c_2}\left(\frac{a_{12}^2}{l_2}+a_{22}^2\frac{c_{3-\psi}c_2+s_{3-\psi}s_2}{h}\right)\quad; \tag{1.69}$$

and finally the angular accelerations are obtained:

$$\begin{Bmatrix}l_2\varepsilon_2\\h\varepsilon_3\end{Bmatrix}=\begin{bmatrix}a_{11}&a_{12}\\a_{21}&a_{22}\end{bmatrix}\begin{Bmatrix}l_1\varepsilon_1\\\ddot{x}_D\end{Bmatrix}+\begin{bmatrix}b_{11}&b_{12}&b_{13}\\b_{21}&b_{22}&b_{23}\end{bmatrix}\begin{Bmatrix}(l_1\omega_1)^2\\l_1\omega_1\dot{x}_D\\(\dot{x}_D)^2\end{Bmatrix} \tag{1.70}$$

The mass center positions, the velocities and accelerations of these are obtained using the relations:

$$\begin{cases}x_1=a_1l_1c_1\quad;\\y_1=a_1l_1s_1\quad.\end{cases}\quad\begin{cases}\dot{x}_1=-a_1l_1\omega_1s_1\quad;\\\dot{y}_1=a_1l_1\omega_1c_1\quad.\end{cases}\quad\begin{cases}\ddot{x}_1=-a_1l_1\varepsilon_1s_1-a_1l_1\omega_1^2c_1\quad;\\\ddot{y}_1=a_1l_1\varepsilon_1c_1-a_1l_1\omega_1^2s_1\quad.\end{cases} \tag{1.71}$$

$$\begin{cases}x_2=l_1c_1+a_2l_2c_2\\y_2=l_1s_1+a_2l_2s_2\end{cases};\begin{cases}\dot{x}_2=-l_1\omega_1s_1-a_2l_2\omega_2s_2\\\dot{y}_2=l_1\omega_1c_1+a_2l_2\omega_2c_2\end{cases};\begin{cases}\ddot{x}_2=-l_1\varepsilon_1s_1-a_2l_2\varepsilon_2s_2-l_1\omega_1^2c_1-a_2l_2\omega_2^2c_2\\\ddot{y}_2=l_1\varepsilon_1c_1+a_2l_2\varepsilon_2c_2-l_1\omega_1^2s_1-a_2l_2\omega_2^2s_2\end{cases}; \tag{1.72}$$

$$\begin{cases}x_3=l_1c_1+l_2c_2+hg\cdot c_{3-\psi-\xi}\\y_3=l_1s_1+l_2s_2+hg\cdot s_{3-\psi-\xi}\end{cases};\quad\begin{cases}\dot{x}_3=-l_1\omega_1s_1-l_2\omega_2s_2-hg\cdot\omega_3s_{3-\psi-\xi}\\\dot{y}_3=l_1\omega_1c_1+l_2\omega_2c_2+hg\cdot\omega_3c_{3-\psi-\xi}\end{cases};$$

$$\begin{cases}\ddot{x}_3=-l_1\varepsilon_1s_1-l_2\varepsilon_2s_2-hg\cdot\varepsilon_3s_{3-\psi-\xi}-l_1\omega_1^2c_1-l_2\omega_2^2c_2-hg\cdot\omega_3^2c_{3-\psi-\xi}\quad;\\\ddot{y}_3=l_1\varepsilon_1c_1+l_2\varepsilon_2c_2+hg\cdot\varepsilon_3c_{3-\psi-\xi}-l_1\omega_1^2s_1-l_2\omega_2^2s_2-hg\cdot\omega_3^2s_{3-\psi-\xi}\quad.\end{cases} \tag{1.73}$$

$$\{a\}=\begin{Bmatrix}\ddot{x}_1\\\ddot{y}_1\\\varepsilon_1\\\ddot{x}_2\\\ddot{y}_2\\\varepsilon_2\\\ddot{x}_3\\\ddot{y}_3\\\varepsilon_3\\\ddot{x}_D\end{Bmatrix}=\begin{Bmatrix}0\\0\\0\\0\\0\\0\\0\\0\\0\\1\end{Bmatrix}\ddot{x}_D+\begin{Bmatrix}-a_1s_1l_1\\a_1c_1l_1\\1\\-s_1l_1\\c_1l_1\\0\\-s_1l_1\\c_1l_1\\0\\0\end{Bmatrix}\varepsilon_1+\begin{Bmatrix}0\\0\\0\\-a_2s_2l_2\\a_2c_2l_2\\1\\-s_2l_2\\c_2l_2\\0\\0\end{Bmatrix}\varepsilon_2+\begin{Bmatrix}0\\0\\0\\0\\0\\0\\-s_{3-\psi-\xi}hg\\c_{3-\psi-\xi}hg\\1\\0\end{Bmatrix}\varepsilon_3+$$

$$+\begin{Bmatrix} -a_1c_1l_1 \\ -a_1s_1l_1 \\ 0 \\ -c_1l_1 \\ -s_1l_1 \\ 0 \\ -c_1l_1 \\ -s_1l_1 \\ 0 \\ 0 \end{Bmatrix}\omega_1^2+\begin{Bmatrix} 0 \\ 0 \\ 0 \\ -a_2c_2l_2 \\ -a_2s_2l_2 \\ 0 \\ -c_2l_2 \\ -s_2l_2 \\ 0 \\ 0 \end{Bmatrix}\omega_2^2+\begin{Bmatrix} 0 \\ 0 \\ 0 \\ 0 \\ 0 \\ 0 \\ -a_3c_{3-\psi-\xi}hg \\ -a_3s_{3-\psi-\xi}hg \\ 0 \\ 0 \end{Bmatrix}\omega_3^2 \tag{1.74}$$

$$\begin{Bmatrix}\omega_2\\ \omega_3\end{Bmatrix}=\begin{bmatrix}\frac{a_{11}l_1}{l_2} & \frac{a_{12}}{l_2}\\ \frac{a_{21}l_1}{h} & \frac{a_{22}}{h}\end{bmatrix}\begin{Bmatrix}\omega_1\\ \dot{x}_D\end{Bmatrix} \tag{1.75}$$

$$\begin{Bmatrix}\varepsilon_2\\ \varepsilon_3\end{Bmatrix}=\begin{bmatrix}\frac{a_{11}l_1}{l_2} & \frac{a_{12}}{l_2}\\ \frac{a_{21}l_1}{h} & \frac{a_{22}}{h}\end{bmatrix}\begin{Bmatrix}\varepsilon_1\\ \ddot{x}_D\end{Bmatrix}+\begin{bmatrix}\frac{b_{11}l_1^2}{l_2} & \frac{b_{12}l_1}{l_2} & \frac{b_{13}}{l_2}\\ \frac{b_{21}l_1^2}{h} & \frac{b_{22}l_1}{h} & \frac{b_{23}}{h}\end{bmatrix}\begin{Bmatrix}\omega_1^2\\ \omega_1\dot{x}_D\\ \dot{x}_D^2\end{Bmatrix} \tag{1.76}$$

$$\{a\}=\begin{Bmatrix}\ddot{x}_1\\ \ddot{y}_1\\ \varepsilon_1\\ \ddot{x}_2\\ \ddot{y}_2\\ \varepsilon_2\\ \ddot{x}_3\\ \ddot{y}_3\\ \varepsilon_3\\ \ddot{x}_D\end{Bmatrix}=\begin{Bmatrix}0\\0\\0\\0\\0\\0\\0\\0\\0\\1\end{Bmatrix}\ddot{x}_D+\begin{Bmatrix}-a_1s_1l_1\\ a_1c_1l_1\\ 1\\ -s_1l_1\\ c_1l_1\\ 0\\ -s_1l_1\\ c_1l_1\\ 0\\ 0\end{Bmatrix}\varepsilon_1+\begin{bmatrix}0 & 0\\ 0 & 0\\ 0 & 0\\ -a_2s_2l_2 & 0\\ a_2c_2l_2 & 0\\ 1 & 0\\ -s_2l_2 & -s_{3-\psi-\xi}hg\\ c_2l_2 & c_{3-\psi-\xi}hg\\ 0 & 1\\ 0 & 0\end{bmatrix}\left(\begin{bmatrix}\frac{a_{11}l_1}{l_2} & \frac{a_{12}}{l_2}\\ \frac{a_{21}l_1}{h} & \frac{a_{22}}{h}\end{bmatrix}\begin{Bmatrix}\varepsilon_1\\ \ddot{x}_D\end{Bmatrix}+\begin{bmatrix}\frac{b_{11}l_1^2}{l_2} & \frac{b_{12}l_1}{l_2} & \frac{b_{13}}{l_2}\\ \frac{b_{21}l_1^2}{h} & \frac{b_{22}l_1}{h} & \frac{b_{23}}{h}\end{bmatrix}\begin{Bmatrix}(\omega_1)^2\\ \omega_1\dot{x}_D\\ (\dot{x}_D)^2\end{Bmatrix}\right)+$$

$$+\begin{Bmatrix} -a_1c_1l_1 \\ -a_1s_1l_1 \\ 0 \\ -c_1l_1 \\ -s_1l_1 \\ 0 \\ -c_1l_1 \\ -s_1l_1 \\ 0 \\ 0 \end{Bmatrix}\omega_1^2+\begin{bmatrix} 0 & 0 \\ 0 & 0 \\ 0 & 0 \\ -a_2c_2l_2 & 0 \\ -a_2s_2l_2 & 0 \\ 0 & 0 \\ -c_2l_2 & -a_3c_{3-\psi-\xi}hg \\ -s_2l_2 & -a_3s_{3-\psi-\xi}hg \\ 0 & 0 \\ 0 & 0 \end{bmatrix}\begin{bmatrix}\left(\frac{a_{11}}{l_2}l_1\right)^2 & 2\frac{a_{11}a_{12}}{l_2^2}l_1 & \left(\frac{a_{12}}{l_2}\right)^2\\ \left(\frac{a_{21}}{h}l_1\right)^2 & 2\frac{a_{21}a_{22}}{h^2}l_1 & \left(\frac{a_{22}}{h}\right)^2\end{bmatrix}\begin{Bmatrix}\omega_1^2\\ \omega_1\dot{x}_D\\ \dot{x}_D^2\end{Bmatrix}= \tag{1.77}$$

$$\{a\}=\begin{Bmatrix}\ddot{x}_1\\ \ddot{y}_1\\ \varepsilon_1\\ \ddot{x}_2\\ \ddot{y}_2\\ \varepsilon_2\\ \ddot{x}_3\\ \ddot{y}_3\\ \varepsilon_3\\ \ddot{x}_D\end{Bmatrix}=\begin{bmatrix} -a_1s_1l_1 & 0\\ a_1c_1l_1 & 0\\ 1 & 0\\ -s_1l_1-a_2s_2a_{11}l_1 & -a_2s_2a_{12}\\ c_1l_1+a_2c_2a_{11}l_1 & a_2c_2a_{12}\\ \frac{a_{11}l_1}{l_2} & \frac{a_{12}}{l_2}\\ -s_1l_1-s_2a_{11}l_1-s_{3-\psi-\xi}hg\frac{a_{21}l_1}{h} & -s_2a_{12}-s_{3-\psi-\xi}hg\frac{a_{22}}{h}\\ c_1l_1+c_2a_{11}l_1+c_{3-\psi-\xi}hg\frac{a_{21}l_1}{h} & c_2a_{12}+c_{3-\psi-\xi}hg\frac{a_{22}}{h}\\ \frac{a_{21}l_1}{h} & \frac{a_{22}}{h}\\ 0 & 1\end{bmatrix}\begin{Bmatrix}\varepsilon_1\\ \ddot{x}_D\end{Bmatrix}+$$

$$+\begin{bmatrix} -a_1c_1l_1 & 0 & 0\\ -a_1s_1l_1 & 0 & 0\\ 0 & 0 & 0\\ -c_1l_1-a_2s_2b_{11}l_1^2 & -a_2s_2b_{12}l_1 & -a_2s_2b_{13}\\ -s_1l_1+a_2c_2b_{11}l_1^2 & a_2c_2b_{12}l_1 & a_2c_2b_{13}\\ \frac{b_{11}l_1^2}{l_2} & \frac{b_{12}l_1}{l_2} & \frac{b_{13}}{l_2}\\ -c_1l_1-s_2b_{11}l_1^2-s_{3-\psi-\xi}hg\frac{b_{21}l_1^2}{h} & -s_2b_{12}l_1-s_{3-\psi-\xi}hg\frac{b_{22}l_1}{h} & -s_2b_{13}-s_{3-\psi-\xi}hg\frac{b_{23}}{h}\\ -s_1l_1+c_2b_{11}l_1^2+c_{3-\psi-\xi}hg\frac{b_{21}l_1^2}{h} & c_2b_{12}l_1+c_{3-\psi-\xi}hg\frac{b_{22}l_1}{h} & c_2b_{13}+c_{3-\psi-\xi}hg\frac{b_{23}}{h}\\ \frac{b_{21}l_1^2}{h} & \frac{b_{22}l_1}{h} & \frac{b_{23}}{h}\\ 0 & 0 & 0\end{bmatrix}\begin{Bmatrix}(\omega_1)^2\\ \omega_1\dot{x}_D\\ (\dot{x}_D)^2\end{Bmatrix}+$$

$$+\begin{bmatrix} 0 & 0 & 0\\ 0 & 0 & 0\\ 0 & 0 & 0\\ \frac{-a_2c_2a_{11}^2l_1^2}{l_2} & -a_2c_2\,2\frac{a_{11}a_{12}}{l_2}l_1 & -a_2c_2\frac{a_{12}^2}{l_2}\\ -\frac{a_2s_2a_{11}^2l_1^2}{l_2} & -a_2s_2\,2\frac{a_{11}a_{12}}{l_2}l_1 & -a_2s_2\frac{a_{12}^2}{l_2}\\ 0 & 0 & 0\\ \frac{-c_2a_{11}^2l_1^2}{l_2}-c_{3-\psi-\xi}hg\left(\frac{a_{21}}{h}l_1\right)^2 & -2c_2\frac{a_{11}a_{12}}{l_2}l_1-2c_{3-\psi-\xi}hg\frac{a_{21}a_{22}}{h^2}l_1 & -c_2\frac{a_{12}^2}{l_2}-c_{3-\psi-\xi}hg\left(\frac{a_{22}}{h}\right)^2\\ -\frac{s_2a_{11}^2l_1^2}{l_2}-s_{3-\psi-\xi}hg\left(\frac{a_{21}}{h}l_1\right)^2 & -2s_2\frac{a_{11}a_{12}}{l_2}l_1-2s_{3-\psi-\xi}hg\frac{a_{21}a_{22}}{h^2}l_1 & -s_2\frac{a_{12}^2}{l_2}-s_{3-\psi-\xi}hg\left(\frac{a_{22}}{h}\right)^2\\ 0 & 0 & 0\\ 0 & 0 & 0\end{bmatrix}\begin{Bmatrix}(\omega_1)^2\\ \omega_1\dot{x}_D\\ (\dot{x}_D)^2\end{Bmatrix}+$$

(1.78)

$$\{a\}=\begin{Bmatrix}\ddot{x}_1\\ \ddot{y}_1\\ \varepsilon_1\\ \ddot{x}_2\\ \ddot{y}_2\\ \varepsilon_2\\ \ddot{x}_3\\ \ddot{y}_3\\ \varepsilon_3\\ \ddot{x}_D\end{Bmatrix}=\begin{bmatrix} -a_1s_1l_1 & 0\\ a_1c_1l_1 & 0\\ 1 & 0\\ -s_1l_1-a_2s_2a_{11}l_1 & -a_2s_2a_{12}\\ c_1l_1+a_2c_2a_{11}l_1 & a_2c_2a_{12}\\ \dfrac{a_{11}l_1}{l_2} & \dfrac{a_{12}}{l_2}\\ -s_1l_1-s_2a_{11}l_1-s_{3-\psi-\xi}hg\dfrac{a_{21}l_1}{h} & -s_2a_{12}-s_{3-\psi-\xi}hg\dfrac{a_{22}}{h}\\ c_1l_1+c_2a_{11}l_1+c_{3-\psi-\xi}hg\dfrac{a_{21}l_1}{h} & c_2a_{12}+c_{3-\psi-\xi}hg\dfrac{a_{22}}{h}\\ \dfrac{a_{21}l_1}{h} & \dfrac{a_{22}}{h}\\ 0 & 1\end{bmatrix}\begin{Bmatrix}\varepsilon_1\\ \ddot{x}_D\end{Bmatrix}+$$

$$+\begin{Bmatrix} -a_1c_1l_1\\ -a_1s_1l_1\\ 0\\ -c_1l_1-\dfrac{a_2s_2b_{11}}{l_1^2}-a_2c_2l_2\left(\dfrac{a_{11}}{l_2}l_1\right)^2\\ -s_1l_1+\dfrac{a_2c_2b_{11}}{l_1^2}-a_2s_2l_2\left(\dfrac{a_{11}}{l_2}l_1\right)^2\\ \dfrac{b_{11}}{l_2l_1^2}\\ -c_1l_1-\dfrac{s_2b_{11}}{l_1^2}-s_{3-\psi-\xi}hg\dfrac{b_{21}}{l_1^2h}-c_2l_2\left(\dfrac{a_{11}}{l_2}l_1\right)^2-c_{3-\psi-\xi}hg\left(\dfrac{a_{21}}{h}l_1\right)^2\\ -s_1l_1+\dfrac{c_2b_{11}}{l_1^2}+c_{3-\psi-\xi}hg\dfrac{b_{21}}{l_1^2h}-s_2l_2\left(\dfrac{a_{11}}{l_2}l_1\right)^2-s_{3-\psi-\xi}hg\left(\dfrac{a_{21}}{h}l_1\right)^2\\ \dfrac{b_{21}}{l_1^2h}\\ 0\end{Bmatrix}\omega_1^2+$$

$$+\begin{Bmatrix} 0\\ 0\\ 0\\ -\dfrac{a_2s_2b_{12}}{l_1}-a_2c_2l_2\,2\dfrac{a_{11}a_{12}}{l_2^2}l_1\\ \dfrac{a_2c_2b_{12}}{l_1}-a_2s_2l_2\,2\dfrac{a_{11}a_{12}}{l_2^2}l_1\\ \dfrac{b_{12}}{l_1l_2}\\ -\dfrac{s_2b_{12}}{l_1}-s_{3-\psi-\xi}hg\dfrac{b_{22}}{l_1h}-2c_2l_2\dfrac{a_{11}a_{12}}{l_2^2}l_1-2c_{3-\psi-\xi}hg\dfrac{a_{21}a_{22}}{h^2}l_1\\ \dfrac{c_2b_{12}}{l_1}+c_{3-\psi-\xi}hg\dfrac{b_{22}}{l_1h}-2s_2l_2\dfrac{a_{11}a_{12}}{l_2^2}l_1-2s_{3-\psi-\xi}hg\dfrac{a_{21}a_{22}}{h^2}l_1\\ \dfrac{b_{22}}{l_1h}\\ 0\end{Bmatrix}\omega_1\dot{x}_D+$$

$$+\begin{Bmatrix} 0 \\ 0 \\ 0 \\ -a_2c_2l_2\left(\frac{a_{12}}{l_2}\right)^2 - a_2s_2b_{13} \\ -a_2s_2l_2\left(\frac{a_{12}}{l_2}\right)^2 + a_2c_2b_{13} \\ \frac{b_{13}}{l_2} \\ -c_2l_2\left(\frac{a_{12}}{l_2}\right)^2 - c_{3-\psi-\zeta}hg\left(\frac{a_{22}}{h}\right)^2 - s_2b_{13} - s_{3-\psi-\zeta}hg\frac{b_{23}}{h} \\ -s_2l_2\left(\frac{a_{12}}{l_2}\right)^2 - s_{3-\psi-\zeta}hg\left(\frac{a_{22}}{h}\right)^2 + c_2b_{13} + c_{3-\psi-\zeta}hg\frac{b_{23}}{h} \\ \frac{b_{23}}{h} \\ 0 \end{Bmatrix}\dot{x}_D^2 \tag{1.79}$$

Finally it can be written:

$$\{a\} = \left[\{A_1\}\{A_2\}\right]\begin{Bmatrix}\varepsilon_1 \\ \ddot{x}_D\end{Bmatrix} + \left[\{B_1\}\{B_2\}\{B_3\}\right]\begin{Bmatrix}(\omega_1)^2 \\ (\omega_1\dot{x}_D) \\ (\dot{x}_D)^2\end{Bmatrix} = [A]\begin{Bmatrix}\varepsilon_1 \\ \ddot{x}_D\end{Bmatrix} + [B]\begin{Bmatrix}(\omega_1)^2 \\ (\omega_1\dot{x}_D) \\ (\dot{x}_D)^2\end{Bmatrix} \tag{1.80}$$

where the notations for the matrix $\{A_1\}$, $\{A_2\}$, $\{B_1\}$, $\{B_2\}$, $\{B_3\}$, $[A] = \left[\{A_1\}\{A_2\}\right]$, $[B] = \left[\{B_1\}\{B_2\}\{B_3\}\right]$ are obvious.

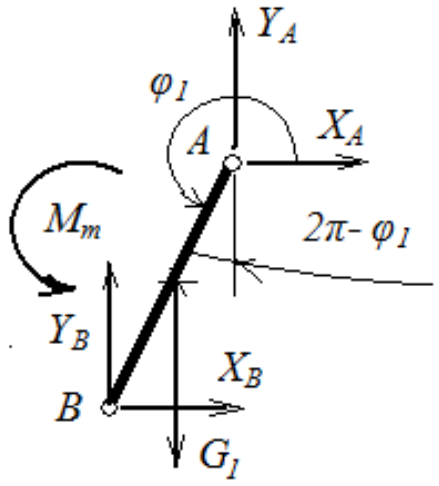

Figure 1.14. Free body diagram of the crank

The motion equations for the crank:

$$m_1\ddot{x}_1 = X_A + X_B$$

$$m_1\ddot{y}_1 = Y_A + Y_B - G_1$$

$$J_1\varepsilon_1 = M_m - X_A a_1 l_1 \cos(\frac{3\pi}{2} - \varphi_1) + Y_A a_1 l_1 \sin(\frac{3\pi}{2} - \varphi_1) + X_B (1 - a_1) l_1 \cos(\frac{3\pi}{2} - \varphi_1) - Y_B (1 - a_1) l_1 \sin(\frac{3\pi}{2} - \varphi_1) \quad (1.81)$$

The last relation become, after some calculus:

$$J_1\varepsilon_1 = M_m + X_A a_1 l_1 s_1 - Y_A a_1 l_1 c_1 - X_B (1 - a_1) l_1 s_1 + Y_B (1 - a_1) c_1 \quad (1.82)$$

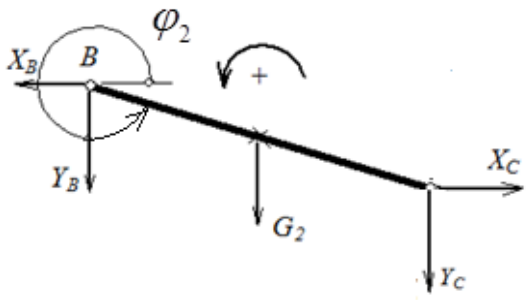

Figure 1.15. Free body diagram of the rod

The motion equations for the rod:

$$m_2\ddot{x}_2 = -X_B + X_C$$

$$m_2\ddot{y}_2 = -Y_B - Y_C - G_2 \quad (1.83)$$

$$J_2\varepsilon_2 = X_B a_2 l_2 \sin(2\pi - \varphi_2) + Y_B a_2 l_2 \cos(2\pi - \varphi_2) + \\ + X_C (1 - a_2) l_2 \sin(2\pi - \varphi_2) + Y_C (1 - a_2) l_2 \cos(2\pi - \varphi_2)$$

The last equation become:

$$J_2\varepsilon_2 = -X_B a_2 l_2 s_2 + Y_B a_2 l_2 c_2 - X_C (1 - a_2) l_2 s_2 - Y_C (1 - a_2) l_2 c_2 \quad (1.84)$$

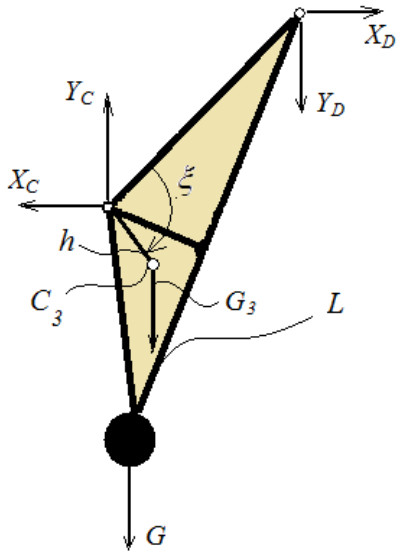

Figure 1.16. Free body diagram of the pendulum

The motion equations for the pendulum:

$$(m_3 + M_3)\ddot{x}_3 = X_D - X_C$$

$$(m_3 + M_3)\ddot{y}_3 = -Y_D + Y_C - G_3 - G$$

$$J_3\varepsilon_3 = -X_D y_D - Y_D x_D + X_C \cdot y_C - Y_C \cdot x_C + G(-x_D + Lc_3) \tag{1.85}$$

where:

$$x_D = -hg\cos(\xi - \varphi_3 + \psi) + h\cos(\varphi_3 - \psi) \tag{1.86}$$

$$y_D = hg\sin(\xi - \varphi_3 + \psi) + hs\sin(\varphi_3 - \psi) \tag{1.87}$$

$$x_C = -hg\cos(\xi - \varphi_3 + \psi) \tag{1.88}$$

$$y_C = hg\sin(\xi - \varphi_3 + \psi) \tag{1.89}$$

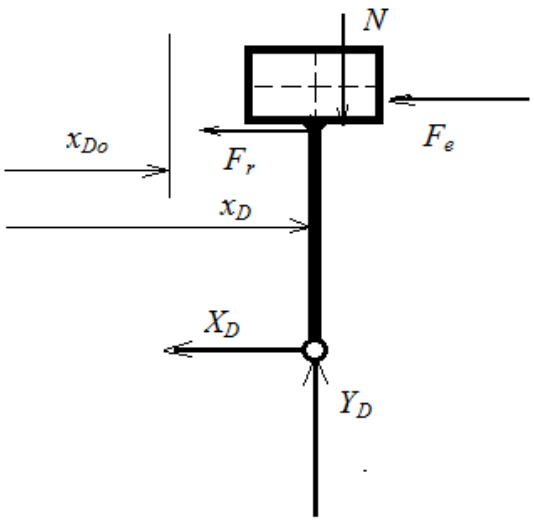

Figure 1.17. Free body diagram for the slider

$$m_D\ddot{x}_D = -X_D - F_r\,\mathrm{sgn}(\dot{x}_D) - k(x_D - x_{Do}) \tag{1.90}$$

We denote:

$$[J] = \begin{bmatrix} m_1 & & & & & & & & & \\ & m_1 & & & & & & & & \\ & & J_1 & & & & 0 & & & \\ & & & m_2 & & & & & & \\ & & & & m_2 & & & & & \\ & & & & & J_2 & & & & \\ & & & & & & m_3 & & & \\ & & 0 & & & & & m_3 & & \\ & & & & & & & & J_3 & \\ & & & & & & & & & m_D \end{bmatrix}$$

Acceleration vector system (1.17, 1.18) contains accelerations centers of mass of elements AB, BC, CD, angular acceleration of the rod and linear acceleration slider D. Corresponding generalized coordinates vector the generalized forces vector is considered:

$$\{Q\}=\begin{Bmatrix} X_A+X_B \\ Y_A+Y_B-G_1 \\ M_m+X_A a_1 l_1 s_1-Y_A a_1 l_1 c_1-X_B(1-a_1)l_1 s_1+Y_B(1-a_1)c_1 \\ -X_B+X_C \\ -Y_B-Y_C-G_2 \\ -X_B a_2 l_2 s_2+Y_B a_2 l_2 c_2-X_C(1-a_2)l_2 s_2-Y_C(1-a_2)l_2 c_2 \\ X_D-X_C \\ -Y_D+Y_C-G_3-G \\ -X_D y_D-Y_D x_D+X_C\cdot y_C-Y_C\cdot x_C+G(-x_D+Lc_3) \\ -X_D-F_r\,\mathrm{sgn}(\dot{x}_D)-k(x_D-x_{Do}) \end{Bmatrix} \tag{1.91}$$

The motion equations can be written in a compact form:

$$[m]\{a\}=\{Q\} \tag{1.92}$$

If in rel. 1.92 the vector of the previously determined acceleration is introduced, is obtained:

$$[m]\left(\left[\{A_1\}\{A_2\}\right]\begin{Bmatrix}\varepsilon_1\\ \ddot{x}_D\end{Bmatrix}+\left[\{B_1\}\{B_2\}\{B_3\}\right]\begin{Bmatrix}\omega_1^2\\ \omega_1\dot{x}_D\\ \dot{x}_D^2\end{Bmatrix}\right)=\{Q\} \tag{1.93}$$

To eliminate the liaison forces it must to premultiply the rel 1.93 with:

$$\begin{bmatrix}\{A_1\}^T\\ \{A_2\}^T\end{bmatrix}$$

and it obtains:

$$\begin{bmatrix}\{A_1\}^T\\ \{A_2\}^T\end{bmatrix}[m]\left(\left[\{A_1\}\{A_2\}\right]\begin{Bmatrix}\varepsilon_1\\ \dot{x}_D\end{Bmatrix}+\left[\{B_1\}\{B_2\}\{B_3\}\right]\begin{Bmatrix}\omega_1^2\\ \omega_1\dot{x}_D\\ \dot{x}_D^2\end{Bmatrix}\right)=\begin{bmatrix}\{A_1\}^T\\ \{A_2\}^T\end{bmatrix}\{Q\} \tag{1.94}$$

If calculations are made it results:

$$\begin{bmatrix}\{A_1\}^T[m]\{A_1\} & \{A_1\}^T[m]\{A_2\}\\ \{A_2\}^T[m]\{A_1\} & \{A_2\}^T[m]\{A_2\}\end{bmatrix}\begin{Bmatrix}\varepsilon_1\\ \ddot{x}_D\end{Bmatrix}+$$

$$+\begin{bmatrix}\{A_1\}^T[m]\{B_1\} & \{A_1\}^T[m]\{B_2\} & \{A_1\}^T[m]\{B_3\}\\ \{A_2\}^T[m]\{B_1\} & \{A_2\}^T[m]\{B_2\} & \{A_2\}^T[m]\{B_3\}\end{bmatrix}\begin{Bmatrix}\omega_1^2\\ \omega_1\dot{x}_D\\ \dot{x}_D^2\end{Bmatrix}=\begin{bmatrix}\{A_1\}^T\{Q\}\\ \{A_2\}^T\{Q\}\end{bmatrix} \tag{1.95}$$

We denote:

$$Q^e = [A]^T \{Q\} =$$

$$= \begin{bmatrix} -a_1 s_1 l_1 & 0 \\ a_1 c_1 l_1 & 0 \\ 1 & 0 \\ -s_1 l_1 - a_2 s_2 a_1 l_1 & -a_2 s_2 a_{12} \\ c_1 l_1 + a_2 c_2 a_1 l_1 & a_2 c_2 a_{12} \\ \frac{a_1 l_1}{l_2} & \frac{a_{12}}{l_2} \\ -s_1 l_1 - s_2 a_1 l_1 - s_{3-\psi-\xi} hg \frac{a_2 l_1}{h} & -s_2 a_{12} - s_{3-\psi-\xi} hg \frac{a_{22}}{h} \\ c_1 l_1 + c_2 a_1 l_1 + c_{3-\psi-\xi} hg \frac{a_2 l_1}{h} & c_2 a_{12} + c_{3-\psi-\xi} hg \frac{a_{22}}{h} \\ \frac{a_2 l_1}{h} & \frac{a_{22}}{h} \\ 0 & 1 \end{bmatrix}^T \begin{Bmatrix} X_A + X_B \\ Y_A + Y_B - G_1 \\ M_m + X_A a_1 l_1 s_1 - Y_A a_1 l_1 c_1 - X_B (1-a_1) l_1 s_1 + Y_B (1-a_1) c_1 \\ -X_B + X_C \\ -Y_B - Y_C - G_2 \\ -X_B a_2 l_2 s_2 + Y_B a_2 l_2 c_2 - X_C (1-a_2) l_2 s_2 - Y_C (1-a_2) l_2 c_2 \\ X_D - X_C \\ -Y_D + Y_C - G_3 - G \\ -X_D xx_D - Y_D yy_D + X_C \cdot xx_C - Y_C \cdot yy_C + G(xx_D - Lc_3) \\ -X_D - F_r \operatorname{sgn}(\dot{x}_D) - k(x_D - x_{Do}) \end{Bmatrix} =$$

$$= \begin{Bmatrix} M_m - G_1 a_1 c_1 l_1 - G_2 (c_1 l_1 + a_{11} a_2 c_2 l_1) - (G_3 + G)(c_1 l_1 + a_{11} c_2 l_1 + a_{21} l_1 c_{3pe} hg / h) + G(xx_D - Lc_3) \frac{a_{21} l_1}{h} \\ - G_2 a_{12} a_2 c_2 - (G_3 + G)(a_{12} c_2 + a_{22} hg c_{3pe} / h) + G(xx_D - Lc_3) \frac{a_{22}}{h} - F_r \operatorname{sgn}(\dot{x}_D) - k(x_D - x_{Do}) \end{Bmatrix} \tag{1.96}$$

and:

$$X = \begin{Bmatrix} \varphi_1 \\ x_D \end{Bmatrix} \quad ; \quad \dot{X} = Y \tag{1.97}$$

then it results the nonlinear system of differential equations:

$$\begin{Bmatrix} \varepsilon_1 \\ \ddot{x}_D \end{Bmatrix} = \{\dot{Y}\} =$$

$$= -\begin{bmatrix} \{A_1\}^T [m] \{A_1\} & \{A_1\}^T [m] \{A_2\} \\ \{A_2\}^T [m] \{A_1\} & \{A_2\}^T [m] \{A_2\} \end{bmatrix}^{-1} \begin{bmatrix} \{A_1\}^T [m] \{B_1\} & \{A_1\}^T [m] \{B_2\} & \{A_1\}^T [m] \{B_3\} \\ \{A_2\}^T [m] \{B_1\} & \{A_2\}^T [m] \{B_2\} & \{A_2\}^T [m] \{B_3\} \end{bmatrix} \begin{Bmatrix} (\omega_1)^2 \\ (\omega_1 \dot{x}_D) \\ (\dot{x}_D)^2 \end{Bmatrix} +$$

$$+ \begin{bmatrix} \{A_1\}^T [m] \{A_1\} & \{A_1\}^T [m] \{A_2\} \\ \{A_2\}^T [m] \{A_1\} & \{A_2\}^T [m] \{A_2\} \end{bmatrix}^{-1} \begin{bmatrix} \{A_1\}^T \{Q\} \\ \{A_2\}^T \{Q\} \end{bmatrix} \tag{1.98}$$

The following will be performed integrations for some situations to check how the integration subroutines work.

Input data: l_1=0.1; l_2=0.4; l3=0.3;a_1=0.5;a_2=0.5;a_3=1.5;L_c=2;g=10;m1=1;m2=4; m_3=10; J_1=0.066;J_2=0.05; M_m=0.2 ;F_r=0.25; g=10; z_0 = 4.1888 3.0000 10.0000 1.0000; t_0=0. With

the initial conditions Z_0=[pi+pi/6 3 10 0]; t_{final} =20; are obtained, after integration, following results (represented in a series of graphs):

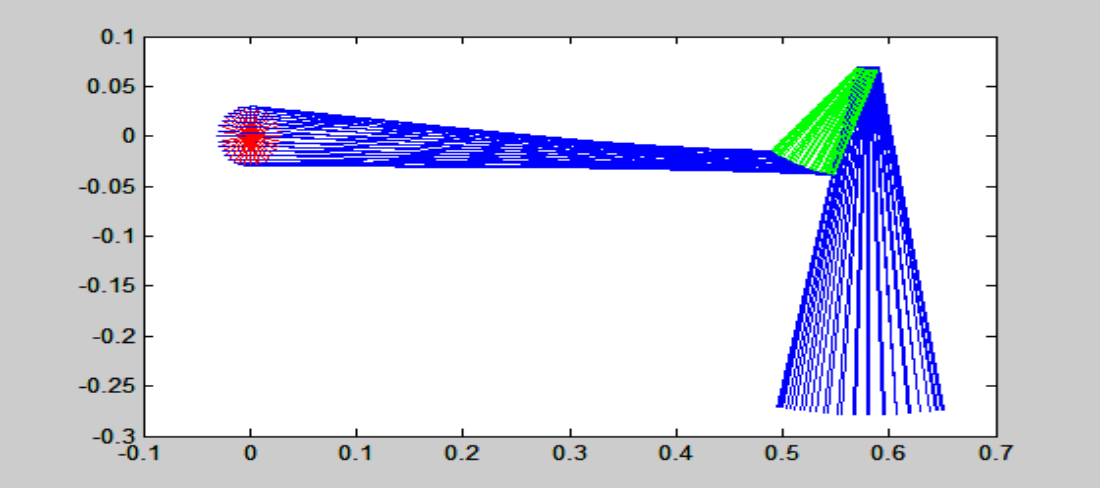

Figure 1.18. Sketch of the motion of the two degree of freedom system for the angular speed 160 rot./min

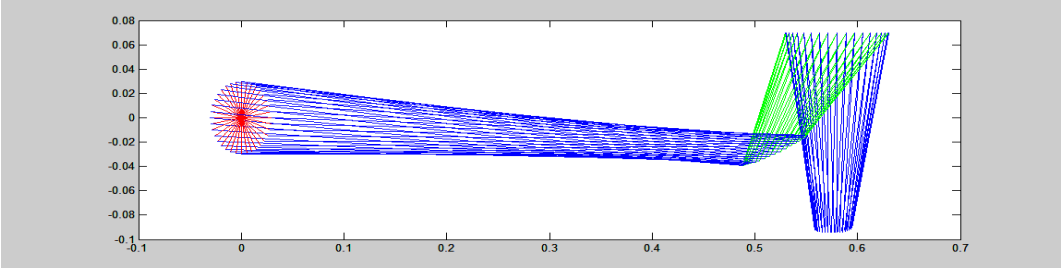

Figure 1.19. Sketch of the motion of the two degree of freedom system for the angular speed 190 rot./min

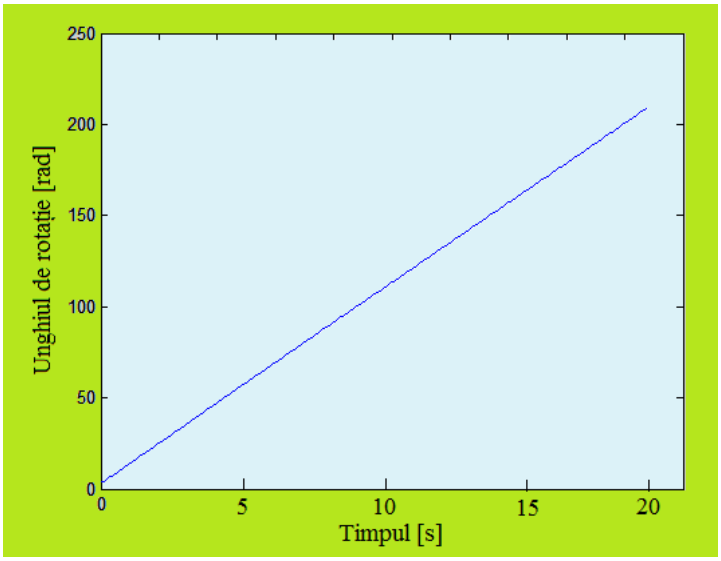

Figure 1.20. Rotation angle of the crank for an integration time t_{final}= 20 sec

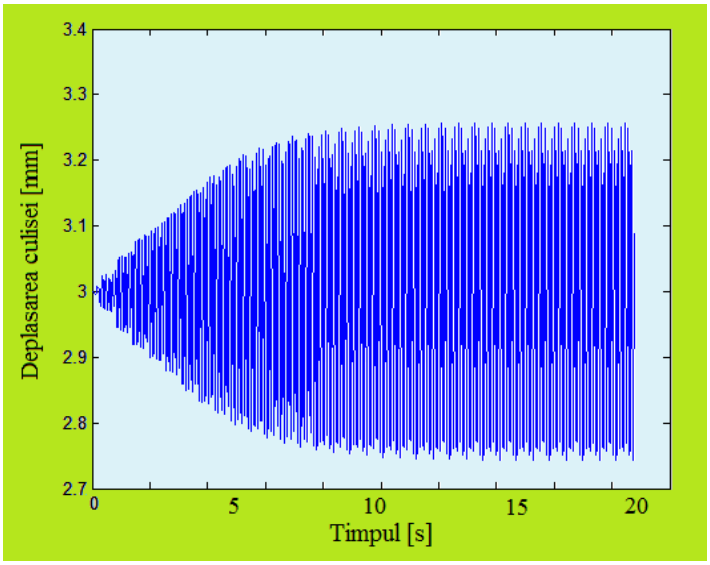

Figure 1.21. Displacement of the slider for t_{final} = 20 sec

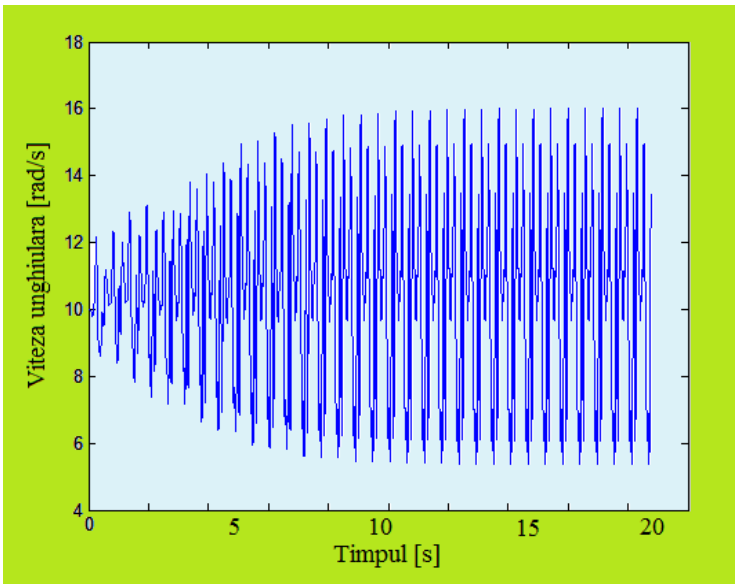

Figure 1.22. Angular velocity of the Time [s] crank for t_{final} = 20 sec

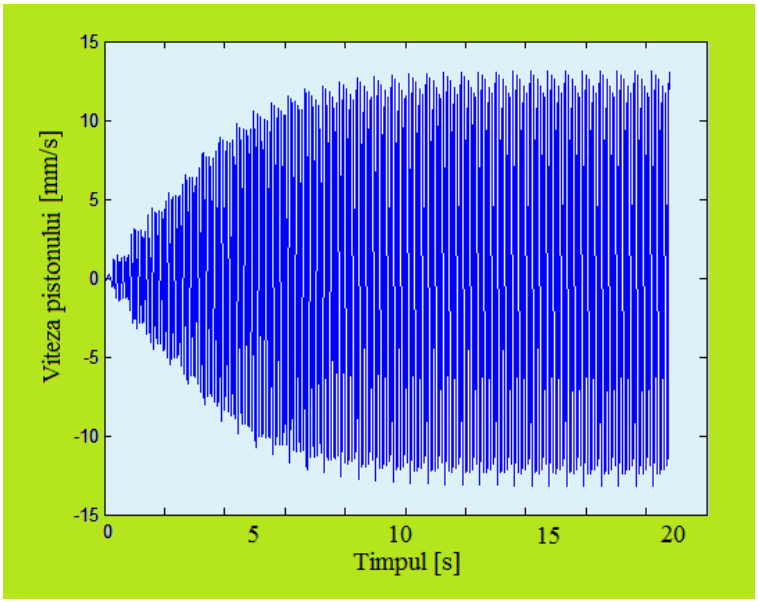

Figure 1.23. Slider velocity [mm/s] for t_{final} = 20 sec

If t_{final}=30 similar graphs are obtained, resulting a good stability of the matlab integration subroutine used (ode23).

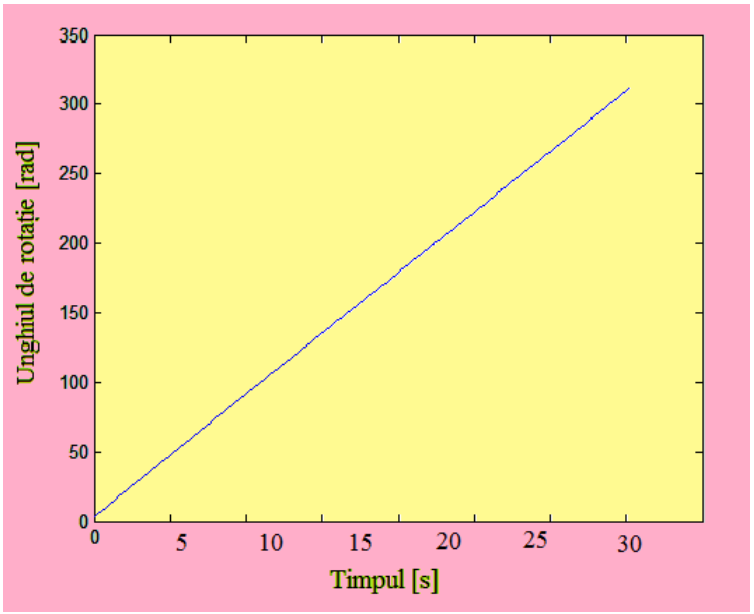

Figure 1.24. Rotation angle of the crank for t_{final} = 30 sec

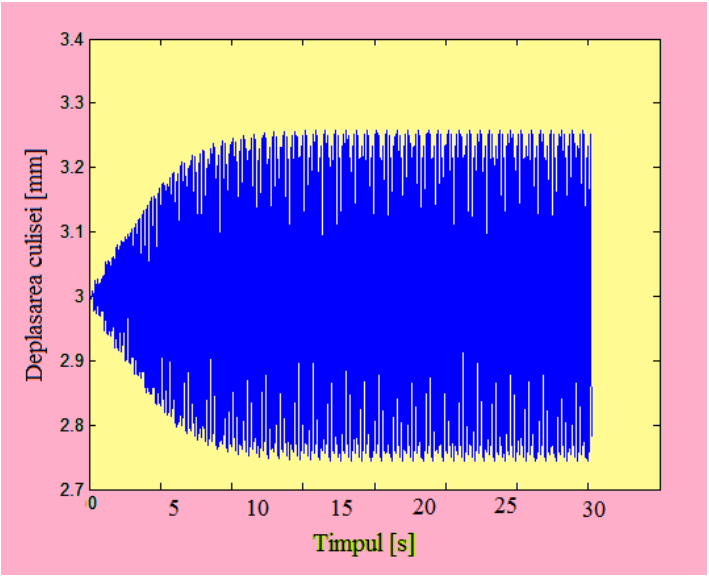

Figure 1.25. Slider displacement for tfinal = 30 sec

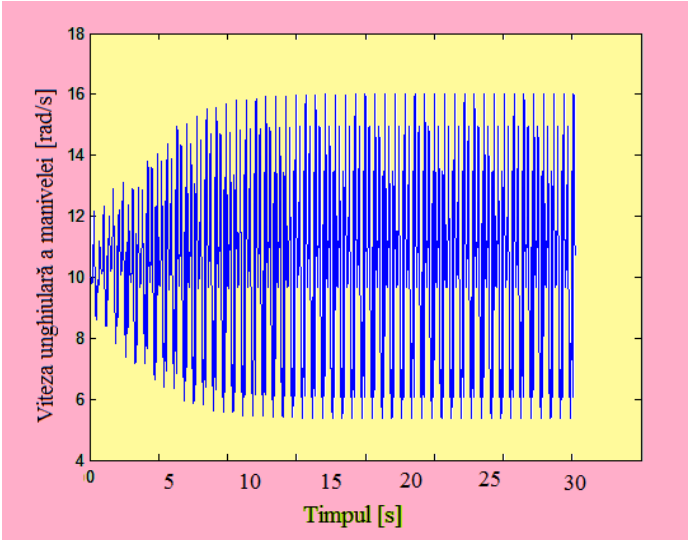

Figure 1.26. Slider velocity for t_{final} = 30 sec

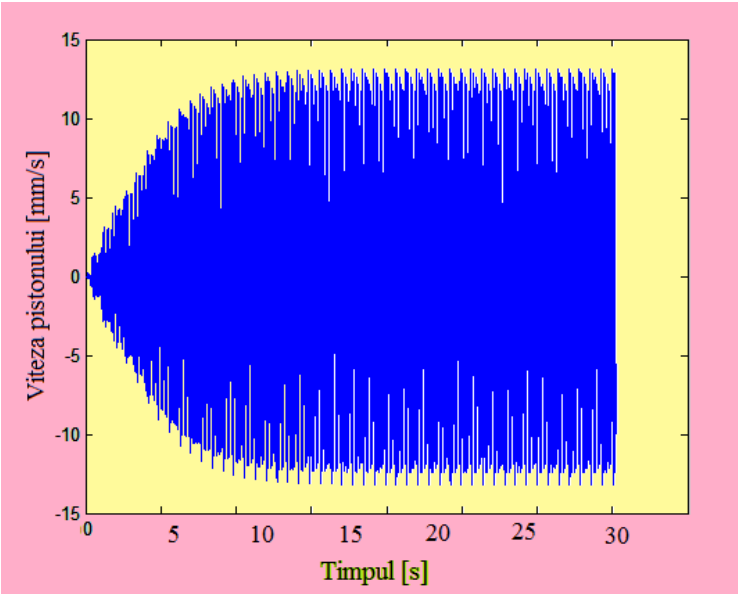

Figure 1.27. Angular velocity of the crank for t_{final} = 30 sec

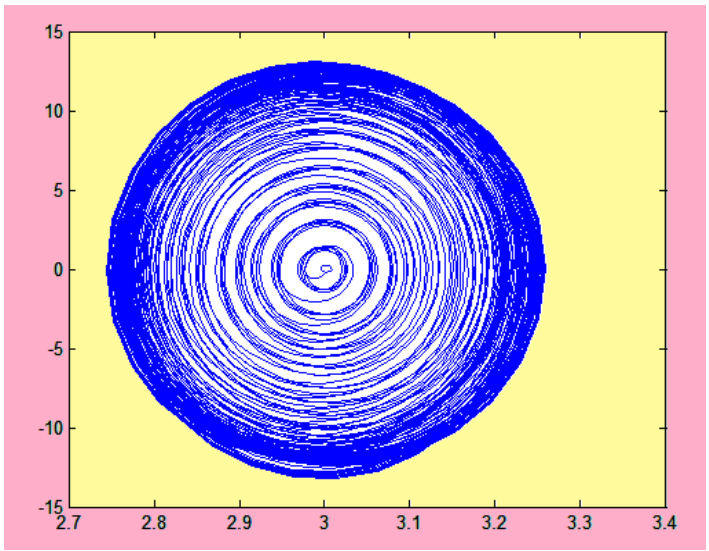

Figure 1.28. Motion representation in the phase space

With the input data: l_1=0.1; l_2=0.4; l_3=0.3;a_1=0.5;a_2=0.5;a_3=1.5;L_c=2;g=10;m_1=1; m_2=4; m_3=10; J_1=0.066; J_2=0.05; M_m=0.2 ;F_r=0.25; g=10; z_0 = 4.1888 3.0000 10.0000 1.0000; t_0=0; t_{final}=200; following representations are obtained by integrating the equations of motion:

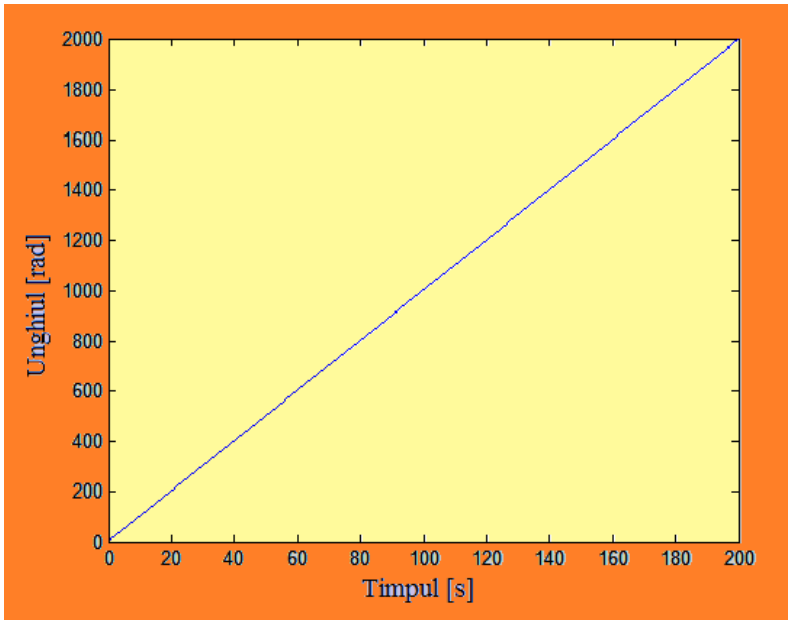

Figure 1.29. Rotation angle of crank for t_{final} = 200 sec

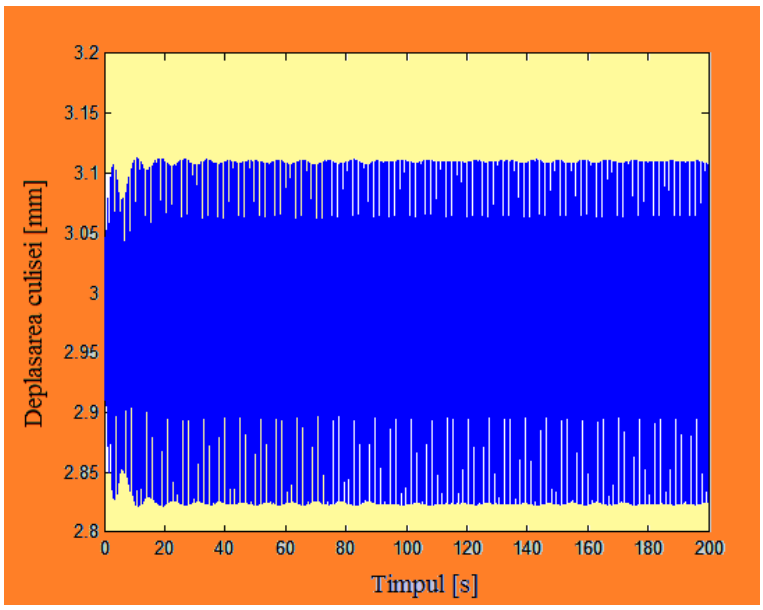

Figure 1.30. Slider displacement for t_{final} = 200 sec

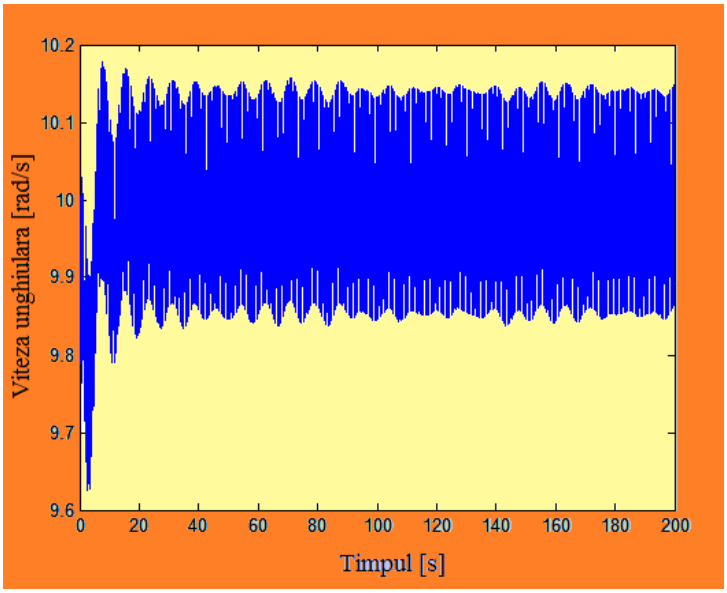

Figure 1.31. Slider velocity for t_{final} = 200 sec

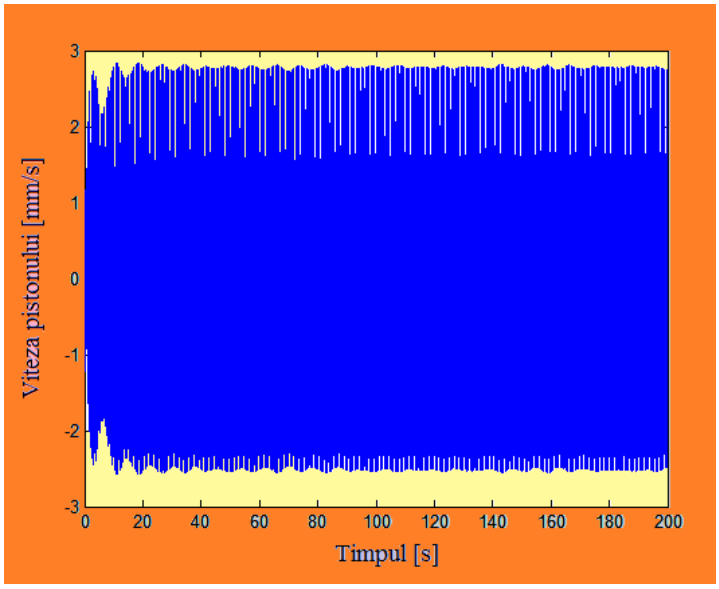

Figure 1.32. Angular velocity of the crank for t_{final} = 200 sec

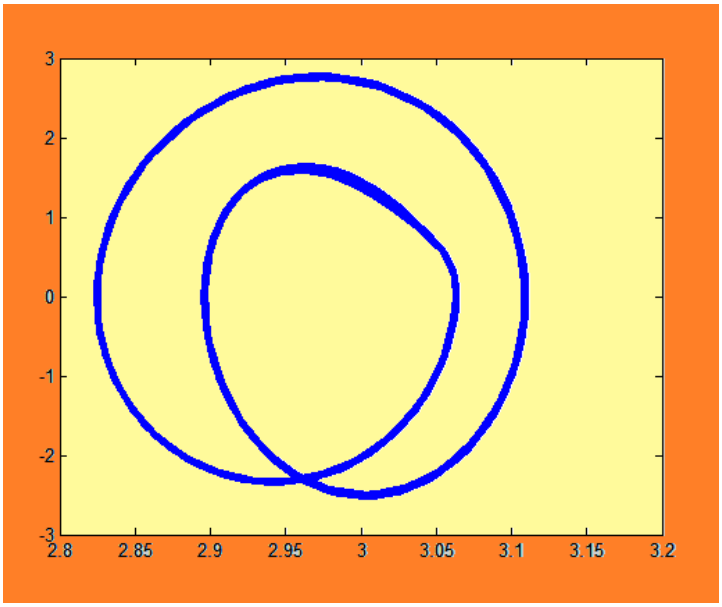

Figure 1.33 Slider motion representation in the phase space

From the graphs above it can be seen that there is a stable integration process for long intervals. In addition to checking subroutines were used to integrate data sets chosen with consideration that could pose problems of integration but after running the program proved that poses no such problems.

The proposed system is a system with two degrees of freedom. As a result the system of differential equations and algebraic (DAE) which is obtained when using the fundamental theorems of dynamics will be made after removing the reactions of two second order differential equations. Integrating this system of equations can lead to numerical stability issues due to high complexity of the system.

We tried several subroutines integration of MATLAB programming environment and found ode23 subroutine has the best behavior. To study the stability of the integration process has sought a quasi stable operating regime and became integration time becoming longer, to determine how long rounded errors lead to instability of the solution. For the latter presented final integration time of 200 s was chosen. This yields stable results.

The problem now becomes processing time of the program. Therefore it can be concluded that the model used is correct and numerical integration subroutine ode23 provide relevant results.

1.6. Experimental confirmation of the theoretical results

1.6.1 The experimental method used in measurements

In order to performhigh-precisiontestsand also useful in verifying and validating accomplished models,I have used an optical recording method of the movement,which provides the opportunity for measurement sunder dynamic loading.

Dynamic analysis of the proposed mechanic small owed the numerical determination of the lawof motion ofthe elements of studied multibody system and the proposed experimental method will serve to validate these numerical results.

1.6.2. The AOS high-speed video camera

Now a days, the current method based on motion analysis using a motion capture system is a particularly efficient and high perspective one. In the Department of Mechanical Engineering, Research Center C02B-Numerical Simulation, Testing and Mechanics of Materials, there is such amotion capture system, consisting of two major components:

- Hardware, represented by video equipment and elements necessary to equip the system, particularly useful for proper operation;
- Software, represented by the applications in which in formation in the video recorded by the camera are processed and made into a form to allow digitize data.

It should be noted the fact that the presenting results is related to the processing part, practically the software used formotion analysis will give a presentation of the results that will be satisfactory from the thesis point of view.

The conditions that make possible the records and the control elements that are required for the proper and efficient work of the system, must meet certain aspects. Thus, the place where the camera will capture the mechanism motion must have good lighting, in order to extract information from videos.

The camera (Fig.1.34) will be mounted on a fixed support and perpendicular to the displacement pump, at a height that should ween sure that the entire mechanism is capture the video.Important to note is the fact that with decreasing distance from the camera position, increases the system efficiency be ingnecessary to find the right balance between the duration of the operation mechanism, that should be sufficient, as well as a small enough distance from the filmed mechanism to not loss from information [AOS07]; [MIH11].

a) The AOS high-speed video camera

b) Lamp light system Elinchrom (1000V, 230W)

Figure 1.34

The motion analysis systems can be classified in accordance with the work, existing two main methods, namely a motion capture method which markers are used and a method in which the markers are not used. In the first method, certain key points are considered to apply markers who se movementis captured and analyzed over time. In the case of the second method, the free of markers method, segments of the moving mechanism considered of interest are captured and analyzed. I have considered it appropriate to use the method with markers for the present research work.

The equipment used is well suited for the records that we want to do as it can ensure shooting in dark surroundings with very good accuracy.

In analyzing the motion with markers, the basic idea is to track the movement of a marker attached to a particular point of interest on the mechanism and then, the trajectory of that point will be extracted and analyzed by methods that correspond to the desired out come to be achieved. A motion capture software will there fore be able to follow the path of a marker over the entiremotion and then to provide at least a list of coordinates of the marker over time, coordinates that define this trajectory. Below is presented how such an application performs these operations.

The first step is to get the film, taken from the camera. It is then loaded into the application of the worked motion analysis and the operator or the person that performs the motion analysis sets the marker's zone. The establishment of this area and how the application will follow it in time are the essential elements for a practical and effective analysis of the motion capture.

Typically, the software will track a pixel area, established by the operator, which ideally contains the area of interest as well as "different" pixels around the area of interest. "Different" pixels refers to pixels of different color against the pixel sof the marked area of interest. In fact, the application intended this composition of pixels along the motion but usually the coordinates of a single pixel too, in the middle of this area belonging to the area of interest. These coordinates will be then obtained as the marker or area of interest coordinates.

The most important factor for such an applicationis the ability to track,with as high precision, this pixels area defined by the user. This factor depends both on the application

quality and of the operator's skill to define a suitable area of interest, skill that will come with experience in use. Also, another feature of interest is the application possibility to ad just the area of interest, frame by frame. Initially, the first area of interest is chosen from the first frame ofthe video, which will become the reference frame for motion. Sometimes, however, the pixels in the area of interes thas under gone major changes during motion, and where the reference frame work would remain the initial one, the area would be lost. Therefore, some applications provide the opportunity that for then-frame, the reference frame should ben-1.

The software that will work to achieve the goals of the thesis,will be able to take data as they are captured by the camera, i.e.in the form of video and also will then have the possibility to process these data by simple methods. Also the final format in which the data are obtained must be one in which data are presented directly, automatically, in a format similar to the ones used by spread sheet applications–(Exceltables).

In view of the above considerations, for the experimental research with in this thesis , the Adobe After Effects have been used, due to:

- Efficiency in terms of how motion is treated, the method of markers recognition and accuracy with which the trajectory of a marker is recognized;
- Accuracy in terms of tracking the trajectory according to several criteria (brightness,color intensity, etc.), but also influence certain aspects of external conditions in which the capture is carried out (brightness, the distance at which the motion is captured);
- The extent to which the results of the application are further processed to obtain the dimensions of the motion parameters that are analyzed in the thesis.

The High Speed Video Camera AOSX-PRI, with a small size, is able to achieve a fairly good accuracy, a sufficient number of records-frames / second-to capture the mechanism motion. Also AOSX-PRI camcorders equipped with an accessory "trigger mechanism" that can replace the command in the software's start recording.

The camera captures images very high speed allowing them to alow speed play back via software(AOS Imaging Studio LIGHT) .These selections can be made only when the camera is connected to turned laptop and the records being started when all LEDs camera control panel are green. On the other hand, the control panel of Imaging Studio Light application is found at the AOS camera also (Fig.1.35).

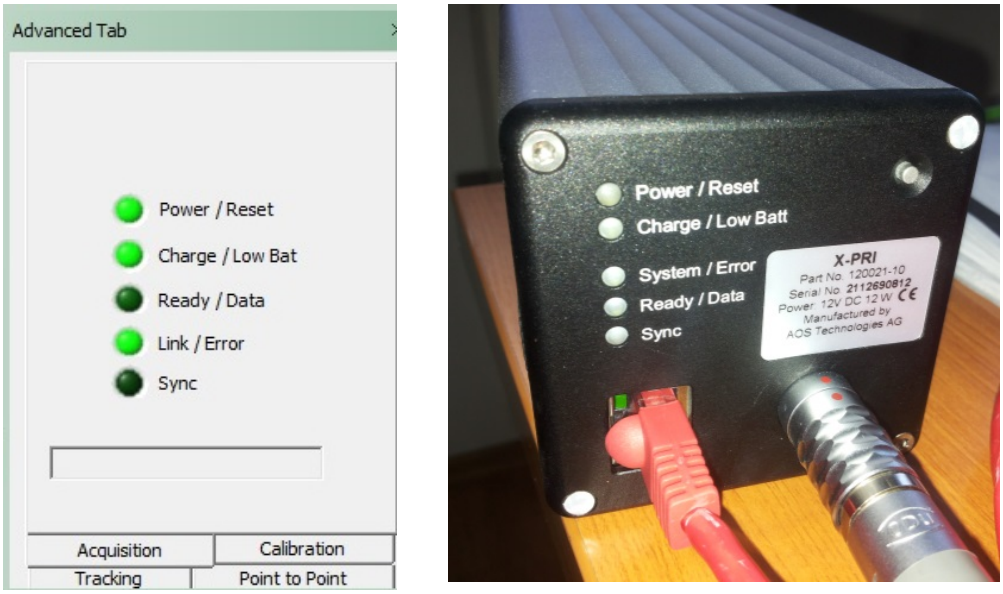

a) Control panel of Imaging Studio Light

b) AOS X-PRI camera

Figure 1.35

Before the actual start of the video footage, the required parameters are established, i.e. the number of frames/second from the "Setting" submenu but also the speed and footage resolution, taken into account that a higher recording time can be obtained with a lower resolution. These last parameters are fixed from the "Camera Setup" menu (Fig.1.36, Fig.1.37).

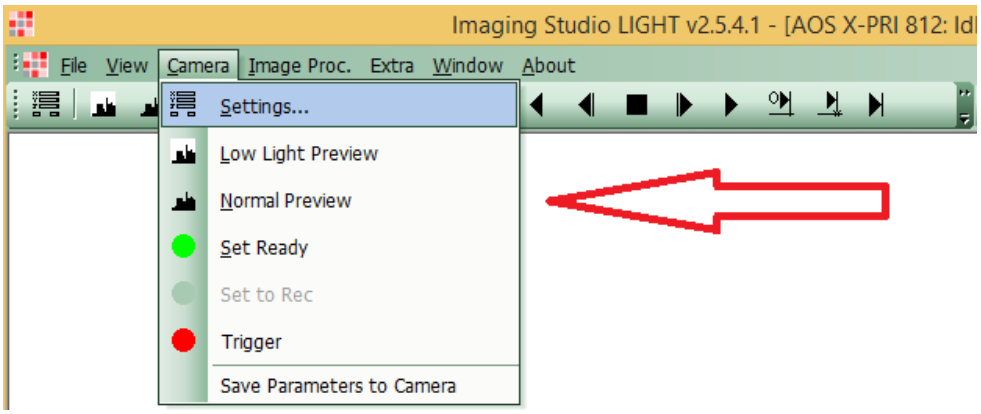

Figure 1.36. Accessing camera settings in AOS Imaging Studio LIGHT software

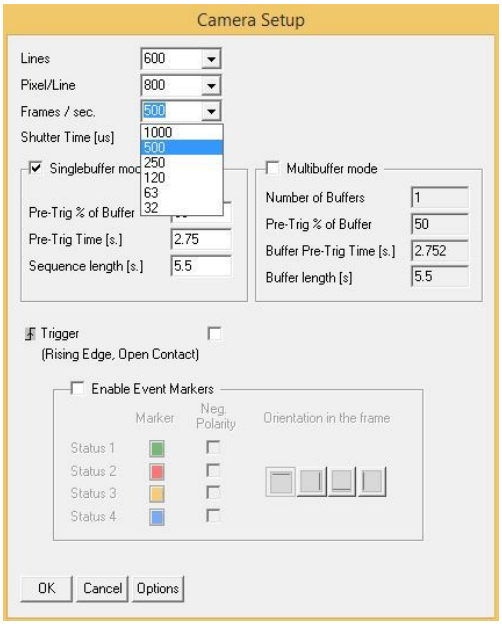

Figure 1.37. Setting the capture of image

Brightness and focal length have been manually adjusted by turning the rings located on lens, in relation to existing natural light intensity at that time and the resulting image sharpness. These setting are indicated to be made when ever the camera position or lighting is changed.

The nextstep is to capture shooting by selecting the Ready Set button, from the Camera Toolbar, followed by accessing the Trigger button, from the same bar or using the manually trigger mechanism. So, the camera takes records with fixed leng the stablished by software, followed by a temporary data storage, but for final storage of shooting for later use as needed, in the bottom panel of the window can be found working tools necessary to adjust shooting in terms of their duration (Fig.1.38).

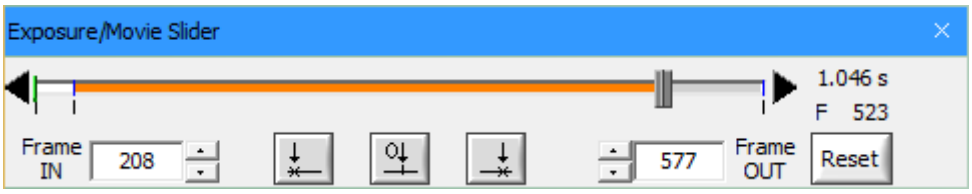

Figure 1.38. The toolbarused to adjust theduration ofshooting

AOS software allows saving shootings in acommonly (.avi) video format being indispensable heir decreasing as duration or their compression. This format has been used because of its compatibility with the application necessary to obtain experimental data. Subsequently indicating the locationin which they are saved, the software displays an unloading confirmation message, this message represents the end stage capture of those shootings. Thus, is the case for each new film, existing the possibility of their access at anytime via soft ware and a new adjustment if necessary.

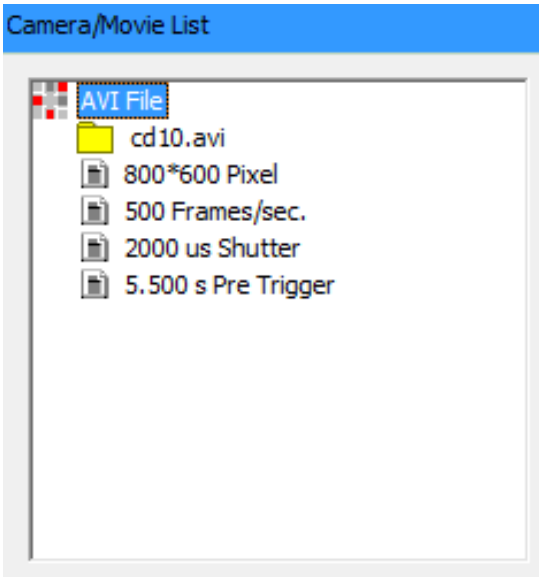

Figure 1.39. Selection from AOS softw are regarding the shooting characteristics

1.6.1. Obtaining experimental data

Next will be presented in detail the process of obtaining and processing experimental data, the computing mode and obtained results.

After fulfilling the conditions for the experiment, the markers are fixed on mechanism after which the mechanism is recorded at different shooting modes, each mode (transformer-rectifier indication) being recorded on the own video. Markers will be centered on the main pump rod as well as on joints mechanism (Fig.1.40).

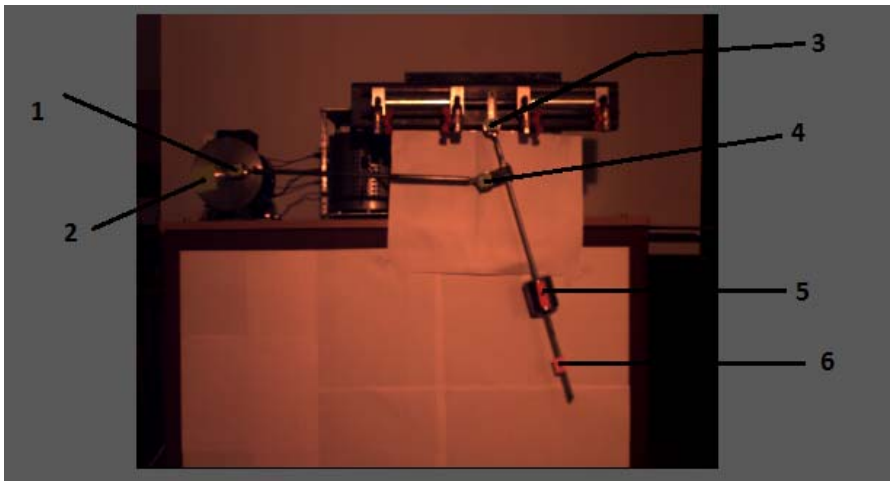

Figure 1.40. Position of the markers on the mechanism elements

The videos are downloaded to your computer then processes the first record. With Adobe After Effects application, the motion coordinates are retrieved for each marker. Once imported, the video is "pull" (drag& drop) in Composition window, and then from Animation menu, the option "Track Motion" has chosen.

So, on screen the element of motion tracking will appear, which will be placed on the desired marker. It sees a "+" in the middle of the element of motion tracking, which is actually the pixel whose coordinates will be tracked over time (called the Attach Point) (Fig.1.41).

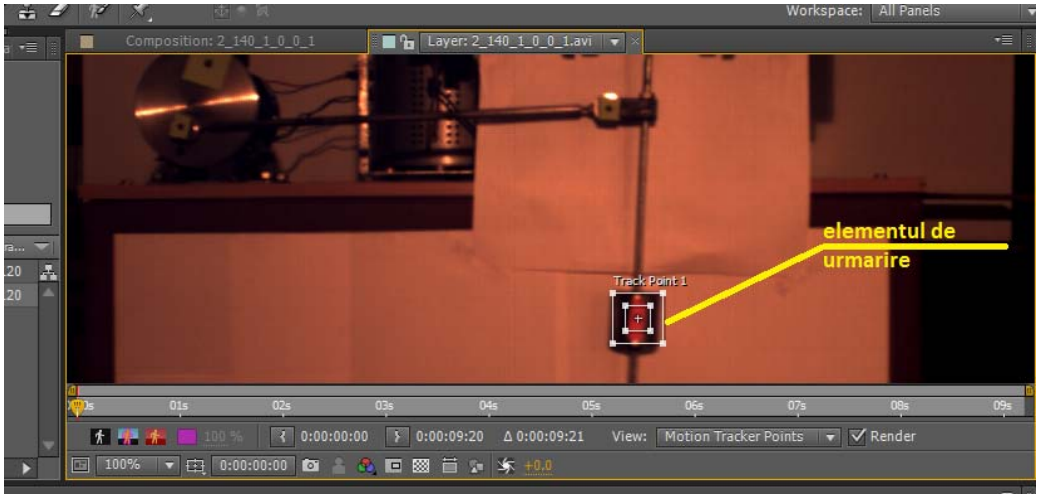

Figure 1.41. Positioning the element of motion tracking on the desired marker

We determine the conditions in which the point of interest will follow a long video. This will access Tracker-> Options (bottom right corner) and for the present experiment the RGB (color tone after tracking) and Track Fields have to be chosen (Fig.1.42).

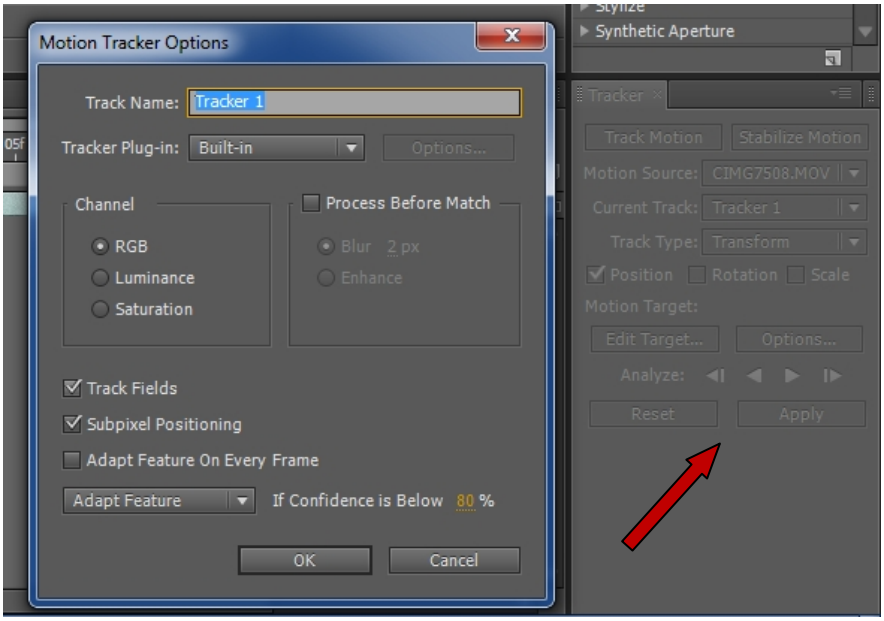

Figure.42. Tracking conditions of point of interest

After establishing the conditions under which the point of interest will follow through out the video, from the same element (bottom right corner) press Play (arrow oriented to the right) and thus the marker begins to be pursued throughout the motion.

.

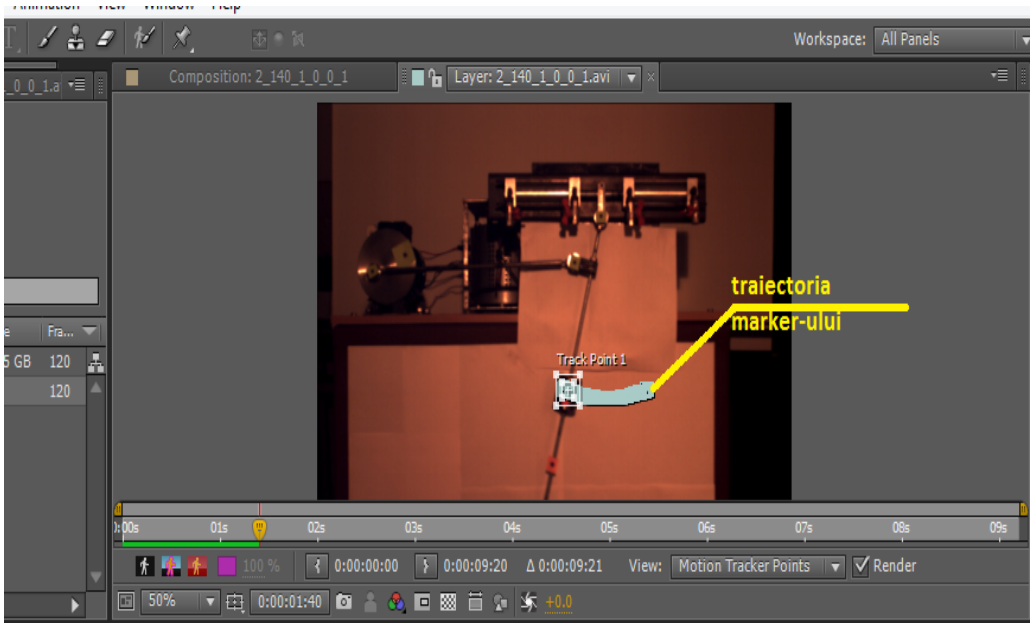

Figure.43. The pathof the analyzed marker

After completing the video material, the experimental data acquisition should be proceed. Since Adobe After Effects does not offer (yet) the possibility to automatically export their take over, this will be made by direct copying in an Excel table following a series of steps.

Thus, in the first step, from the lower right corner, where you select information from motion tracking element (MotionTracker), the Attach Point can be selected (shown in the table on the right selection key frames corresponding to this element-their color changes to yellow) and information are copied to the Clipboard using (Ctrl-C).

Working with Adobe After Effects for current marker ended and the information contained in this application, being now in the Clipboard, have to be exported to an Excel spread sheet (Ctrl-V). Obtaining the marker coordinates in the first phase involves the removal of information "ballast" which comes from the Adobe After Effects, (Fig.1.44).

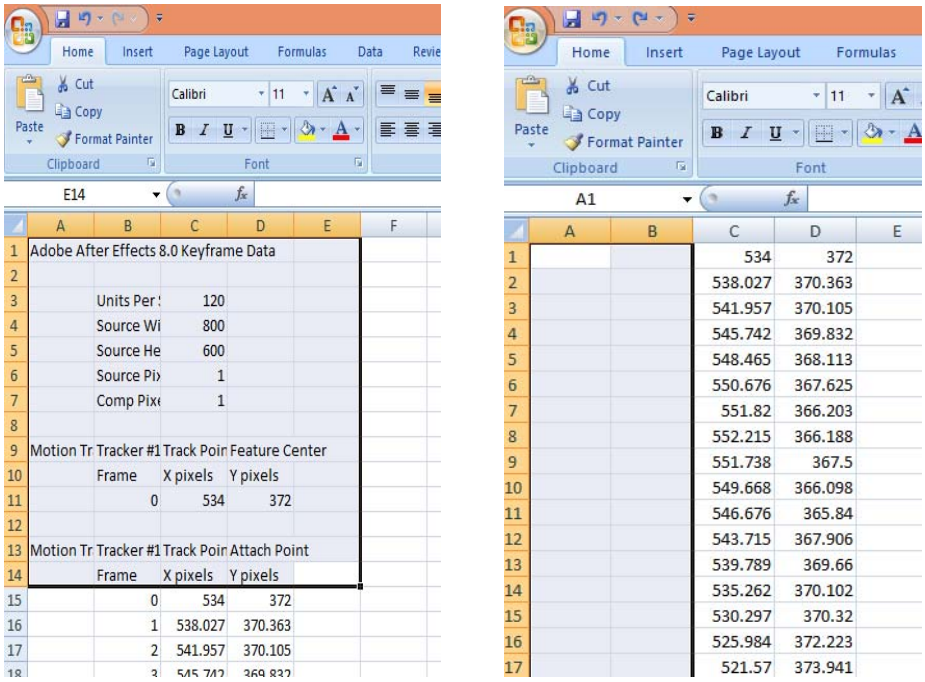

Figure.44. Moving data in Excel and removing ballast information

The next step is to change the format of text data innumerical values due to the fact that the information was done through copying to the Clipboard (Fig.1.45).

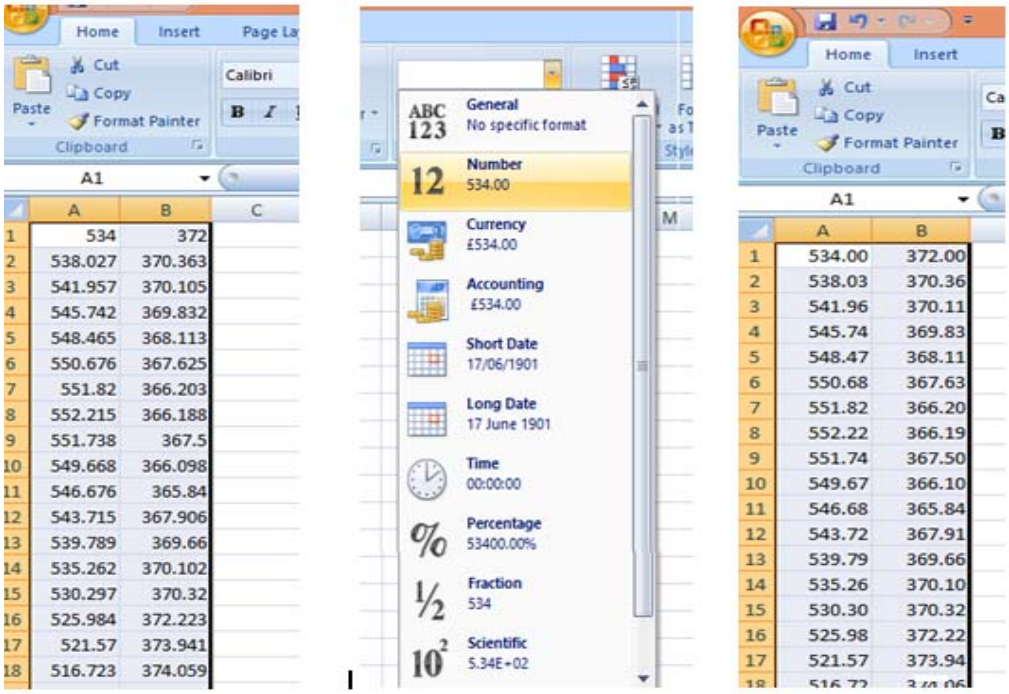

Figure1.45. Transforming data from digital format into text format

The result (which should look like the table at right) is saved and represents the time evolution of the coordinates of a marker.

The same process will be covered for other markers of the video (pump marker and the pendulum marker) too. This returns to Adobe After Effects, either by closing the project and will take all over again, or by returning to Undo (Ctrl-Z) until the element motion tracking is attached. It will be reposition new marker and the process will continue from that point.

Thus, the data for the first recording have been obtained. The above steps are repeated for other records of the mechanism to finally get its corresponding database, followed by data processing.

1.6.2. Design and accomplishment of the experimental setup

The experimental setup allows testing the behavior of a mechanism with two degrees of freedom - "closed kinematic chain through inertia" [DEL05] for different engine speeds. The test program described previously allow experimental tests and evaluation of certain kinematic parameters.

The proposed mechanism for the study (mechanism with two degrees of freedom - "closed kinematic chain through inertia ") [DEL05] has been developed at the Department of Mechanical Engineering, University of Braşov and conducted in collaboration with the INAR Institute of Brasov, the mechanism's components are shown in Fig. 1.46

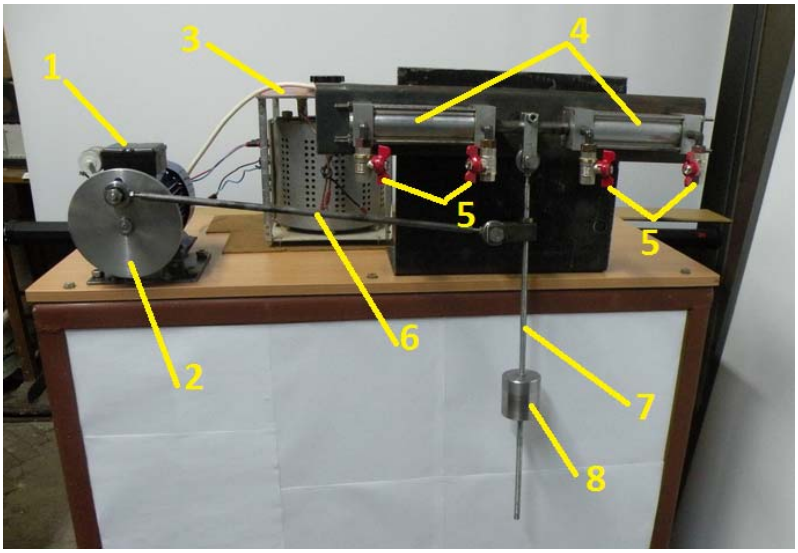

Figure 1.46. Experimental setup for testing
1-motor; 2- disc drive; 3 -transformer;
4 -pump; 5-valves; 6-rod; 7- pendulum rod; 8- weight

1.6.3. Tests achievement, processing and interpretation of the obtained data

This chapter presents the results obtained from testing the mechanism with two degrees of freedom. The test represents the video recording of markers motion for three different load situations of piston pump. By processing the obtained results, the motion identification of predetermined points of the mechanism has been aimed.

As I stated at the beginning of the chapter, the tests have been carried out using an AOS high-speed camera and the data processing has been made through the use of Adobe After Effects. With this software, the area of interest within the area of contrast can be followed, that means practically that two areas of different pixels are aimed, well-defined in plane to each other, thus avoiding the loss of much of the area of interest in the background. A focus area in which the point that we want to follow it should be established as well as a zone around the area of interest, which ideally contain pixels of another color for contrast (Fig.1.47-1.48).

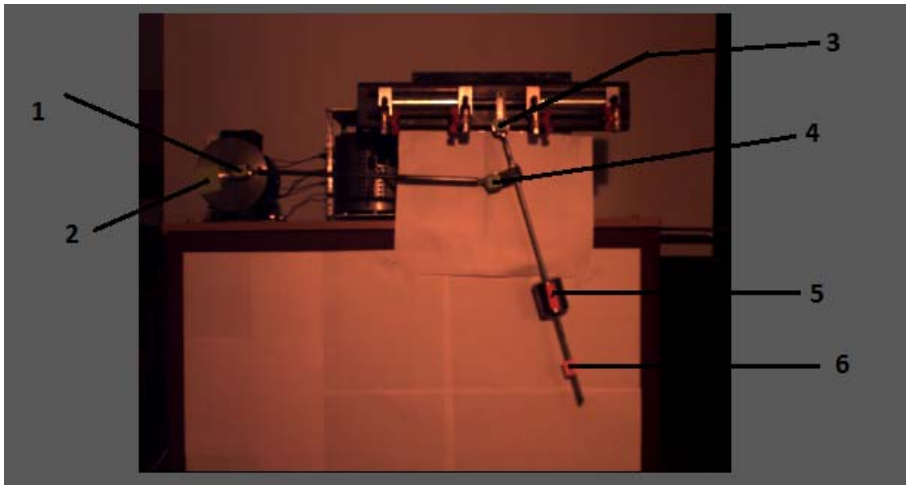

Figure 1.47. Highlighting the markers

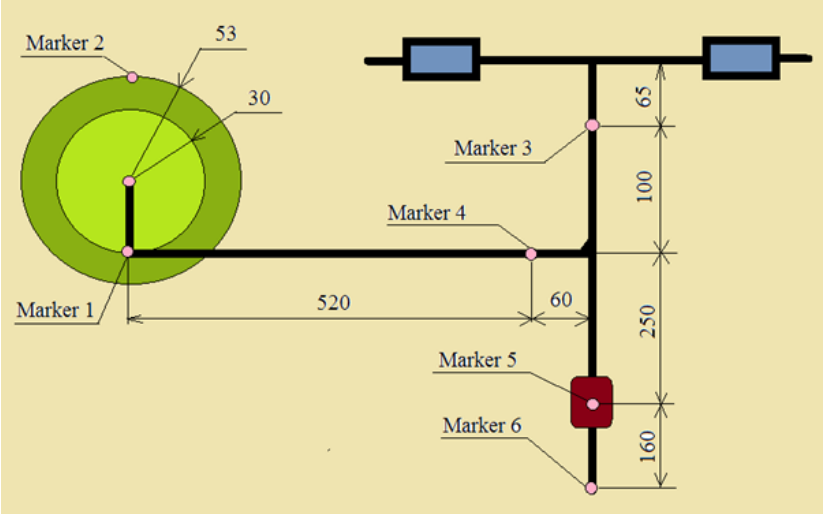

Figure 1.48. Sketch of the mechanism with markers highlighting

Applications to track a motion trajectory present the disadvantage that when the tracked entity merges with the background or is accidentally covered for a short time by an element of decor, the signal is lost.

In terms of the analysis that we will do, significant will be the determination of markers 1 and 3 coordinates, but interesting is to study and to analyze the motion of others' markers to verify the results.

The research has been carried out in three different regimes and different valve positions. In order to track, process and evaluate the experimental data, following notations have been made:

- movement with all valves open: 0_0_0_0;
- movement with all extremity valves closed: 1_0_0_1
- movement with all valves closed: 1_1_1_1

Regimes that tests have been carried out were 100, 120, 140, 160, numbers that are indications shown by transformer-rectifier element 3 on the stand. Based on the records, the speeds at established regimes have been determined.

Throughout the shooting the markers positioned on the mechanism have been followed, their trajectory being visible on the screen at the end of shooting (Fig. 1.49). Due to the fact that the used application (Adobe After Effects) has not been designed specifically for motion analysis - the trajectory tracking way being designed in order to apply the effect of motion on that path of some elements of video material, so this does not provide a direct possibility to export them in a known format. But markers coordinates (X and Y) can be copied in an Excel file, where, after some minor adjustments can be retrieved by other applications for further processing.

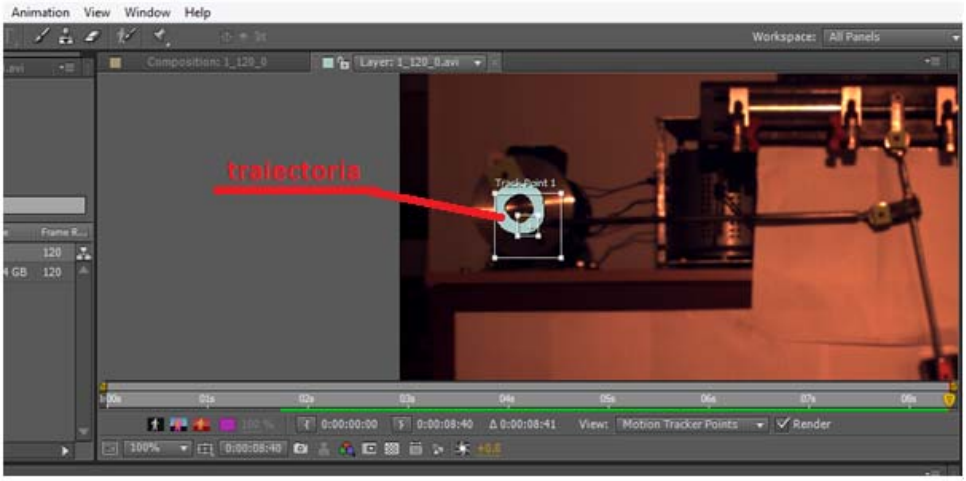

Figure 49. The path of marker 1

After the completion of the experimental tests, video recordings have been obtained representing the coordinates of the six markers corresponding to the four operating modes (100, 120, 140, 160) in the three loading cases (0_0_0_0, 1_0_0_1, 1_1_1_1).

Since experimental data showed by the Adobe After Effects are in pixels, it was necessary to establish a transformation scale from pixels in metric units because these data have to be scaled. On the other hand, in Adobe After Effect, the origin of the coordinate axes is in the upper left corner of the screen, which led to proper positioning of the axes system, which was made possible by simple subtracting operation of values obtained on Y axis of a fixed value.

Mathematical processing of experimental data from videos has led to some results presented in graphical form (Fig.1.50-1.55)

The motion study of the markers 1 and 2 is useful for determining the speed of the drive motor. The marker 3 will give the pistons motion and marker 5 allows determination of swinging motion.

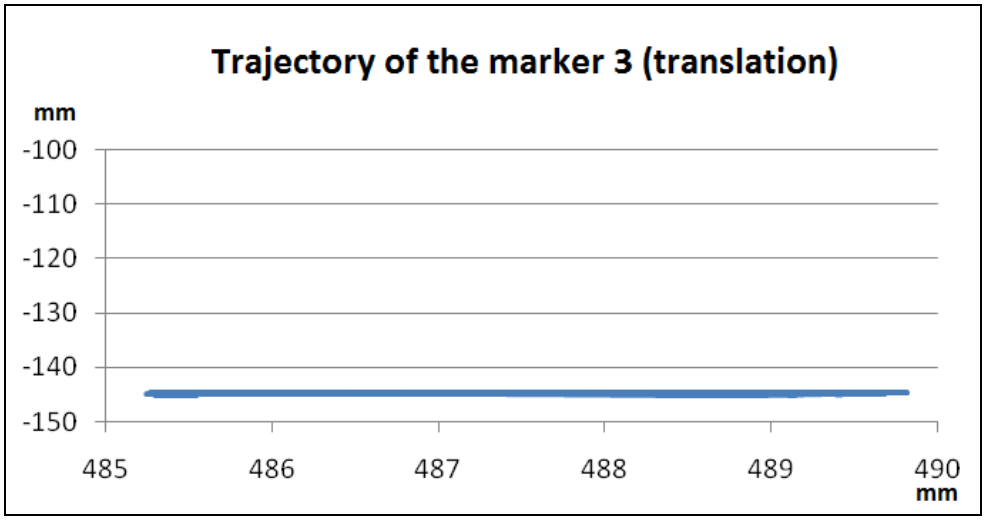

Figure 1.50. The graph of motion of the marker 3 (mm)

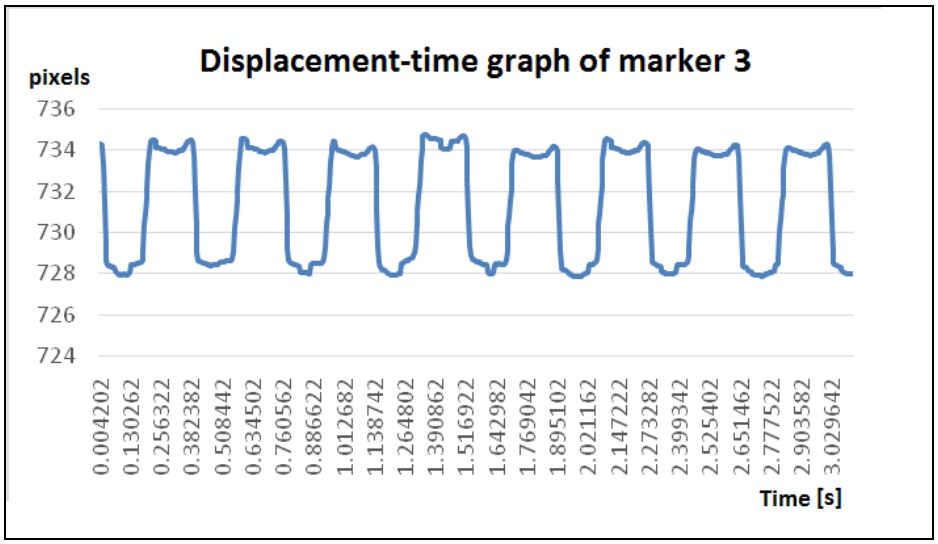

Figure 1.51. Horizontal displacement of the marker 3

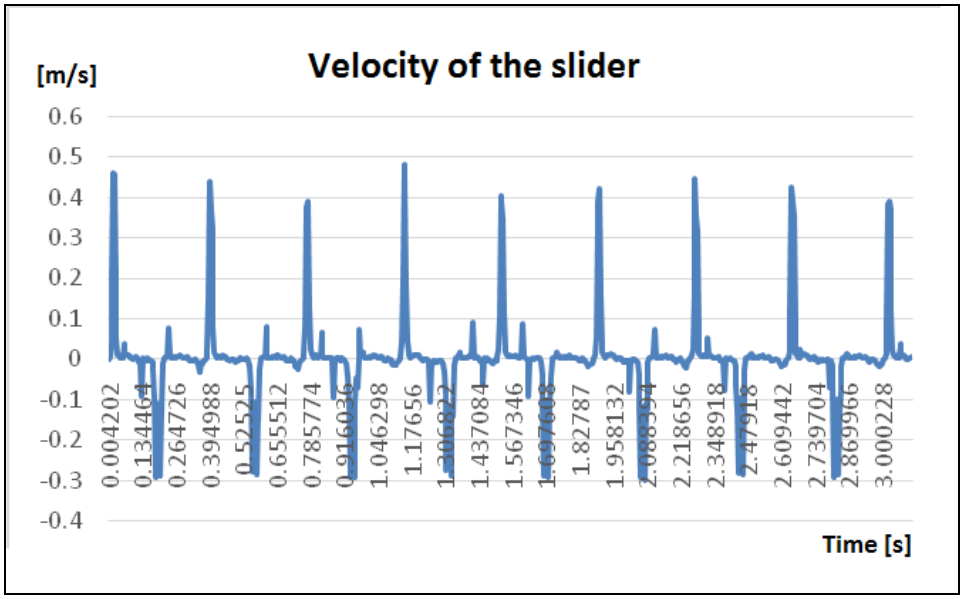

Figure 1.52. Horizontal speed of the slide

The study of marker 5 motion has determined following motion graphics.

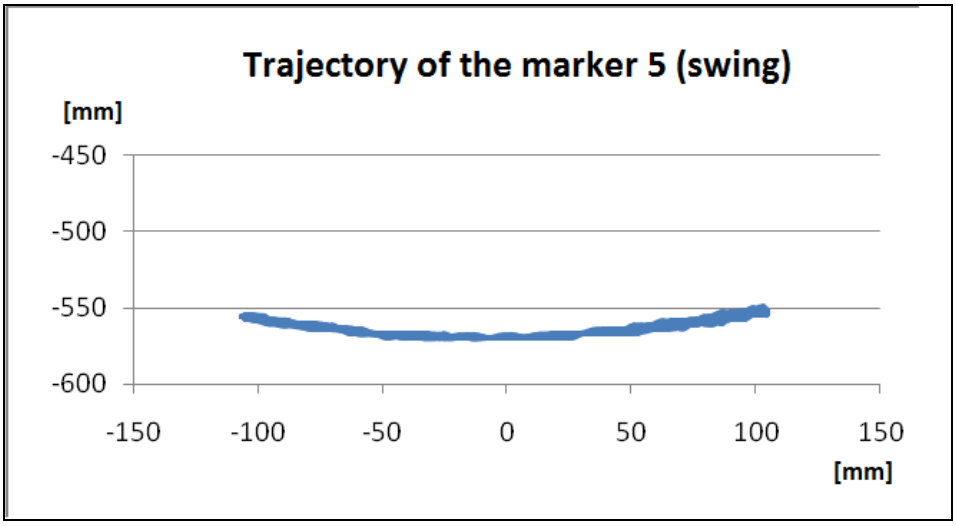

Figure 1.53. Trajectory of marker 5

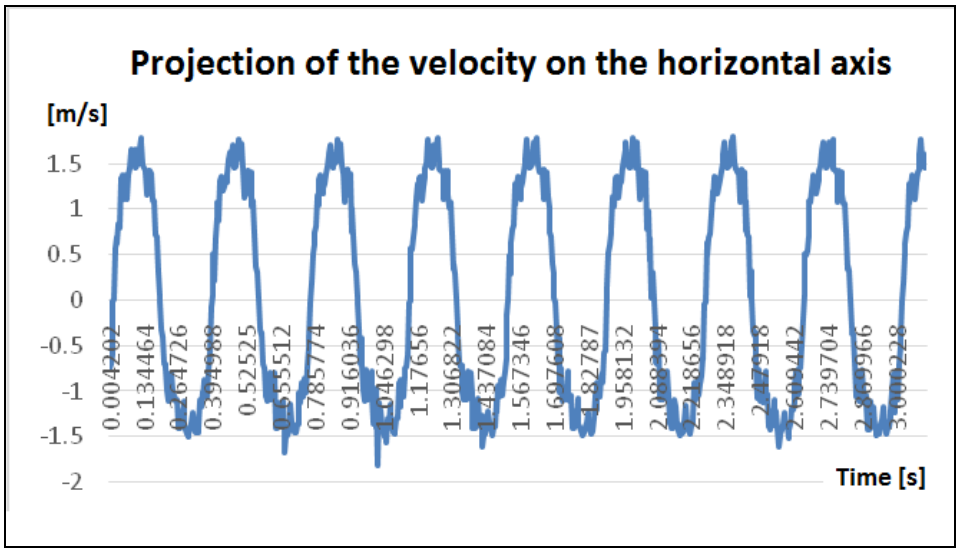

Figure 1.54. The projection of the speed on the horizontal axis of marker 5

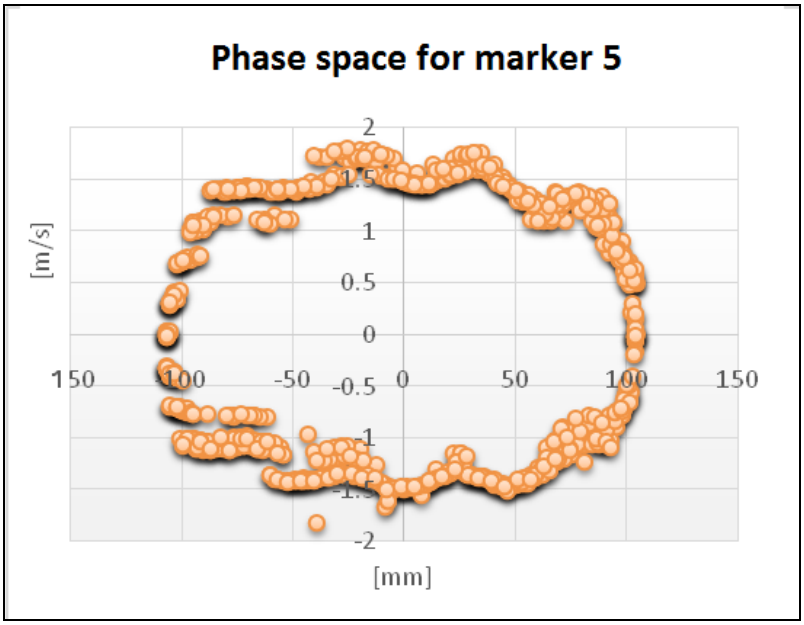

Figure 1.55. Phase space representation of displacement on the horizontal axis for the marker 5

Graphical representation "displacement versus engine speed" required as a first step to determine the engine speed for all operating modes in the three situations. Thus from the analysis of marker 1 I have determined the engine speed, taking into consideration 120 frames/sec, and marker 3 analysis led to the result of the piston stroke in the same conditions.

Data have been summarized in tabular form (Tab.1.1) and then plotted (fig.1.56-1.57).

For example, for the operating mode 120, from the graphs analysis of marker 1, the speed value 183.1543 rot/min have been determined.

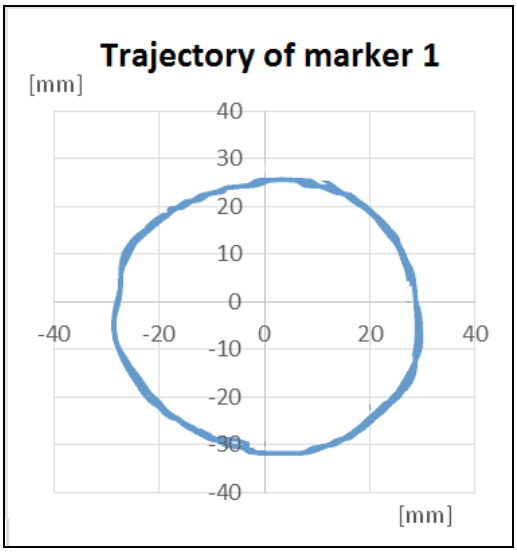

Figure 1.56. Trajectory of marker 1

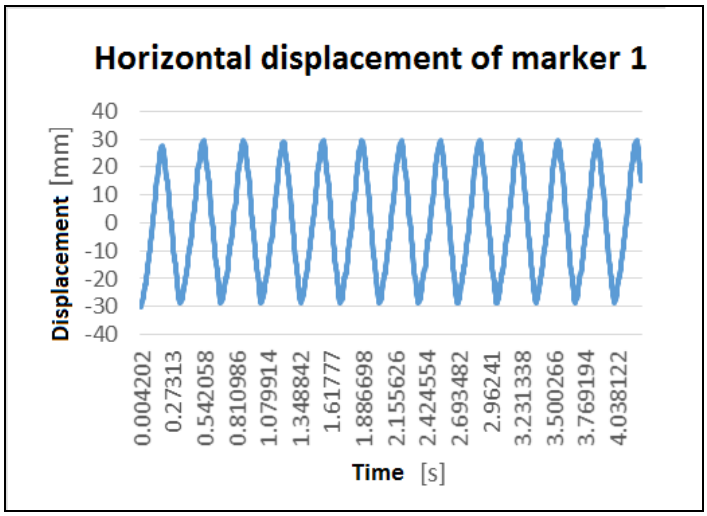

Figure 1.57. Horizontal displacement of marker 1

Tabelul 1.1.

Operating mode 120			Time from a frame 0.004166 s		
	Intervalul	No. of data	No. of frames	Period	No. of rot/min
	1	83	82	0.344564	174.1331
	2	80	79	0.331958	180.7458
	3	80	79	0.331958	180.7458
	4	81	80	0.33616	178.4864
	5	77	76	0.319352	187.8805
	6	77	76	0.319352	187.8805
	7	78	77	0.323554	185.4405
	8	78	77	0.323554	185.4405
	9	78	77	0.323554	185.4405
	10	78	77	0.323554	185.4405
	11	79	78	0.327756	183.063

Average angular speed	**183.1543**	**rot/min**

The analysis in terms of marker 3 graphics led to the determination of the piston stroke (Fig.1.56-1.57).

Similarly is the case for all operating modes, in all established variants (0_0_0_0, 1_0_0_1, 1_1_1_1), the data being obtained from the centralized spreadsheet (Tab.1.2) for plotting. (Fig.1.58-1.60)

Table 1.2.

Regime	**TAP POSITION**					
	0_0_0_0		**1_0_0_1**		**1_1_1_1**	
	Angular speed (rot/min)	**Displa-cement (mm)**	**Angular speed (rot/min)**	**Displa-cement (mm)**	**Angular speed (rot/min)**	**Displa-cement (mm)**
100	165.36	6.84	165.24	6.16	161.73	6.05
120	183.15	9.58	176.93	8.74	163.71	8.04
140	191.21	14.67	185.26	12.76	184.18	11.62
160	197.11	15.86	192.56	15.30	191.67	15.04

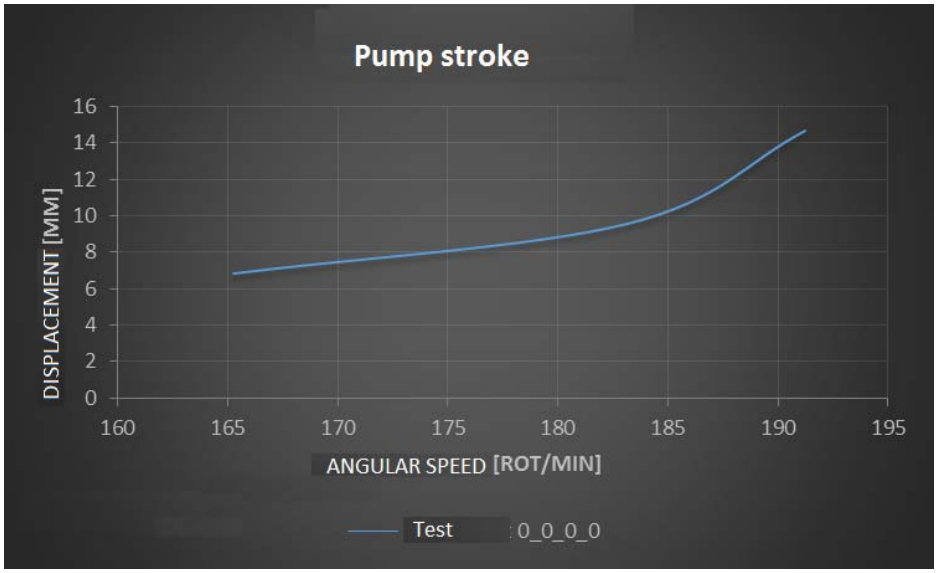

Figure 1.58. The displacement of the piston 0_0_0_0

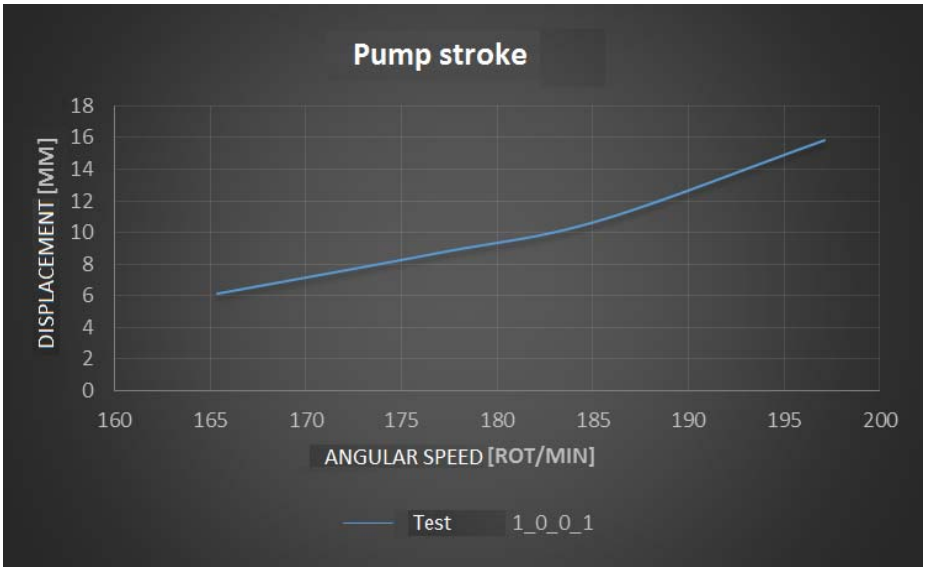

Figure 1.59. The displacement of the piston 1_0_0_1

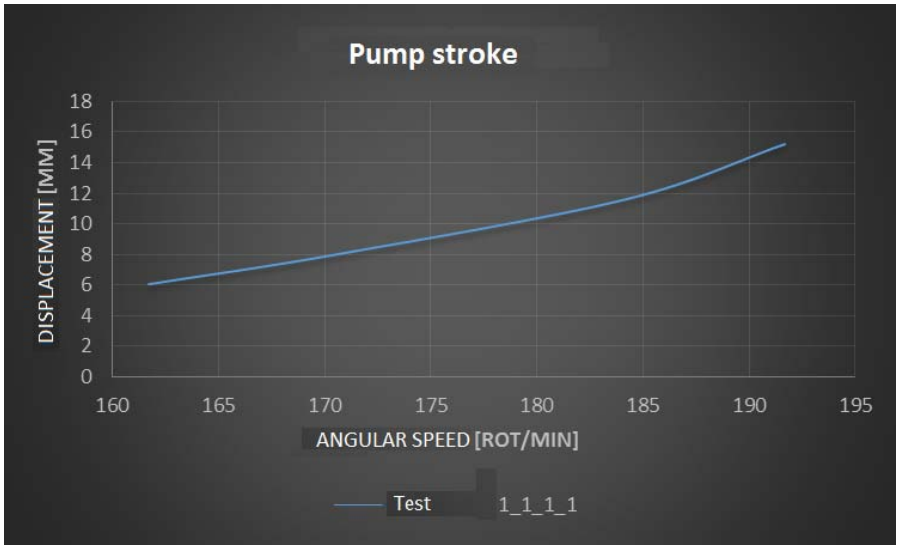

Figure 1.60. The displacement of the piston 1_1_1_1

Based on the results obtained in the investigation the following conclusions and original contributions can be drawn:

- A stand on a small scale of the mechanism with two degrees of freedom has been carried out;
- An experiment has been designed in which significant motion mechanism points can be registered to determine finally the motion of all elements of the multibody system;
- Tests were performed on the stand mechanism with two degrees of freedom;
- The motion mechanism through position markers has been analysed, making video recordings of markers;
- The obtained results have been digitized, applying for this the Adobe After Effects software;
- The numerical results of tests based on tables and charts have been synthesized and processed.

The main advantage of studied mechanism with two degrees of freedom is in its transmission flexibility ratio. By this we mean that, unlike the classical connecting rod-crank mechanism that has a constant transmission ratio - in that, independently of the speed of the crank, the stroke is the same – the proposed two degrees of freedom mechanism carries out at low speeds of the crank, a very low (or even zero) stroke, and as the frequency of rotation of the crank increases (i.e. wind speed increases), the stroke increases also, not only its frequency alternating motion.

This mechanism property provides the following benefits:

- Allow startup of vertical axis wind turbine at low wind speed (thus avoiding the disadvantage of this type of wind turbines);

- Achieved an increase in efficiency of turbine-pump unit with increasing wind speed. This is obvious if you notice that as speed increases, both the number of piston strokes in unit time and the length of its stroke increase;
- Limits the speed in case of strong wind, by substantially increasing the power consumed by the pump.

1.7. Conclusions

Theoretical and experimental study carried out in thesis have the aim to research the dynamic behavior of wind-driven pumps, focusing on dynamic analysis of these pumps transmissions.

In a first step the theoretical research has focused mainly on the analysis of existing systems, studying the way they behave in normal loading conditions that occur in operation.

Then comes the analysis of these types of pumps in order to see whether constructive solutions can be optimized, the study is justified by the spread that the power converters have, primarily due to their simplicity and then due to the fact that wind is a free resource and practically inexhaustible. The challenge was to finally get a simple, easy to maintain, inexpensive and reliable system that incorporates current technology's new conquests.

It should be noted that determining the type and capacity of wind power, involves prior analysis of wind potential in the local area of installation, and the use and maintenance of pumps involves that also the motion transmission of the rotor pump driven by wind to be accomplished by simpler systems. The most used pump drive system is a connecting rod-crank mechanism which converts the rotation motion of the turbine into an alternating translation motion.

The main methods used to increase the efficiency of adaptation between the rotor and wind pump have been highlighted and several aspects regarding the balance of the depth piston pumps have been treated. The presentation of the methods analysis of multibody systems has been conducted in order to find some fundamental theorems of transmission elements of multibody system from the pump to turbine.

These theorems allow a simple representation and numerical approach by help of software. The method of eliminating the reactions that occur in the constraints of the considered multibody system (reactions in joints and traveler) has been established, method that uses the existent perpendicularity between virtual displacements from the constraints and the forces that occur in connections.

Applying these methods, the equations of motion for a pump that uses at motion transmission, a simple rod-crank mechanism have been written. The presentation of these equations of motion has been carried out in matrix form, so that it becomes quite easy to approach them using computer programs. Based on these computer programs, the equations of motion have been integrated in a first step for connecting rod-crank system with one degree of freedom.

Finally, in the thesis, the kinematics and dynamics of a transmission with two degrees of freedom, represented by a inertia closed kinematic chain have been studied. [DEL05]

We made a stand on a small scale of the mechanism with two degrees of freedom. We designed an experiment where significant motions of the mechanism points have been registered to determine, finally, the motions of multibody system elements. Tests have been conducted on a stand of the mechanism with two degrees of freedom. We have analyzed the mechanism motion through position markers, making video recordings of markers. The results have been digitized, applying for this the Adobe Photoshop program.

The results of tests based on tables and charts have been numerically processed and synthesized.

Finally, in the thesis were studied the kinematics and dynamics of a transmission with two degrees of freedom, represented by a inertia closed kinematic chain. [DEL05]

We made a stand on a small scale of the mechanism with two degrees of freedom. We designed an experiment where was registered significant movement mechanism points to determine, finally, the motions of multibody system element's. Tests were conducted on a stand of the mechanism with two degrees of freedom. We analyzed the movement mechanism through position markers, making video recordings of markers. The results were digitized, applying for this program Adobe Photoshop.

Were synthesized and processed numerical results of tests based on tables and charts.

1.8. Original contributions of the author in the field

Analysis of researches conducted in the field of construction of low power drive pumps used to pump water, from which it can be noticed that both the study and research of such systems has developed dramatically, obtaining numerous results presented in a large number of publications.

- Developing an appropriate mathematical model for dynamic analysis of the transmission of classical pump-turbine aggregates. This enables the proposed model in the first instance, the removal of the connecting forces and obtaining the equations of motion of a system of differential equations of second order which allowed the numerical integration, using MATLAB software, to determine the law of motion of the classic mechanism used in the transmission of wind driven pumps;
- Since the main type of transmission in case of wind pump is a mechanical one, the conversion of the rotation motion into translation motion achieved by use of the connecting rod-crank system, this type of transmission has been computed and the results have been compared with those obtained for the solution proposed by the author, in the system with two degrees of freedom mechanism.;
- Critical analysis of power converters used in wind turbines, analysis aimed to identify the main problems arising from the use of such facilities. Numerous published results on small wind installations used for water pumps, highlighting the main types used in practice have been also presented;
- A mechanism with two degrees of freedom to transmit and convert the rotation motion into translation one has been proposed. This type of mechanism has some structural

advantages, one of which is that it can run the turbine at weak wind. At weak wind, the mechanism can function as a pendulum driven by turbine rotation, but as the turbine speed increases, the pendulum inertia moves the pump. This produces an increasing stroke of the piston, which increases the consumption of energy taken over by the pump and limits the turbine speed;

- The main advantage of mechanism with two degrees of freedom is studied in its transmission flexibility ratio. By this we mean that, unlike the classical connecting rod-crank mechanism that has a constant transmission ratio, - in the sense that the piston stroke is the same, irrespective of the crank, the proposed mechanism of two degrees of freedom carries out very low (or even zero) stroke at low speeds of the crank, and as the frequency of rotation of the crank increases (i.e. wind speed increases) the stroke increases also, not only its frequency alternating motion.

This mechanism property provides the following benefits:

- Allow startup of the vertical axis wind turbine at low wind speeds (thus avoiding the disadvantage of this type of wind turbines);
- Accomplishes an increase of pump turbine efficiency with the increase of wind speed. This is obvious if you notice that as speed increases, both the number of racing pistons in unit time and the length of its stroke increase;
- Limits the speed in case of strong wind turbine, by substantially increasing the power consumed by the pump;
- Dynamic analysis of the proposed mechanism with two degrees of freedom;
- Numerically integration of the motion equations has been performed, determining the forces that act in the mechanism elements, preliminary stage of a calculation of resistance. For this purpose we used models - proposed in work and presented above - on which algorithms in Matlab have been written. Mixed system of differential equations, with algebric unknowns, liaison forces (DAE - differential algebraic equations), has been reduced to a system of two second order differential equations with two unknowns (DOE - ordinary differential equations). By numerical integration of the motion equations, using simple relations, the liaison forces have been computed, which allows determination of loadings from the system;
- Execution to a certain scale of the transmission mechanism with two degrees of freedom, model that serves to highlight the characteristics of this solution and to confirm its veracity;
- Check of the obtained experimental results in different phases of the work. Using modern methods of measuring mechanical quantities as well as videos, recordings of this mechanism motion have been carried out, being confirmed the hypothesis of the thesis.

Chapter 2

Analysis of the Motion Equations and Dynamic Response of a Multibody System with Elastic Elements

2.1. Modeling the multibody systems with elastic elements

This section presents known results in the dynamic analysis of the multibody systems with elastic elements in order to introduce the main notions for a good understanding of the contributions and personal researches.

2.1.1. Introduction

In many application in the domain of the multibody systems the element composing the mechanical system are considered rigid. This hypothesis corresponds for a large class of problems but, in some cases, when the elasticity of components is significantly, the dynamic response can be different both quantitatively and qualitatively. For example, especially in the field of high speed vehicles and robotics can be necessary to consider the elasticity of elements and to use an adequate models in order to obtain pertinent results. Generally, a multibody system containing some elastic elements presents a high complexity and a strong non-linearity where difficulties arise to address this topic.

The study of mechanical system with elastic elements using the classic theorems of the applied mechanics does not represent ussualy a practical task, the obtained equations of motions do not generally have an analytical solutions. For this for the dynamical analysis the numerical methods of discretization are used where the infinite displacement field is replace with a finite displacement field. The main discretisation method remains finite element method (FEM), which is now one of the strongest instruments for differential equations systems solving. In the section will be presented how can be obtained the equations of motion in a general case, a three-dimensional finite element involved in a three-dimensional motion within a mechanical system.

For every type of finite element used the chosen shape functions will determine the final form of the equation but a presentation in a general situation can be perform, without considering certain particular shape functions. In what follows the common hypothesis used in the elasticity of the solids is made: deformations are small and have not influence on the general rigid motion of the whole system.

In the literature results considering one-dimensional finite elements are obtained by many researchers (see for example [BAG83], [BAH76] , [CLE81] , [FAN03] , [SUN86]). For a truss finite element, having a plane motion, the equations of motion have been obtained in the case of the planar mechanisms with bars. In these applications different types of finite elements

have been considered. In [CLE81] and [THO86] the study for a one-dimensional truss finite element with a three-dimensional motion has been carried out. The researches published presented some aspects regarding the calculation, experimental checks and control in case of simple applications ([DEU08] , [MAY96] , [PIR05]. Other influences as influence of damping, the lost of the stability, the use of some composite materials (see [NET06], [SHI01], [ZHA07]) or thermal problems (see [HOU09]) has been studied. The major difficulty consists in the symbolic representation of the equations of motions and in finding an adequate method for integration. Models for uni-dimensional finite element with a two- and three-dimensional motions have been developed by [THO86] .

In such type of dynamical problems it is also considered that beforehand a dynamical analysis of the whole mechanical system with the elements considered rigid has been carried out and the kinematics of this system is solved (the field of velocities and accelerations has been determined).

The model considers a chosen arbitrary finite element participating to the entire rigid motion of the mechanical system. The classical mechanics show us that the field of the velocities and accelerations of a point of this finite element shall be entirely determined if are known:

- the velocity and acceleration of the origin of coordinate system the finite element and
- the angular velocity and angular acceleration of the origin of the coordinate system related to the finite element considered.

A simplifying assumption is that the solid are considered linearly elastic. The method used to obtain the motion equations are the Lagrange method. To use this is necessary to write the kinetic energy and the strain energy for the considered finite element and the work of the distributed and concentrated forces.

2.1.2. Theoretical background and modelling

It is presented a model in order to obtain the motion equations for a single finite element. Let's consider a finite element resulting after a discretisation of an elastic element of the mechanical system studied. In Finite Element Method the displacements of all the points of a continuous system shall be expressed depending on a finite number of nodal coordinates. For this the finite element considered shall be refer to the local mobile coordinate system, being in a general rigid motion (fig.1.1).

Choosing the origin O in the mass center of the finite element can be a convenient procedure, useful in mechanics (the general theorems become simpler). We shall note with $\bar{v}_o(\dot{X}_o,\dot{Y}_o,\dot{Z}_o)$ the velocity and with $\bar{a}_o(\ddot{X}_o,\ddot{Y}_o,\ddot{Z}_o)$ the acceleration of the origin of the local coordinate refer to the global coordinate system OXYZ, to which the motion of the whole system (as a "rigid body") will relate. We shall note the angular velocity with $\bar{\omega}(\omega_x,\omega_y,\omega_z)$ and with $\bar{\varepsilon}(\varepsilon_x,\varepsilon_y,\varepsilon_z)$ the angular acceleration of the mobile coordinate system. These four kinematic vectors will define the general time depending finite rigid motion of the element. The multi-body system analised consisting of several solids, these vectors will be different for each solid composing the system. The transformation of the components of a vector from the local

system of coordinates into the global system of coordinates occurs by means of a matrix of rotation $\boldsymbol{R}$.

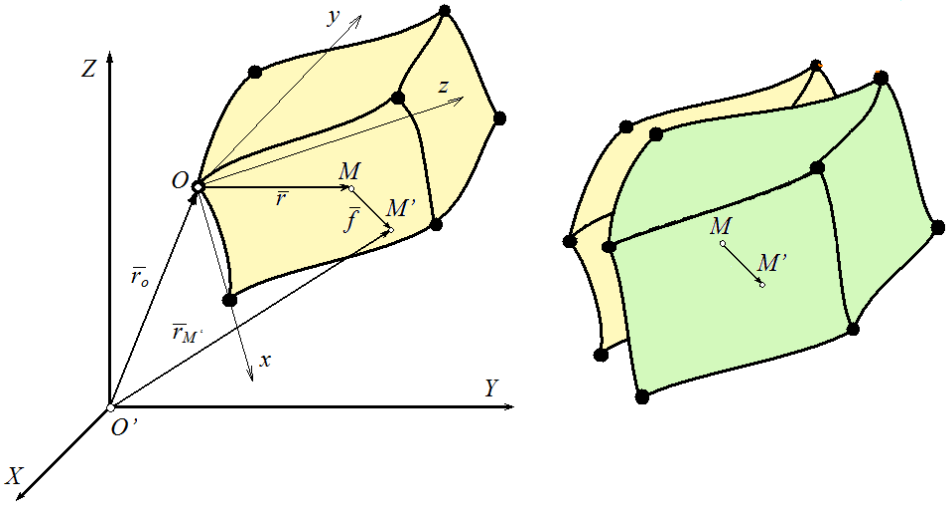

Figure 2.1. One finite element method ([VLA12])

Now we will express the position vector of a current point M with $\boldsymbol{r}_{M,G}$:

$$\boldsymbol{r}_{M,G} = \boldsymbol{r}_{O,G} + \boldsymbol{r}_{G} = \boldsymbol{r}_{O,G} + \boldsymbol{R} \cdot \boldsymbol{r}_{L} \tag{2.1}$$

where index G indicates a vector with the components expressed in the global coordinate system and index L indicates a vector with the components expressed in the local coordinate system.

The displacement of the point M is f_L and he becomes M':

$$\boldsymbol{r}_{M',G} = \boldsymbol{r}_{O,G} + \boldsymbol{R} \cdot (\boldsymbol{r}_{L} + f_L) \tag{2.2}$$

where $\boldsymbol{r}_{M',G}$ represents the position vector of point M ' with his components expressed in the global coordinate system. The continuous displacement field $\boldsymbol{f}(x,y,z)_L$ is approximated in the finite element method by the relation:

$$\boldsymbol{f}_{L} = \boldsymbol{N}(x,y,z)\ \boldsymbol{\delta}_{e}(t)_L \tag{2.3}$$

where the shape functions $\boldsymbol{N}$ will depend on the type of the finite element chosen. Differentiation (2.2) is possible to obtain the velocity of point M' :

$$\boldsymbol{v}_{M',G} = \dot{\boldsymbol{r}}_{o} + \dot{\boldsymbol{R}}\,\boldsymbol{r}_{L} + \dot{\boldsymbol{R}}\,\boldsymbol{f}_{L} + \boldsymbol{R}\,\dot{\boldsymbol{f}}_{L} = \dot{\boldsymbol{r}}_{o} + \dot{\boldsymbol{R}}\,\boldsymbol{r}_{L} + \dot{\boldsymbol{R}}\,\boldsymbol{N}\,\boldsymbol{\delta}_{e,L} + \boldsymbol{R}\,\boldsymbol{N}\,\dot{\boldsymbol{\delta}}_{e,L} \tag{2.4}$$

In the following the non-indexed vectors are considered to be written in the global system of coordinates.

The orthogonallity conditions for the rotation matrix are [VLA07]:

$$\boldsymbol{R}\,\boldsymbol{R}^{T} = \boldsymbol{R}^{T}\,\boldsymbol{R} = \boldsymbol{E} \tag{2.5}$$

where $\boldsymbol{E}$ is the unit matrix. If we differentiate the relation (2.5) we obtain:

$$\dot{\boldsymbol{R}}\ \boldsymbol{R}^T+\boldsymbol{R}\ \dot{\boldsymbol{R}}^T=0 \tag{2.6}$$

The skew symmetric matrix:

$$\tilde{\boldsymbol{\omega}}_G=\dot{\boldsymbol{R}}\ \boldsymbol{R}^T=\begin{bmatrix} 0 & -\omega_{zG} & \omega_{yG} \\ \omega_{zG} & 0 & -\omega_{xG} \\ -\omega_{yG} & \omega_{xG} & 0 \end{bmatrix} \tag{2.7}$$

represents the angular velocity operator, corresponding to the angular velocity:

$$\boldsymbol{\omega}_G=\begin{Bmatrix} \omega_{zG} \\ \omega_{yG} \\ \omega_{zG} \end{Bmatrix} \tag{2.8}$$

The angular acceleration operator is defined by:

$$\tilde{\boldsymbol{\varepsilon}}_G=\dot{\tilde{\boldsymbol{\omega}}}_G=\ddot{\boldsymbol{R}}\ \boldsymbol{R}^T+\dot{\boldsymbol{R}}\ \dot{\boldsymbol{R}}^T . \tag{2.9}$$

It will result, after elementary calculation:

$$\ddot{\boldsymbol{R}}\ \boldsymbol{R}^T=\tilde{\boldsymbol{\varepsilon}}_G-\dot{\boldsymbol{R}}\ \dot{\boldsymbol{R}}^T=\tilde{\varepsilon}_G+\tilde{\boldsymbol{\omega}}_G\ \tilde{\boldsymbol{\omega}}_G \tag{2.10}$$

relation used in the following.

2.1.3. Use of the Lagrange equations

To write the motion equations a good method is to use the Lagrange equations using the Lagrange function. For the considered element the Lagrangean is:

$$L=E_c-E_p+W+W^c \tag{2.11}$$

We apply the equations of Lagrange (see Teodorescu, 2007):

$$\frac{d}{dt}\left\{\frac{\partial L}{\partial \dot{\delta}_e}\right\}-\left\{\frac{\partial L}{\partial \delta_e}\right\}=0 \tag{2.12}$$

By $\left\{\dfrac{\partial L}{\partial \delta_e}\right\}$ we understand:

$$\left\{\frac{\partial L}{\partial X}\right\}=\begin{Bmatrix} \dfrac{\partial L}{\partial x_1} \\ \dfrac{\partial L}{\partial x_2} \\ \vdots \\ \dfrac{\partial L}{\partial x_n} \end{Bmatrix} \quad \text{where: } \{X\}=\begin{Bmatrix} x_1 \\ x_2 \\ \vdots \\ x_n \end{Bmatrix} \tag{2.13}$$

Using these equations, after a series of elementary calculations and rearranging of terms we get the equations of motion for the finite element considered:

$$(\int_V \boldsymbol{N}^T \boldsymbol{N}\, \rho dV)\, \ddot{\boldsymbol{\delta}}_{e,L} + 2\,(\int_V \boldsymbol{N}^T \boldsymbol{R}^T \dot{\boldsymbol{R}}\, \boldsymbol{N}\, \rho dV)\, \dot{\boldsymbol{\delta}}_{e,L} + (\boldsymbol{k}_e + \int_V \boldsymbol{N}^T \boldsymbol{R}^T \ddot{\boldsymbol{R}}\, \boldsymbol{N}\, \rho dV)\, \boldsymbol{\delta}_{e,L} =$$

$$= \boldsymbol{q}_e + \int_V \boldsymbol{N}^T \boldsymbol{p}_L dV - (\int_V \boldsymbol{N}^T \rho dV)\, \boldsymbol{R}^T \ddot{\boldsymbol{r}}_o - \int_V \boldsymbol{N}^T \boldsymbol{R}^T \ddot{\boldsymbol{R}}\, \boldsymbol{r}\, \rho dV \qquad (2.14)$$

Is denoted with: $\boldsymbol{N}_i$ the row *i* of matrix $\boldsymbol{N}$. If are used the notations:

$$\boldsymbol{m}_{ix} = \int_V N_i^T x\, \rho dV \;; \quad \boldsymbol{m}_{iy} = \int_V \boldsymbol{N}_i^T y\, \rho dV \;; \quad \boldsymbol{m}_{iz} = \int_V \boldsymbol{N}_i^T z\, \rho dV$$

$$\boldsymbol{m}_{ij} = \int_V \boldsymbol{N}_i^T \boldsymbol{N}_i^T\, \rho dV \;; \quad \boldsymbol{q}^*_{e,L} = \int_V \boldsymbol{N}^T \boldsymbol{p}_L dV \;; \quad \boldsymbol{m}^i_{Oe} = \int_V \boldsymbol{N}^T \rho dV;$$

$$\boldsymbol{m}_e = \int_V \boldsymbol{N}^T \boldsymbol{N}\, \rho dV = \boldsymbol{m}_{11} + \boldsymbol{m}_{22} + \boldsymbol{m}_{33} \;;$$

$$\boldsymbol{c}_e(\omega) = \int_V \boldsymbol{N}^T \boldsymbol{R}^T \dot{\boldsymbol{R}}\, \boldsymbol{N}\, \rho dV = \int_V \boldsymbol{N}^T \tilde{\boldsymbol{\omega}}_L\, \boldsymbol{N}\, \rho dV \;;$$

$$\boldsymbol{k}_e(\varepsilon) + \boldsymbol{k}_e(\omega^2) = \int_V \boldsymbol{N}^T \boldsymbol{R}^T \ddot{\boldsymbol{R}}\, \boldsymbol{N}\, \rho dV = \int_V \boldsymbol{N}^T \tilde{\boldsymbol{\varepsilon}}_L\, \boldsymbol{N}\, \rho dV + \int_V \boldsymbol{N}^T \tilde{\boldsymbol{\omega}}_L \tilde{\boldsymbol{\omega}}_L\, \boldsymbol{N}\, \rho dV \;;$$

$$\boldsymbol{k}_e(\varepsilon) = \int_V \boldsymbol{N}^T \tilde{\boldsymbol{\varepsilon}}_L\, \boldsymbol{N}\, \rho dV \;; \quad \boldsymbol{k}_e(\omega^2) = \int_V \boldsymbol{N}^T \tilde{\boldsymbol{\omega}}_L \tilde{\boldsymbol{\omega}}_L\, \boldsymbol{N}\, \rho dV \;;$$

$$\boldsymbol{q}^i_{e,L}(\omega) = \int_V \boldsymbol{N}^T \tilde{\boldsymbol{\omega}}_L \tilde{\boldsymbol{\omega}}_L\, \boldsymbol{r}_L\, \rho dV \;; \quad \boldsymbol{q}^i_{e,L}(\varepsilon) = \int_V \boldsymbol{N}^T \tilde{\boldsymbol{\varepsilon}}_L\, \boldsymbol{r}_L\, \rho dV \qquad (2.15)$$

A condensed form for the equations of motion is:

$$\boldsymbol{m}_e \ddot{\boldsymbol{\delta}}_{e,L} + 2\boldsymbol{c}_e \dot{\boldsymbol{\delta}}_{e,L} + [\boldsymbol{k}_e + \boldsymbol{k}_e(\varepsilon) + \boldsymbol{k}_e(\omega^2)]\, \boldsymbol{\delta}_{e,L}$$

$$= \boldsymbol{q}_e + \boldsymbol{q}^*_{e,L} - \boldsymbol{q}^i_{e,L}(\varepsilon) - \boldsymbol{q}^i_{e,L}(\omega^2) - \boldsymbol{m}^i_{Oe} \boldsymbol{R}^T \ddot{\boldsymbol{r}}_o \qquad (2.14')$$

It must mention that the equations of motion are related to the local system of coordinates. These equations can be linearized considering the reference as " frozen" in that particular position, in which the field of velocities and accelerations is known.

The matrix coefficients can be calculated after choosing the shape functions and the nodal coordinates for expressing the displacement of a point.

Finally the equations of motion are obtained in terms of a set of independent nodal coordinates. We can observe, comparing with the equations obtained in case of the study of the steady state response, that some additional terms occur. The additional terms are due to the relative motion of nodal coordinates relative to the mobile coordinate systems attached to the finite element considered - Coriolis effects – and causes a change in the stiffness. The inertia terms will be also modified.

Obtaining the equations of motion represents a first step in solving this kind of problems. The next step is to relate the equations of motion for one single finite element to the global coordinate system. The third step is to assemble them for obtaining the set of differential equations which will describe the dynamical response in terms of independent nodal coordinates.

2.2. Eigenvalues and eigenmodes of a cardan joint

2.2.1. Introduction

First part of the chapter presented the motion equations for a single finite element having a general three-dimensional motion. In the following the obtained equations will be applied in order to determine the behavior of shaft of cardan joint. The shaft is in a rotation around his axisi. This axis is not fixed, being in a motion in a vertical plane but can be considered, in a first approximation, unchanged. In this a way is possible to obtain the motion equation for the whole structure in more simplier form. These equations will be used to study the motion of the shaft.

2.2.2. Simplified form of the motion equations

In the case of the rotation arround the axis of the shaft with the angular velocity $\vec{\omega}$ this will be considered constant and will have the direction with the angular acceleration $\vec{\varepsilon}$. We refer the rotation to the overall coordinate system OXYZ and we will considered the local coordinate system attached to the finite element (Fig.2.2). The rotation axis will be OZ and we will consider that the axis Oz remain identic with OZ. The rotation of the shaft axis will be defined by the rotation angle θ.

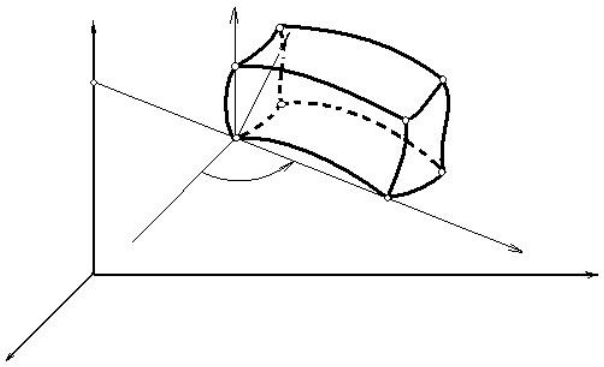

Figure 2.2. A finite element in rotation arround an axis

The symplify form of the motion equations is obtained from rel. (25) previously obtained in 2.1. Considering the null components of the angular velocity and acceleration re. (25) become, after some calculus:

$$(\boldsymbol{m}_{11}+\boldsymbol{m}_{22}+\boldsymbol{m}_{33})_{\mathrm{e}}\,\ddot{\boldsymbol{\delta}}_{e,L}+2\omega(\boldsymbol{m}_{21}-\boldsymbol{m}_{12})_{\mathrm{e}}\,\dot{\boldsymbol{\delta}}_{e,L}+[\boldsymbol{k}_{e}+\varepsilon(m_{21}-m_{12})_{\mathrm{e}} \quad + \quad \omega^{2}(m_{11}+m_{22})_{\mathrm{e}}]$$
$$\boldsymbol{\delta}_{e,L}=\boldsymbol{q}_{e}^{ext}+\boldsymbol{q}_{e}^{liaison}-\varepsilon(\boldsymbol{m}_{2x}-\boldsymbol{m}_{1y})_{\mathrm{e}}-\omega^{2}(\boldsymbol{m}_{1x}+\boldsymbol{m}_{2y})_{\mathrm{e}}-\boldsymbol{m}\,{}^{i}_{Oe}\boldsymbol{R}^{T}\,\ddot{\boldsymbol{r}}_{O} \qquad (2.16)$$

The values $\omega_x = \omega \neq 0$; $\omega_y = \omega_z = 0$; $\varepsilon_x = \varepsilon \neq 0$; $\varepsilon_y = \varepsilon_z = 0$ are considered. The rotation matrix for the plane rotation with the angle θ become:

$$R = \begin{bmatrix} \cos\theta & -\sin\theta & 0 \\ \sin\theta & \cos\theta & 0 \\ 0 & 0 & 1 \end{bmatrix}$$

If we denote with d_o the distance from O to the axis O'Z it can be written:

$$\dot{r}_o = \begin{Bmatrix} -\omega d_o \sin\theta \\ \omega d_o \cos\theta \\ 0 \end{Bmatrix} = \omega d_o \begin{Bmatrix} -\sin\theta \\ \cos\theta \\ 0 \end{Bmatrix} \quad ; \tag{2.17}$$

$$\ddot{\boldsymbol{r}}_{\boldsymbol{o}} = \varepsilon d_o \begin{Bmatrix} -\sin\theta \\ \cos\theta \\ 0 \end{Bmatrix} - \omega^2 d_o \begin{Bmatrix} \cos\theta \\ \sin\theta \\ 0 \end{Bmatrix} \quad ; \tag{2.18}$$

$$\boldsymbol{R}^T \ddot{\boldsymbol{r}}_{\boldsymbol{o}} = \varepsilon d_o \begin{Bmatrix} 0 \\ 1 \\ 0 \end{Bmatrix} - \omega^2 d_o \begin{Bmatrix} 1 \\ 0 \\ 0 \end{Bmatrix} \quad ; \tag{2.19}$$

Finally, the motion equations become:

$$(\boldsymbol{m}_{11}+\boldsymbol{m}_{22}+\boldsymbol{m}_{33})_e \ddot{\boldsymbol{\delta}}_{e,L} + 2\omega(\boldsymbol{m}_{21}-\boldsymbol{m}_{12})_e \dot{\boldsymbol{\delta}}_{e,L} + [\boldsymbol{k}_e + \varepsilon(\boldsymbol{m}_{21}-\boldsymbol{m}_{12})_e + \omega^2(\boldsymbol{m}_{11}+\boldsymbol{m}_{22})_e]$$

$$\boldsymbol{\delta}_{e,L} = \boldsymbol{q}_e^{ext} + \boldsymbol{q}_e^{liaison} - \varepsilon\left(\boldsymbol{m}_{2x} - \boldsymbol{m}_{1y} + \boldsymbol{d}_o \boldsymbol{m}_{oe}^i \begin{Bmatrix} 0 \\ 1 \\ 0 \end{Bmatrix}\right) - \omega^2\left(\boldsymbol{m}_{1x} + \boldsymbol{m}_{2y} - \boldsymbol{d}_o \boldsymbol{m}_{oe}^i \begin{Bmatrix} 1 \\ 0 \\ 0 \end{Bmatrix}\right). \tag{2.20}$$

2.2.3. Motion equation in a global coordinate system

Every finite element is related to a local coordinate system. In order to assemble these equations in a differential equation system is necessary to express all the equation in the same coordinate system. The nodal displacements vector in the global reference system $\boldsymbol{\Delta}_e = \boldsymbol{\delta}_{e,G}$ can be express can be expressed in terms of components of the same vector in local coordinate system $\boldsymbol{\delta}_{e,L}$ using the relations [vlase , cinematica]:

$$\boldsymbol{\delta}_{e,L} = \boldsymbol{R}_e^T \boldsymbol{\Delta}_e \tag{2.21}$$

Using rel. (2.21) in (2.20) it obtains:

$$(\boldsymbol{m}_{11}+\boldsymbol{m}_{22}+\boldsymbol{m}_{33})_e \boldsymbol{R}^T \ddot{\Delta}_e + 2\omega\,(\boldsymbol{m}_{21}-\boldsymbol{m}_{12})_e \boldsymbol{R}^T \dot{\boldsymbol{\Delta}}_e + [\boldsymbol{k}_e + \varepsilon(\boldsymbol{m}_{21}-\boldsymbol{m}_{12})_e + \omega^2(\boldsymbol{m}_{11}+\boldsymbol{m}_{22})_e] \text{x x}$$

$$\boldsymbol{R}^T \boldsymbol{\Delta}_e = \boldsymbol{q}_e^{ext} + \boldsymbol{q}_e^{liaison} - \varepsilon\left(m_{2x} - m_{1y} + d_o m_{oe}^i \begin{Bmatrix} 0 \\ 1 \\ 0 \end{Bmatrix}\right) - \omega^2\left(\boldsymbol{m}_{1x} + \boldsymbol{m}_{2y} - \boldsymbol{d}_o \boldsymbol{m}_{oe}^i \begin{Bmatrix} 1 \\ 0 \\ 0 \end{Bmatrix}\right) \tag{2.22}$$

and multiplying with $\boldsymbol{R}$ it is possible to obtain the motion equations written in the global coordinate system for one single finite element.

$$\boldsymbol{R}\ (\boldsymbol{m}_{11}+\boldsymbol{m}_{22}+\boldsymbol{m}_{33})_e\ \boldsymbol{R}^T\ \ddot{\boldsymbol{\Delta}}_e+2\omega\ \boldsymbol{R}\ (\boldsymbol{m}_{21}-\boldsymbol{m}_{12})_e\ \boldsymbol{R}^T\ \dot{\boldsymbol{\Delta}}_e+$$

$$+\boldsymbol{R}\ [\boldsymbol{k}_e+\varepsilon(\boldsymbol{m}_{21}-\boldsymbol{m}_{12})_e+\omega^2(\boldsymbol{m}_{11}+\boldsymbol{m}_{22})_e]\ \boldsymbol{R}^T\ \boldsymbol{\Delta}_e=$$

$$=\boldsymbol{R}\ \boldsymbol{q}_e^{ext}+\boldsymbol{R}\ \boldsymbol{q}_e^{liaison}-\boldsymbol{R}\ \varepsilon\left(\boldsymbol{m}_{2x}-\boldsymbol{m}_{1y}+\boldsymbol{d}_o\boldsymbol{m}_{oe}^i\begin{Bmatrix}0\\1\\0\end{Bmatrix}\right)-\boldsymbol{R}\ \omega^2\left(\boldsymbol{m}_{1x}+\boldsymbol{m}_{2y}-\boldsymbol{d}_o\boldsymbol{m}_{oe}^i\begin{Bmatrix}1\\0\\0\end{Bmatrix}\right). \tag{2.23}$$

After some calculus it results, in a compact form:

$$\boldsymbol{M}_e\ddot{\boldsymbol{\Delta}}_e+\boldsymbol{C}_e\dot{\boldsymbol{\Delta}}_e+\left(\boldsymbol{K}_e+\boldsymbol{K}_e(\varepsilon)+\boldsymbol{K}_e(\omega^2)\right)\boldsymbol{\Delta}_e=\mathbf{Q}_e^{ext}+\mathbf{Q}_e^{liaison}-\mathbf{Q}_e^i(\varepsilon)-\mathbf{Q}_e^i(\omega^2)-R\ \mathbf{M}^i{}_{oe}\mathbf{R}^T\ddot{\mathbf{r}}_o \tag{2.24}$$

where they made notations:

$$\boldsymbol{M}_e=\boldsymbol{R}\ (\boldsymbol{m}_{11}+\boldsymbol{m}_{22}+\boldsymbol{m}_{33})_e\ \boldsymbol{R}^T\ ;\quad \boldsymbol{C}_e=\ 2\omega\ \boldsymbol{R}\ (\boldsymbol{m}_{21}-\boldsymbol{m}_{12})_e\ \boldsymbol{R}^T\ ;$$

$$\boldsymbol{K}_e=\boldsymbol{R}\ \boldsymbol{k}_e\ \boldsymbol{R}^T\ ;\quad \boldsymbol{K}_e(\varepsilon)=\ \varepsilon\boldsymbol{R}(\boldsymbol{m}_{21}-\boldsymbol{m}_{12})_e\ \boldsymbol{R}^T\ ;\quad \boldsymbol{K}_e(\omega^2)=\omega^2\boldsymbol{R}(\boldsymbol{m}_{11}+\boldsymbol{m}_{22})\ \boldsymbol{R}^T\ ;$$

$$\boldsymbol{Q}_e^{ext}=\boldsymbol{R}\ \boldsymbol{q}_e^{ext}\ ;\ \boldsymbol{Q}_e^{liaison}=\boldsymbol{R}\ \boldsymbol{q}_e^{liaison}\ ;\ \boldsymbol{Q}_e^i(\varepsilon)=\ \boldsymbol{R}\ \varepsilon(\boldsymbol{m}_{2x}-\boldsymbol{m}_{1y})\ ;$$

$$\boldsymbol{Q}_e^i(\omega^2)=\omega^2\ \boldsymbol{R}\ (\boldsymbol{m}_{1x}+\boldsymbol{m}_{2y})\ ;\quad \boldsymbol{R}\ \boldsymbol{M}^i{}_{oe}\boldsymbol{R}^T\ddot{\boldsymbol{r}}_o=d_0\ \boldsymbol{R}\ \boldsymbol{m}_{oe}^i\left(\varepsilon\begin{Bmatrix}0\\1\\0\end{Bmatrix}-\omega^2\begin{Bmatrix}1\\0\\0\end{Bmatrix}\right)\quad .$$

We shall write down

$$\boldsymbol{Q}_e^{inertia}=-\boldsymbol{Q}^i{}_e(\varepsilon)-\boldsymbol{Q}^i{}_e(\omega^2)-\boldsymbol{R}\,\boldsymbol{M}^i{}_{oe}\boldsymbol{R}^T\ddot{\boldsymbol{r}}_o$$

We obtain the final form of equations of motion in the global coordinate system, in which the kinematic conditions have not been considered (the liaisons between elements, the link between bodies):

$$\boldsymbol{M}_e\ddot{\boldsymbol{\Delta}}_e+\boldsymbol{C}_e\dot{\boldsymbol{\Delta}}_e+\left(\boldsymbol{K}_e+\boldsymbol{K}_e(\varepsilon)+\boldsymbol{K}_e(\omega^2)\right)\boldsymbol{\Delta}_e=\ \boldsymbol{Q}_e^{ext}+\boldsymbol{Q}_e^{liaison}+\boldsymbol{Q}_e^{inertia} \tag{2.24'}$$

2.2.4. Motion equations assembling

In the dynamical analysis of a multibody system with elastic elements the unknowns occuring can be classified in: nodal displacements unknowns and liaison forces unknowns. By a proper assembly of motion equations written for each finite element in a global reference system we can eliminate the algebraic unknowns ([BLA11] , [KHA11], [VLA87]) (which usually are liaison forces); in this case the unknowns nodal displacement remain the only unknowns.

The liaisons between the finite elements are achieved by nodes which defining the considered element. Generally the relationships between the displacements of nodes and the

independent coordinates of the system can be expressed, for the *e* - th element, by a linear relation :

$$\boldsymbol{\Delta_e = A_e d} \tag{2.25}$$

or, in a compact form, for the all elements:

$$\boldsymbol{\Delta} = \begin{Bmatrix} \boldsymbol{\Delta}_1 \\ \boldsymbol{\Delta}_2 \\ \vdots \\ \boldsymbol{\Delta}_n \end{Bmatrix} = \begin{bmatrix} \boldsymbol{A}_1 & & & 0 \\ & \boldsymbol{A}_2 & & \\ & & \ddots & \\ 0 & & & \boldsymbol{A}_n \end{bmatrix} = \boldsymbol{A\,d} \tag{2.26}$$

By differentiation we obtain:

$$\dot{\boldsymbol{\Delta}} = \boldsymbol{A}\dot{\boldsymbol{d}} \tag{2.27}$$

and

$$\ddot{\Delta} = \boldsymbol{A}\ddot{\boldsymbol{d}}\,. \tag{2.28}$$

Here $\boldsymbol{\Delta}$ represents the vector of nodal displacements, $\boldsymbol{\Delta_e}$ the vector of nodal displacements of element *e* with components expressed in the fixed (global) coordinates system and $\boldsymbol{d}$ the vector of independent coordinates:

$$\boldsymbol{d} = \left[d_1\ d_2 \cdots d_s\right]^T \quad .$$

If we take into account relations (2.26)-(2.28) , (2.24') can be written:

$$\boldsymbol{M\,A}\ddot{d} + \boldsymbol{C\,A}\dot{d} + \left(\boldsymbol{K} + \boldsymbol{K}(\varepsilon) + \boldsymbol{K}(\omega^2)\right)\boldsymbol{A}\,d = \boldsymbol{Q^{ext} + Q^{liaison} + Q^{inertia}} \tag{2.29}$$

The work of the liaison forces can be written, using the velocity expressions, as:

$$dL_e = \dot{\Delta}_e{}^T \boldsymbol{Q}_e^{\,liaison}\,dt \tag{2.30}$$

If we write the equations for all the elements of the system is obtained:

$$dL = \left(\dot{\Delta}_1{}^T \mathbf{Q}_1^{\,liaison} + \dot{\Delta}_2{}^T \mathbf{Q}_2^{\,liaison} + \ldots \quad + \dot{\Delta}_n{}^T \mathbf{Q}_n^{\,liaison}\right)dt = \dot{\boldsymbol{\Delta}}^T \boldsymbol{Q}^{liaison}\,dt = \dot{\boldsymbol{q}}^T \boldsymbol{A}^T \boldsymbol{Q}^{liaison}\,dt \tag{2.31}$$

The work of the liaison forces for an ideal system must be null references [2.1],[2.4] ([BLA11] , [VLA87]) thus:

$$\boldsymbol{A}^T \boldsymbol{Q}^{liaison} = 0 \tag{2.32}$$

Lets pre-multiply the relation (2.29) by $\boldsymbol{A}^T$ resulting in:

$$\boldsymbol{A}^T \boldsymbol{M A}\ddot{d} + \boldsymbol{A}^T \boldsymbol{C A}\dot{d} + \boldsymbol{A}^T \left(\boldsymbol{K} + \boldsymbol{K}(\varepsilon) + \boldsymbol{K}(\omega^2)\right)\boldsymbol{A}\,d = \mathbf{A}^T \mathbf{Q}^{ext} + \mathbf{A}^T \mathbf{Q}^{liaison} + \mathbf{A}^T \mathbf{Q}^{inertia} \tag{2.33}$$

If relation (2.32) is taken into account the liaison forces will disappear because of their orthogonality with respect to the displacements. It results:

$$\boldsymbol{A}^T \boldsymbol{M\,A}\ddot{d} + \boldsymbol{A}^T \boldsymbol{C\,A}\dot{d} + \boldsymbol{A}^T \left(\boldsymbol{K} + \boldsymbol{K}(\varepsilon) + \boldsymbol{K}(\omega^2)\right)\boldsymbol{A}\,d = \boldsymbol{A^T Q^{ext} + A^T Q^{inertia}} \tag{2.34}$$

or, shortly:

$$\boldsymbol{m}\ddot{\boldsymbol{d}} + \boldsymbol{c}\dot{\boldsymbol{d}} + \boldsymbol{k}\,\boldsymbol{d} = \boldsymbol{q} \tag{2.35}$$

where:

$$\boldsymbol{m} = \boldsymbol{A}^T \boldsymbol{M}\,\boldsymbol{A} \;\; ; \;\; \boldsymbol{c} = \boldsymbol{A}^T \boldsymbol{C}\,\boldsymbol{A} \;\; ; \;\; \boldsymbol{k} = \boldsymbol{A}^T \left(\boldsymbol{K} + \boldsymbol{K}(\varepsilon) + \boldsymbol{K}(\omega^2)\right)\boldsymbol{A} \;\; ; \;\; \boldsymbol{q} = \boldsymbol{A}^T \boldsymbol{Q}^{ext} + \boldsymbol{A}^T \boldsymbol{Q}^{inertia} .$$

The differential equation system obtained is nonlinear, the matrices from the left term depending on the instantaneous configuration of the mechanical system with liaisons .

2.2.5. The cardan joint analysis

Consider a cardan joint used in thansmission of a truck (fig.2.3). If a stady state response is considered, the cardan joint will have angular velocity $\vec{\omega}$. For a short period Δt it can be made the hypothesis of constant angular velocity. The motion can be considered "frozen" and it is possible to determine the eigenvalues and the eigenvectors for the cardan joint, using the well known procedure provided by the numerical calculus enviroment. [2.3] [PEN09]. The obtained results will be compare with the results obtained considering the stady state response.

Figure 2.3. The cardan joint analysed

Table 2.1. The eigenvalues

MODE NUMBER (WITHOUT RIGID BODY MODE)	CLASSIC MODEL – EIGENVALUES (HZ)	PROPOSED MODEL – EIGENVALUES (HZ)
4	5514	5865
5	5514	5865
6	7045	7323
7	7045	7323
8	8959	9180
9	8959	9180
10	9416	9626
11	10641	10827
12	10641	10827
13	11713	11883
14	11713	11883
15	12767	12923
16	14284	14423
17	14284	14423
18	14910	15044

In Fig. 2.4 are presented the eigenvalus in both two cases, calculated in Table 2.1.

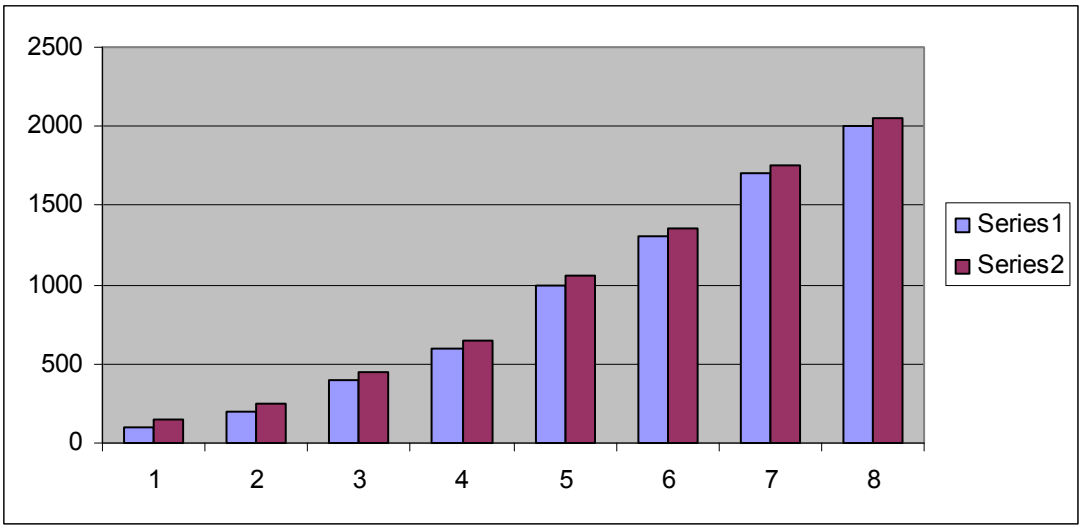

Figure 2.4. The eigenvalues in two different cases presented

The eigenmodes are represented in Fisg. 2.5-2.12.

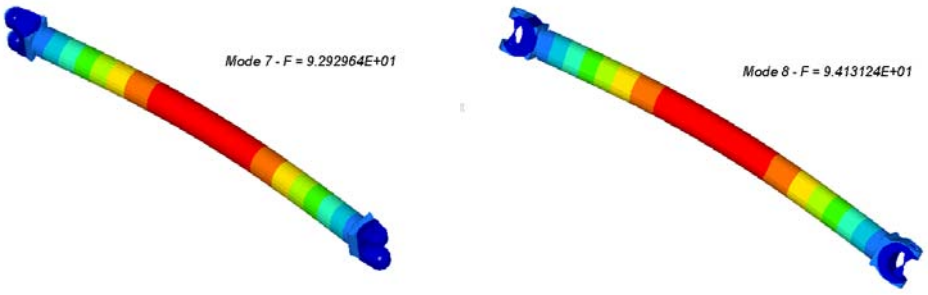

Figure 2.5. Modes 7 and 8

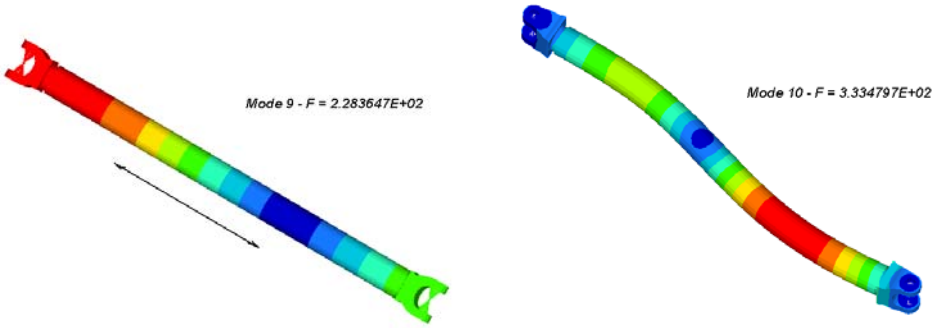

Figure 2.6. Modes 9 and 10

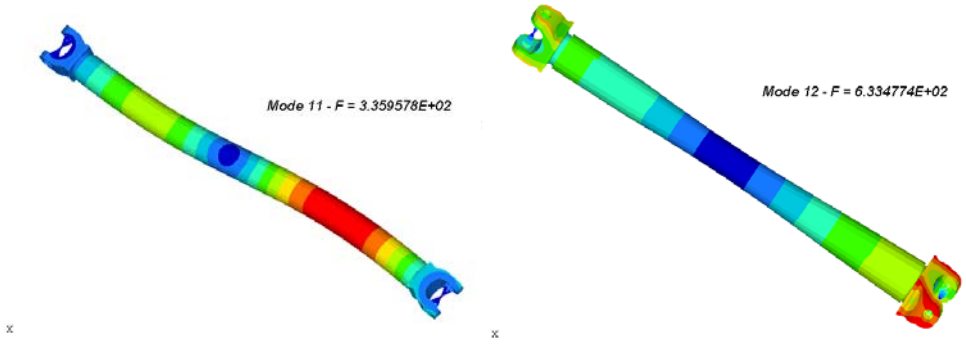

Figure 2.7. Modes 11 and 12

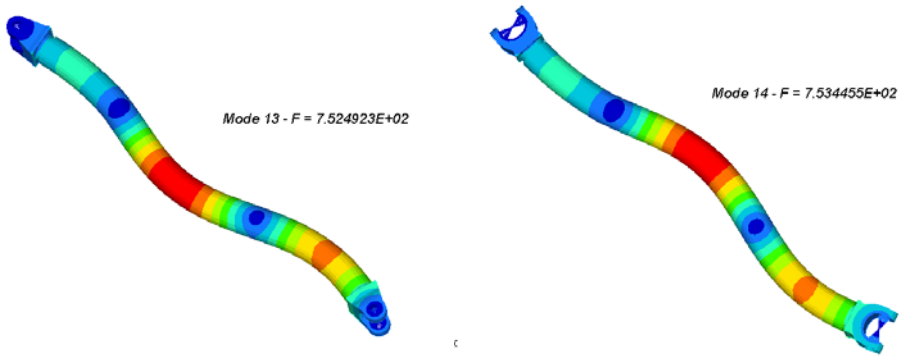

Figure 2.8. Modes 13 and 14

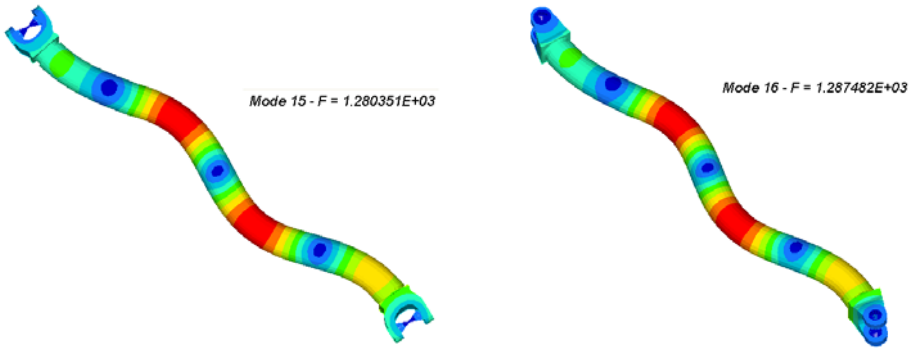

Figure 2.9. Modes 15 and 16

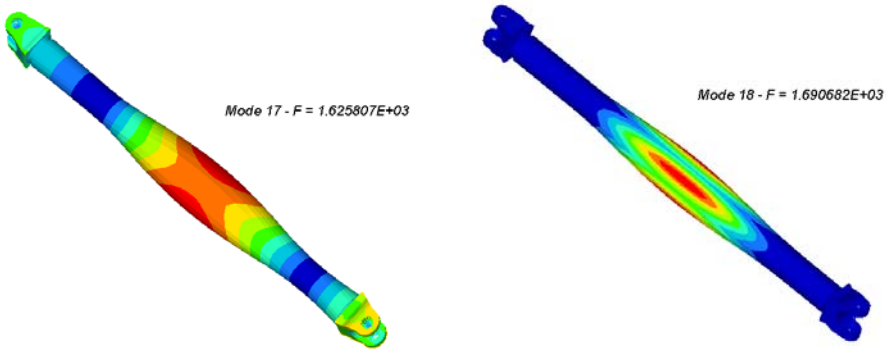

Figure 2.10. Modes 17 and 18

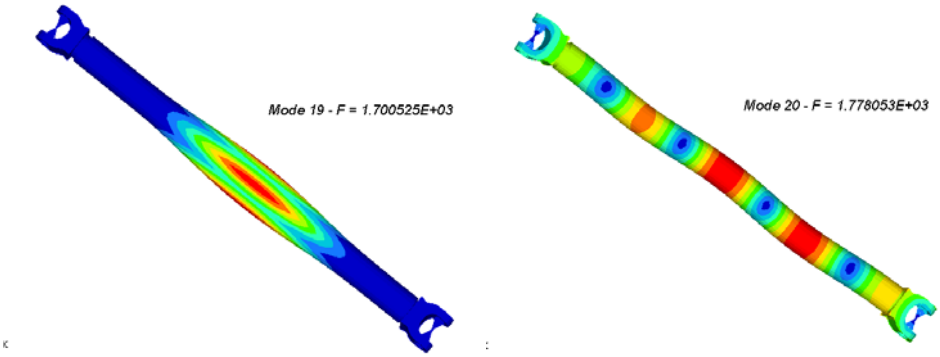

Figure 2.11. Modes 19 and 20

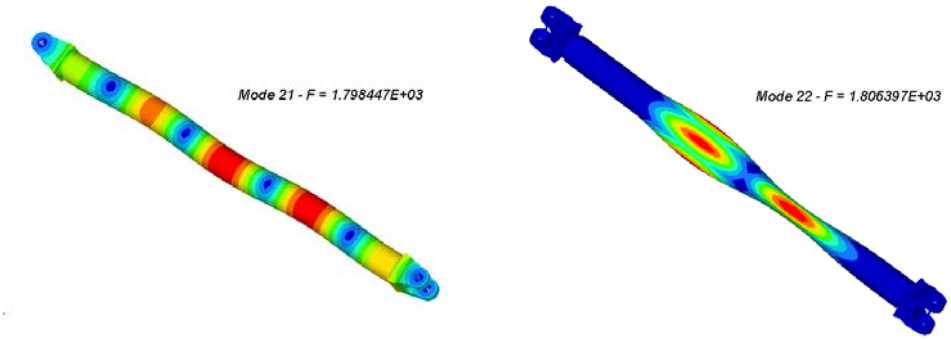

Figure 2.12. Modes 21 and 22

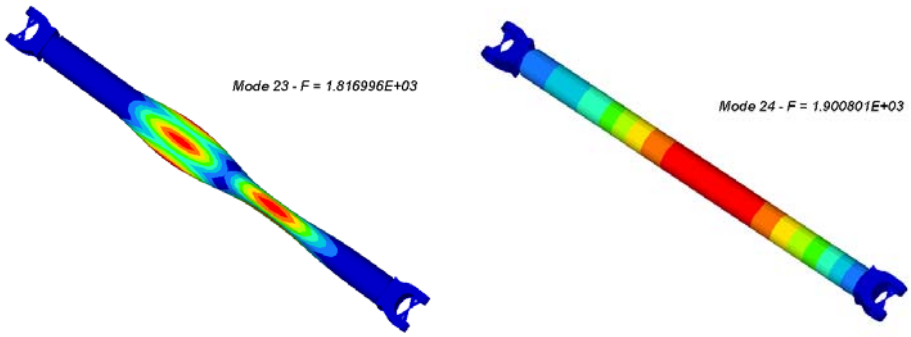

Figure 2.13. Modes 23 and 24

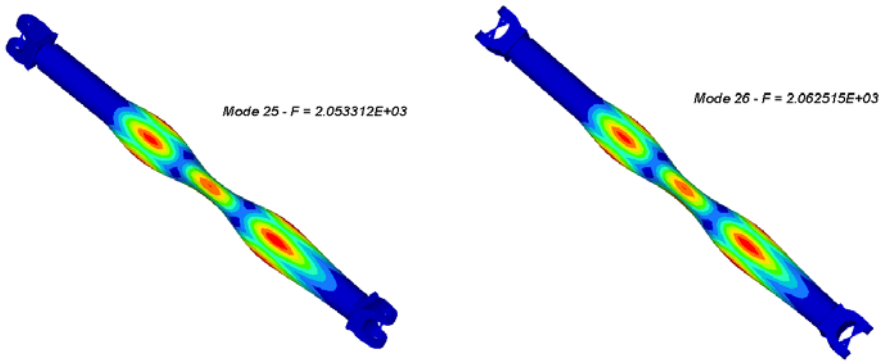

Figure 2.14. Modes 25 and 26

2.2.6. Conclusions

In section 2.2.1 of the chapter we presented the form of motion equations containing the new terms of the motion equations :

- $2\boldsymbol{c}_e(\omega)\ \dot{\boldsymbol{\delta}}_{e,L}$ - are Coriolis forces as a result of the relative motions $\dot{\boldsymbol{\delta}}_{e,L}$ of nodal coordinates relative to the mobile coordinate system; the matrix $\boldsymbol{c}_e$ is a skew symmetric one;
- $\boldsymbol{k}_e(\varepsilon) + \boldsymbol{k}_e(\omega^2)$ - change of the stiffness matrix as a result of the action of the accelerations of rotation;

The influence of these terms will modify the dynamic response of the system. In the section 2.2 was analysed how big is this influence. It can observe a differenece between the eigenvalues in these two case considered.

2.3. Finite Element Analysis of a Two-Dimensional Linear Elastic Systems with a Plane "Rigid Motion"

The results presented in this section are a presentation of the problem of a two-dimensional finite element in plane motion ([VLA12], [VLA87a], [VLA87b]) with applications to a disk ([VLA13a]). Discretizing a mechanical structure as part of finite element procedure makes it necessary to use a variety of finite elements, according to the shape and geometry of the analyzed system. Two-dimensional finite elements are widely used in finite element analysis and using them is generally easy and fast.

Dynamic analysis of a system using finite element finite enforces the use of numerous additional terms that can no longer be neglected. In this section will be determine the motion equations for a two-dimensional finite element where we distinguish the additional terms that can eventually change the qualitative and quantitative behavior of the system. The motion equations are obtained using classic theorems of mechanics and Lagrange's equations.

2.3.1. Introduction

This section aims to perform the dynamic response and to determine the equations of motion for a two-dimensional finite element, having a "rigid" plan-parallel motion. In this way it is possible to study the phenomena of resonance and loss of stability as manifestations of elasticity.

It is previously considered that the field of velocities and accelerations was already determined for all the elements of the system (considered as “rigid”). A finite element in a "rigid" motion along with the body which it discretizes will be analyzed. In order to determine the equations of motion, the Lagrange equations will be used. For this, it is necessary to determine the kinetic energy and the internal energy for the elements of the mechanical system (considered linear elastic).

If the obtained equations will be compared with the steady state response equations, new terms will be found. These appear due to the relative motion of independent coordinates relative to the mobile reference systems which are attached to the elements of the mechanical system (Coriolis effects) and they will determine changes in stiffness and in the inertial terms along with the appearance of some conservative damping.

2.3.2. Motion Equations

Let's consider a two-dimensional finite element with a plan parallel motion. The type of finite element which will be used will determine finally the shape functions and the last form for the matrix coefficients. In what follows it is used the hypothesis that the deformations are small enough not to influence the general rigid motion of the system.

The field of velocities and accelerations for each two-dimensional element of the multicorp systems are considered to be solved (see [PEN09]). The finite element is related to the local coordinates system Oxy, which participates to the motion (Fig. 2.15) with the element, so it has a known rigid motion. Let's consider $\boldsymbol{v}_o\ (\dot{\boldsymbol{X}}_o, \dot{\boldsymbol{Y}}_o, 0)$ being the velocity and $\boldsymbol{a}_o\ (\ddot{\boldsymbol{X}}_o, \ddot{\boldsymbol{Y}}_o, 0)$ being the acceleration of the origin of the mobile reference system related to the fixed reference system OXY, to which the whole motion of the mechanical system relates. We will consider $\boldsymbol{\omega}\,(0,\ 0,\ \omega)$ as being the angular velocity of the solid containing the finite element and $\boldsymbol{\varepsilon}\ (0, 0, \varepsilon)$ as being the angular acceleration of the same solid.

If we consider $\boldsymbol{r}_{M,G}$ as being the position vector of the M point, we have:

$$\boldsymbol{r}_{M,G} = \boldsymbol{r}_{O,G} + \boldsymbol{r}_{G} = \boldsymbol{r}_{O,G} + \boldsymbol{R} \cdot \boldsymbol{r}_{L} \tag{2.36}$$

where we consider G defining the vectorial entities which have their components relating to the global reference system and L defining the vectorial entities which have their components relating to the local reference system.

For the plane motion the rotation transformation matrix $\boldsymbol{R}$ has a very simple form:

$$\boldsymbol{R} = \begin{bmatrix} \cos\theta & -\sin\theta \\ \sin\theta & \cos\theta \end{bmatrix}. \tag{2.37}$$

If the current point M is subjected to a displacement $\boldsymbol{f}_L$, transforming into the M' point, the position vector of M' become:

$$\boldsymbol{r}_{M',G} = \boldsymbol{r}_{O,G} + \boldsymbol{R} \cdot (\boldsymbol{r}_L + \boldsymbol{f}_L) \tag{2.38}$$

where the position vector of the point M' has the components relating to the global reference system. The continuous displacement field $\boldsymbol{f}(x,y)_L$ is approximated in the finite element method, using the relationship:

$$\boldsymbol{f}_L = \boldsymbol{N}(x,y)\ \boldsymbol{\delta}_e(t)_L \tag{2.39}$$

where the elements of the $\boldsymbol{N}$ matrix (which contains the interpolation functions) depend on the type of the chosen finite element.

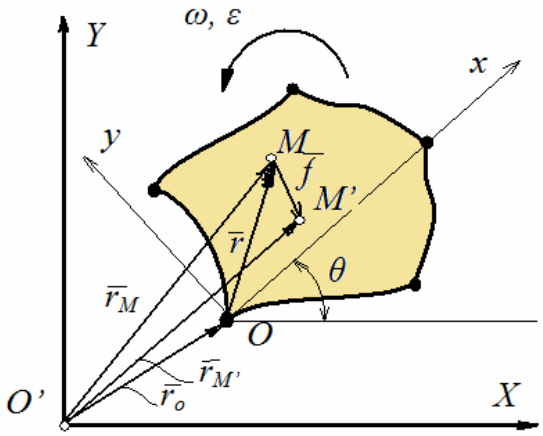

Figure 2.15. A two-dimensional finite element with plan motion

The velocity of the *M'* point, related to the fixed coordinate system, will be:

$$\boldsymbol{v}_{M',G} = \dot{\boldsymbol{r}}_O + \dot{\boldsymbol{R}}\,\boldsymbol{r}_L + \dot{\boldsymbol{R}}\,\boldsymbol{f}_L + \boldsymbol{R}\,\dot{\boldsymbol{f}}_L = \dot{\boldsymbol{r}}_O + \dot{\boldsymbol{R}}\,\boldsymbol{r}_L + \dot{\boldsymbol{R}}\,\boldsymbol{N}\,\boldsymbol{\delta}_{e,L} + \boldsymbol{R}\,\boldsymbol{N}\,\dot{\boldsymbol{\delta}}_{e,L} \tag{2.40}$$

The equations of motion will be obtained in the local coordinates system. The kinetic energy of the considered element will be determined using the relationship:

$$E_c = \frac{1}{2}\int_V \rho v^2 dV = \frac{1}{2}\int_V \rho\, \boldsymbol{v}^T_{M',L}\, \boldsymbol{v}_{M',L}\, dV \tag{2.41}$$

The classic form for the deformation energy is:

$$E_p = \frac{1}{2}\int_V \boldsymbol{\sigma}^T\ \boldsymbol{\varepsilon}\ dV \tag{2.42}$$

For the ease of understanding, we remember that the generalized Hooke law is:

$$\boldsymbol{\sigma} = \boldsymbol{D}\ \boldsymbol{\varepsilon} \tag{2.43}$$

where, for a two-dimensional finite element (plane state of deformation) we have:

$$\boldsymbol{D} = \frac{E}{(1-\mu)(1-2\mu)}\begin{bmatrix} 1-\mu & 0 & 0 \\ 0 & 1-\mu & 0 \\ 0 & 0 & \frac{1-2\mu}{2} \end{bmatrix} \tag{2.44}$$

The relation between the specific deformations and the finite deformations of the nodes can be expressed as:

$$\boldsymbol{\varepsilon} = \boldsymbol{a}\,\boldsymbol{f} \tag{2.45}$$

where $\boldsymbol{a}$ is a differentiation operator:

$$\boldsymbol{a} = \begin{bmatrix} \frac{\partial}{\partial x} & 0 & 0 \\ 0 & \frac{\partial}{\partial y} & 0 \\ \frac{\partial}{\partial y} & \frac{\partial}{\partial x} & 0 \end{bmatrix} . \tag{2.46}$$

Considering all this, for the deformation energy we have:

$$E_p = \frac{1}{2}\int_V \boldsymbol{\delta}_{e,L}^{T}\, \boldsymbol{k}_e\, \boldsymbol{\delta}_{e,L}\, dV \tag{2.47}$$

with $\boldsymbol{k}_e$ being the stiffness element matrix:

$$\boldsymbol{k}_e = \int_V \boldsymbol{N}^T \boldsymbol{a}^T \boldsymbol{D}^T \boldsymbol{a}\, \boldsymbol{N}\, dV. \tag{2.48}$$

If $\boldsymbol{p} = \boldsymbol{p}(x,y)$ is the vector of the distributed forces, then the external work of those forces is:

$$W = \int_V \boldsymbol{p}_L^{T}\, \boldsymbol{f}_L\, dV = \left(\int_V \boldsymbol{p}_L^{T}\, \boldsymbol{N}\, dV\right) \boldsymbol{\delta}_{e,L} \tag{2.49}$$

The nodal forces $\boldsymbol{q}_e^T$ give an external work:

$$\boldsymbol{W}^c = \boldsymbol{q}_{e,L}^{T}\, \boldsymbol{\delta}_{e,L} . \tag{2.50}$$

Now it is possible to write the Lagrangean for the considered element:

$$L = E_c - E_p + W + W^c =$$

$$= \frac{1}{2}\int_V \rho\, \dot{\boldsymbol{r}}_o^{T}\, \dot{\boldsymbol{r}}_o\, dV - \frac{1}{2}\int_V \boldsymbol{\delta}_{e,L}^{T}\, \boldsymbol{k}_e\, \boldsymbol{\delta}_{e,L}\, dV + \left(\int_V \boldsymbol{p}_L^{T}\, \boldsymbol{N}\, dV\right) \boldsymbol{\delta}_{e,L} + \boldsymbol{q}_{e,L}^{T}\, \boldsymbol{\delta}_{e,L} \tag{2.51}$$

The equations of motion can be obtained by applying the Lagrange equations. After some ordering, we can write the equations of motion for the finite element in the form:

$$\left(\int_V \boldsymbol{N}^T\, \boldsymbol{N}\, \rho dV\right) \ddot{\boldsymbol{\delta}}_{e,L} + 2\left(\int_V \boldsymbol{N}^T \boldsymbol{R}^T\, \dot{\boldsymbol{R}}\, \boldsymbol{N}\, \rho dV\right) \dot{\boldsymbol{\delta}}_{e,L} + \left(\boldsymbol{k}_e + \int_V \boldsymbol{N}^T \boldsymbol{R}^T\, \ddot{\boldsymbol{R}}\, \boldsymbol{N}\, \rho dV\right) \boldsymbol{\delta}_{e,L} =$$

$$\boldsymbol{q}_e + \int_V \boldsymbol{N}^T \boldsymbol{p}_L\, dV - \left(\int_V \boldsymbol{N}^T \rho dV\right) \boldsymbol{R}^T\, \ddot{\boldsymbol{r}}_o - \int_V \boldsymbol{N}^T \boldsymbol{R}^T\, \ddot{\boldsymbol{R}}\, \boldsymbol{r}\, \rho dV \tag{2.52}$$

The equations of motion can be written in a concentrated form:

$$\boldsymbol{m}_{e}\ddot{\boldsymbol{\delta}}_{e,L}+2\boldsymbol{c}_{e}\dot{\boldsymbol{\delta}}_{e,L}+[\boldsymbol{k}_{e}+\boldsymbol{k}_{e}(\varepsilon)+\boldsymbol{k}_{e}(\omega^{2})]\,\boldsymbol{\delta}_{e,L}=$$

$$=\boldsymbol{q}_{e}+\boldsymbol{q}^{*}_{e,L}-\boldsymbol{q}^{i}_{e,L}(\varepsilon)-\boldsymbol{q}^{i}_{e,L}(\omega^{2})-\boldsymbol{m}^{i}_{Oe}\boldsymbol{R}^{T}\ddot{\boldsymbol{r}}_{O} \tag{2.53}$$

where is denoted:

$$\boldsymbol{q}^{*}_{e,L}=\int_{V}\boldsymbol{N}^{T}\boldsymbol{p}_{L}dV\ ;\ \boldsymbol{m}^{i}_{Oe}=\int_{V}\boldsymbol{N}^{T}\rho dV;\quad \boldsymbol{m}_{e}=\int_{V}\boldsymbol{N}^{T}\boldsymbol{N}\,\rho dV=\boldsymbol{m}_{11}+\boldsymbol{m}_{22}\ ;$$

$$\boldsymbol{c}_{e}(\omega)=\int_{V}\boldsymbol{N}^{T}\boldsymbol{R}^{T}\dot{\boldsymbol{R}}\,\boldsymbol{N}\,\rho dV\ ;$$

$$\boldsymbol{k}_{e}(\varepsilon)+\boldsymbol{k}_{e}(\omega^{2})=\int_{V}\boldsymbol{N}^{T}\boldsymbol{R}^{T}\ddot{\boldsymbol{R}}\,\boldsymbol{N}\,\rho dV\ ;$$

$$\boldsymbol{q}^{i}_{e,L}(\varepsilon)+\boldsymbol{q}^{i}_{e,L}(\omega)=\int_{V}\boldsymbol{N}^{T}\boldsymbol{R}^{T}\ddot{\boldsymbol{R}}\boldsymbol{r}\ \rho dV \tag{2.54}$$

The matrix products where the rotation transformation matrix appears can easily be calculated, as this matrix is determined by only one element, the angle θ. The skew-symmetric matrix:

$$\boldsymbol{\omega}=\dot{\boldsymbol{R}}\,\boldsymbol{R}^{T}=\begin{bmatrix}0 & -\omega\\ \omega & 0\end{bmatrix}=\omega\begin{bmatrix}0 & -1\\ 1 & 0\end{bmatrix} \tag{2.55}$$

represents the angular velocity operator. We also have:

$$\ddot{\boldsymbol{R}}\,\boldsymbol{R}^{T}=\varepsilon\begin{bmatrix}0 & -1\\ 1 & 0\end{bmatrix}-\omega^{2}\begin{bmatrix}1 & 0\\ 0 & 1\end{bmatrix}. \tag{2.56}$$

If we consider $\boldsymbol{N}_{(1)}$ and $\boldsymbol{N}_{(2)}$ being the rows of the matrix N, with the notations:

$$\boldsymbol{m}_{1x}=\int_{V}N^{T}_{(1)}x\,\rho dV\ ;\ \boldsymbol{m}_{1y}=\int_{V}\boldsymbol{N}^{T}_{(1)}y\,\rho dV\ ;\quad \boldsymbol{m}_{11}=\int_{V}\boldsymbol{N}_{(1)}\boldsymbol{N}^{T}_{(1)}\,\rho dV\ ;$$

$$\boldsymbol{m}_{2x}=\int_{V}N^{T}_{(2)}x\,\rho dV\ ;\ \boldsymbol{m}_{2y}=\int_{V}\boldsymbol{N}^{T}_{(2)}y\,\rho dV\ ;\quad \boldsymbol{m}_{22}=\int_{V}\boldsymbol{N}_{(2)}\boldsymbol{N}^{T}_{(2)}\,\rho dV\ ; \tag{2.57}$$

we can obtain the equations of motion for the finite element, with explicit dependencies on the angular velocity ω and angular acceleration ε. We can made the notations:

$$\boldsymbol{m}_{e}=(\boldsymbol{m}_{11}+\boldsymbol{m}_{22})_{e};\ \boldsymbol{c}_{e}(\omega)=\omega\ \left(m_{21}-m_{12}\right)_{e}$$

$$\boldsymbol{k}_{e}(\varepsilon)+\boldsymbol{k}_{e}(\omega^{2})=\varepsilon\left(\boldsymbol{m}_{21}-\boldsymbol{m}_{12}\right)_{e}-\omega^{2}\left(\boldsymbol{m}_{11}-\boldsymbol{m}_{22}\right)_{e}$$

$$\boldsymbol{q}^{i}_{e,L}(\varepsilon)+\boldsymbol{q}^{i}_{e,L}(\omega)=\varepsilon\left(\boldsymbol{m}_{2x}-\boldsymbol{m}_{1y}\right)_{e}-\omega^{2}\left(\boldsymbol{m}_{1x}+\boldsymbol{m}_{2y}\right)_{e} \tag{2.58}$$

With these notations the equations of motion will be:

$$(\boldsymbol{m}_{11}+\boldsymbol{m}_{22})_{e}\ddot{\boldsymbol{\delta}}_{e,L}+2\omega(\boldsymbol{m}_{21}-\boldsymbol{m}_{12})_{e}\dot{\boldsymbol{\delta}}_{e,L}+[\boldsymbol{k}_{e}+\varepsilon\left(\boldsymbol{m}_{21}-\boldsymbol{m}_{12}\right)_{e}-\omega^{2}\left(\boldsymbol{m}_{11}+\boldsymbol{m}_{22}\right)_{e}]\,\boldsymbol{\delta}_{e,L}=$$

$$=\boldsymbol{q}_{e}^{ext}+\boldsymbol{q}_{e}^{liaison}-\varepsilon\left(\boldsymbol{m}_{2x}-\boldsymbol{m}_{1y}\right)_{e}+\omega^{2}\left(m_{1x}+m_{2y}\right)_{e}-\boldsymbol{m}^{i}_{Oe}\boldsymbol{R}^{T}\ddot{\boldsymbol{r}}_{O}\ . \tag{2.59}$$

Using a correct assembly of the equations of motion, written by each finite element, the algebraic unknowns (the contact forces) can be removed (see [BLA11], [KHA11], [VLA87a] , [VLA87b]) The equations of motion for the whole multibody system will be possible to be written as a system of 2nd order non-linear differential equations. The matrix coefficients of this system of equations have the following properties:

- The inertial matrix ***m*** is symmetric;
- The damping matrix ***c*** is a skew symmetric matrix. The terms defined by this matrix represent the Coriolis accelerations, due to relative motions of nodal displacements with respect to the mobile reference coordinate system, linked to the moving parts of the studied system;
- The stiffness matrix ***k*** contains both symmetric and skew symmetric terms. Moreover, this matrix can have singularities due to the rigid motion of the system that have to be removed before conducting the study of the system.

2.3.3. Modal Analysis of a Rotatings Disk

Let's now consider a rotating disk. If we consider a stady state motion, the disk will rotate with an angular velocity ω. In a very small interval Δt we may consider that the angular velocity is constante and we intend to achieve the modal analysis of rotating disk. We will use the method previously presented for carrying out the calculation and compare the results with that obtained by applying the classic version of the method of finite elements. We consider two cases:

A. The rotating disk has a plan motion and the finite element is in a plane displacement field. The eigenvalues are presented in Table 1 and the eigenvector in Fig.2.16-Fig.2.20

Table 2.3. The eigenvalues of the disk

MODE NUMBER (WITHOUT RIGID BODY MODE)	CLASSIC MODEL – EIGENVALUES (HZ)	PROPOSED MODEL – EIGENVALUES (HZ)
4	5514	5865
5	5514	5865
6	7045	7323
7	7045	7323
8	8959	9180
9	8959	9180
10	9416	9626
11	10641	10827
12	10641	10827
13	11713	11883
14	11713	11883
15	12767	12923
16	14284	14423
17	14284	14423
18	14910	15044

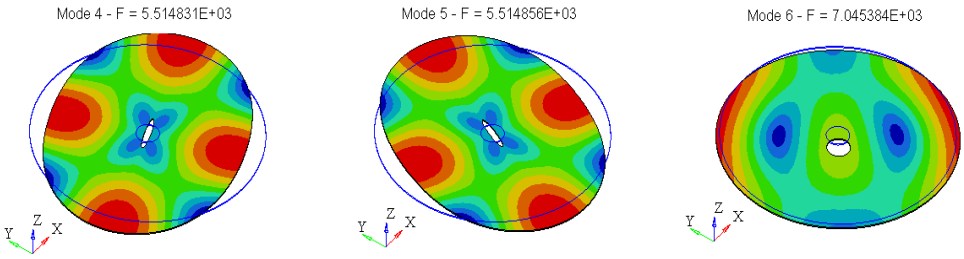

Figure 2.16. Eigenmodes 4,5 and 6

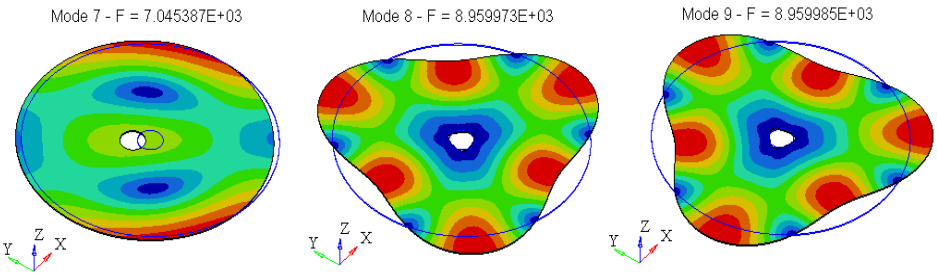

Figure 2.17. Eigenmodes 7,8 and 9

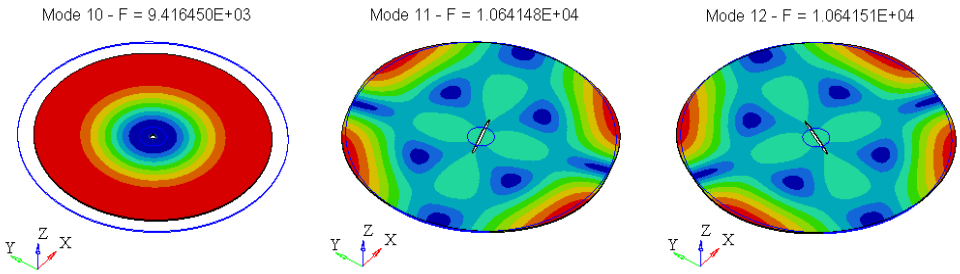

Figure 2.18. Eigenmodes 10,11 and 12

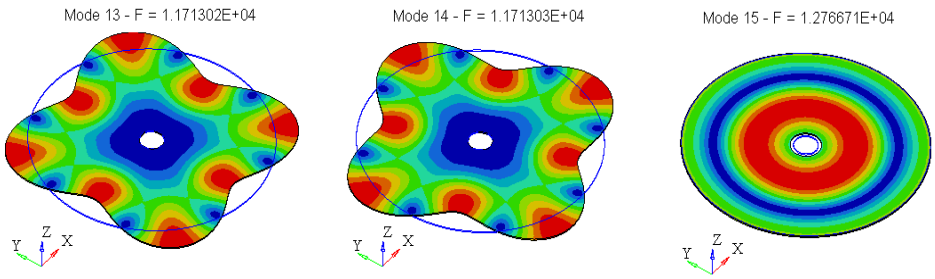

Figure 2.19. Eigenmodes 13, 14 and 15

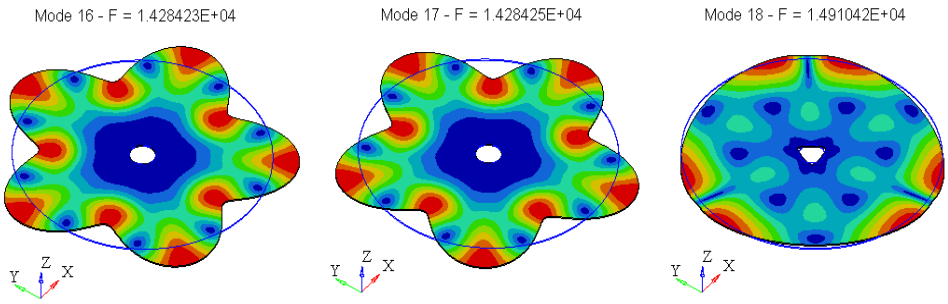

Figure 2.20. Eigenmodes 16,17 and 18

B. The rotating disk has a plan motion and the finite element is in a general displacement field. The eigenmodes are presented in Fig.2.21-Fig.2.25.

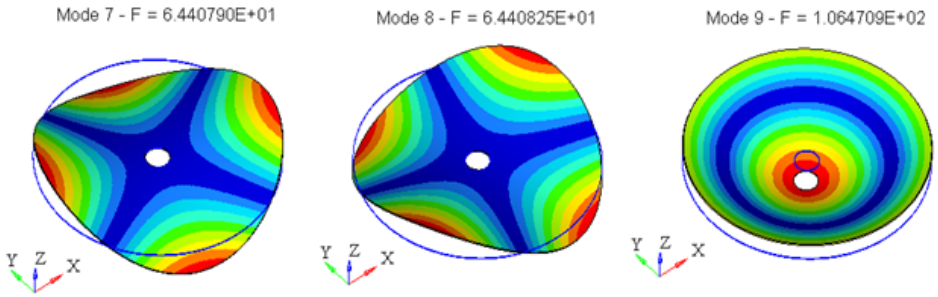

Figure 2.21. Eigenmodes 7,8 and 9

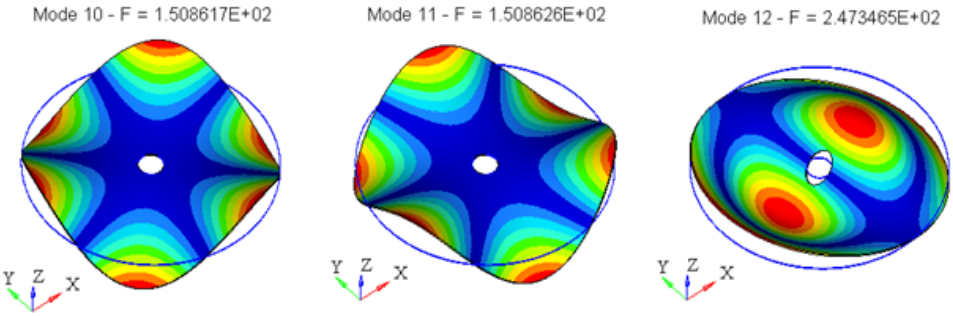

Figure 2.22. Eigenmodes 10,11 and 12

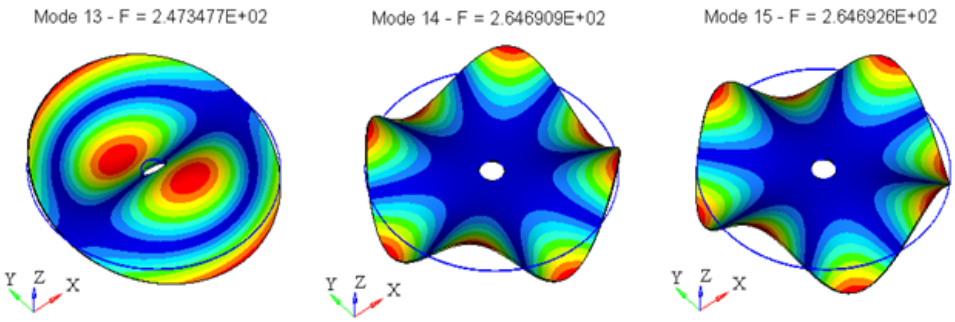

Figure 2.23. Eigenmodes 13,14 and 15

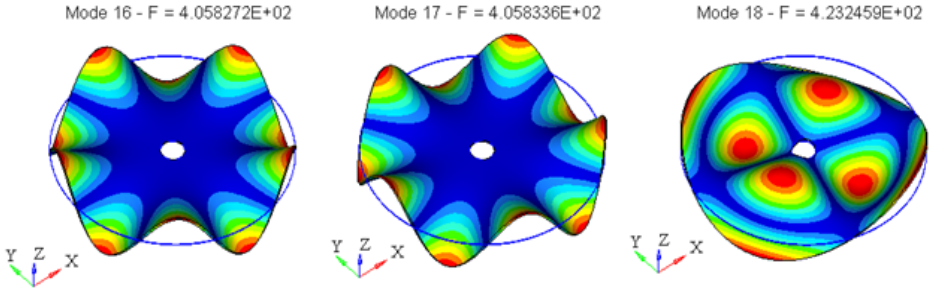

Figure 2.24. Eigenmodes 16,17 and 18

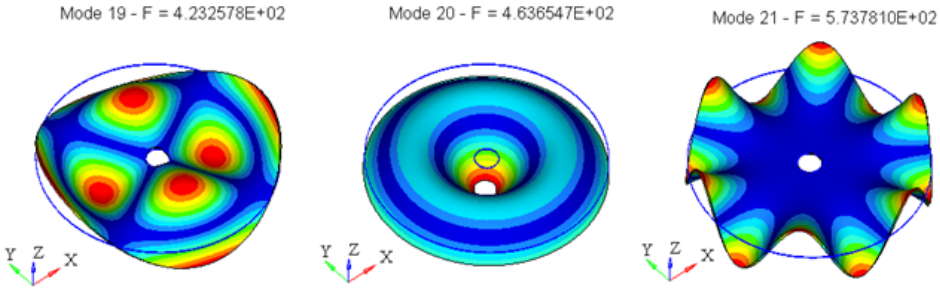

Figure 2.25. Eigenmodes 19,20 and 21

2.3.4. Conclusions

The additional terms in the equations of motion will influence the dynamic response of the system. It may happen that a resonant state or a loss of stability state to be reached. The changes in the values of eigenvalues considering a rotating disk (along its own axis) were presented previously. An upwards displacement for all the eigenvalues can be observed - this happens because an increase in stiffness takes place in this situation (rotation), due to the inertial forces. The vibration modes remain practically the same, while a small change in the amplitudes

can be observed. The presence of inertial and Coriolis effects can significantly modify, in some situations, the dynamic response of the system.

2.4. Some properties of motion equations

2.4.1. Introduction

The industrial applications use instruments and machines operating at high speeds, developing high forces, low temperatures, corrosive environments, extreme pressures, and so forth. Under these conditions, the elasticity of elements such a machine is built of cannot be ignored anymore, and models are needed to more accurately "grasp" the mechanical phenomena accompanying the operation. The vibrations and the loss of stability are the main effects occurring under these conditions. For the study on this kind of systems with rigid motion and elastic elements, numerous models have been elaborated, the main idea being the discretization of the elements and the use of finite element method. Finally, second-order differential equations with variable coefficients are obtained; these equations are strong nonlinear ones due to the time-dependent values of angular speed and acceleration, and they can be linearized considering a very short period of time, in which the motion is considered to be "frozen."

The aim of this paper is to present some characteristic properties of these systems. A mechanical system, a machine or instrument, is made up of elastic elements, the elasticity manifesting itself more or less. The rigid elements assumption generally made when studying such technical systems represents a first approximation leading to rapid results closer to reality. Depending on the given instrument operation conditions, this assumption may lead to correct results or to results considerably deviating from the real situation. If the instrument or the machine works with low operation speeds or if it is subjected to lower loads, then the model built based on the rigid elements assumption may lead to excellent results.

The elasticity becomes a significant element if the loads occurred are high and/or the operation speeds are high (Figure 2.26). In this case, the deformations of the machine element will influence, usually in a negative way, the correct operation of the system. The resonance and the loss of stability represent the main forms of manifestation of elasticity. They will occur in the case of an inadequate design leading to a fast machine damage.

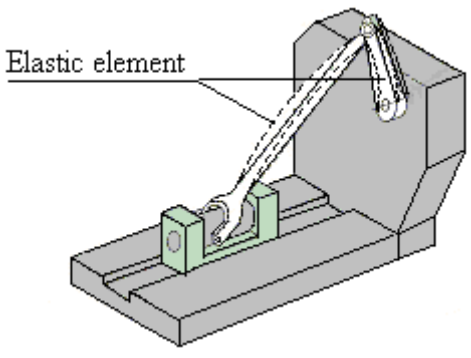

Figure 2.26. Mechanical system with elastic elements

The main method of approach of such a problem is the method of finite elements, a method used in a lot of works for elaborating models describing the behavior of machines containing elastic elements**.**

As a result of modeling a set of differential equations having a complex nonlinear form is obtained. It contains a series of additional terms due to the relative movements of nodal coordinates and the general motion, and the operation motion is called "rigid motion" of the system. As the geometrical configuration of a mechanical system with rigid motion changes from one moment to the other, the motion equations are valid for that very moment, in which the system motion is to be considered to be "frozen". In this case, periods of time, when the coefficients can be approximate as constant, are being considered.

It is difficult to estimate the length of this interval that depends on the topology and geometry of the multibody system. We consider that it is short enough in order to regard the motion as "frozen." The analysis made is an incremental analysis. The motion equations written in the local coordinate system may be expressed under the form ([VLA12], [BAG83], [ERD72], [NAT80]): , [VLA87a], [VLA87b], [MAY96], [ZHA01])

$$[m_e]\{\ddot{\delta}_e\}+2[c_e(\omega)]\{\dot{\delta}_e\}+\left([k_e]+[k_e(\varepsilon)]+\left[k_e(\omega^2)\right]+\left[k_e^G\right]\right)\{\delta_e\}=$$

$$=\{q_e\}+\{q_e^*\}-\{q_e^i(\varepsilon)\}-\{q_e^i(\omega^2)\}-[m_{Ee}^i][I]\{\varepsilon\}_L-[m_{oe}^i][R]^T\{\ddot{r}_o\}_G \qquad (2.60)$$

where:,

$[m_e]$ - inertia matrix, symmetric;
$[c_e(\omega)]$ - matrix of Coriolis terms, skew-symmetric;
$[k_e]$ - classical matrix stiffness, symmetric;
$[k_e(\varepsilon)]$ - stiffness change due to the angular acceleration of the mobile reference system;
$\left[k_e(\omega^2)\right]$ - stiffness change due to the angular speed of the mobile reference system;
$\left[k_e^G\right]$ - rigidity due to the second order effects;
$\{q_e\}+\{q_e^*\}$ - the external forces concentrated and distributed;
$\{q_e^i(\varepsilon)\}$ - inertial forces due to the angular acceleration of the mobile reference system;
$\{q_e^i(\omega^2)\}$ - inertial forces due to the angular speed of the mobile reference system;
$[m_{Ee}^i][I]\{\varepsilon\}_L$ - inertial forces due to rotation only in the case of truss elements;
$[m_{oe}^i][R]^T\{\ddot{r}_o\}_G$ - inertial forces due to the motions of the mobile reference system .

After passing to a global coordinate system (neglecting the second-order effects), finally, the second-order differential equations system with variable coefficients is obtained referinte ([HOU09], [PIR05], [XIA07]):

$$[M]\{\ddot{\Delta}\}+[C]\{\dot{\Delta}\}+\left([K]+[K(\varepsilon)]+\left[K(\omega^2)\right]\right)\{\Delta\})=\{0\} \qquad (2.61)$$

where:

$[M]$ - inertia matrix, symmetric;
$[C]$ - matrix of Coriolis terms, skew-symmetric;
$[K]$ - rigidity matrix, symmetric;

$[K(\varepsilon)]$ - change of the stifness due to the angular accelerations, skew-symmetric;
$[K(\omega^2)]$ - change of stifness due to the angular speeds, symmetric;
$\{Q\}$ - vector of the total nodal loads.

To summarize, matrices „ of the whole structure" are symmetric or skew symmetric. New researches increase the complexity of the problem of the study of the multibody systems with flexible elements **(**[XIA07], [HAR61], [MAS07]**)** but there are not many useful results concerning the solution of the differential equations. Some properties of such a system will be presented underneath.

2.4.2. Some properties of the motion equations

The motion equations of such system have properties allowing an easier solution of the system obtained but also a qualitative interpretation of the dynamic response of the system. The obtained results were published in (hindawi). [SCUd12] The properties are presented in the following:

P1. In the Reyleigh quotient the eigenvalues do not depend directly on the damping matrix

There is a very short period of time in which the variation of the matrix coefficients of motion equations is of no importance (varies very slowly). In this situation, the motion equation, nonlinear, depending on time, can be considered, on short time interval, having constant coefficient. The nonlinear differential system of equations can be consider linear on short periods. The theory of the differential system of equation (well known) make possible to show some important properties. The system solution of the following form is selected:

$$\{\Delta\} = \{A\}\cos(\omega t + \varphi) \tag{2.62}$$

By differentiation is obtained:

$$\{\dot{\Delta}\} = -\omega\{A\}\sin(\omega t + \varphi) \quad ; \quad \{\ddot{\Delta}\} = -\omega^2\{A\}\cos(\omega t + \varphi) \tag{2.63}$$

Introducing into the homogeneous system associated to (2.61) we get:

$$-\omega^2[M]\{A\}\cos(\omega t + \varphi) - \omega[C]\{A\}\sin(\omega t + \varphi) + \left([K] + [K(\varepsilon)] + [K(\Omega^2)]\right)\{A\}\cos(\omega t + \varphi) = 0 \tag{2.64}$$

By pre-multiplying (2.64) by $\{A\}$ we get:

$$-\omega^2\{A\}^T[M]\{A\}\cos(\omega t + \varphi) - \omega\{A\}^T[C]\{A\}\sin(\omega t + \varphi) +$$

$$+\{A\}^T\left([K]+[K(\varepsilon)]+\left[K\left(\Omega^2\right)\right]\right)\{A\}\cos(\omega t+\varphi)=0 \tag{2.65}$$

Since $[C]$ and $[K(\varepsilon)]$ are skew-symmetrical, we have:

$$\{A\}^T[C]\{A\}=0\,; \qquad \{A\}^T[K(\varepsilon)]\{A\}=0 \tag{2.66}$$

and (2.65) becomes:

$$\left[-\omega^2\{A\}^T[M]\{A\}+\{A\}^T\left([K]+\left[K\left(\Omega^2\right)\right]\right)\{A\}\right]\cos(\omega t+\varphi)=0 \tag{2.67}$$

where from:

$$\omega^2=\frac{\{A\}^T\left([K]+\left[K\left(\Omega^2\right)\right]\right)\{A\}}{\{A\}^T[M]\{A\}}\,. \tag{2.68}$$

Thus we have the following property:

In the Reyleigh quotient the eigenvalues do not depend directly on the damping matrix

Moreover, these values are real and positive, since $[K]+\left[K\left(\Omega^2\right)\right]$ and $[M]$ are symmetrical and positive definite; thus there is no damping in the system. It results that the matrix $[C]$, having in equations the significance a viscous damping, does not introduce a damping term in the obtained solutions. Its skew-symmetry denotes the system property of not dissipating the energy to the exterior.

Lets now write the relation (2.62) as follows:

$$\{\Delta\}=\{A_1\}\cos\omega t+\{A_2\}\sin\omega t\,. \tag{2.62'}$$

P2. The values of vector components $\{A_1\}$ and $\{A_2\}$ depend on the skew-symmetrical matrices $[C]$.

By introducing into (2.61) the solution (2.62') and putting the condition of checking the system at any time moment t it follows that $\{A_1\}$ and $\{A_2\}$ should satisfy the homogeneous linear system:

$$\begin{bmatrix}[K]+[K(\Omega)]-\omega^2[M] & -\omega[C]\\ -\omega[C] & [K]+[K(\Omega)]-\omega^2[M]\end{bmatrix}\begin{Bmatrix}A_1\\A_2\end{Bmatrix}=\{0\} \tag{2.63}$$

If this did not depend on $[C]$, the system (2.61) would be satisfied when $[C]$=0 and (2.63) became:

$$\begin{aligned}\left([K]+\left[K\left(\Omega^2\right)\right]-\omega^2[M]\right)\{A_1\}=\{0\}\\ \left([K]+\left[K\left(\Omega^2\right)\right]-\omega^2[M]\right)\{A_2\}=\{0\}\end{aligned} \tag{2.64}$$

It follows there from : $\{A_1\}=y\{A_2\},\quad y\in R$ (2.65)

If for instance $\{A_1\}=\{A_2\}$ from (2.63) we get:

$$\left([K]+[K(\Omega)]-\omega^2[M]-\omega[C]\right)\{A_1\}=\{0\} \tag{2.66}$$

or:

$$\left([K]+[K(\Omega)]-\omega^2[M]\right)\{A_1\}-\omega[C]\{A_1\}=\{0\} \tag{2.66'}$$

If (2.64) is taken into account we will have:

$$-\omega[C]\{A_1\}=\{0\} \tag{2.67}$$

This relation is generally not valid because if on the one hand det $[C]\neq 0$ the linear homogenous system $\omega[C]\{A_1\}=0$ is impossible and if det $[C]=0$ (for instance when the dimension of $[C]$ is an odd number on the other hand, from (2.66') and (2.67) would result that also $[K]+[K(\Omega)]-\omega^2[M]$ and $[C]$ are proportional, a fact that cannot be admitted since $[K],[K(\Omega)],[M]$ are symmetrical and $[C]$ skew-symmetric.

It results that $\{A_1\}$ and $\{A_2\}$ depend on $[C]$ and also the value of ω^2 from the Rayleigh quotient.

P3. Matrix $[A]$ defined by relation (2.71) has two null eigenvalues

First we simply teh problem and we neglect the matrices $[K(\varepsilon)]$ and $\left[K\left(\Omega^2\right)\right]$; they have generally a small contribution to the rigidity matrix. We propose ourselves to solve the homogeneous system (2.63) which becomes under this assumption:

$$[M]\{\ddot{\Delta}\}+[C]\{\dot{\Delta}\}+[K]\{\Delta\}=0 \tag{2.68}$$

with $[M]$ and $[K]$ symmetric and $[C]$ skew-symmetric. With the classical substitution:

$$\{\Delta\}=\{x_1\};\ \{\dot{\Delta}\}=\{x_2\} \tag{2.69}$$

the first order linear system is obtained:

$$\begin{Bmatrix} \dot{x}_1 \\ \dot{x}_2 \end{Bmatrix} = \begin{bmatrix} 0 & [E] \\ -[M]^{-1}[K] & -[M]^{-1}[C] \end{bmatrix} \begin{Bmatrix} x_1 \\ x_2 \end{Bmatrix}; \tag{2.70}$$

or:

$$\{\dot{x}\} = [A]\{x\}, \tag{2.70'}$$

where:

$$\{x\} = \begin{Bmatrix} x_1 \\ x_2 \end{Bmatrix}; \quad [A] = \begin{bmatrix} 0 & [E] \\ -[M]^{-1}[K] & -[M]^{-1}[C] \end{bmatrix}. \tag{2.71}$$

and the unit matrix was named with $[E]$

If *n* is the system dimension then the dimension of matrix $[A]$ will be *2n x 2n*.

Let $\lambda_1, \lambda_2, ..., \lambda_{2n}$ be the eigenvalues for matrix $[A]$ and $\{V_1\}, \{V_2\}, ..., \{V_{2n}\}$ the corresponding eigenvectors. We denote:

$$[Q] = \begin{bmatrix} V_1 & V_2 & \dots & V_{2n} \end{bmatrix}.$$

the matrix of eigenvectors. Using the transformation $\{x\} = [Q]\{q\}$ the system is reduced to:

$$\{\dot{q}\} = [\lambda]\{q\} \tag{2.72}$$

where:

$$[\lambda] = \begin{bmatrix} \lambda_1 & & & \\ & \lambda_2 & & 0 \\ 0 & & \ddots & \\ & & & \lambda_{2n} \end{bmatrix}, \quad \lambda_j \in C \tag{2.73}$$

The equations: $\dot{q}_i = \lambda_i q_i$ allow the solutions: $q_i = C_i \exp(\lambda_i t)$.

If in the condition: $\det([A] - \lambda[E]) = 0$ we plug in $\lambda = 0$ we get the condition: $\det[A]$=0.

Proof: Developing on rows we get finally:

$$\det[A] = (-1)^n \det([M]^{-1}[K]) = (-1)^n \det[M]^{-1} \det[K] = 0 \tag{2.74}$$

because $[K]$ is singular.

We will show in what follows that $[A]$ allows another eigenvalue 0. If an eigenvalue λ_1 is known matrix $[A]$ can be reduced to a matrix of dimension (2n-1)x(2n-1) which has 2n-1 eigenvalues equal to the eigenvalues of $[A]$ wherefrom λ_1 has been eliminated. It is known [2.7] that matrix $[B]=[T]^{-1}\ [A]\ [T]$ has the same eigenvalues as $[A]$ but the eigenvectors are:

$$\{V'\}=[T]^{-1}\{V\} \tag{2.75}$$

Then if a matrix $[B]$ has the form:

$$[B]=\begin{bmatrix} \lambda_1 & \vdots & b_{12} & \cdots & & b_{1n} \\ \cdots & \vdots & \cdots & \cdots & \cdots & \cdots \\ & \vdots & b_{22} & \cdots & & b_{2n} \\ 0 & \vdots & & & & \\ & \vdots & b_{n2} & \cdots & & b_{nn=} \end{bmatrix}=\begin{bmatrix} \lambda_1 & \vdots & [B_{12}] \\ \cdots & \cdots & \cdots \\ 0 & \vdots & [B_{22}] \end{bmatrix} \tag{2.76}$$

with:

$$[B_{22}]=\begin{bmatrix} b_{22} & \cdots & b_{2n} \\ & & \\ & & \\ b_{n2} & \cdots & b_{nn} \end{bmatrix};\quad [B_{12}]=[b_{12} \quad \cdots \quad b_{1n}] \tag{2.76'}$$

then the problem of eigenvalues:

$$\det([B_{12}]-\lambda[E])=0 \tag{2.77}$$

is to be written $(\lambda-\lambda_1)\det([B_{22}]-\lambda[E])=0$ resuming to determine the eigenvalues of $[B_{22}]$.

It is checked by direct computation that the transformation $[T]$ is as follows:

$$[T]=\begin{bmatrix} & \vdots & & 0 & \\ & \vdots & \cdots & \cdots & \cdots \\ & \vdots & & & \\ V & \vdots & & E_{2n-1} & \\ & \vdots & & & \\ & \vdots & & & \end{bmatrix}=\begin{bmatrix} 1 & \vdots & & 0 & \\ \cdots & \cdots & \cdots & \cdots & \cdots \\ e_2 & \vdots & & & \\ e_3 & \vdots & & E_{2n-1} & \\ \vdots & \vdots & & & \\ e_{2n} & \vdots & & & \end{bmatrix} \tag{2.78}$$

By simple computation we get:

$$[T]^{-1}=\begin{bmatrix} 1 & \vdots & & 0 & & \\ \cdots & \vdots & \cdots & \cdots & \cdots & \cdots \\ -e_2 & \vdots & & & & \\ -e_3 & \vdots & & E_{2n-1} & & \\ & \vdots & & & & \\ -e_{2n} & \vdots & & & & \end{bmatrix} \tag{2.79}$$

It results in the possibility of avoiding the computation of the eigenvalues for matrix $[A]$ with $\det[A]=0$, considering the fact that we know an eigenvalue $\lambda_1=0$ and by the transformation presented we shall compute the other eigenvalues as eigenvalues of $[B_{22}]$.

For $\lambda_1=0$ the eigenvector $\{V_1\}$ corresponding to matrix $[A]$ will be computed. We shall have:

$$[A]\{V_1\}=\{0\} \tag{2.80}$$

or:

$$\begin{bmatrix} & & & \vdots & & & \\ & 0_n & & \vdots & & E_n & \\ & & & \vdots & & & \\ \cdots & \cdots & \cdots & \cdots\ \vdots & \cdots & \cdots & \cdots \\ & & & \vdots & & & \\ & -[M]^{-1}[K] & & \vdots & & -[M]^{-1}[C] & \\ & & & \vdots & & & \end{bmatrix} \begin{Bmatrix} e_1 \\ e_2 \\ \vdots \\ e_n \\ \cdots \\ e_{n1} \\ \vdots \\ e_{2n} \end{Bmatrix} = \begin{Bmatrix} 0 \\ 0 \\ \vdots \\ \vdots \\ \vdots \\ \vdots \\ \vdots \\ 0 \end{Bmatrix} \tag{2.80'}$$

The first rows n give us : $e_{n+1}=0$; $e_{n+2}=0$; … … $e_{2n}=0$.

Using these results the other rows *n* give us:

$$\begin{bmatrix} & \vdots & \\ -[M]^{-1}[K] & \vdots & -[M]^{-1}[C] \\ & \vdots & \end{bmatrix} \begin{Bmatrix} e_1 \\ e_2 \\ \vdots \\ e_n \\ \cdots \\ 0 \\ \vdots \\ 0 \end{Bmatrix} = 0 \tag{2.81}$$

or, carrying out the multiplications of the matrix- blocks:

$$\begin{bmatrix} & & \\ & -[M]^{-1}[K] & \\ & & \end{bmatrix} \begin{Bmatrix} e_1 \\ e_2 \\ \vdots \\ e_n \end{Bmatrix} = 0 \qquad (2.81')$$

the result will be that the first n components of the eigenvector are components of the vector corresponding to value $\lambda_1 = 0$ for matrix $[M]^{-1}[K]$ which characterizes the system:

$[M]\{\ddot{\Delta}\} + [K]\{\Delta\} = \{0\}$.

With these components we build:

$$[T] = \begin{bmatrix} 1 & \vdots & & 0 & \\ \cdots & \cdots & \cdots & \cdots & \cdots \\ e_2 & \vdots & & & \\ \vdots & \vdots & & & \\ e_n & \vdots & & & \\ \cdots & \vdots & & E_{2n-1} & \\ & \vdots & & & \\ 0 & \vdots & & & \\ & \vdots & & & \end{bmatrix}; \quad [T]^{-1} = \begin{bmatrix} 1 & \vdots & & 0 & \\ \cdots & \cdots & \cdots & \cdots & \cdots \\ -e_2 & \vdots & & & \\ \vdots & \vdots & & & \\ -e_n & \vdots & & & \\ \cdots & \vdots & & E_{2n-1} & \\ & \vdots & & & \\ 0 & \vdots & & & \\ & \vdots & & & \end{bmatrix} \qquad (2.82)$$

where $e_1 = 1$. We compute: $[B] = [T]^{-1}[A][T]$.

$$[B] = \begin{bmatrix} 1 & \vdots & & 0_{1x(n-1)} & \\ \cdots & \cdots & \cdots & \cdots & \cdots \\ -e_2 & \vdots & & & \\ \vdots & \vdots & & & \\ -e_n & \vdots & & & \\ \cdots & \vdots & & E_{2n-1} & \\ & \vdots & & & \\ 0 & \vdots & & & \\ & \vdots & & & \end{bmatrix} \cdot \begin{bmatrix} & \vdots & \\ & \vdots & \\ 0_{nx1} & \vdots & E_n \\ & \vdots & \\ & \vdots & \\ \cdots & \vdots & \cdots \\ & \vdots & \\ -[M]^{-1}[K] & \vdots & -[M]^{-1}[C] \\ & \vdots & \end{bmatrix} \cdot \begin{bmatrix} 1 & \vdots & & 0 & \\ \cdots & \cdots & \cdots & \cdots & \cdots \\ e_2 & \vdots & & & \\ \vdots & \vdots & & & \\ e_n & \vdots & & & \\ \cdots & \vdots & & E_{2n-1} & \\ & \vdots & & & \\ 0 & \vdots & & & \\ & \vdots & & & \end{bmatrix} =$$

$$= \begin{bmatrix} 1 & \vdots & & 0 & \\ \cdots & \cdots & \cdots & \cdots & \cdots \\ -e_2 & \vdots & & & \\ \vdots & \vdots & & & \\ -e_n & \vdots & & & \\ \cdots & \vdots & & E_{2n-1} & \\ & \vdots & & & \\ 0 & \vdots & & & \\ & \vdots & & & \end{bmatrix} . \begin{bmatrix} & & \vdots & & \\ & 0 & \vdots & E_n & \\ & & \vdots & & \\ & & \vdots & & \\ \cdots & \cdots & \cdots & \cdots & \cdots \\ 0 & & \vdots & & \\ \vdots & [\alpha^*] & \vdots & -[M]^{-1}[C] & \\ \vdots & & \vdots & & \\ 0 & & \vdots & & \end{bmatrix} =$$

$$= \begin{bmatrix} & & & \vdots & 1 & & & & \\ & & & \vdots & -e_2 & 1 & & & \\ & 0_{n\,x\,n} & & \vdots & -e_3 & & 1 & & \\ & & & \vdots & \vdots & & & \cdots & \\ & & & \vdots & -e_n & & & & 1 \\ \cdots & \cdots & \cdots & \vdots & \cdots & \cdots & \cdots & \cdots & \cdots \\ 0_{nx1} & \vdots & [\alpha^*] & \vdots & & & -[M]^{-1}[C] & & \\ & \vdots & & \vdots & & & & & \end{bmatrix} \qquad (2.83)$$

where $[\alpha^*]$ is the matrix having the dimensions *2n* x (*2n-1*), it is obtained from $[M]^{-1}[K]$ having the dimension *2n* x *2n* by eliminating the first column.

We have:

$$[B_{22}] = \begin{bmatrix} & & & \vdots & -e_2 & 1 & & & \\ & & & \vdots & -e_3 & 0 & 1 & & \\ & 0 & & \vdots & \vdots & & & \ddots & \\ & & & \vdots & -e_n & & & \cdots & 1 \\ & & & \vdots & & & & & \\ \cdots & \cdots & \cdots & \vdots & \cdots & \cdots & \cdots & \cdots & \cdots \\ & [\alpha^*] & & \vdots & & & -[M]^{-1}[C] & & \\ & & & \vdots & & & & & \end{bmatrix} =$$

$$= \begin{bmatrix} & & \vdots & -e_2 & 1 & & \\ & & \vdots & -e_3 & & & \\ & 0 & \vdots & \vdots & & \ddots & \\ & & \vdots & -e_n & & & 1 \\ \cdots & \cdots & \cdots & \vdots & \cdots & \cdots & \cdots & \cdots \\ & & & \vdots & & & & \\ & [\alpha^*] & & \vdots & C_1 & C_2 & & C_n \\ & & & \vdots & & & & \end{bmatrix} \tag{2.84}$$

where the matrix columns $[M]^{-1}[C]$ have been named $C_1, C_2, .. \quad C_n$. We calculate by developing the matrix determinant B_{22} on rows:

$$\det[B_{22}] = (-1)^n e_2 \begin{bmatrix} & & \vdots & 0 & 1 & & \\ & & \vdots & 0 & & & \\ & 0 & \vdots & \vdots & & \ddots & \\ & & \vdots & 0 & & & 1 \\ \cdots & \cdots & \cdots & \vdots & \cdots & \cdots & \cdots & \cdots \\ & & & \vdots & & & & \\ & [\alpha^*] & & \vdots & C_1 & C_2 & & C_n \\ & & & \vdots & & & & \end{bmatrix} + (-1)^n x \begin{bmatrix} & & \vdots & -e_3 & 1 & & \\ & & \vdots & -e_4 & & & \\ & 0 & \vdots & \vdots & & \ddots & \\ & & \vdots & -e_n & & & 1 \\ \cdots & \cdots & \cdots & \vdots & \cdots & \cdots & \cdots & \cdots \\ & & & \vdots & & & & \\ & [\alpha^*] & & \vdots & C_1 & C_2 & & C_n \\ & & & \vdots & & & & \end{bmatrix} =$$

$$= e_2 \det[\alpha^* \vdots C_2] + e_3 \det[\alpha^* \vdots C_3] + ... + e_n \det[\alpha^* \vdots C_n] + e_1 \det[\alpha^* \vdots C_1] =$$

$$= \det[\ [\alpha^*]\ \vdots\ \ e_1C_1 + e_2C_2 + ... + e_nC_n\ ] \tag{2.85}$$

(we took into account that $1=e_1$).

In what follows the following relation has been considered:

$\det[A][B] = \det[A]\det[B]$;

We have:

$$1 = \det\begin{bmatrix} 1 & & 0 \\ & 1 & \\ & \ddots & \\ 0 & & 1 \end{bmatrix} = \det\left(\begin{bmatrix} \frac{1}{e_1} & & & 0 \\ & \frac{1}{e_2} & & \\ & & \ddots & \\ 0 & & & \frac{1}{e_n} \end{bmatrix} \cdot \begin{bmatrix} e_1 & & & 0 \\ & e_2 & & \\ & & \ddots & \\ 0 & & & e_n \end{bmatrix}\right) \tag{2.86}$$

Taking into account the previous relation we may write:

$$\det[B_{22}]=$$

$$=\det\begin{pmatrix}\begin{bmatrix}\frac{1}{e_1} & & 0\\ & \frac{1}{e_2} & \\ 0 & & \frac{1}{e_n}\end{bmatrix}\cdot\begin{bmatrix}e_1 & & 0\\ & e_2 & \\ 0 & & e_n\end{bmatrix}\end{pmatrix} x \det\begin{bmatrix}\vdots & \\ \alpha^* & \vdots \quad e_1C_1+e_2C_2+.....+e_nC_n\\ \vdots & \end{bmatrix}=$$

$$=\det\begin{bmatrix}\frac{1}{e_1} & & 0\\ & \frac{1}{e_2} & \\ 0 & & \frac{1}{e_n}\end{bmatrix}\cdot\det\left(\begin{bmatrix}e_1 & & 0\\ & e_2 & \\ 0 & & e_n\end{bmatrix} x\begin{bmatrix}\vdots & \\ \alpha^* & \vdots \quad e_1C_1+e_2C_2+.....+e_nC_n\\ \vdots & \end{bmatrix}\right)$$

$$=\det\begin{bmatrix}\frac{1}{e_1} & & 0\\ & \frac{1}{e_2} & \\ 0 & & \frac{1}{e_n}\end{bmatrix}\det\begin{bmatrix}\alpha^*_{L_1}e_1 & \vdots & e_1^2C_{11}+e_1e_2C_{12}+.....+e_1e_nC_{1n}\\ \alpha^*_{L_2}e_2 & \vdots & e_1e_2C_{21}+e_2^2C_{22}+.....+e_2e_nC_{2n}\\ & \vdots & \\ \alpha^*_{L_n}e_n & \vdots & e_1e_nC_{n1}+e_ne_2C_{n2}+.....+e_n^2C_{n2}\end{bmatrix}=0 \qquad (2.87)$$

since:

$$\alpha^*_{L_1}e_1+\alpha^*_{L_2}e_2+\ldots \quad \ldots+\alpha^*_{L_n}e_n=\{V_1\}^T\begin{bmatrix}V_2 & V_3 & & V_n\end{bmatrix}=0,$$

and:

$$\left(e_1^2c_{11}+e_2e_1c_{12}+..... \quad .....e_ne_1c_{n1}\right)+$$

$$+\left(e_2e_1c_{21}+e_2^2c_{22}+..... \quad ....e_2e_nc_{n2}\right)+...+$$

$$+\left(e_ne_1c_{n1}+e_ne_2c_{n2}+..... \quad .....e_n^2c_{nn}\right)=\sum_{i,j}e_ie_j\left(c_{ij}+c_{ji}\right)=0,\ \left(c_{ij}=-c_{ji}\right). \qquad (2.88)$$

with $\alpha^*_{L_1}$, $\alpha^*_{L_2}$, ..., $\alpha^*_{L_n}$ the lines 1,2,.. ., n of the matrix α^* have been named .

It results in $\det[B_{22}]=0$, thus the matrix $[B_{22}]$ has a null eigenvalue. Matrix B shall have two null eigenvalues .

To these two eigenvalues corresponds the non-harmonic solution: $q=C_1t+C_2$ which will represent the rigid motion of the multibody system in a first approximation. The other values are different from null for a multibody system with only one degree of mobility generally being different from each other.

2.4.3. Conclusions

In section 2.4 are presented some mathematical properties of motion equations in the case of multibody systems having elastic elements. These properties are due to the existence of the skew symmetrical matrix C, by which the relative motion of nodal coordinates is manifested by the Coriolis effects and the additional term introduced in equations (applying the finite element method). Using these properties is possible to allow a qualitative analysis of the obtained motion equations. Thus, the Coriolis effects due to the relative motions will determine a modification (generally small) of the systems eigenpulsations. The Coriolis damping is not dissipative, that means the systems energy is not being influenced by the terms in which the skew symmetrical matrix C occurs.

Chapter 3

Mechanical Propertie's Identification and Tests on Advanced Composite Materials

The chapter presents the results obtained in a period of more ten years in the Laboratory of Composite Materials of the Department of Mechanical Engineering of the TRANSILVANIA University of Brasov. I was member of a team with many results in the domain of the composite materials. These results were published in many papers as: [SVL11b] , [KAT11], [HTE11b] , [SVL11c], [HTE11c] , [RPU12], [AST12] , [SVL12d] , [THE13], [CNI13].

The chapter presents only the papers where my contribution was more consistent.

3.1. Mechanical Properties of a Sandwich Composite with twill weave carbon and EPS

3.1.1. Introduction

Many type of materials where analyzed and tested in the laboratory. The chapter present some interesting materials for applications in the field of the automotive engineering. In this section are presented the most important mechanical properties obtained in a simple tensile test on a 0.4 mm thickness 2/2 carbon twill weave fabric impregnated with epoxy resin, used as skins for an ultralight sandwich composite structure. As core was used the expanded polystyrene. This sandwich panel was subjected to a classical flexural load-unload tests. The main property of the fabric is a very good drapeability and is suitable to reinforce a quite large range of epoxy resins used in many applications.

This kind of fabric is used to obtain thin structures with complex shapes and geometry and high stiffness (the applications are presume to be mainly in automotive engineering). A comparison with a sandwich structure with EWR-300 glass fabric/epoxy resin skins has been accomplished. Due to its high stiffness, the twill weave carbon fabric is used as skins in large sandwich structures even with low stiffness cores. The flexural load-unload tests show an outstanding stiffness of the whole sandwich panel. For this research various specimens' thickness have been used. The results obtained were published in [THE13].

In the current applications carbon fiber-reinforced epoxy resins are used extensively to build composite structures with an outstanding specific weight/strength ratio. Such structures, usually called laminates, present a relative poor tensile stiffness and the flexural stiffness remains at a low level due to low sensitivity at flexural loads of the carbon fibers, especially of the unidirectional reinforced ones [DBM01] , [IMD05], [JRV05]. A method to increase a little bit this flexural stiffness is the use of a large variety of fabrics as reinforcing material. A common fabric is a so called twill weave. The main feature of this weave is that the warp and the

weft threads are crossed in a programmed order and frequency, to obtain a flat appearance with a distinct diagonal line. A twill weave fabric needs at least three threads. More threads can be used for fabrics with high specific weight depending on their complexity and utility [LCB06], [DGL07], [ABS07].

After the plain weave, the twill is the second most common weave. It is often denoted as a fraction, for instance three twill weaves can be designated, in the following way:

- 2/1 in which two threads are raised and one is lowered when a weft thread is inserted;
- 2/2 in which two threads are raised and two are lowered when a weft thread is inserted;
- 3/1 in which three threads are raised and one is lowered when a weft thread is inserted.

The characteristic structure of the twill weave fabric makes it to present a very good dreapability. In general, composite laminates are manufactured from thin layers called laminae. These laminates present a quite low stiffness and flexural rigidity. A solution to increase their stiffness could be the use of stiffening ribs [BFB08]. Not all constructive situations require built-in ribs. A solution could be the increase of the layers but this leads to the disadvantage of increasing the overall weight as well as the resin and reinforcement consumption.

For pre-impregnated composites, to predict their elastic properties, homogenizations and averaging methods can be used [HTE11a]. A better solution to increase the overall stiffness of a composite laminate is to use a thin non-woven polyester mat as core material embedded in the structure [SVL11a], [SVL11b]. This core of non-continuous and non-woven mat presents the advantage to absorb the excessive resin [THE11b]

A composite laminate with this kind of embedded core material presents following main advantages: weight saving, stiffness increase, quick build of the structure's thickness, saving of resin and reinforcement as well as an increased possibility to obtain a better surface finish when it is applied against the "gelcoat". This mat when is impregnated with resin presents high drapeability being suitable for complex shapes and for hand lay-up and spray-up processes [HTE11c]. The results presented in the following are obtained by the foreward mentioned team with many commun researches in the field of the composite materials.

3.1.2 Sandwich structure of the specimens

The sandwich presents two carbon/epoxy skins reinforced with 300 g/mm^2 twill weave carbon fabric and an expanded polystyrene (EPS) 9 mm thick core with a density of 30 kg/m^3. The final thickness of the structure is 10 mm. Other input data are [SVL11c] structure's thickness: 10 mm; skins plies number: two; thickness of each ply: 0.175 mm; skins thickness: 0.35 mm; core thickness: 9 mm; fibers' disposal angle of each ply: 90° and 0°; fibers' volume fraction of each ply: 56%. The data regarding the structure features are: skins reinforcement: HM carbon fibers; fabric type: twill weave; fibers' specific weight: 0.3 kg/m^2; matrix type: epoxy resin; core type: expanded polystyrene.

Other useful data are: core density: 30 kg/m^3; core Young's modulus: 30 MPa; core Poisson's ratio: 0.35; core shear modulus: 11 MPa; fiber Young's modulus in longitudinal direction: 540 GPa; fiber Young's modulus in transverse direction: 27 GPa; fiber Poisson's ratio: 0.3; fibers' shear modulus: 10.38 GPa; matrix Young's modulus: 3.5 GPa; matrix Poisson's ratio: 0.34; matrix shear modulus: 1.42 GPa.

3.1.3 Tests and results

During the flexural tests of the sandwich panel, following experimental determinations have been accomplished:

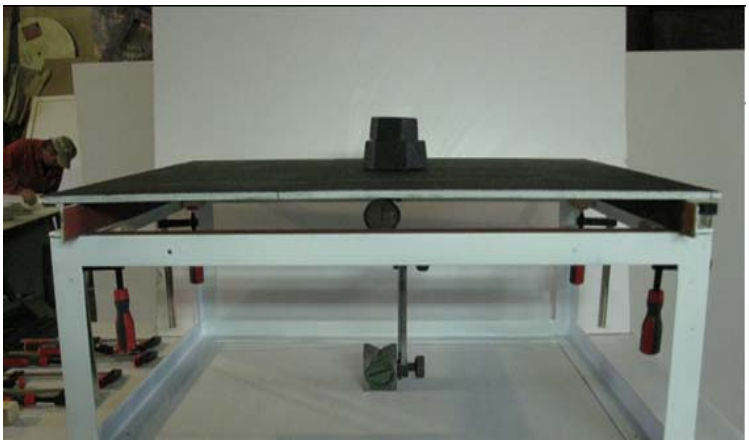

Figure 3.1. Flexural load-unload test detail. Sandwich panel clamped on contour

- Two flexural load-unload tests of the sandwich panel clamped on contour (Fig. 3.1);
- One simple three-point bend test (load-unload) of the sandwich panel supported linearly on two opposite edges (Fig. 3.2).

A loads was applied in the middle of the panel and a displacements' measuring device has been placed under panel at its center. The tensile test on one layer 2/2 twill weave carbon fabric impregnated with epoxy resin has been accomplished on a LR-5KPlus materials testing machine produced by Lloyd Instruments (Fig. 3.3).

The testing machine presents the following characteristics:

- Force range: 5 kN;
- Speed accuracy: <0.2%;
- Load resolution: <0.01% from the load cell used;
- Analysis software: NEXYGEN Plus.

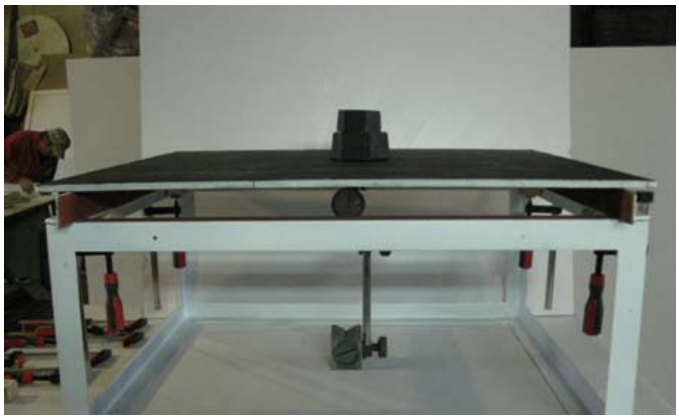

Figure 3.2. Three-point bend load-unload test detail. Sandwich panel supported linearly on two opposite edges.

Figure 3.3. Tensile test detail on an epoxy impregnated 2/2 twill weave carbon fabric.

The features of the 2/2 twill weave carbon fabric is presented below:

- Fabric type: twill weave;
- Fibres type: HM carbon;
- Fabric specific weight: 300 g/m^2;
- Type of resin impregnation: epoxy resin;
- Impregnation process: vacuum bag moulding;
- Impregnation resin: epoxy;
- Fabric thickness: 0.4 mm.

The specimen has been subjected to a test speed of 1 mm/min and the length between extensometer's lamellae is 50 mm. The tensile test results on an epoxy impregnated 2/2 twill weave carbon fabric are presented in Table 1.1. Following main features have been determined: Stiffness; Young's modulus;Load at Maximum Load; Stress at Maximum Load; Extension from preload at Maximum Load; Strain at Maximum Load; Load at Maximum Extension; Stress at Maximum Extension; Extension from preload at Maximum Extension; Strain at Maximum Extension; Load at Minimum Load; Stress at Minimum Load; Extension from preload at

Minimum Load; Strain at Minimum Load; Load at Minimum Extension; Stress at Minimum Extension; Extension from preload at Minimum Extension; Strain at Minimum Extension; Tensile Strength; Extension at Maximum Load; Extension at Maximum Extension; Extension at Minimum Load; Extension at Minimum Extension; Load at Break; Stress at Break.

Due to the non-linear behaviour of the carbon fibre subjected to tensile loads, the stress-strain as well as the load-extension distributions of an epoxy impregnated 2/2 twill weave carbon fabric subjected to tensile loads follows the same non-linear behaviour. The results of the flexural load-unload tests applied to the sandwich panel are presented in Figs. 3.4-3.6.

Table 3.1. Tensile test results on an epoxy impregnated 2/2 twill weave carbon fabric

Characteristics	Value
Length between extensometer's lamellae (mm)	50
Preload stress (kN)	0.0056
Preload speed (mm/min)	21
Test speed (mm/min)	1
Fabric width (mm)	18.5
Fabric thickness (mm)	0.4
Stiffness determined as ratio between load and extension (N/m)	578 5656.99
Young's modulus (MPa)	31273.82
Load at maximum load (kN)	1.92
Stress at maximum load (MPa)	207.61
Strain at maximum load (-)	0.009
Strain at maximum extension (-)	0.344
Strain at minimum load (-)	0.07
Load at minimum extension (kN)	0.005
Stress at minimum extension (MPa)	0.582
Load at break (kN)	1.919
Stress at break (MPa)	207.55
Strain at break (-)	0.009
Tensile strength (MPa)	207.61

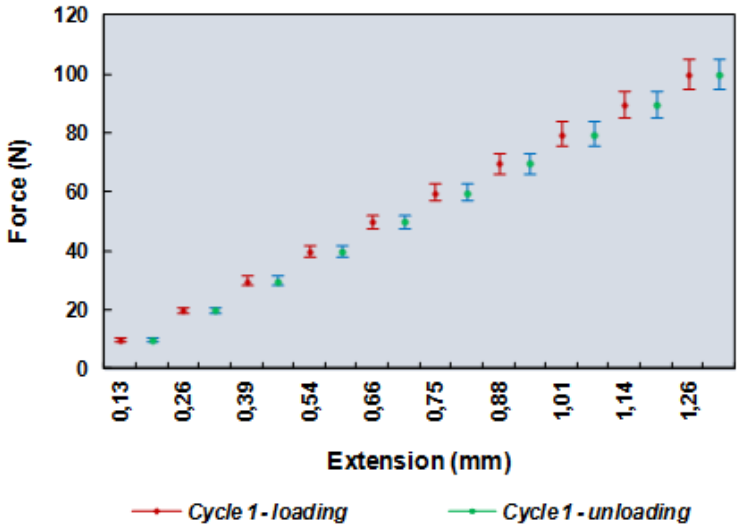

Figure 3.4. Flexural test of the sandwich panel clamped on contour
Cycle 1 loading-unloading

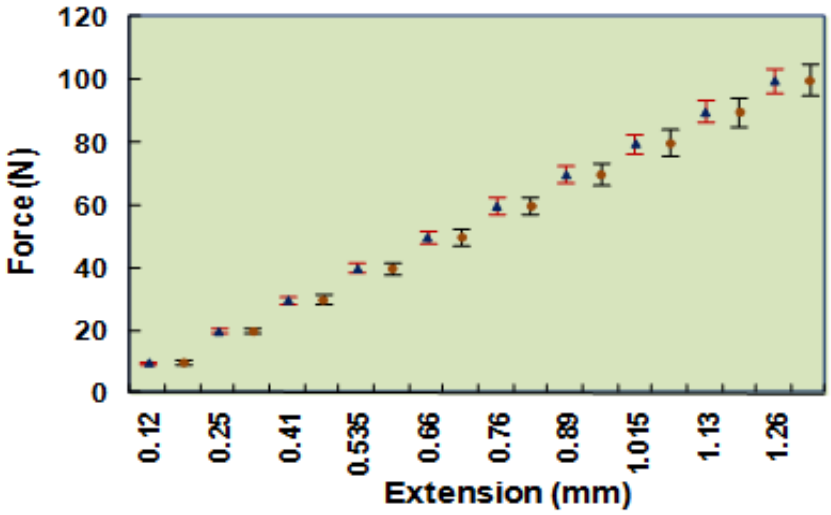

Figure 3.5. Flexural test of the sandwich panel clamped on contour.
Cycle 2 loading-unloading.

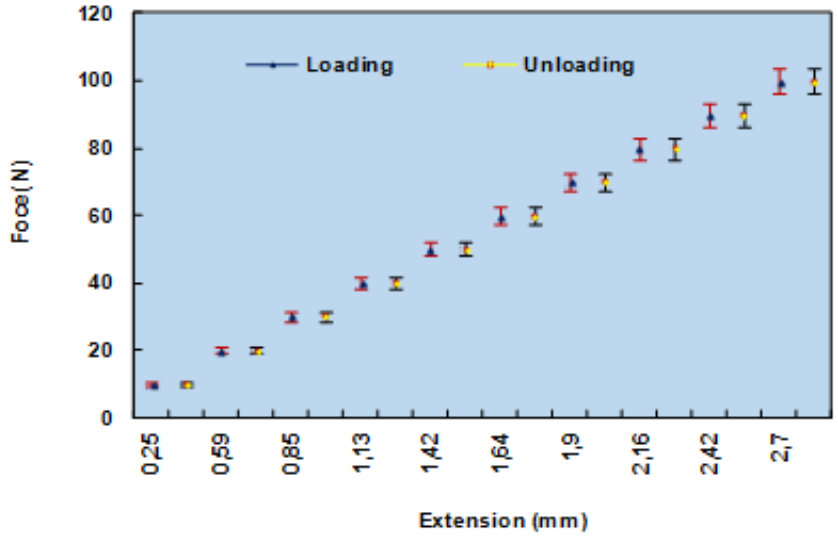

Figure 3.6. Three-point bend test of the sandwich panel supported linearly on two opposite edges.

Various specimens with different thickness (10, 20, 30 and 40 mm) have been manufactured and subjected to three-point bend tests until break occurs. Force-extension distributions of these specimens are presented in Figs. 3.7-3.10.

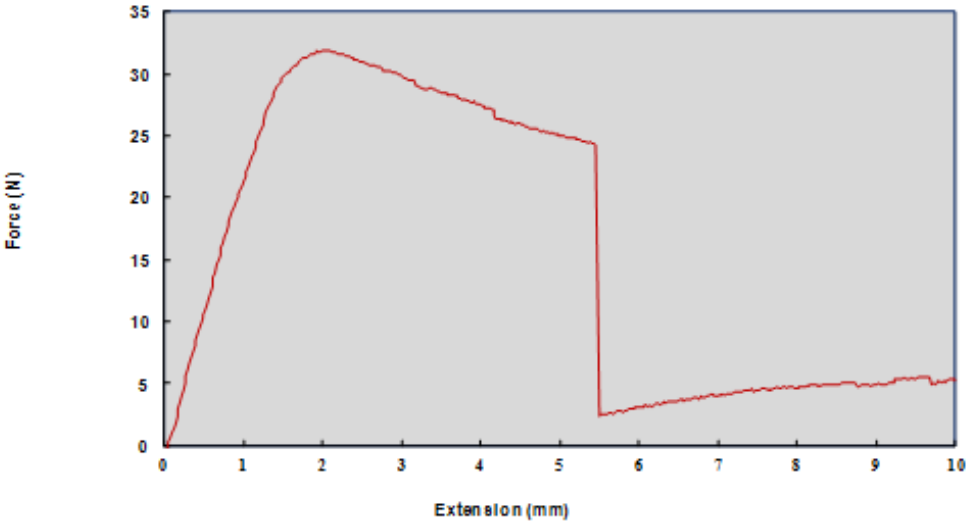

Figure 3.7. Force-extension distribution on 10 mm thickness specimen subjected to three-point bend test.

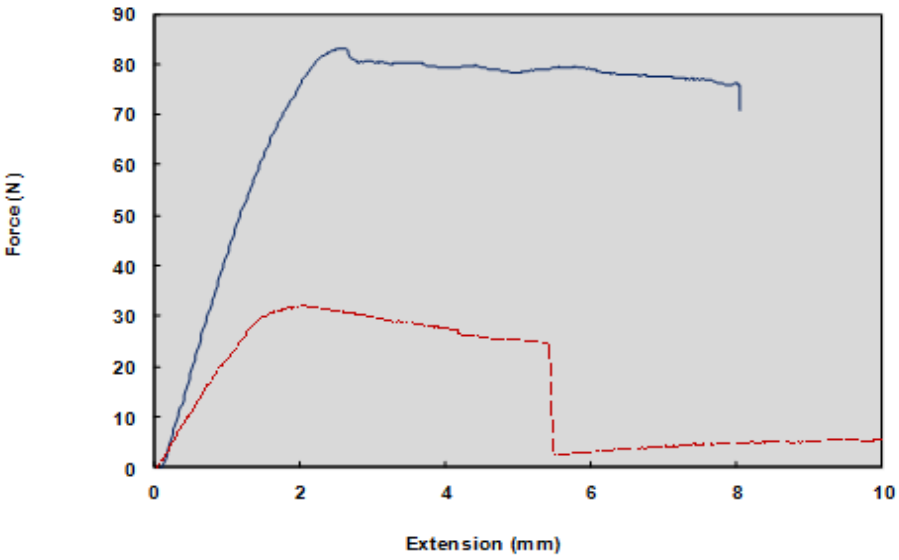

Figure 3.8. Force-extension distribution on 20 mm thickness specimen subjected to three-point bend test.

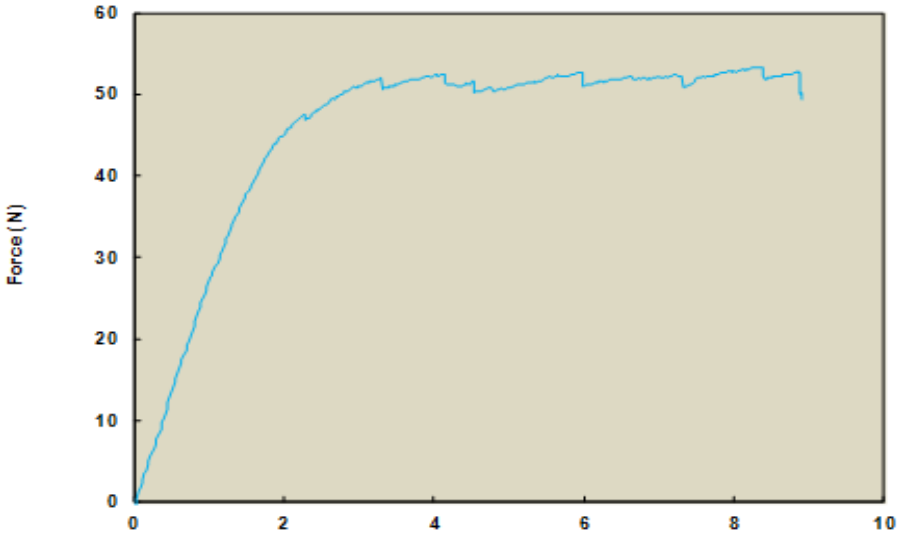

Figure 3.9. Force-extension distribution on 30 mm thickness specimen subjected to three-point bend test.

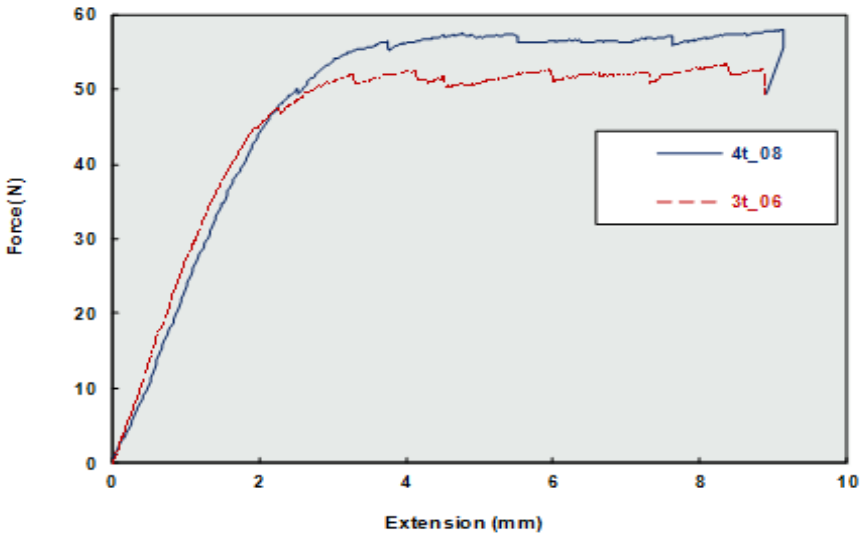

Figure 3.10. Comparison betwwen force-extension distributions on 30 mm and 40 mm thickness specimens subjected to three-point bend tests.

3.1.4. Conclusions

Due to its high stiffness and good dreapeability the epoxy impregnated 2/2 twill weave carbon fabric can be used as skins in large sandwich panels even with low stiffness cores, with applications in the automotive industry.

Carbon fibers are suitable to fit special structures and devices for the future car due to their excellent thermal and electric conductivity. The comparison between the flexural rigidity of the structure obtained experimentally and that obtained through the theoretical approach shows a good agreement between the experimental data and the theoretical approach. The following conclusions can be drawn:

- The sandwich structure with two carbon/epoxy skins reinforced with a 300 g/m^2 twill weave fabric and an expanded polystyrene (EPS) 9 mm thick core with a density of 30 kg/m^3, fulfils following special requirements:
  - Panel dimensions: 10 × 2350 × 4070 mm;
  - Overall weight: maximum 10 kg.
- The sandwich structure's strains with skins based on twill weave carbon fabric reinforced epoxy resin are comparable with those of the structure with skins based on EWR-300 glass fabric/epoxy resin;
- Stresses in fibres direction in case of the sandwich structure with carbon fabric/epoxy resin reinforced skins, are up to six times higher than those existent in EWR-300 glass fabric/epoxy resin skins;
- Stresses transverse to the fibres direction in case of the sandwich structure with carbon fabric/epoxy resin reinforced skins are 20% lower than those existent in EWR-300 glass

fabric/epoxy resin skins;

- The shear stresses in carbon fabric/epoxy resin reinforced skins' plies are almost identical with those existent in EWR-300 glass fabric/epoxy resin skins' plies;
- The core stresses are almost zero, so the loading is taken over exclusively by skins;
- Using a 9 mm thick expanded polystyrene core (EPS) the stiffness of the sandwich structure with carbon fibres reinforced epoxy resin skins is more than ten times higher than the skins' plies stiffness.

3.2. On the polylite composite laminate material behavior to tensile stress on weft direction

3.2.1. Introduction

Basic mechanical properties have been experimentally determined on twelve layers glass fabric-reinforced polyester resin specimens subjected to tensile loads on weft direction until break. Glass fabric of type RT300 (300 g/m^2 specific weight) has been used to reinforce Polylite 440-M888 polyester resin. From a cured composite laminate plate, fifteen specimens have been cut on weft direction using a diamond powder mill to avoid introducing supplementary internal stresses in the laminate.

Eight specimens have been tested with 1 mm/min test speed and seven have been tested with 2 mm/min test speed. Young's modulus, tensile strength, load at maximum load, extension at maximum load and other important features have been experimentally determined on a "LS100 Plus" Lloyd Instruments materials testing machine using Nexygen software. The obtained results were presented in [SVL12].

Glass fabrics manufactured from unidirectional roving of type RT represent the second most used reinforcing material after chopped strand mats (CSMs). These fabrics present certain number of nodes on square centimeter, certain width and thickness, certain eye width, bending strength and feature certain surface aspect [NDC03] , [HTE09]. The most used weaving methods are:

- Plain weave (in which warp and weft threads pass in a certain sequence one above each other);
- Diagonal weave (in which the fabric forms a characteristic pattern with diagonal lines on its surface);
- Satin weave (in which the fabric surface is formed either by threads belonging to warp or to weft).

The weaving method, threads thickness as well as their twist degree plays a significant role in mechanical characterization of a composite structure. In case of two-phase composite (e.g. matrix and reinforcement), the elastic properties can be quite easy computed using the basic elasticity properties of each compound in the rule of mixtures formula. Things are not so simple in case of three or more compounds. Here, homogenization and averaging methods can be used

to compute elastic properties of such composite materials (e.g. pre-impregnated composites) [HTE11a].

Extended experimental researches have been carried out on glass-fiber-reinforced polymer matrix composites subjected to cyclic tensile-compression loadings with various numbers of cycles and load limits [HTE11b], [SVL11c]. Both experimental and numerical methods have been used to determine mechanical properties of various fiber-reinforced composite laminates, with and without fillers, subjected to off-axis loading systems, tensile and bending loads, biaxial loadings as well as thermal loads [SVL11d], [HTE11c], [HTE10], [RPU12], [AST12]

3.2.2. Material used and testing method

The composite laminate used in tensile tests is a thermosett polymer (i.e. unsaturated polyester resin of type Polylite 440-M888) reinforced with twelve plies of glass fabric of type RT300 (300 g/m^2 specific weight). In general, the RT fabrics are manufactured from roving with cut margins and strengthened with Dreher threads (Fig. 3.11). These fabrics are used to reinforce polyester and epoxy resins and present good impregnation properties.

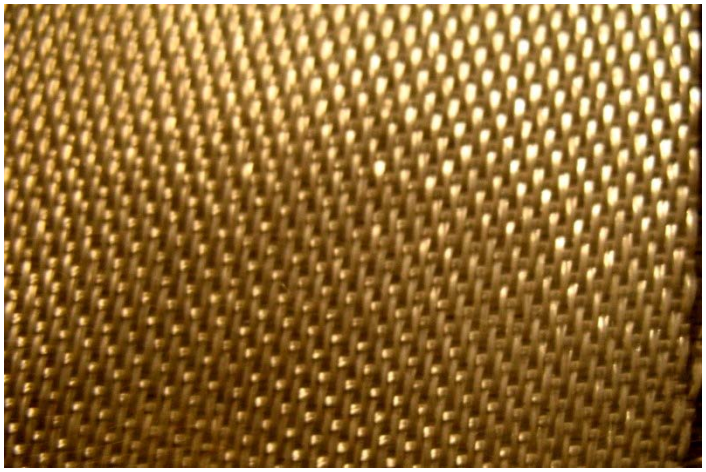

Figure 3.11. RT300 glass fabric reinforcing material

From a cured plate, fifteen specimens have been cut on weft direction using a diamond powder mill with added water to avoid introduce internal stresses and especially thermal stresses that can appear in the cutting process. The specimens have been tempered for 24 hours at a temperature of 20°C and then subjected to tensile loads until break according to SR EN 527-1: „Determination of tensile properties of fiber reinforced composite materials" (Fig. 3.12). A "LS100 Plus" Lloyd Instruments materials testing machine have been used without extensometer to perform the tensile tests.

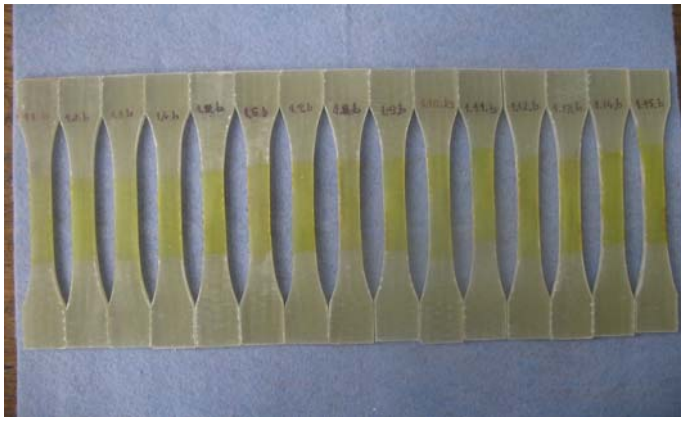

Figure 3.12. RT300 glass fabric-reinforced Polylite 440-M888 polyester resin specimens cut on weft direction

Following main features have been experimentally determined: Stiffness (N/m); Young's modulus (MPa); Load/stress/strain at maximum load; Load/stress/strain at maximum extension; Load/stress/strain at minimum load; Load/stress/strain at minimum extension; Tensile strength; Load/stress at break; Work to maximum load/extension; Work to minimum load/extension.

Test and specimens features are:

- Test speed: 1 and 2 mm/min;
- Number of specimens: 8 for 1 mm/min test speed and 7 for 2 mm/min test speed;
- Specimens mean width: 9.63 mm for 1 mm/min test speed and 9.61 mm for 2 mm/min test speed;
- Specimens mean thickness: 3.65 mm for 1 mm/min test speed and 3.62 mm for 2 mm/min test speed;
- Mean cross-sectional area: 35.2 mm^2 for 1 mm/min test speed and 34.88 mm^2 for 2 mm/min test speed.

The materials testing machine allows determination of experimental results in electronic format by help of the NEXYGEN Plus software.

3.2.3. Tensile test and results

Maximum mechanical properties of twelve layers RT300 glass fabric-reinforced Polylite 440-M888 polyester resin specimens cut on weft direction determined in tensile tests with 1 mm/min test speed are presented in table 3.2. For 2 mm/min test speed, maximum mechanical properties are presented in table 3.3. Both load-extension and stress-strain distributions have been generated for two test speeds (Fig. 3.13-3.14).

Table 3.2. Specimens' maximum mechanical properties with 1 mm/min test speed

Feature	Value
Load at maximum load (kN)	11.57
Load at break (kN)	11.567
Young's modulus (MPa)	7446.2
Tensile strength (MPa)	312.74
Stress at break (MPa)	312.61
Strain at break (-)	0.077
Stress at minimum extension (MPa)	0.109
Strain at maximum load (-)	0.077

Table 3.3. Specimens' maximum mechanical properties with 2 mm/min test speed

Feature	Value
Load at maximum load (kN)	10.778
Load at break (kN)	10.386
Tensile strength (MPa)	320.76
Stress at break (MPa)	309.11
Strain at break (-)	0.078
Stress at minimum extension (MPa)	0.104
Strain at maximum load (-)	0.077
Strain at maximum extension (-)	0.078

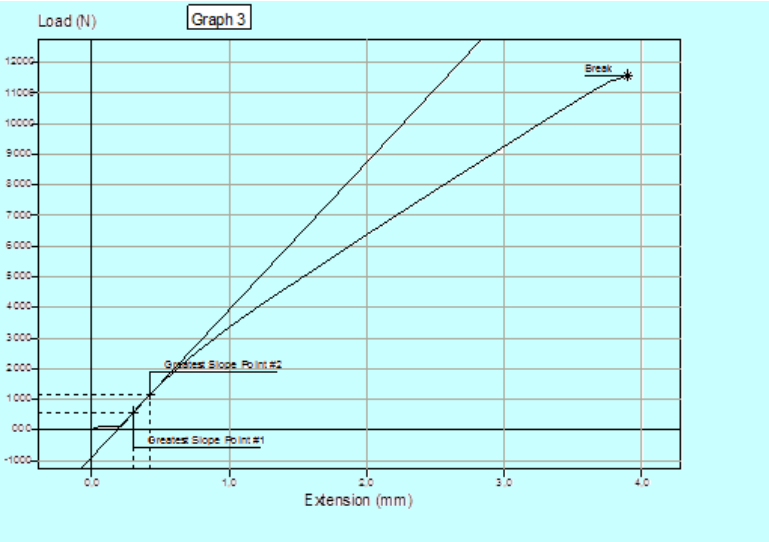

Figure 3.13. Load-extension distribution of specimen 3
(1 mm/min test speed)

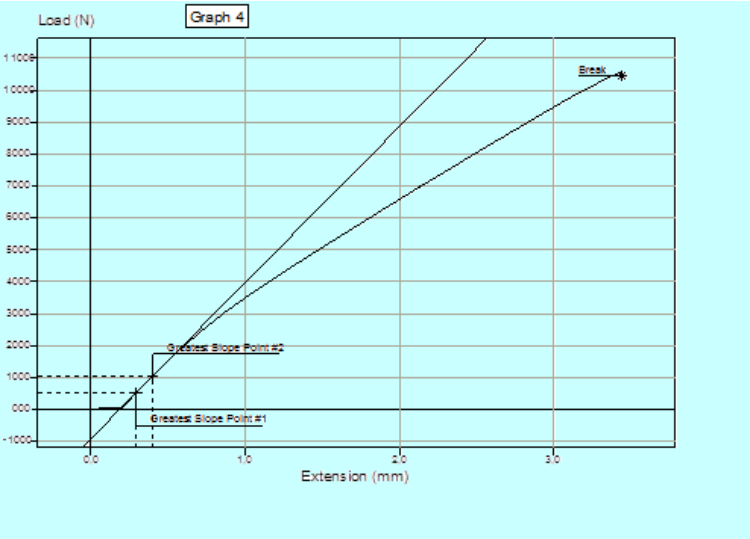

Figure 3.14. Load-extension distribution of specimen 4
(1 mm/min test speed)

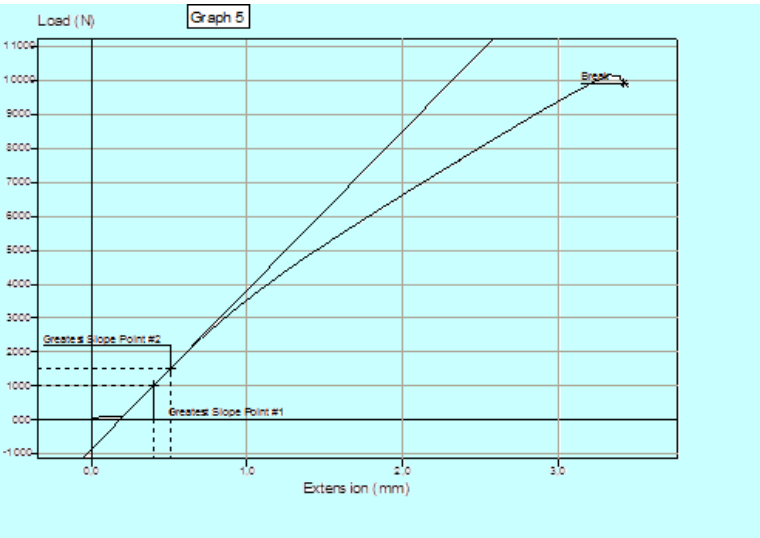

Figure 3.15. Load-extension distribution of specimen 5
(1 mm/min test speed)

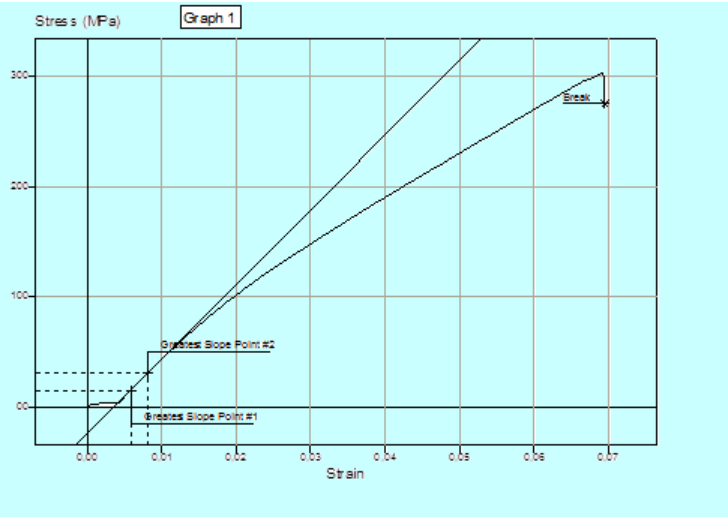

Figure 3.16. Stress-strain distribution of specimen 1
(1 mm/min test speed)

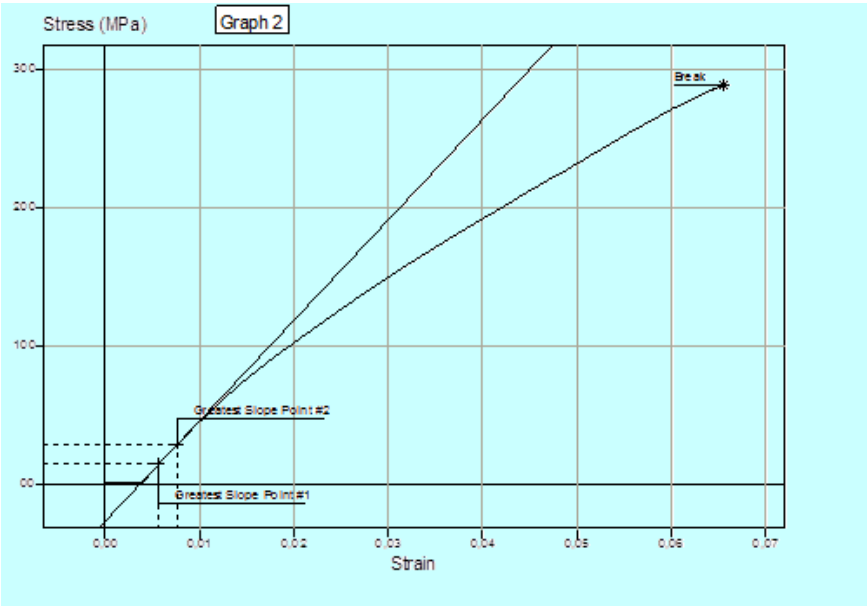

Figure 3.17. Stress-strain distribution of specimen 2
(1 mm/min test speed)

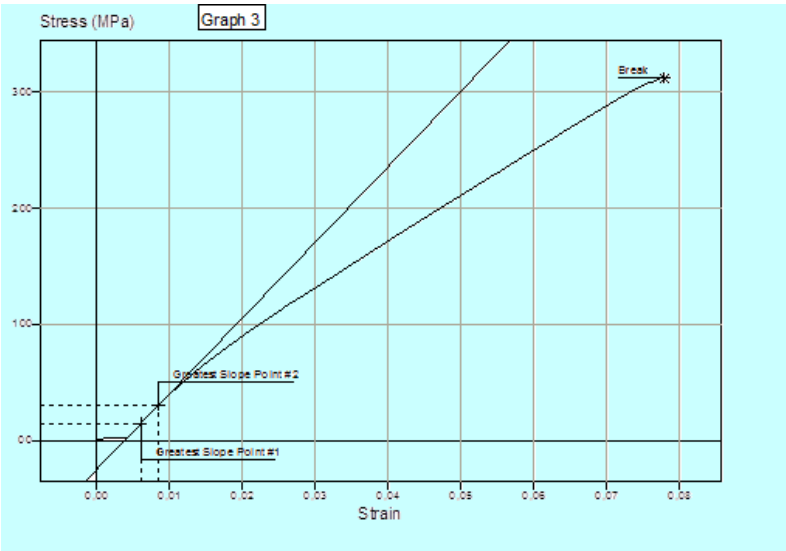

Figure 3.18. Stress-strain distribution of specimen 3
(1 mm/min test speed)

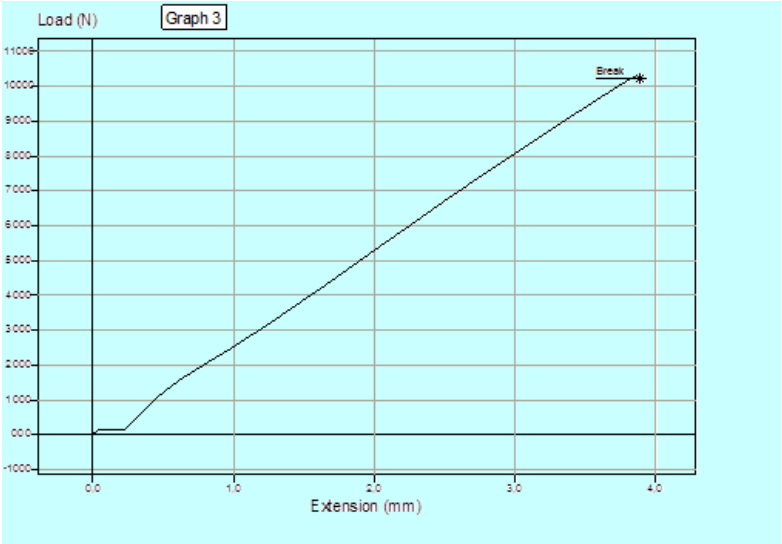

Figure 3.19. Load-extension distribution of specimen 3
(2 mm/min test speed)

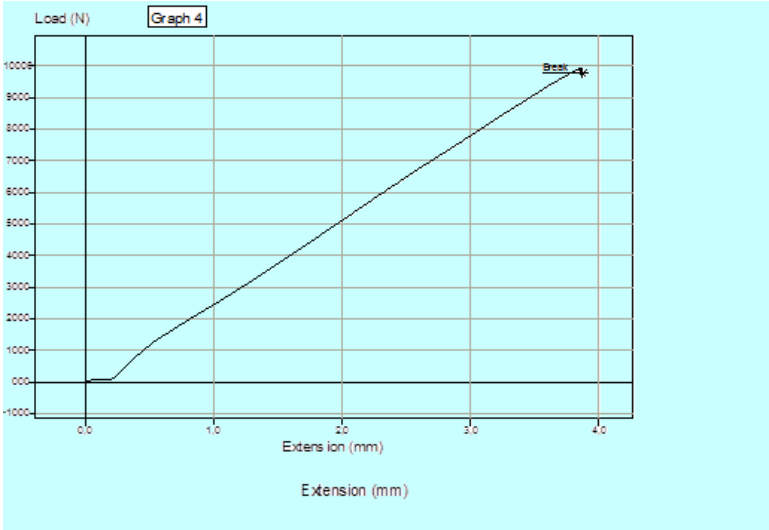

Figure 3.20. Load-extension distribution of specimen 4
(2 mm/min test speed)

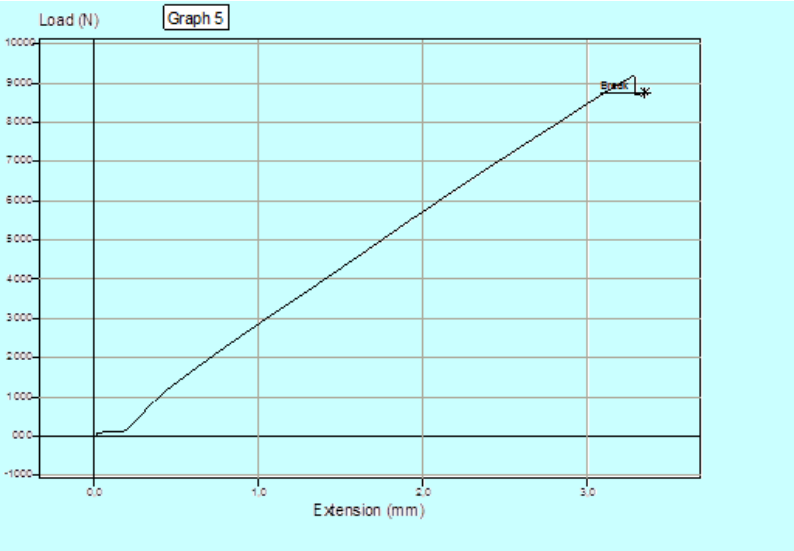

Figure 3.21. Load-extension distribution of specimen 5
(2 mm/min test speed)

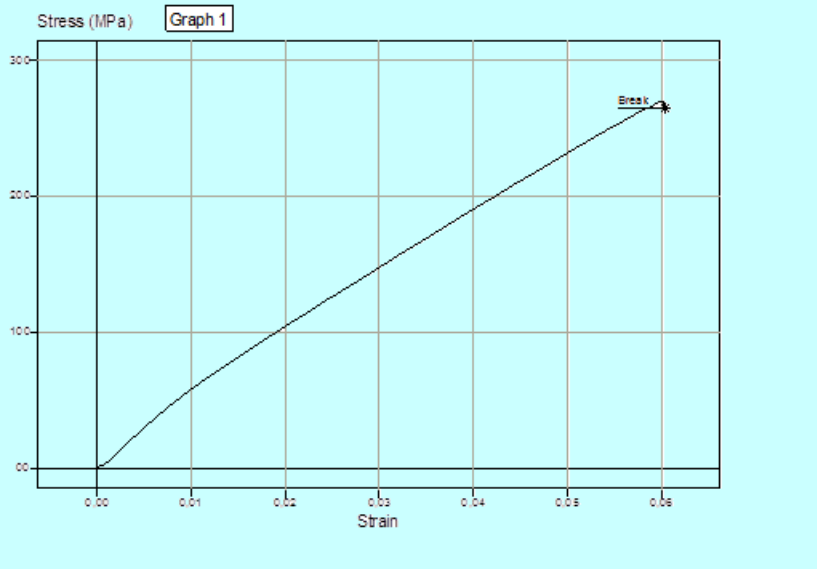

Figure 3.22. Stress-strain distribution of specimen 1
(2 mm/min test speed)

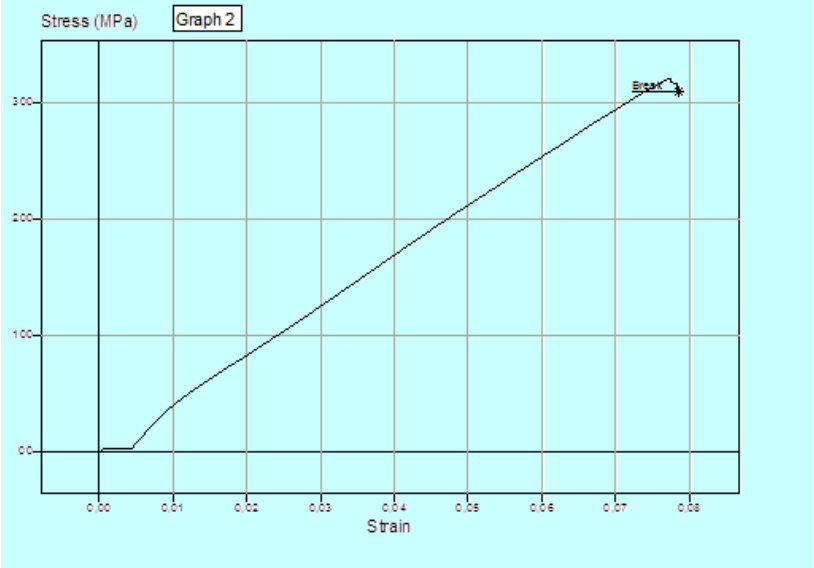

Figure 3.23. Stress-strain distribution of specimen 2
(2 mm/min test speed)

In the distributions presented in Figs. 3.16-3.18 and 3.22-3.24, the Young's modulus is computed between two points with the greatest slope belonging to the graph. These points are automatically generated at the end of each tensile test by the Nexygen software.

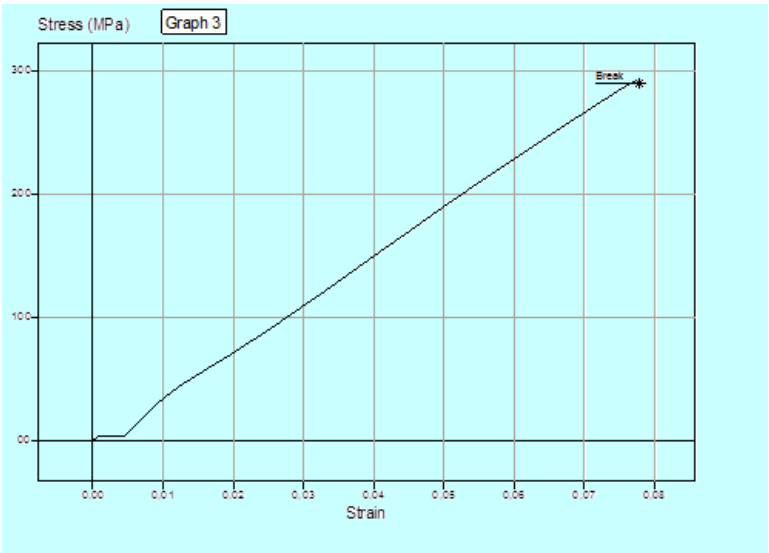

Figure 3.24. Stress-strain distribution of specimen 3
(2 mm/min test speed)

Young's modulus distributions of twelve layers RT300 glass fabric-reinforced Polylite 440-M888 polyester resin specimens cut on weft direction are presented in fig. 3.25 as well as a distribution between Young's modulus and tensile strength (fig. 3.26).

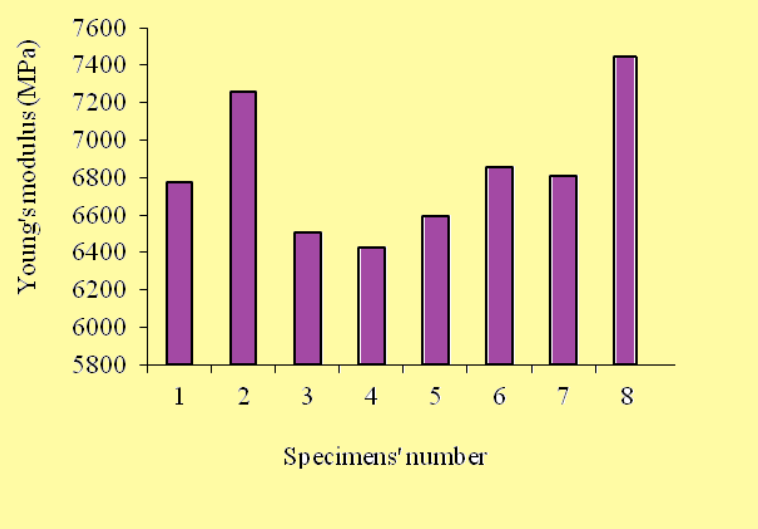

Figure 3.25. Young's modulus distribution of eight RT300 glass fabric-reinforced Polylite 440-M888 polyester resin specimens (1 mm/min test speed)

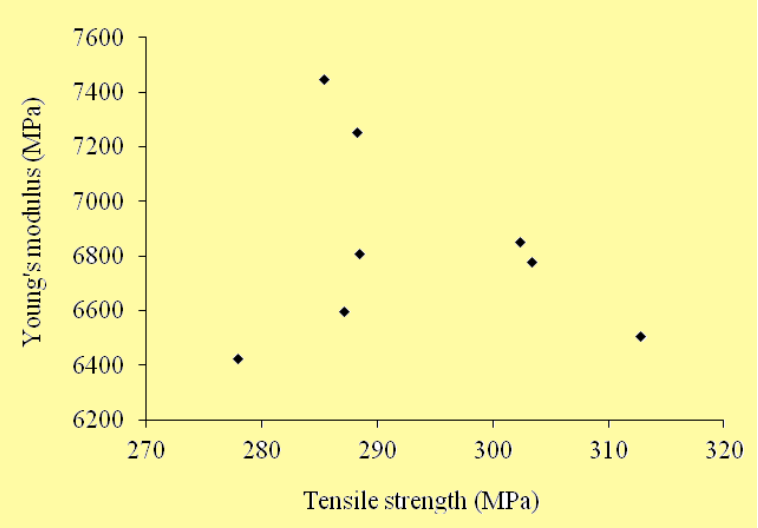

Figure 3.26. Young's modulus distribution versus tensile strength of eight RT300 glass fabric-reinforced Polylite 440-M888 polyester resin specimen (1 mm/min test speed)

3.2.4. Discussion and conclusion

Regarding the load-extension distributions of twelve layers RT300 glass fabric-reinforced Polylite 440-M888 polyester resin specimens cut on weft direction, all these behaviors shown in figs. 3.13-3.24 present nonlinear distributions. This phenomenon is due to the nonlinear behavior of the Polylite 440-M888 polyester resin since is well known that glass fibers present perfect

linear distribution in tensile test. The load-extension and stress-strain distributions for both 1 mm/min and 2 mm/min test speeds present close values.

The Young's modulus distribution of twelve layers RT300 glass fabric-reinforced Polylite 440-M888 polyester resin specimens cut on weft direction presents a maximum value of 7446.16 MPa at specimen 8 and a minimum value of 6424.94 MPa at specimen 4 (fig. 3.25). These values have been determined using the machine extensometer. Regarding the Young's modulus distribution versus tensile strength of twelve layers RT300 glass fabric-reinforced Polylite 440-M888 polyester resin specimens cut on weft direction presented in fig. 3.26, the eight values of Young's modulus are scattered between 277.86 MPa and 285.35 MPa tensile strength.

The first failures take place at a strain value of 0.025 – 0.035 for both test speeds. These failures appear due to delamination. The delamination is not so spectacular than in case of chopped strand mats reinforced polyester resin laminates. The crack that leads to break presents a development on a smaller length than in case of chopped strand mats reinforced polyester resin specimens. The tensile tests stopped at specimens' break. Due to good drape ability of RT300 glass fabrics, these reinforcing materials are widely used in most common polyester based composite structures.

3.3. Study of a RT300 glass fabric/Polylite composite laminate simulation

3.3.1. Fundamental considerations

This section presents numerical simulations regarding the elastic properties of ten plies RT300 glass fabric laminate impregnated with Polylite 440-M888 resin subjected to off-axis loading system as well as a comparison with experimental results obtained in tensile tests on thirteen specimens. To compute the elastic properties, the glass fabric laminate may be equivalent with a new laminate with plies sequence $[0/90]_{10}$ formed of unidirectional reinforced laminae. This equivalence can be considered accurate.

Axial, transverse and shear moduli as well as axial-transverse Poisson ratio have been computed. The comparison between numerical simulations and experimental results obtained on "LS100 Plus" Lloyd Instruments materials testing machine show a good accordance between both types of data.

Glass fabrics manufactured from unidirectional roving represent the second most used reinforcing material after chopped strand mats. These fabrics present certain number of nodes on square centimeter, certain width and thickness, certain porosity (eye width), bending strength and feature certain surface aspect. The weaving method, threads thickness as well as their twist degree plays a significant role in mechanical characterization of a composite structure. In case of two-phase composite (e.g. matrix and reinforcement), the elastic properties can be quite easy computed using the basic elasticity properties of each compound in the rule of mixtures formula.

Things are not so simple in case of three or more compounds. Here, homogenization and averaging methods can be used to compute elastic properties of such composite materials (e.g. pre-impregnated composites) [HTE11a]. Extended experimental researches have been carried

out on glass-fiber-reinfrced polymer matrix composites subjected to cyclic tensile-compression loadings with various numbers of cycles and load limits [HTE11b], [SVL11c]. Both experimental and numerical methods have been used to determine mechanical properties of various fiber-reinforced composite laminates, with and without fillers, subjected to off-axis loading systems, tensile and bending loads, biaxial loadings as well as thermal loads.

3.3.2. A theoretical model

Fibers-reinforced polymer matrix composite materials are heterogeneous and anisotropic materials so that their mechanics is more complex than that of conventional materials. A theoretical model, proposed by Teodorescu-Drăghicescu H. is presented. The basic element of a composite laminate structure is the individual layer (called lamina) unidirectional reinforced with fibers inserted into a resin system (called matrix). For in-plane stress state condition by superimposing three loadings $\sigma_{\parallel}$, $\sigma_{\perp}$ and $\tau_{\#}$, following law of elasticity can be given:

$$\begin{bmatrix} \varepsilon_{II} \\ \varepsilon_{\perp} \\ \gamma_{\#} \end{bmatrix} = \begin{bmatrix} \frac{1}{E_{II}} & -\frac{\upsilon_{II\perp}}{E_{\perp}} & 0 \\ -\frac{\upsilon_{\perp II}}{E_{II}} & \frac{1}{E_{\perp}} & 0 \\ 0 & 0 & \frac{1}{G_{\#}} \end{bmatrix} \cdot \begin{bmatrix} \sigma_{II} \\ \sigma_{\perp} \\ \tau_{\#} \end{bmatrix}, \tag{3.1}$$

where the second matrix is called the compliances matrix.

Transverse contraction coefficients $\upsilon_{\parallel\perp}$ and $\upsilon_{\perp\parallel}$ are not independent of each other. If we assume the existence of small deformations and a linear elastic behavior of the composite material than, between the coefficients of transverse contraction υ and the Young's moduli E, there is following relationship [HSC05]:

$$\frac{\upsilon_{\perp II}}{E_{II}} = \frac{\upsilon_{II\perp}}{E_{\perp}}. \tag{3.2}$$

The unidirectional reinforced lamina can be described by four basic elasticity terms: $E_{\parallel}$, $E_{\perp}$, $\upsilon_{\perp\parallel}$ and $G_{\#}$. If desired, the expression (3.1) in terms of stresses versus strains can be written as following:

$$\begin{bmatrix}\sigma_{II}\\ \sigma_{\perp}\\ \tau_{\#}\end{bmatrix}=\begin{bmatrix}\frac{E_{II}}{1-\upsilon_{\perp II}\cdot\upsilon_{II\perp}} & \frac{\upsilon_{II\perp}\cdot E_{\perp}}{1-\upsilon_{\perp II}\cdot\upsilon_{II\perp}} & 0\\ \frac{\upsilon_{\perp II}\cdot E_{II}}{1-\upsilon_{\perp II}\cdot\upsilon_{II\perp}} & \frac{E_{\perp}}{1-\upsilon_{\perp II}\cdot\upsilon_{II\perp}} & 0\\ 0 & 0 & G_{\#}\end{bmatrix}\cdot\begin{bmatrix}\varepsilon_{II}\\ \varepsilon_{\perp}\\ \gamma_{\#}\end{bmatrix}, \tag{3.3}$$

where the second matrix is called the stiffness matrix.

Expressing the strains versus stresses lead to the advantage to compute the compliances as a function of lamina's basic elastic properties. These basic elastic properties are also called technical constants. These constants can be determined from the lamina's micromechanics using the fibers and matrix elastic properties [HSC05]

$$E_{II}=E_F\cdot\varphi+E_M\cdot(1-\varphi), \tag{3.4}$$

$$\upsilon_{\perp II}=\varphi\cdot\upsilon_F+(1-\varphi)\cdot\upsilon_M\ , \tag{3.5}$$

$$E_{\perp}=\frac{E_M}{1-\upsilon_M^2}\cdot\frac{1+0{,}85\cdot\varphi^2}{(1-\varphi)^{1{,}25}+\frac{\varphi\cdot E_M}{(1-\upsilon_M^2)\cdot E_F}}, \tag{3.6}$$

$$\upsilon_{II\perp}=\upsilon_{\perp II}\cdot\frac{E_{\perp}}{E_{II}}, \tag{3.7}$$

$$G_{\#}=G_M\cdot\frac{1+0{,}6\cdot\varphi^{0{,}5}}{(1-\varphi)^{1{,}25}+\varphi\cdot\frac{G_M}{G_F}}. \tag{3.8}$$

Considering lamina being in the stress plane state, its strains can be expressed versus stresses using the transformed components of the compliances matrix:

$$\begin{bmatrix}\varepsilon_{xx}\\ \varepsilon_{yy}\\ \gamma_{xy}\end{bmatrix}=\begin{bmatrix}c_{11} & c_{12} & c_{13}\\ c_{12} & c_{22} & c_{23}\\ c_{13} & c_{23} & c_{33}\end{bmatrix}\cdot\begin{bmatrix}\sigma_{xx}\\ \sigma_{yy}\\ \tau_{xy}\end{bmatrix}. \tag{3.9}$$

These transformed compliances can be computed as following [HSC05].:

$$c_{11}=\frac{\cos^4\alpha}{E_{II}}+\frac{\sin^4\alpha}{E_{\perp}}+\frac{1}{4}\cdot\left(\frac{1}{G_{\#}}-\frac{2\cdot\upsilon_{\perp II}}{E_{II}}\right)\cdot\sin^2 2\alpha, \tag{3.10}$$

$$c_{22}=\frac{\sin^4\alpha}{E_{II}}+\frac{\cos^4\alpha}{E_{\perp}}+\frac{1}{4}\cdot\left(\frac{1}{G_{\#}}-\frac{2\cdot\upsilon_{\perp II}}{E_{II}}\right)\cdot\sin^2 2\alpha, \tag{3.11}$$

$$c_{33}=\frac{\cos^2 2\alpha}{G_{\#}}+\left(\frac{1}{E_{II}}+\frac{1}{E_{\perp}}+\frac{2\cdot\upsilon_{\perp II}}{E_{II}}\right)\cdot\sin^2 2\alpha, \tag{3.12}$$

$$c_{12}=\frac{1}{4}\cdot\left(\frac{1}{E_{II}}+\frac{1}{E_{\perp}}-\frac{1}{G_{\#}}\right)\cdot sin^2 2\alpha -$$

$$-\frac{\upsilon_{\perp II}}{E_{II}}\cdot\left(sin^4\alpha+cos^4\alpha\right), \tag{3.13}$$

$$c_{13}=\left(\frac{2}{E_{\perp}}+\frac{2\cdot\upsilon_{\perp II}}{E_{II}}-\frac{1}{G_{\#}}\right)\cdot sin^3\alpha\cdot cos\alpha-\left(\frac{2}{E_{II}}+\frac{2\cdot\upsilon_{\perp II}}{E_{II}}-\frac{1}{G_{\#}}\right)\cdot\cos^3\alpha\cdot\sin\alpha, \tag{3.14}$$

$$c_{23}=\left(\frac{2}{E_{\perp}}+\frac{2\cdot\upsilon_{\perp II}}{E_{II}}-\frac{1}{G_{\#}}\right)\cdot cos^3\alpha\cdot sin\alpha-\left(\frac{2}{E_{II}}+\frac{2\cdot\upsilon_{\perp II}}{E_{II}}-\frac{1}{G_{\#}}\right)\cdot sin^3\alpha\cdot cos\,\alpha. \tag{3.15}$$

When stresses are expressed versus strains, the relations are:

$$\begin{bmatrix}\sigma_{xx}\\ \sigma_{yy}\\ \tau_{xy}\end{bmatrix}=\begin{bmatrix}r_{11} & r_{12} & r_{13}\\ r_{12} & r_{22} & r_{23}\\ r_{13} & r_{23} & r_{33}\end{bmatrix}\cdot\begin{bmatrix}\varepsilon_{xx}\\ \varepsilon_{yy}\\ \gamma_{xy}\end{bmatrix}, \tag{3.16}$$

where r_{ij} represent the transformed components of the stiffness matrix.

A laminate composite structure is considered formed of N unidirectional reinforced laminae subjected to a general set of in-plane loads. The elasticity law of a unidirectional reinforced K lamina can be expressed as following:

$$\begin{bmatrix}\sigma_{xx\,K}\\ \sigma_{yy\,K}\\ \tau_{xy\,K}\end{bmatrix}=\begin{bmatrix}r_{11\,K} & r_{12\,K} & r_{13\,K}\\ r_{12\,K} & r_{22\,K} & r_{23\,K}\\ r_{13\,K} & r_{23\,K} & r_{33\,K}\end{bmatrix}\cdot\begin{bmatrix}\varepsilon_{xx\,K}\\ \varepsilon_{yy\,K}\\ \gamma_{xy\,K}\end{bmatrix}, \tag{3.17}$$

where r_{ijK} represents the transformed stiffness, σ_{xxK} and σ_{yyK} are medium stresses of a K lamina on x and y-axes, τ_{xyK} represent the medium shear stress according to x-y coordinate system.

The laminate balance equations are:

$$n_{xx}=\underline{\sigma}_{xx}\cdot t=\sum_{K=1}^{N}\left(\sigma_{xxK}\cdot t_K\right)=\sum_{K=1}^{N}n_{xxK}, \tag{3.18}$$

$$n_{yy}=\underline{\sigma}_{yy}\cdot t=\sum_{K=1}^{N}\left(\sigma_{yyK}\cdot t_K\right)=\sum_{K=1}^{N}n_{yyK}, \tag{3.19}$$

$$n_{xy}=\underline{\tau}_{xy}\cdot t=\sum_{K=1}^{N}\left(\tau_{xyK}\cdot t_K\right)=\sum_{K=1}^{N}n_{xyK}, \tag{3.20}$$

where n_{xx} and n_{yy} are the normal forces, n_{xy} is the shear force, $\underline{\sigma}_{xx}$ and $\underline{\sigma}_{yy}$ represent the normal stresses, $\underline{\tau}_{xy}$ is the shear stress of the composite laminate, t_K and t are the K lamina thickness respective the laminate thickness, n_{xxK} and n_{yyK} are normal forces on the unit length of the K lamina and n_{xyK} is the in-plane shear force on the unit length of the K lamina.

With relations (3.17)-(3.20) the composite laminate elasticity law can be obtained:

$$\begin{bmatrix} \underline{\sigma}_{xx} \\ \underline{\sigma}_{yy} \\ \underline{\tau}_{xy} \end{bmatrix} = \begin{bmatrix} \sum_{K=1}^{N}\left(r_{11K}\cdot\frac{t_K}{t}\right) & \sum_{K=1}^{N}\left(r_{12K}\cdot\frac{t_K}{t}\right) & \sum_{K=1}^{N}\left(r_{13K}\cdot\frac{t_K}{t}\right) \\ \sum_{K=1}^{N}\left(r_{12K}\cdot\frac{t_K}{t}\right) & \sum_{K=1}^{N}\left(r_{22K}\cdot\frac{t_K}{t}\right) & \sum_{K=1}^{N}\left(r_{23K}\cdot\frac{t_K}{t}\right) \\ \sum_{K=1}^{N}\left(r_{13K}\cdot\frac{t_K}{t}\right) & \sum_{K=1}^{N}\left(r_{23K}\cdot\frac{t_K}{t}\right) & \sum_{K=1}^{N}\left(r_{33K}\cdot\frac{t_K}{t}\right) \end{bmatrix} \cdot \begin{bmatrix} \varepsilon_{xx} \\ \varepsilon_{yy} \\ \gamma_{xy} \end{bmatrix}, \tag{3.21}$$

and from these relations, the composite laminate stiffness can be determined:

$$\underline{r}_{ij} = \sum_{K=1}^{N}\left(r_{ijK}\cdot\frac{t_K}{t}\right). \tag{3.22}$$

In these conditions, the composite laminate elasticity law becomes:

$$\begin{bmatrix} \underline{\sigma}_{xx} \\ \underline{\sigma}_{yy} \\ \underline{\tau}_{xy} \end{bmatrix} = \begin{bmatrix} \underline{r}_{11} & \underline{r}_{12} & \underline{r}_{13} \\ \underline{r}_{12} & \underline{r}_{22} & \underline{r}_{23} \\ \underline{r}_{13} & \underline{r}_{23} & \underline{r}_{33} \end{bmatrix} \cdot \begin{bmatrix} \varepsilon_{xx} \\ \varepsilon_{yy} \\ \gamma_{xy} \end{bmatrix}, \tag{3.23}$$

where $\underline{r}_{ij}$ are functions of the basic elastic properties of each lamina $E_{\parallel K}$, $E_{\perp K}$, $\upsilon_{\perp\parallel K}$, $G_{\#K}$ and of the fibers disposal angle. Analogue to stresses, a strains analysis can be carried out. From relation (3.23) the strains ε_{xx}, ε_{yy} and γ_{xy} can be computed.

The individual strains of each lamina can be determined through transformation as following:

$$\begin{bmatrix} \varepsilon_{II\,K} \\ \varepsilon_{\perp K} \\ \gamma_{\#K} \end{bmatrix} = [T] \cdot \begin{bmatrix} \varepsilon_{xx\,K} \\ \varepsilon_{yy\,K} \\ \gamma_{xy} \end{bmatrix}, \tag{3.24}$$

where [T] represents the transformation matrix with following expression:

$$[T] = \begin{bmatrix} cos^2\alpha_K & sin^2\alpha_K & sin\alpha_K cos\alpha_K \\ sin^2\alpha_K & cos^2\alpha_K & -sin\alpha_K cos\alpha_K \\ -2sin\alpha_K cos\alpha_K & 2sin\alpha_K cos\alpha_K & \left(cos^2\alpha_K - sin^2\alpha_K\right) \end{bmatrix} \tag{3.25}$$

Finally, from the strains presented in relation (3.24), the stresses in each individual lamina can be computed:

$$\sigma_{II\,K}=\frac{E_{II\,K}}{1-\upsilon_{\perp II\,K}\cdot\upsilon_{II\perp K}}\cdot\varepsilon_{II\,K}+\frac{\upsilon_{\perp II\,K}\cdot E_{\perp K}}{1-\upsilon_{\perp II\,K}\cdot\upsilon_{II\perp K}}\cdot\varepsilon_{\perp K}, \tag{3.26}$$

$$\sigma_{\perp K}=\frac{\upsilon_{\perp II\,K}\cdot E_{\perp K}}{1-\upsilon_{\perp II\,K}\cdot\upsilon_{II\perp K}}\cdot\varepsilon_{II\,K}+\frac{E_{\perp K}}{1-\upsilon_{\perp II\,K}\cdot\upsilon_{II\perp K}}\cdot\varepsilon_{\perp K}, \tag{3.27}$$

To carry out a prediction regarding the failure of the individual laminae, a break criterion is usually used. The system of coordinates ∥-⊥-z represents the local system of coordinates and is applied to each individual lamina. The x-y-z system of coordinates represents the global system of coordinates and is usually applied to the entire laminate.

3.3.3. Numerical simulations and results

To compute the elastic properties of a composite laminate, a glass fabric-reinforced composite laminate with following features have been considered:

- Type of glass fabric: RT300;
- Type of weave: plain;
- Type of resin: Polylite 440-M888;
- Number of plies: 10.

These ten plies of the considered glass fabric laminate may be equivalent with a new laminate with $[0/90]_{10}$ plies sequence that will be considered in numerical simulations.

The computational method is based on the approach presented in reference [DHU96]. All plies present same fibers and matrix properties, fibers content and plies thickness. The axial Young's moduli of every lamina and the axial-transverse Poisson ratio have been computed using an equal strain expression (rule of mixtures). The transverse Young's moduli of every lamina as well as the axial-transverse shear modulus have been computed using either equal stress or Haplin-Tsai expressions. Following material input data have been considered:

- Matrix axial and transverse Young's modulus: 3.2 GPa;
- Fibers axial and transverse Young's modulus: 73 GPa;
- Matrix axial-transverse Poisson ratio: 0.3;
- Fibers axial-transverse Poisson ratio: 0.28;
- Matrix shear modulus: 1.23 GPa;

- Fibers shear modulus: 28.5 GPa;
- Fibers volume fraction: 0.35.

The results are presented in Figs. 3.37-3.39.

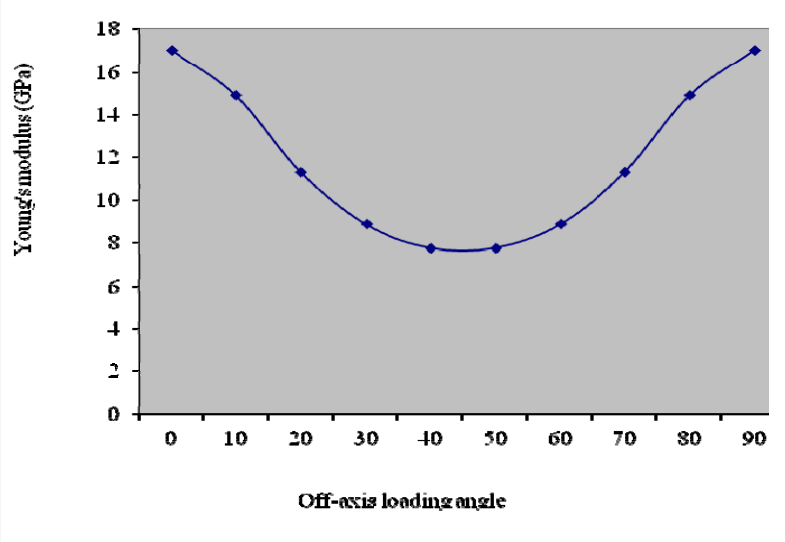

Figure 3.27. Axial and transverse Young's modulus distribution

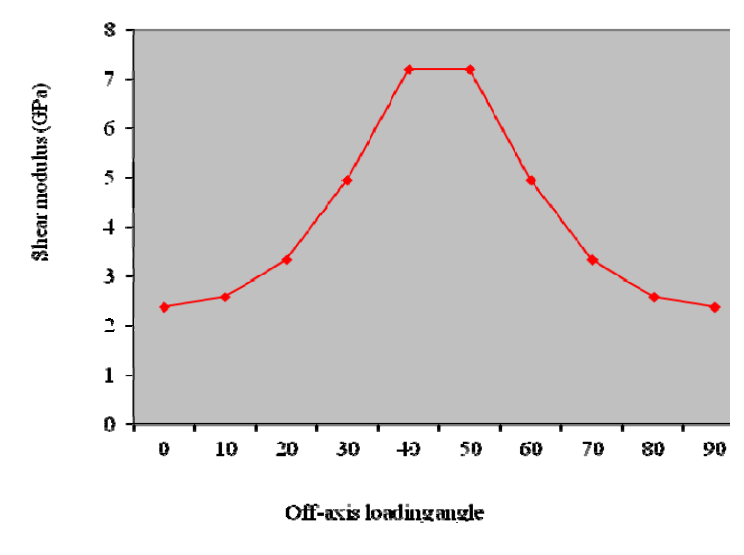

Figure 3.28. Axial-transverse shear modulus distribution

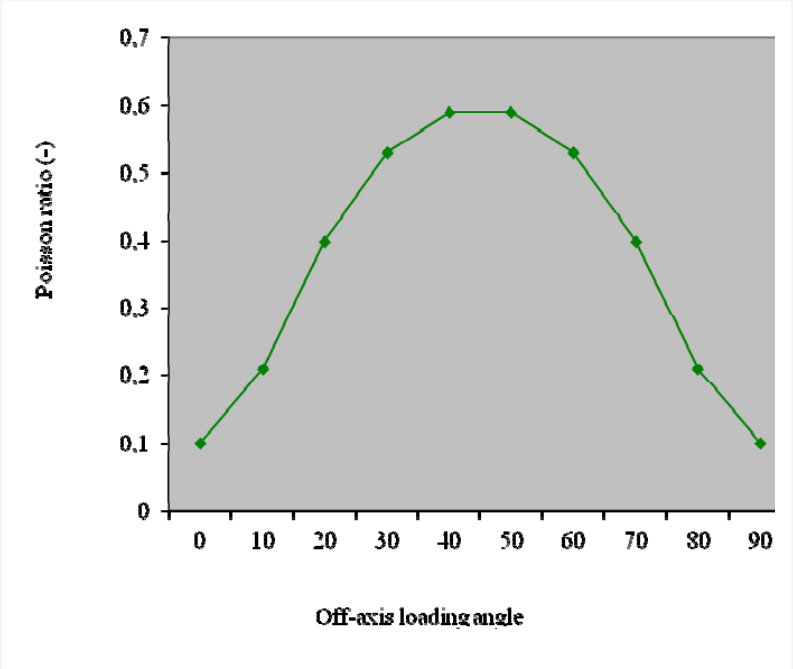

Figure 3.29. Axial-transverse Poisson ratio distribution

3.3.4. Experimental approach and results

The composite laminate used in tensile tests is a thermosett polymer (i.e. unsaturated polyester resin of type Polylite 440-M888) reinforced with twelve plies of glass fabric of type RT300 (300 g/m^2 specific weight). In general, the RT fabrics are manufactured from roving with cut margins and strengthened with Dreher threads. From a cured plate of 3 mm thickness, several specimens have been cut using a diamond powder mill with added water to avoid introduce internal stresses and especially thermal stresses that can appear in the cutting process. The specimens have been tempered for 24 hours at a temperature of 20°C and then subjected to tensile loads until break according to SR EN 527-1 (Fig. 3.30).

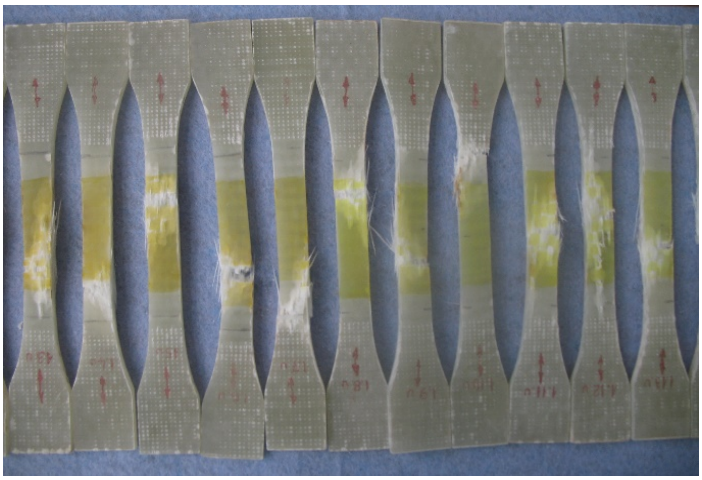

Figure 3.30. Tensile tested RT300 glass fabric-reinforced Polylite 440-M888 polyester resin specimens

The maximum mechanical properties of ten plies RT300 glass fabric-reinforced Polylite 440-M888 polyester resin specimens determined in tensile tests are presented in table 3.5. Young's modulus distributions of eight specimens and versus tensile strength are shown in Figs. 3.31-3.32. An example of load-extension from preload distribution of one specimen is presented in Fig. 3.33.

Table 3.5. Specimens' maximum mechanical properties

Feature	Value
Load at maximum load (kN)	1.36
Load at break (kN)	1.2
Young's modulus (MPa)	8894.7
Tensile strength (MPa)	339.37
Machine extension at maximum load (mm)	3.6
Stress at break (MPa)	334.45
Strain at break (-)	0.069
Stress at minimum extension (MPa)	0.014
Strain at maximum load (-)	0.068

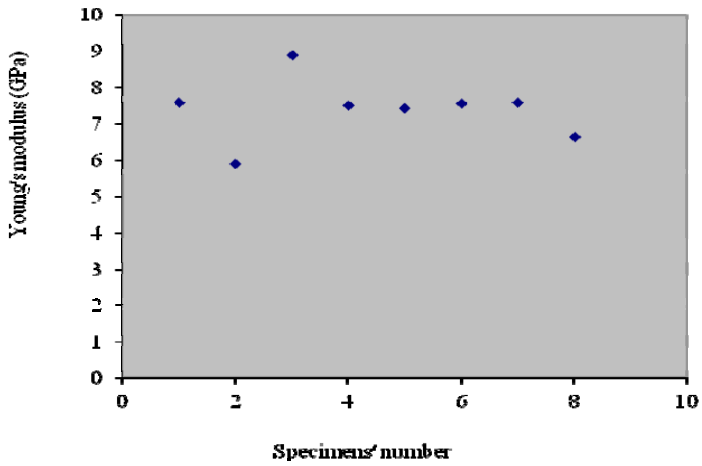

Figure 3.31. Young's modulus distribution of eight RT300 glass fabric-reinforced Polylite 440-M888 specimens

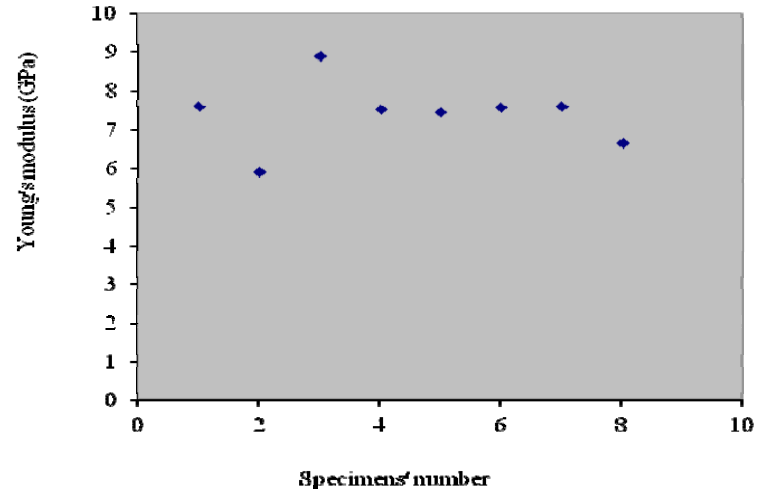

Figure 3.31. Young's modulus distribution of eight RT300 glass fabric-reinforced Polylite 440-M888 specimens

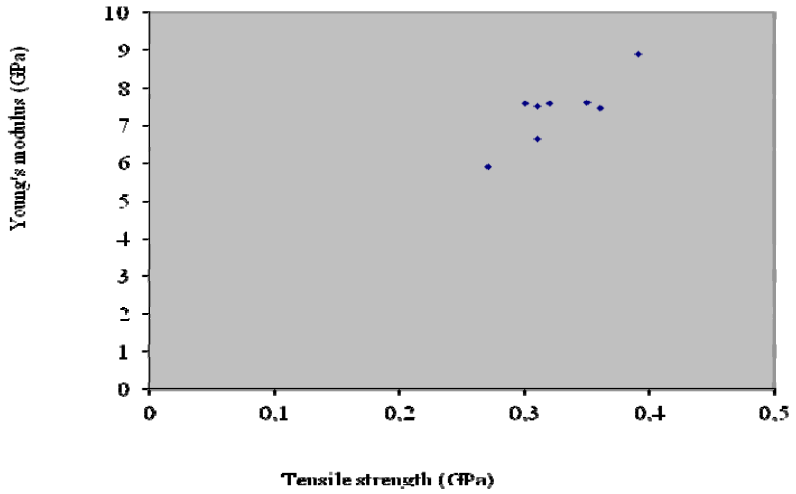

Figure 3.32. Young's modulus distribution versus tensile strength of eight RT300 glass fabric-reinforced Polylite 440-M888 specimens

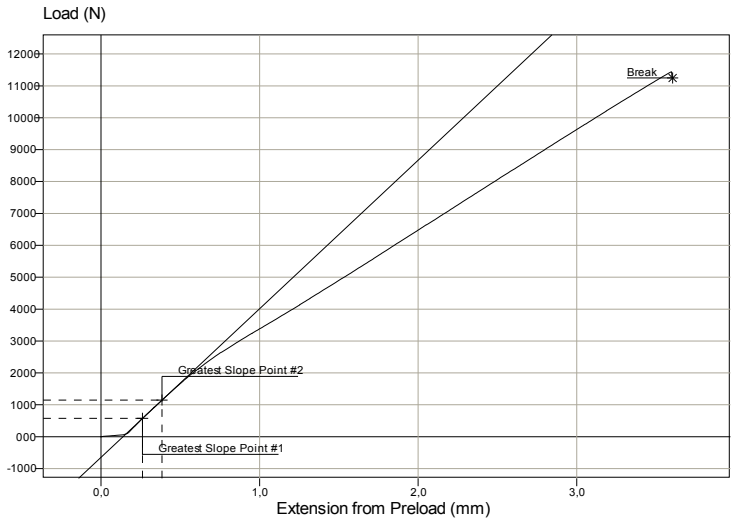

Figure 3.33. Example of load-extension from preload distribution

3.3.5. Discussion and conclusions

A comparison between numerical simulations and experimental results carried out on ten plies RT300 glass fabric laminate impregnated with Polylite 440-M888 resin subjected to tensile loads until break is presented in Fig. 3.34. Numerical simulations of axial and transverse Young's modulus at 0° off-axis loading system show greater values than those obtained in tensile tests.

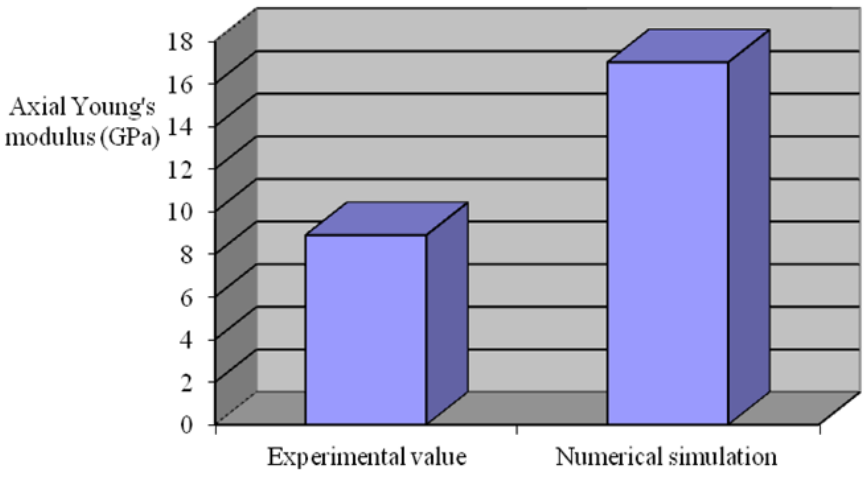

Figure 3.34. Stiffness evaluations of RT300 glass fabric/Polylite laminate

The first failures take place at a strain value of 0.03. These failures appear because of delamination. The delamination is not so spectacular than in case of chopped strand mats reinforced polyester resin laminates. The crack that leads to break presents a development on a smaller length than in case of chopped strand mats reinforced polyester resin specimens.

Another useful comparison between numerical simulations and experimental results carried out on ten plies RT300 glass fabric laminate impregnated with Polylite 440-M888 resin subjected to a general set of in-plane loads (e.g. normal axial stress: 380 MPa; normal transverse stress: 38 MPa and shear stress: 19 MPa) show the same difference between normal axial stress determined at 0° off-axis loading system at lamina number 11 and the stress at break value (Fig. 3.35).

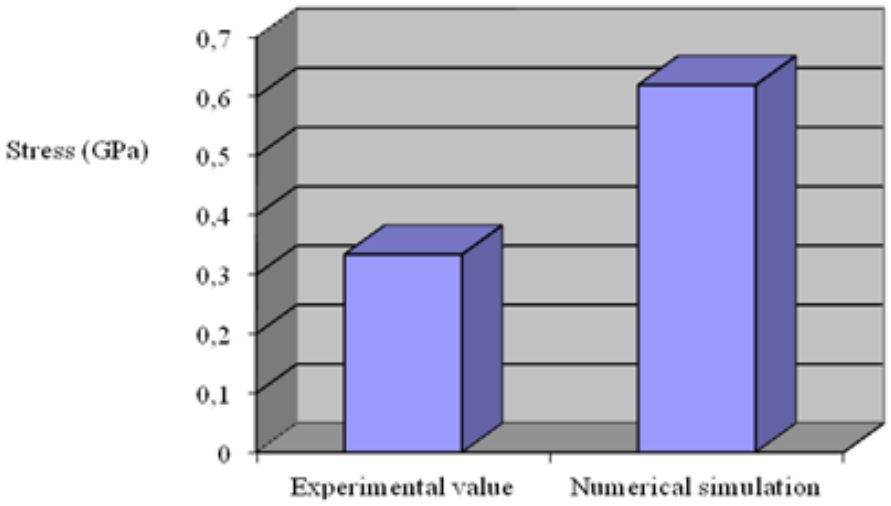

Figure 3.35. Normal axial stress at 0° off-axis loading system in lamina 11 and the stress at break determined experimentally for the entire laminate

Due to good drape ability of RT300 glass fabrics, these reinforcing materials are widely used in most common polyester based composite structures. These fabrics are used to reinforce polyester as well as epoxy resins and present good impregnation properties.

3.4. High rigidity thin sandwich composite laminate with COREMAT and dissimilar skins

3.4.1. General considerations

Within this section, the most important mechanical properties determined in simple tensile tests of a thin sandwich composite laminate with nonwoven polyester mat used as core and dissimilar skins are presented. This nonwoven polyester mat known as COREMAT increases the overall stiffness of a composite laminate by the increase of the entire thickness of the laminate avoiding stacking a specific number of layers.

The skins are dissimilar, the upper one has a polyester reinforced RT glass fabric and the lower one is a gelcoat layer. Following main mechanical properties have been determined: stiffness, Young's modulus, load/stress/strain at maximum load, load/stress/strain at maximum extension, load/stress/strain at minimum load, load/stress/strain at minimum extension, tensile

strength, work to maximum load/extension, work to minimum load/extension and load/stress at break.

For a sandwich structure, the core represents the most important part which influences the overall structure's stiffness and flexural rigidity. The COREMAT material is a random oriented noncontinuous nonwoven polyester mat which contains microspheres that prevent excessive resin consumption in the manufacturing of thin composite laminates.

The nonwoven polyester mat is a soft material which presents excellent resin impregnation and high drapeability and therefore is suitable for complex shapes. It is most often applied against the gelcoat layer to create a superior surface finish for instance on hull sides and to prevent the appearance of the glass fibers reinforcement especially when dark gelocoats are used.

This material has a good compatibility with polyester, vinylester and epoxy resins and is suitable to use it for common composite laminate processes like hand lay-up and spray-up. The COREMAT material is used to increase the overall stiffness of the whole sandwich structure avoiding stacking together a high number of layers to obtain the same stiffness for a composite laminate [SVL13] . The most important characteristics of a sandwich structure using this kind of core are:

- Weight saving;
- Important saving in resin and reinforcement consumption;
- Overall stiffness increase of the whole sandwich structure;
- Fast build of the structure's thickness;
- Superior surface finish.

Usually, composite laminates present quite low stiffness and flexural rigidities. For pre-impregnated composite materials with more than two phases, to predict their elastic properties, averaging and homogenization methods can be used [HTE11a].

For a three-phase polymer matrix composite material subjected for instance to static cyclic tensile-compression loadings, hysteresis phenomena can appear [HTE11b]. It would be very interesting to quantify the influence of the COREMAT material in the overall hysteresis of a composite laminate with this kind of core.

For a multiphase polymer matrix composite material with ceramic filler, the same hysteresis phenomena have been determined on samples subjected to static cyclic loadings S. [SVL11c] . For unidirectional reinforced polymer matrix composite laminates subjected to off-axis loading systems, their elastic properties vary as a function of their plies sequence [SVL11d] , [HTE11c]. For a thin sandwich structure with COREMAT material, a thermomechanical response including the coefficients of thermal expansion have been determined [HTE10].

3.4.2. Tests to determine the properties of the new material

Following plies sequence has been used in the manufacturing of the composite laminate:

- 1 x RT500 glass roving fabric;
- 2 x RT800 glass roving fabric;
- 1 x 450 g/m^2 chopped glass fibres mat;
- Nonwoven polyester mat as core;
- 1 x 450 g/m^2 chopped glass fibres mat;
- A gelcoat layer.

From the laminate plate, twelve specimens have been cut according to SR EN ISO 527-4: 2000 and subjected to tensile test until break occur. The composite laminate plate has been manufactured at Compozite Ltd., Brasov and tested in the Materials Testing Laboratory within Transilvania University of Brasov, Romania. The materials testing machine used in tests is a LS100 Plus type, produced by Lloyd Instruments, UK, with following characteristics: Force range: up to 100 kN; Test speed accuracy: < 0.2 %; Load resolution: < 0.01 % from the force cell; Extension resolution: < 0.1 microns; Type of force cell: XLC-100K-A1; Extensometer: type Epsilon Technology; Analysis software: NEXYGEN Plus.

Test and specimens features are: Length between extensometer's lamellae: 50 mm; Test speed: 1 mm/min; Median specimens width: 10 mm; Median specimens thickness: 8 mm; Median cross-sectional area: 80 mm^2.

The materials testing machine allows determination of experimental results in electronic format by help of the NEXYGEN Plus software.

3.4.3. Tensile test results

The basic mechanical properties determined in tensile tests have been presented in table 3.6

Table 3.6. Basic mean mechanical properties of thin sandwich composite laminate with nonwoven polyester mat as core

Feature	Value
Stiffness (N/m)	15448000
Young's modulus (MPa)	9635.1
Stress at maximum load (MPa)	71.966
Load at break (kN)	1.2691
Stress at break (MPa)	15.754
Strain at break (-)	-0.058935

A typical stress-strain distribution is presented in Fig. 3.36. This distribution is influenced by the extensometer used during tests.

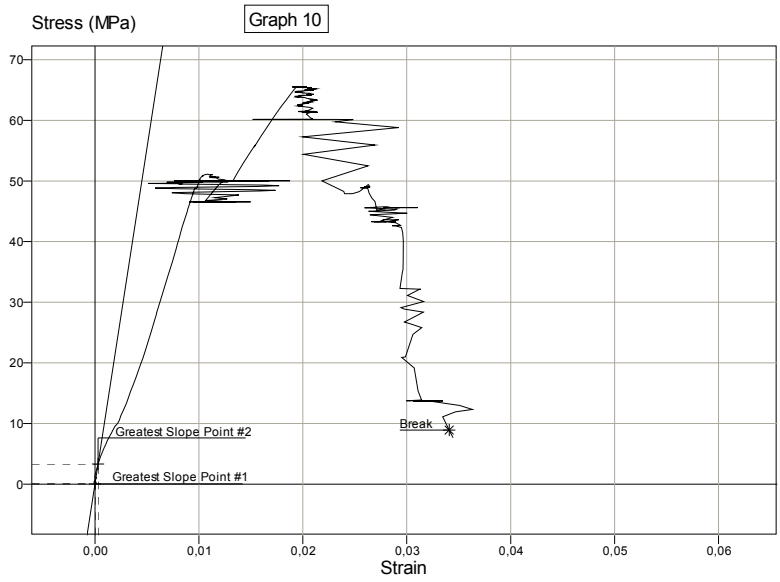

Figure 3.36. Stress-strain distribution of specimen 10

Load-extension distributions for all twelve specimens subjected to tensile loads as well as other important features are presented in Fig. 3.7-3.42.

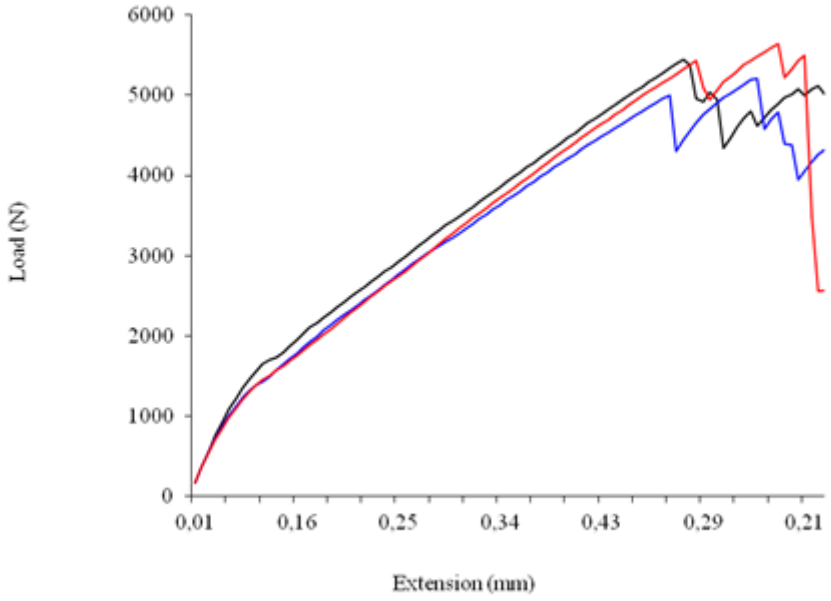

Figure 3.37. Load-extension distribution of specimens 1-3

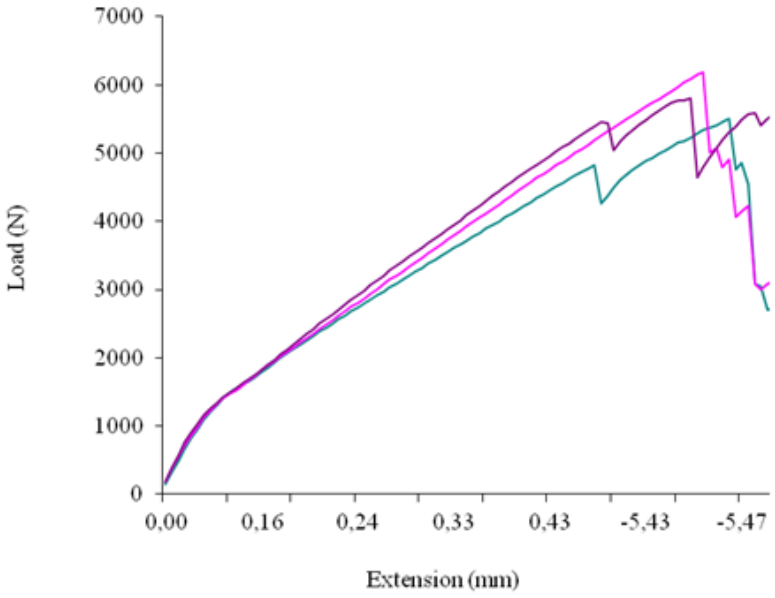

Figure 3.38. Load-extension distribution of specimens 4-6

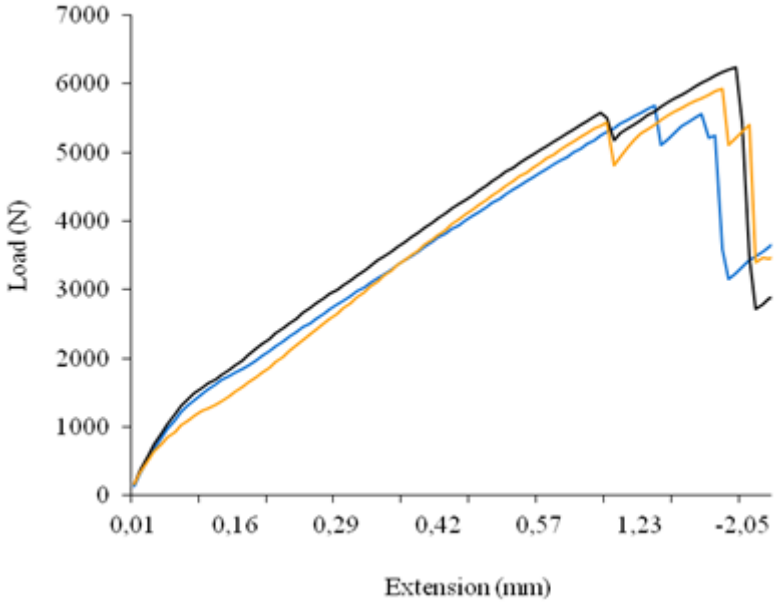

Figure 3.39. Load-extension distribution of specimens 7-9

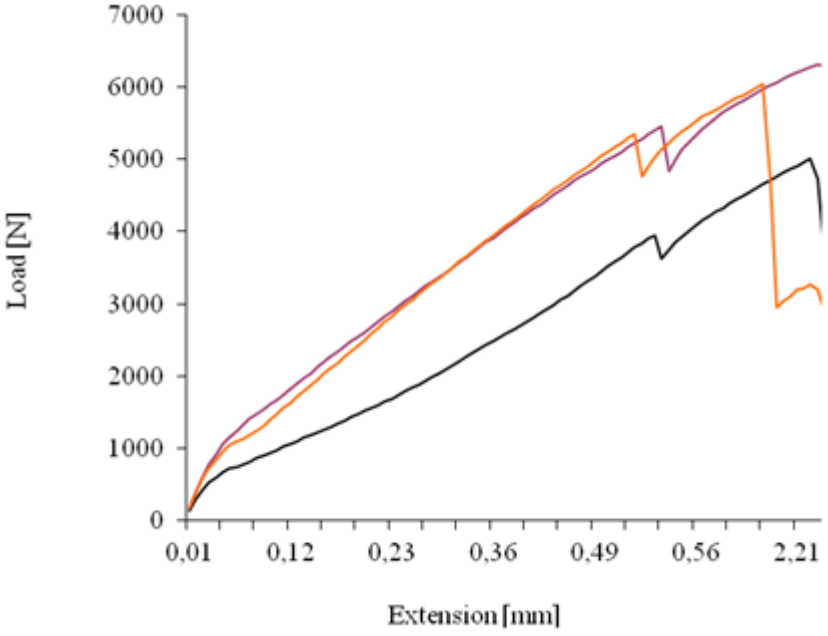

Figure 3.40. Load-extension distribution of samples 10-12

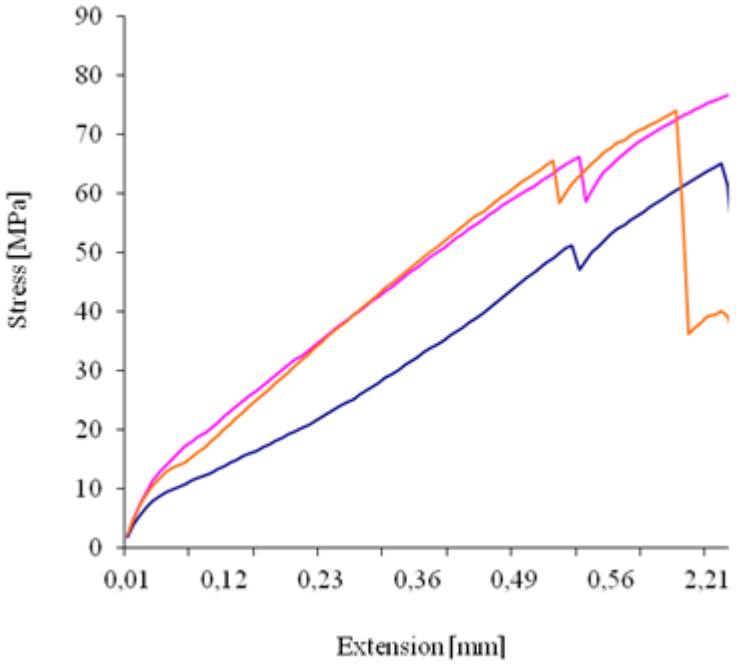

Figure 3.41. Stress-extension distribution of specimens number 10-12

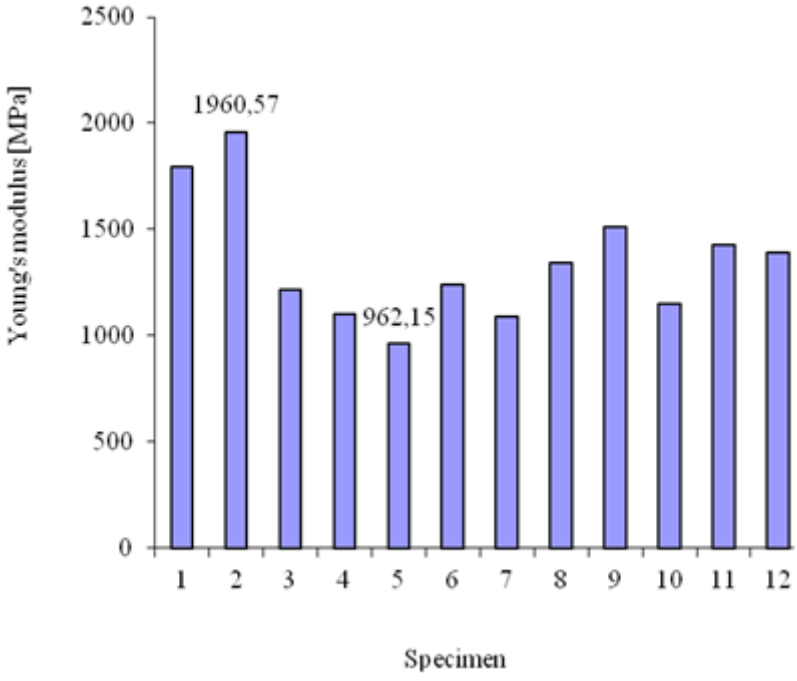

Figure 3.42. Young's modulus distribution of COREMAT nonwoven polyester mat

3.4.4. Final remarks

Regarding the stress-strain distribution of specimen number 10 as shown in Fig. 3.36, in the strain range between 0 and 0.01 the stress-strain distribution is almost linear. The first stiffness decrease occurred at 0.013 strain and aproximately 50 MPa stress due to the inter-fibre break. The tensile stress increased up to 66 MPa corresponding to a 0.018 strain while the stiffness presented a rapid breakdown.

Finally, the specimen has been broken at 0.034 strain and a stress of 8.9 MPa. Regarding the failure modes of the specimens, some of them presented delamination between RT glass fabric of the upper skin and core at specific strain values. Other specimens presented both delamination and core break at high strain values. Some failure modes of the whole sandwich structure with nonwoven polyester mat as core are presented as side views in Figs. 3.43-3.45.

Figure 3.43. Typical failure mode in side view 1

Figure 3.44. Typical failure mode in side view 2

Figure 3.45. Typical failure mode in side view 3

The use of COREMAT nonwoven polyester mat as core for thin composite laminates increases the overall structure's stiffness unlike the stiffness for a composite laminate without COREMAT. An outstanding median stiffness of 15397000 N/m has been achieved. Instead to manufacture a composite laminate with high number of laminae to achive a certain stiffness but

with significant dissadvantages, the nonwoven polyester mat represents an excellent choice to increase the stiffness structure without important resin and reinforcement consumption with environmental consequences.

3.5. Hybrid carbon-hemp composite laminate used in automotive engineering impact applications

3.5.1. Introduction

This section presents a study regarding the impact testing of some hybrid composite laminate panels based on polyester resin reinforced with both carbon and hemp fabric. The effects of different impact speeds on the mechanical behavior of these panels have been analyzed. The paper lays stress on the characterization of this hybrid composite laminate regarding the impact behavior of these panels by dropping a weight with low velocity. Some results of the researches were presented in [MLS14a]. The use of carbon-hemp in laminate used in automotive engineering is proposed by the author.

Composite materials are used in a wide range of applications; however, they are used with prudence in applications where transverse loadings appear, for instance, loadings given by transverse impact with low velocity. In general, failures and imperfections are inevitable in composite structures. In this context, design concepts of composite structures are used to take into account these failures, such as damage tolerance and damage resistance.

Damage resistance is connected on the material's capability to minimize the failures' effects given by impact, while damage tolerance is given by the material's capability to maintain its properties even after failures' appearance in material. Usually, these properties are called residual properties. One of the difficulties regarding the properties and evaluation of composites is, ironically, an advantage, namely, the capability to allow users to tailor their properties to suit the design needs [NDC03] , [HTE11a].

There are a huge number of fibers ranges and combination ways, resins for matrix, additives, stacking and orientation ways of laminae in a laminate, manufacturing possibilities (thermal treatments) and therefore is very difficult to extrapolate the composite behavior depending on these parameters for a certain combination of them [HTE12], [SVL11b], , [HTE11a], [HTE09]. In applications, the use of composites based on natural fibers is yet limited at the so-called non-structural components such as inner components of cars. One of the main reasons for this limitation consists in the sensitivity of these composites at impact and the difficulty in critical evaluation regarding damages caused at impact.

3.5.2. Material and method

The research has been carried out on ten composite panels presenting a rectangular shape and being underpinned on all edges. All panels have the same material's structure:

- a layer of thermosetting resin reinforced with carbon fabric;

- a layer of thermosetting resin reinforced with hemp fabric;
- a layer of thermosetting resin reinforced with carbon fabric;
- a layer of thermosetting resin reinforced with hemp fabric.

The plies sequence has been carried out in the hand lay-up process using a roll for resin impregnation of carbon and hemp fibers. Finally, the structure's thickness has been 4 mm. The laminate panel has been maintained at room temperature for two weeks from which ten specimens of rectangular shape (150 x 100 mm) have been cut.

The specimens have been subjected to impact by dropping a weight according to the standard ASTM-D5420-98a (Fig. 3.47). The impact testing by dropping a weight is used to characterize the dynamic behavior of a material. The experimental setup consists in a two column frame and a weight which can be lifted and released in free fall with minimum friction by sliding along columns under own weight (Fig. 3.46). The indentor presents a hemispherical head with a 16 mm diameter and its mass is equal to 1.9 kg. This indentor hits the middle of the rectangular specimen. The accelerometer is fixed on the upper part of the indentor and the signal (acceleration) is taken over in computer by help of an acquisition device type NI USB 6521 BNC. Using this kind of testing, some data regarding the mechanical properties of a material can be obtained, namely:

- The energy, U, absorbed during impact;
- The variation of impact force, F, at the impact moment;
- The variation of indentor's displacement, d, versus time, etc.

In case of impact testing by weight falling, the only measured feature versus time is the contact force, $F(t)$, exerted by the weight which falls on specimen while the specimen's deflection is determined as a function of time by numerical integration of the indentor's motion equation. The acquisition of experimental data (acceleration) as well as computing the response parameters described above have been carried out using a block diagram conceived by the LabView program.

Figure 3.46. The impact device

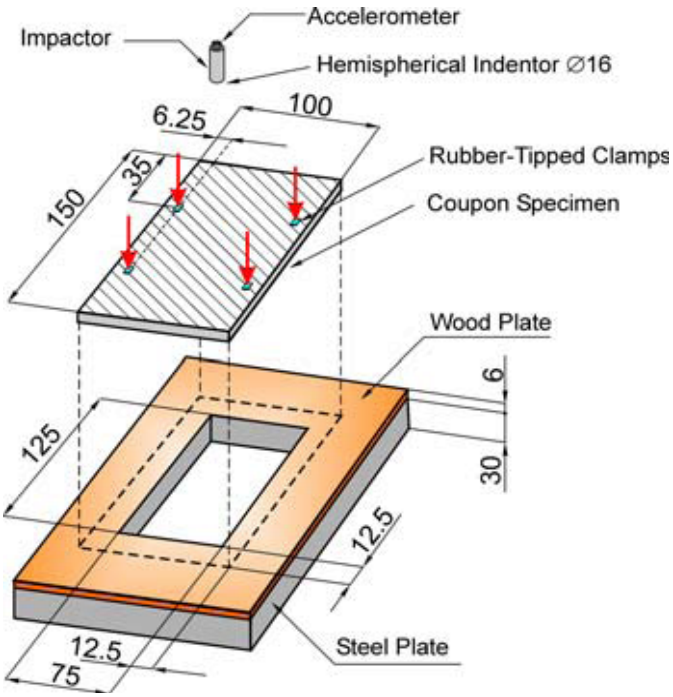

Figure 3.47. The specimen's geometry and fixing mode

The height from which the weight is released has been computed with the well known relation:

$$H = \frac{v^2}{g}[m] \tag{3.28}$$

where *g* represents the gravitational acceleration. The indentor's motion equation can be written by help of the following relation:

$$a(t) = g - \frac{F(t)}{m}\left(m/s^2\right) \tag{3.29}$$

where *m* represents the impactor's mass.

The absorbed energy can be computed according to the relation:

$$U(t) = \int_0^t F(t) \cdot v(t) \cdot t \quad \text{(J)} \tag{3.30}$$

3.5.3. Results

Using the LabView program, the variation of force *F* has been computed at the impact's moment after the signal has been recorded with the accelerometer through the acquisition device (Fig. 3.48). In the same way, following distributions have been represented:

- The variation of impact force *F* versus the displacement δ at the impact's moment (see Fig. 3.49);
- The variation of indentor's displacement δ at the impact's moment (Fig. 3.50);
- The variation of energy *U* at the impact's moment (Fig. 3.51).

The results obtained after the impact testing of hybrid carbon-hemp composite laminate are presented in table 3.7 as well.

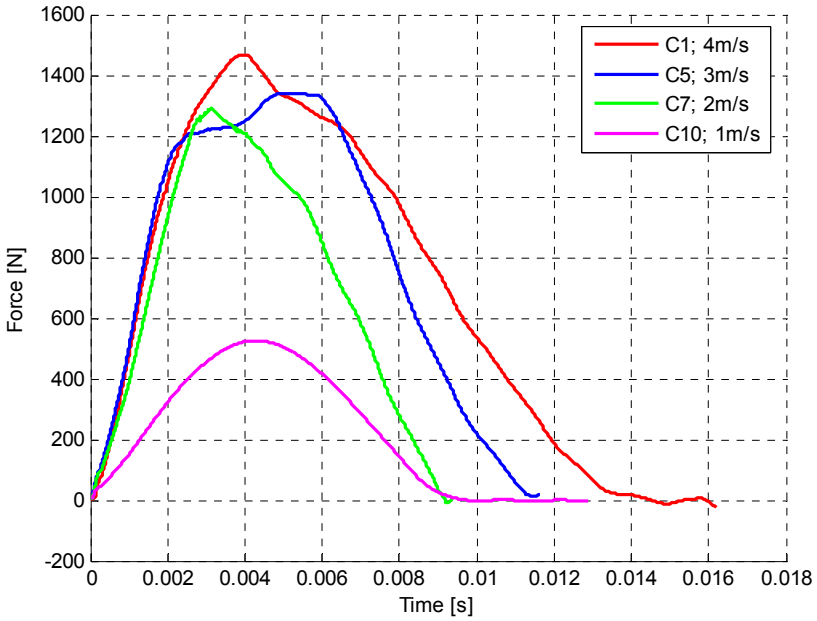

Figure 3.48 Force-time (F-t) distribution at the impact's moment

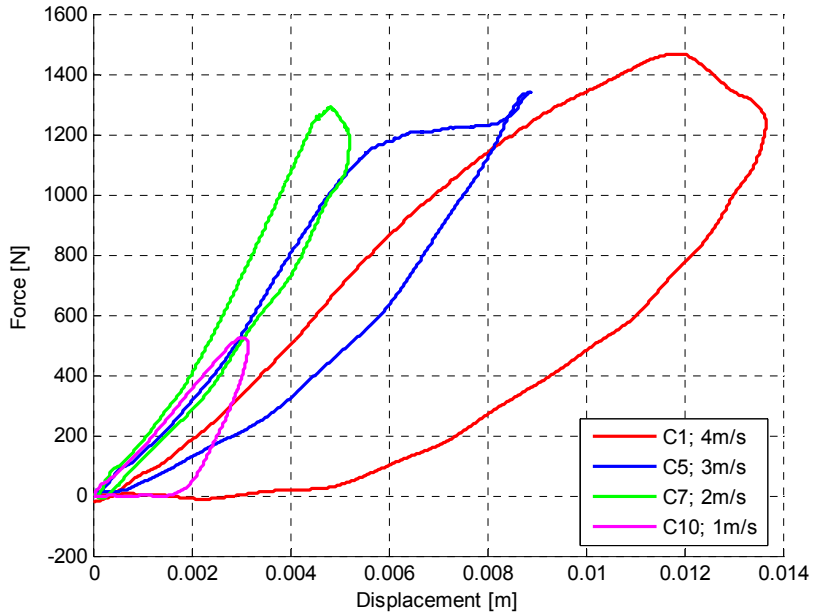

Figure 3.49. Force-displacement (F- δ) curves at the impact's moment

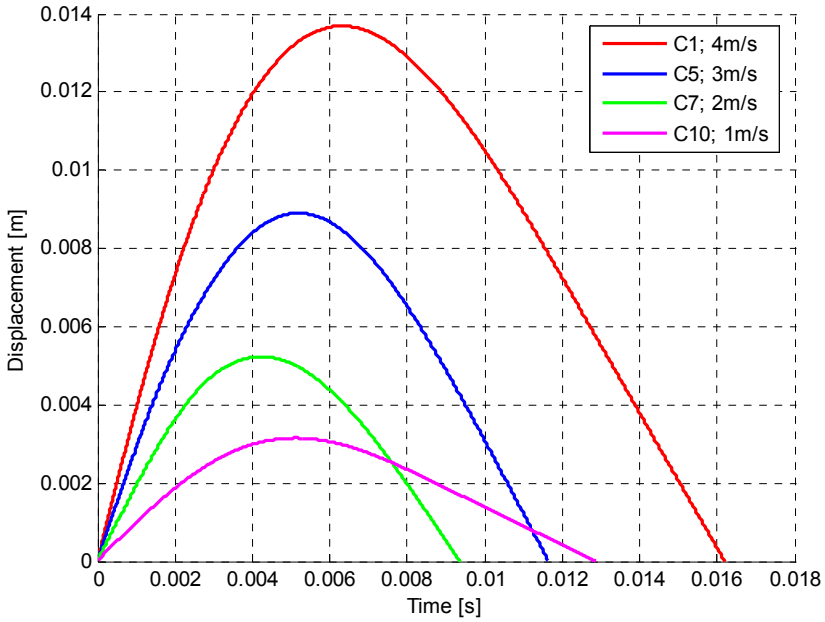

Figure 3.50. The variation of indentor's displacement δ at the impact's moment

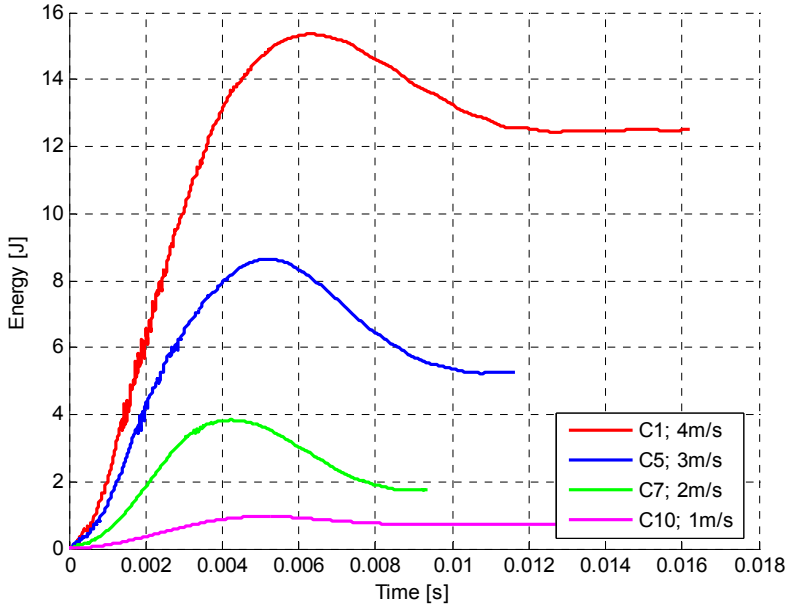

Figure 3.51. The variation of energy U at the impact's moment

Table 3.7. Results after impact testing

Specimen	Results			Observations
	Specimen thickness [mm]	Falling height [m]	Impact speed [m/s]	
1	4	0.815	4	Total break
2				
3				
4				
5		0.458	3	Break at first ply
6				
7		0.203	2	Trace on specimen is slightly marked
8				
9		0.05	1	Trace on specimen is not visible
10				

The indentor's falling height has been computed as following:

$$v^2 = 2gh \quad \Rightarrow \quad h = v^2 / 2g \tag{3.31}$$

3.5.4. Discussion and conclusions

Analysing especially the graphics from Fig. 3.51, we can say that these curves present leaps and inflexions due to the presence of delaminations. Integrating the area under the loading curve (force-displacement, Fig. 3.48) until the maximum value of the force (according to the first failure) the energy required to initiate the failure can be obtained. At the impact's moment, the energy accumulates in time and is direct proportional with the force and increases until reach a constant landing.

After reaching a maximum value of the force, this decreases in time, the energy *U* being absorbed in material and the force's decrease took place after reaching the landing of *U*. In general, at the composite laminates the energy is frequently absorbed by creating some delamination surfaces called delamination breaks that lead to the strength and stiffness decrease. Analysing the specimens after impact testing (Fig. 3.52) it can be noticed that the failure areas localized on the specimens' surface (where the intendor hits) are smaller than those localized on the backfront.

This lead to the conclusion that the cracks have been propagated from the place where the intedor hits to the backfront of the panel. Thus, we can conclude that the panel manufactured

from the hybrid composite material involved in this study is stiff. On the other hand, as expected, the grater the impact speed, the grater the failured area has been noticed.

3.62.a

3.62.b

Figure 3.52. Specimen after impact testing

Chapter 4

Toward the use of irradiation for the composite materials properties improvement

The aims of this chapter is the development of advanced composite materials with high strength to radiations, with applications in automotive industry but also in making automotive components to reduce their weight and manufacturing costs, as well as to improve recycling, in the same time meeting the structural and performance of passive protection. An important application of the study of the irradiated composite is in aeronautical industry. A composite material may be subjected to radiations because it is part of a constituent material operating in an environment with radiations or may be subjected to radiations deliberately, in order to obtain superior properties of the material.

In this second sense, the challenge is to achieve high structural static and dynamic performances, by developing composite materials with enhanced properties that bring better value to the concept of composite type structure. Another main applications of these materials are in the nuclear devices used for the nuclear centrals. The main results in this field were presented in the papers ([SCU14a], ([SCU14b], [SCU14c], ([SCU14d]). The results presented are obtained by the author in the last three years and are a main topics studied to this moment.

4.1. Composite materials properties improvement using irradiation

4.1.1. Introduction

Because the composite materials is an interdisciplinary field and more than a stable connection between disciplines such as chemistry, physics or engineering, experience of this is essential for the development of new materials with well-defined applications. The triangle: synthesis and manufacture - composition and structure - properties and performance are essential relationships in the field of composite materials.

The properties of a given material composition depend to a large extent on the method by which it was manufactured, which are the consequence of different structures [HSC05] Conversely, special applications require specific structural properties, and therefore a precise composition, which involves proper synthesis procedures and manufacturing processes.

The idea of using composite materials does not reduce only to the replacement of metals or other composite materials but also to use in a constructive way these materials, taking into account the special properties and possibilities of manufacturing to create innovative structures,

new forms, to be used for private construction. So, first, a material with increased fatigue strength is designed, recyclable, easy to manufacture and then it is irradiated and is looking to integrate this type of material, taking into account the properties of the practical structures used in mechanical engineering and beyond [SVL11b]

4.1.2. Material and method used

In order to investigate the mechanical behavior of composites, the industrial method of sterilization by irradiation has been used. This method is best understood from the scientific point of view, inducing a clear, precise and nuanced methodology, with strong theoretical base, implemented in ISO, EN and ASTM. Very important in this method is to achieve the total absorbed dose that can be achieved by incremental additions. More specifically, this method is a sterilization method for irradiation used to improve product performances.

The technological irradiation IRASM Center operates a gamma irradiator of type SVST Co-60/B (Fig. 4.1) with Co-60 sources and current activity of ~ 300k/Ci.

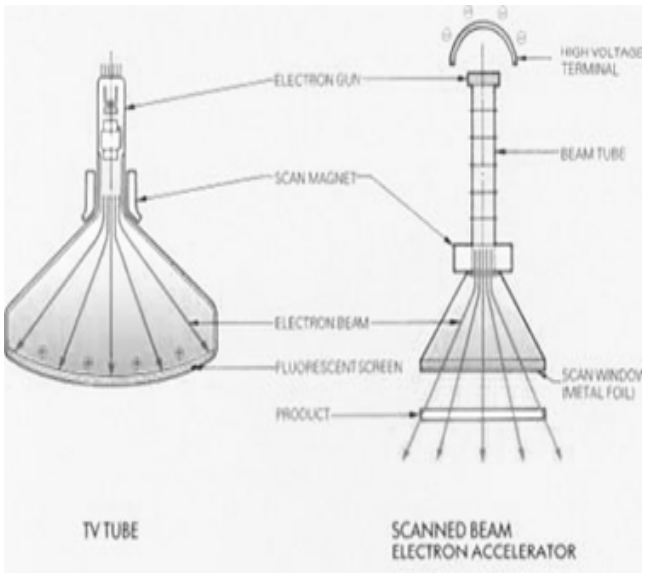

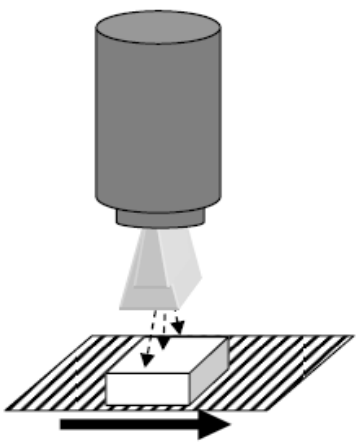

Figure 4.1. Schematic representation of an irradiator with electrons accelerator

SVST Co-60/B irradiator presents following characteristics:

• Irradiation source: Co-60 encapsulated in stainless steel;

• Source type: Type CoS-43 HH, ø11x451mm;

• Type of source grid: rectangular, split;

• The number of racks of sources: 3;

• The number of source modules (in a rack): 4;

• Number of sources in a module: 33;

• Ability grid sources: up to 396 pcs. Sources;

• The movement of the source: pneumatic;

• Lowering the source: gravity;

• Storage: water (pool);

• The basis for shielding: up to 74 PBQ (2Mci) activity of Co-60 source;

• The surface dose rate allowed at the irradiation room wall: max. 2μSv / h;

• Transport products: system "tote-box";

• Dimensions of the products container (tote-box): 50x50x90 cm;

• Useful dimensions of container products: 47x47x88 cm;

• Useful capacity to container products: approx. 200 l;

• Maximum load per container products: 120kg;

• Present ability sterilization (medical devices): 1 500 m^3/year;

• Maximum capacity sterilization (medical devices): 30000 m^3/year;

• Storage of 500 m^2.

Intense fields of ionizing radiations required for sterilization process are obtained with equipment called irradiators: gamma irradiators (with isotopic sources of gamma radiations) and electron accelerators.

In case of gamma irradiators, the irradiation takes place in a chamber called chamber of irradiation which must maintain the gamma radiation (very penetrating) avoiding the personnel and population affecting as well as the environment. The gamma irradiators should have a storage system of radiations source (when the irradiation does not operate) and a transport system of the products in the chamber of irradiation.

For gamma irradiators is very important that the geometry of gamma irradiation should allow the best possible uniformity of the radiation throughout the volume irradiated product. The transport system of products presents multiple passes around the source of radiation.

Several passes around the source means better efficiency in use of radiation. The factor characterizing the uniformity of radiation is called absorbed dose uniformity factor (ratio of absorbed dose to the minimum and maximum absorbed dose irradiation) for a certain category of products (which have a certain apparent density = mass of products/ irradiated volume).

Such composite made of hemp-based fabric and being tested a number of eight specimens in order to study the behavior of this material at static tensile loadings [AMO13], [DHU96]. The irradiation of specimens for testing has been conducted on IRASM irradiator (www.irasm.ro) and the absorbed dose has been measured with the ECB dosimetry. Irradiations have been performed in the 1-250 kGy range covering the doses used in most applications of radiation technology, but very high doses also, where the effects of degradation can be put in evidence with certainty. Thus, specimens made of composite materials based on thermosetting resin and hemp fibers have been irradiated part with a dose of 2 kGy and a part with a dose of 56.7 kGy. After this "operation" we performed a macroscopic analysis, after which failures could be highlighted that have been formed in various stages of the manufacturing processes.

According to current standards eight specimens have been cut (Fig. 4.2) from a panel with five layers of thermosetting resin with hardener, type DERAKANE 411-350 epoxy vinyl esther resin reinforced with unidirectional hemp fabric of type CERTEX PVR-R1 with an average length of 3-6 mm fibers. These specimens have been subjected to tensile loads at a constant rate until break or until stress (load) or strain (extension) reached a predetermined value [SVL11b] , [CNI11] , [SVL13].

.

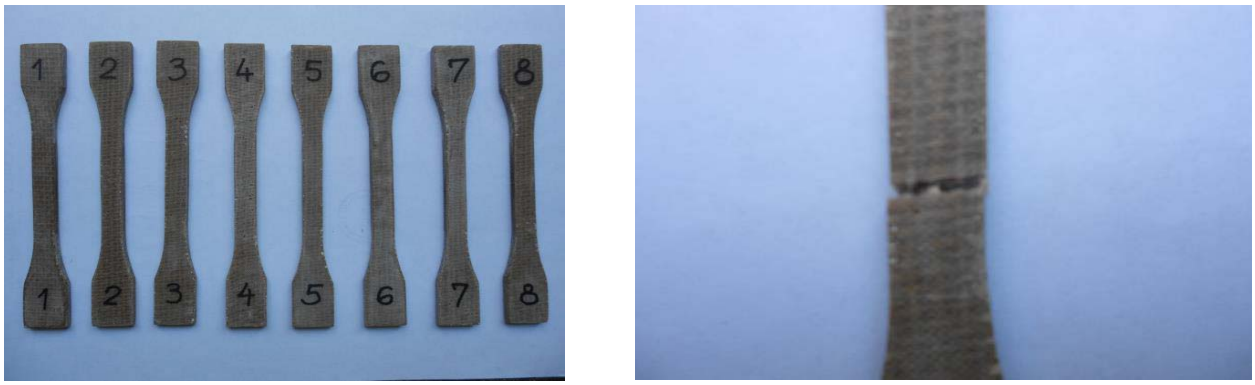

a) Befor b) After

Figure 4.2. Hemp fabric based specimens before and after tensile testing

Another batch of specimens have been cut and irradiated with 56.7 kGy dose and 2kGy respectively, after which they have been tested at tensile loads in order to track the changing in mechanical properties (Figs. 4.3).

a) Specimens irradiated with 2 kGy dosis b) Specimens irradiated with 56.7 kGy dosis

Figure 4.3. Hemp fabric based specimens irradiated after tensile testing

4.1.3. Results

The visualization in detail has been done with a powerful microscope that can enlarge the studied area 500 times to 2000 times, and the images have bee made as clear as possible and even to the depth of the material. Microscopy results have been carried out both in 2D and 3D, noting also how the structure of these materials has been changed (Figs. 4.4-4.7).

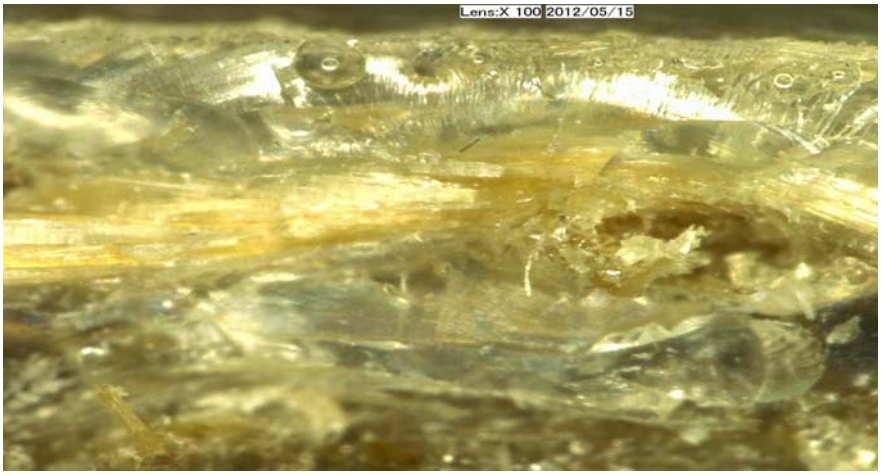

Figure 4.4. Cross-section through a hemp fabric based specimen irradiated with 2 kGy dosis (100X magnitude)

Figure 4.5. Cross-section through a hemp fabric based specimen irradiated with 56.7 kGy dosis (100X magnitude)

Figure 4.6. Side view of an irradiated hemp fabric based specimen (20X magnitude)

Figure 4.7. Side view of a non-irradiated hemp fabric based specimen (20X magnitude)

The synthesis of experimental data obtained at tensile tests of non-irradiated as well as irradiated specimens with 2 kGy respective 56.7 kGy doses are presented in Tables 4.1-4.2. From these tables, the Young's modulus as well as the tensile strength distributions are graphically shown in Figs. 4.9-4.10.

Table 4.1. Young's modulus [MPa] of hemp fabric based specimens subjected to tensile tests

Specimen	Non-irradiated	Irradiated with 2 kGy dosis	Irradiated with 56.7 kGy dosis
	6131,09235	9673,29606	6605,46446
2	7611,57485	91675,9776	6242,42647
3	7236,70744	6349,83073	6520,34653
4	12138,8127	5613,87164	35292,4633
5	8222,60575	15225,2716	6512,11349

Table 4.2. Tensile strength [MPa] of hemp fabric based specimens subjected to tensile tests

Specimen	Non-irradiated	Irradiated with 2 kGy dosis	Irradiated with 56.7 kGy dosis
1	6180141,09	9005838,63	7133901,61
2	7826221,26	111477989	6741820,58
3	7233812,76	7365803,64	7100657,38
4	12133957,2	6682752,8	37946456,5
5	7967704,97	16747798,8	6764783,5

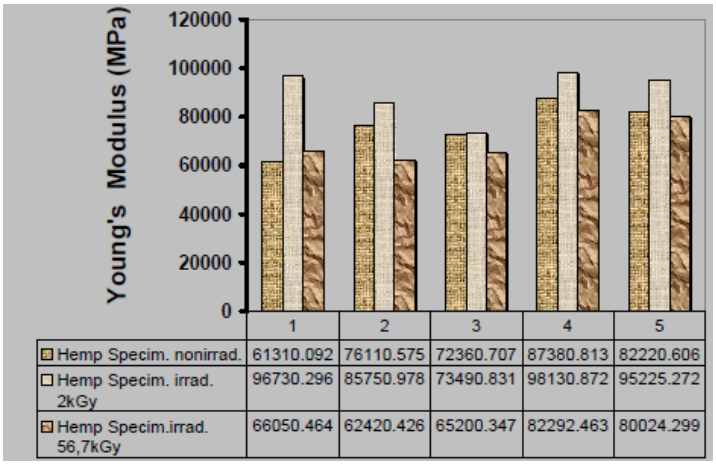

	1	2	3	4	5
Hemp Specim. nonirrad.	61310.092	76110.575	72360.707	87380.813	82220.606
Hemp Specim. irrad. 2kGy	96730.296	85750.978	73490.831	98130.872	95225.272
Hemp Specim.irrad. 56,7kGy	66050.464	62420.426	65200.347	82292.463	80024.299

Figure 4.8. Young's modulus distribution of irradiated and non-irradiated hemp fabric based specimens

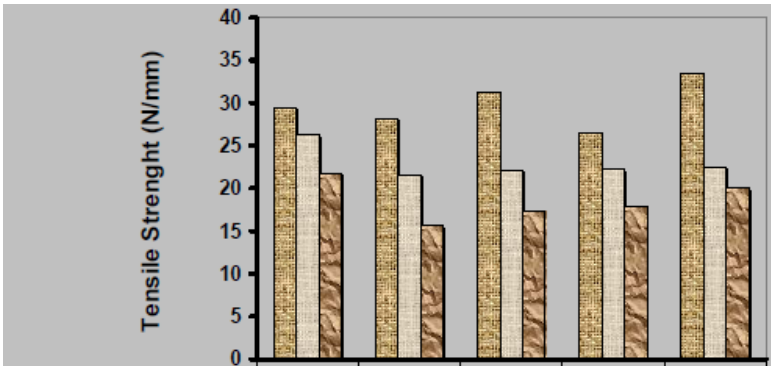

	1	2	3	4	5
Hemp Specim.nonirrad.	29.4146904	28.140153	31.1485591	26.4340371	33.4502294
Hemp Specim. irrad. 2kGy	26.2166018	21.5379625	22.1331365	22.2298688	22.5113346
Hemp Specim. irrad. 56,7kGy	21.7983509	15.6112946	17.3457608	17.8423582	20.0242993

Figure 4.9. Tensile strength distribution of irradiated and non-irradiated hemp fabric based specimens

4.1.4. Discussions and conclusions

The hemp fabric based specimens irradiated with 2 kGy dosis presents higher Young's modulus values than the specimens irradiated with 56.7 kGy dosis showing that the maximum Young's modulus is between these two radiation doses.

In Figs. 4.10-4.11, the mechanical work as well as the tensile strength distributions of non-irradiated and irradiated hemp fabric based specimens with 2 kGy and 56.7 kGy doses put in evidence the higher mechanical properties of 2 kGy dosis irradiated specimens than those irradiated with 56.7 kGy dosis.

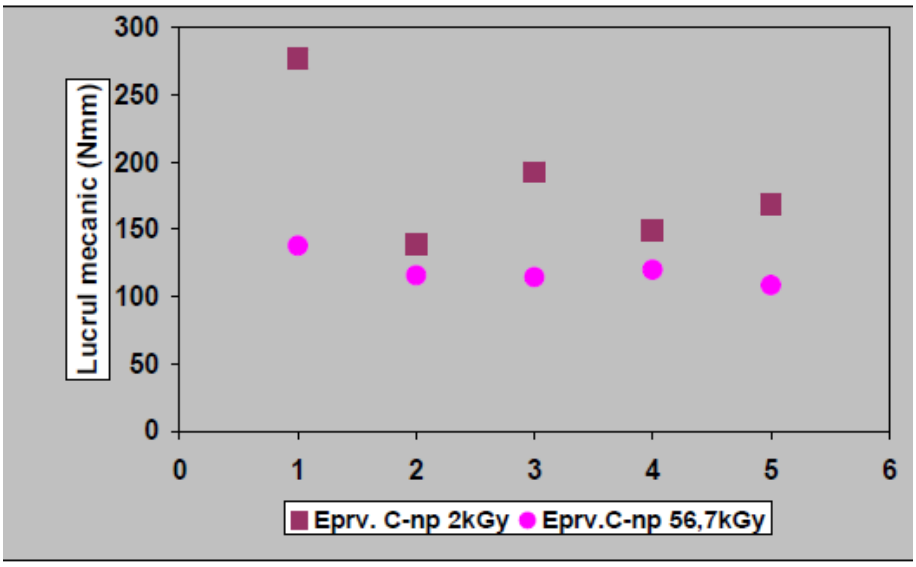

Figure 4.10. Mechanical work distribution of irradiated hemp fabric based specimens with 2 and 56.7 kGy doses

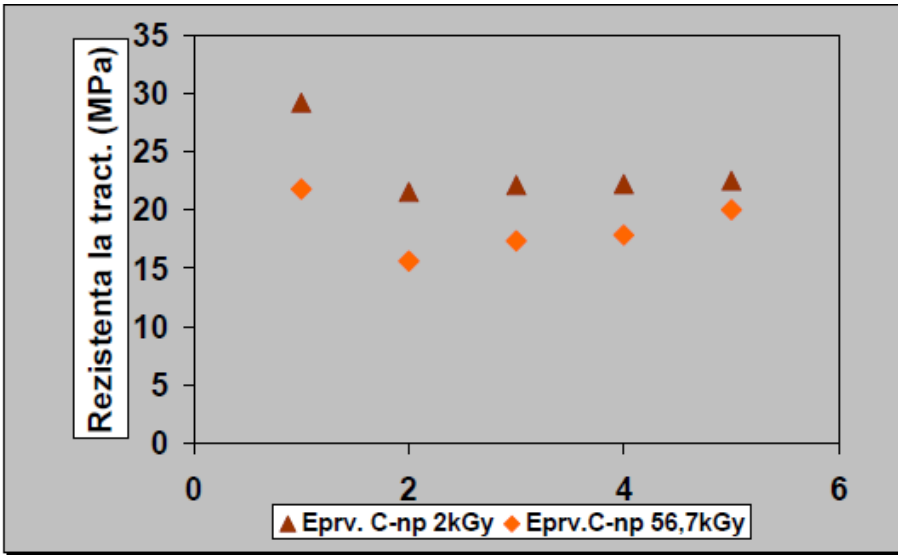

Figure 4.11. Tensile strength distribution of irradiated hemp fabric based specimens with 2 and 56.7 kGy doses

The hemp fabric based composite material irradiated with small doses of radiation meets the requirements of structural and passive protection for medium loaded automotive parts.

4.2. Irradiation influence on a new hybrid hemp bio-composite

4.2.1. Introduction

This section are presented theoretical and experimental issues regarding the behavior at static bending due to irradiation of a new hybrid composite reinforced with glass and hemp fibers, used especially in automotives industry. The advantages of fibers-reinforced composites

are given by their high optimization capability, so that the final material's properties can be imposed according to a given application by choosing of a unique combination between matrix and fibers that lead to manufacturing of a light and ergonomic structure.

A composite material may be subjected to radiations because it is part of a constituent material operating in an environment with radiations or can be subjected to radiations deliberately, in order to obtain higher properties of the material. In this second sense, the challenge is related to reach high static and dynamic structural performances by accomplishment of composite materials with enhanced properties that put as well value to the concept of composite structure.

The products manufactured from polymer matrix biocomposites use environmentally raw materials that after use, through biodegradation will be given to the nature's circuit. Polymer matrix bio-composites will play in future an increasingly more important role in manufacturing of important low weight products specific to interior parts as well as engine and suspension parts. Analyzing the implications regarding the replacement of metals with such materials, it should be mentioned that the advantage does not limit only to reduce weight but often at equal or superior operation.

It is known that fibrous structures can be used as strength structures, only inserted in a support material called matrix. In composite constructions, most of the times, entirely different substances may be combined in such a way that their individual properties should achieve an optimal action. Usually, it is the pair of materials in which one has a bearing function, while the other is intended to contribute to the take over of moment of inertia. În hybrid constructions, the strength and rigidity of the various functions are taken over from many different materials, and at fibers-reinforced polymer matrix composite structures, the composite properties depend essentially on the type, orientation and fibers volume fraction. In such structures, the most used are laminates reinforced with glass, carbon and aramid fibers [HSC05]. Generally there is a particular fascination for natural fiber composites, and even more in manufacturing automotives, composites prove competitive in terms of both price and the possibilities of substitution and successful completion of traditional materials (metals, ceramics, glass etc..), thus carrying out a great weight reduction of the vehicle [SVL11b], [HTE11a] , [AMO13]. Most applications include the construction of car body elements such as wings, doors, pavilions, hoods, etc [DHU96].

4.2.2. Material and method

In order to investigate the mechanical behavior of hemp-glass hybrid composite, it was irradiated (sterilization) with Gamma ray in order to achieve a composite material having good mechanical properties, composite that can be tailored to achieve bio-composites used in automotive industry, so auto parts will ensure a reduction in mass of transport vehicle. Irradiation of samples for testing have been conducted on IRASM irradiator (www.irasm.ro) and absorbed dose has been measured with the ECB dosimetry.

Irradiations have been performed in the 1-250 kGy range, covering the doses used in most applications of radiation technology, but very high doses also, in which the effects of degradation can be put into evidence with certainty. Thus, specimens made of composite materials based on thermosetting resin and hemp fibers have been irradiated some with a dose of 2 kGy and a some with a dose of 56.7 kGy.

The new glass-hemp fabric hybrid composite consists of four layers of thermosetting resin reinforced with glass fibers having 35% fibers volume fraction and hemp fabric with the fibers volume fraction of 20%. The process for producing the glass-hemp fabric hybrid composite material consists that to form layers, hand lay-up technology has been used which provides the use of a roller to impregnate with resin both glass fibers and hemp fabric.

The mechanical characteristics of the thermosetting resin with hardener are: tensile stress at break: 86 MPa; Youn's modulus: 3200 MPa; resistance to impact: 40 kJ/m^2.

The composite laminate panel is accomplihed from a glass fibers layer with a thickness of 1.5 mm alternating with a second layer of hemp fabric with a thickness of 0.5 mm, the operation is repeated to obtain a composite board consisting of four layers. Finally, the composite laminate panel thickness is 4 mm.

The panel thus obtained has been kept at room temperature for two weeks after which the eight specimens have been cut corresponding to the shape bending test in accordance with EN ISO 527-2 standard [SVL11b], [CNI11] [SVL13] ,- (Fig. 4.12).

a) before

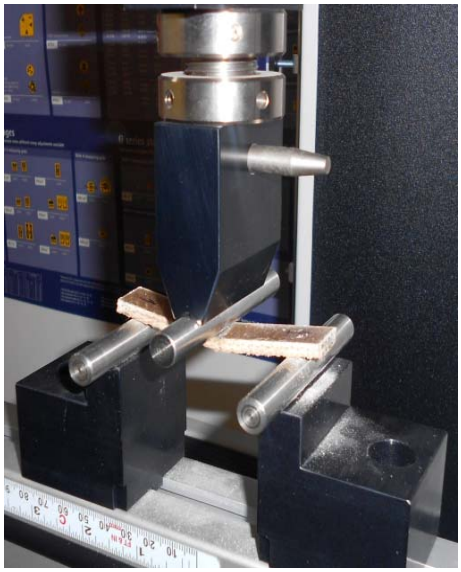

b) during

Figure 4.12. Hybrid glass-hemp specimens, before (a) and during the three-point bend test (b)

The specimens being carried out as an alternating structure, the first four specimens have been tested on "glass face" (Fig. 4.13) and the next four on "hemp face".

a) b)

Figure 4.13. Hybrid glass-hemp specimens after bending tests

4.2.3. Results and conclusions

After processing the data summarized in Table 4.3, following distributions have been illustrated in Figs. 4.14-4.15.

Table 4.3. Mechanical properties of hybrid glass-hemp composite determined in bending tests

Specimen	Load at max. load [kN]	Stress at max. load [MPa]	Rigidity at bending [Nm^2]	Young's modulus [MPa]
1	0.26	105.7	0.26	3251.5
2	0.28	114,21	0.23	295.0
3	0.26	104.02	0.20	2611.8
4	0.27	108.05	0.21	2691.4
5	0.23	93.34	0.20	2537.6
6	0.32	129.26	0.12	1620
7	0.35	141.94	0.03	379.1
8	0.26	105.7	0.20	3251.5

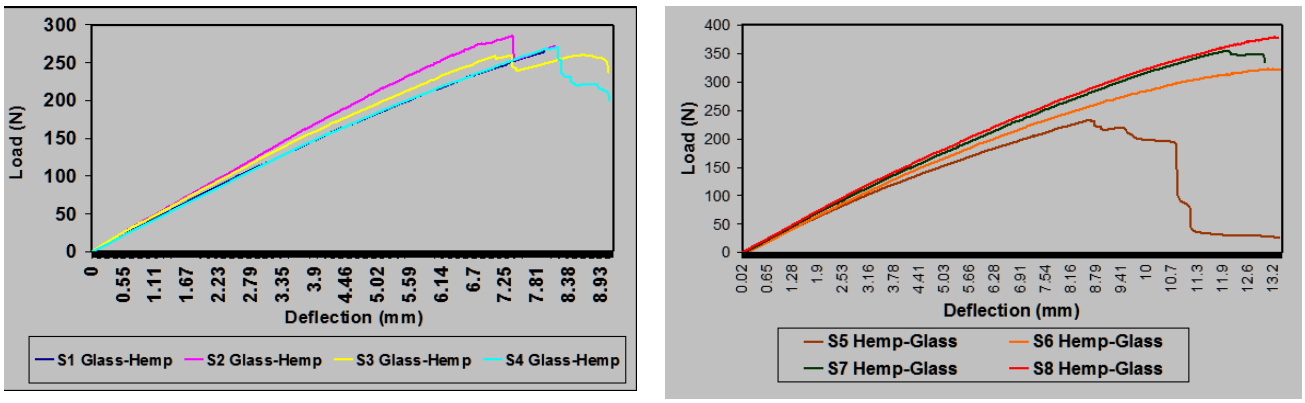

a) b)

Figure 4.14. Load-deflection distributions of hybrid glass-hemp specimens

Specimens made of hybrid glass-hemp composite have been irradiated with the same dose of 2kGy, respectively 56.7kGy, after which they have been tested in bending on the materials testing machine of type LR5K Plus, that provides maximum force of Fmax = 5 kN (Figs. 4.16-4.17). They have been subjected to bending with a constant speed of 5 mm/min until break, or until the stress (load) and deformation (deflection) have reached a predetermined value (Figs. 7-9). Bending test results for the hybrid glass-hemp composite material irradiated with 2kGy and 56.7 kGy are based on the data summarized in Tables 4.4-4.5.

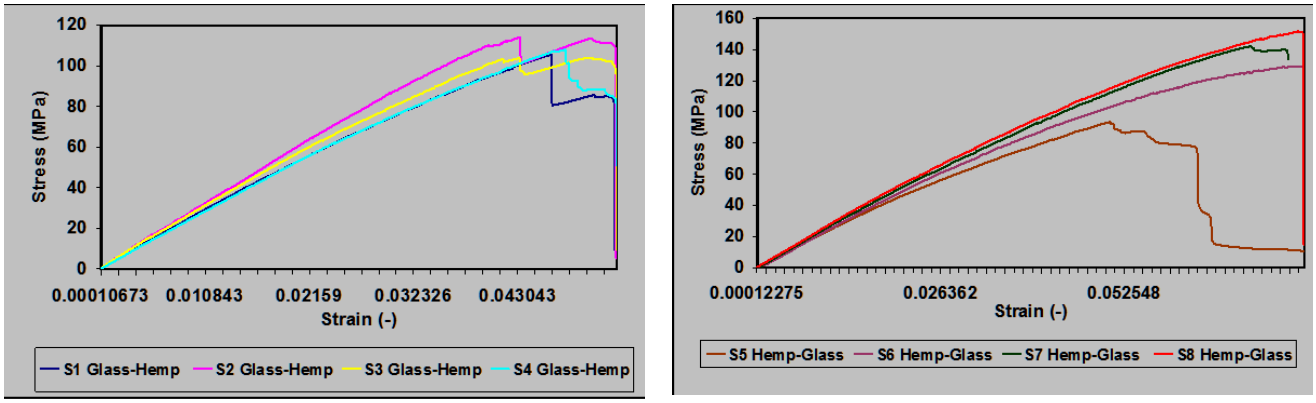

a) b)

Figure 4.15. Stress-strain distributions of hybrid specimens

a) b)

Figure 4.16. Specimens irradiated with 2 kGy dosis

a) b)

Figure 4.17. Specimens irradiated with 56.7 kGy dosis

Table 4.4. Mechanical properties of hybrid glass-hemp composite irradiated with 2 kGy dosis subjected to bending tests

Specimen	Max. load [kN]	Stiffness [N/mm]	Strain [-]	Young's modulus [MPa]
1	0.14	21726.9	0.05	2224.8
2	0.14	19310	0.05	1977.3
3	0.15	22956.3	0.05	2350.7
4	0.12	20833.6	0.04	2133.3
5	0.21	20168.4	0.07	2065.2
6	0.16	18889.3	0.05	1934.2
7	0.15	19777.9	0.06	2025.2
8	0.18	21400	0.06	2191.3

Table 4.5. Mechanical properties of hybrid glass-hemp composite irradiated with 56.7 kGy dosis subjected to bending tests

Specimen	Max. load [kN]	Stiffness [N/mm]	Strain [-]	Young's modulus [MPa]
1	0.18	31259.9	0.05	2134
2	0.22	36880.4	0.04	2517.7
3	0.24	38258.4	0.04	2611.7
4	0.20	31932.9	0.05	2179.9
5	0.34	27759.4	0.06	1895
6	0.28	23240.6	0.08	1586.5
7	0.30	31044.4	0.05	2119.3
8	0.32	31605.5	0.06	2157.6

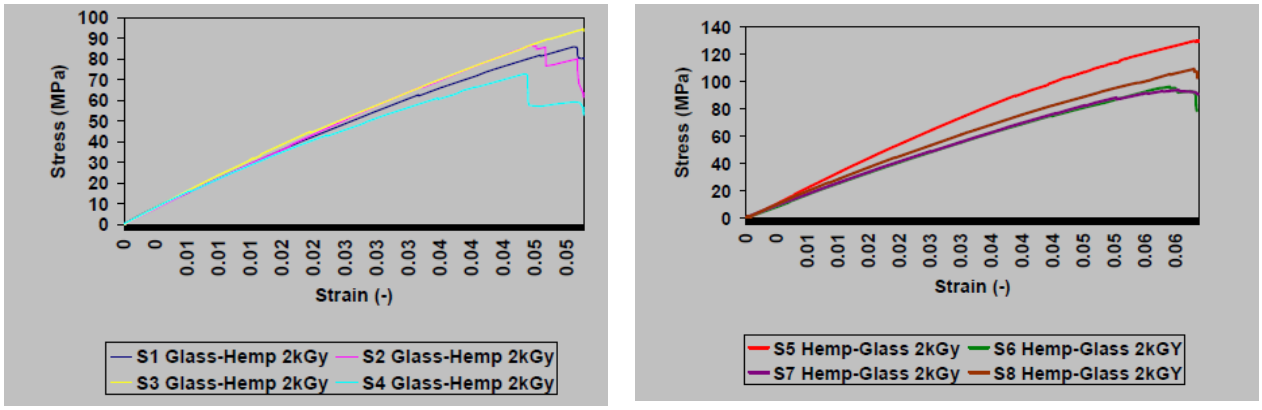

a) b)

Figure 4.18. Stress-strain distributions of hybrid glass-hemp specimens irradiated with 2 kGy dosis

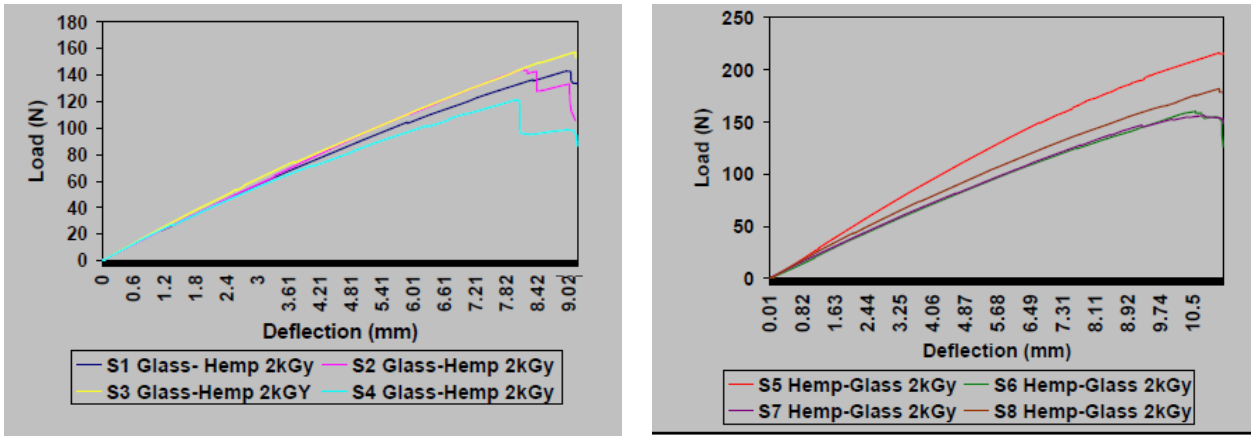

a) b)

Figure 4.19. Load-deflection distributions of hybrid glass-hem specimens irradiated with 56.7 kGy dosis

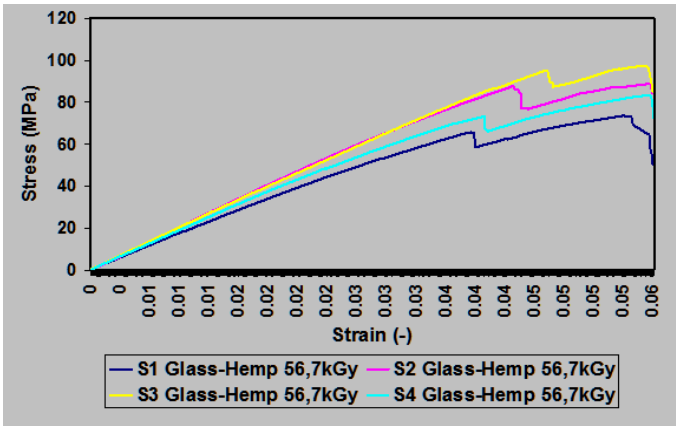

a)

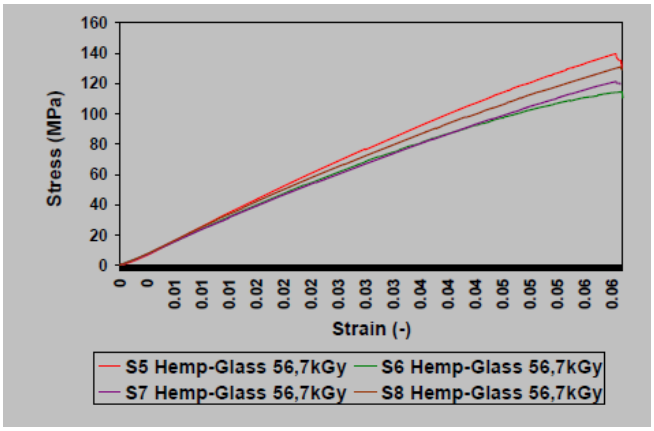

b)

Figure 4.20. Stress-strain distributions of hybrid glass-hemp specimens irradiated with 56.7 kGy dosis

From Table 4.4 can be seen that the stiffness is directly related to the material's structure. Analyzing the stress-strain characteristic curves we can see that their distribution is nearly linear due to the elasticity of the glass fibers (see Fig. 4.18).

Regarding to the comparison of specimens made of the hybrid glass-hemp composite material, graphics have been carried out from which it result the properties of irradiated hybrid composite with both dosis of 2 kGy and 56.7 kGy as well as a comparison regarding the non-irradiated and irradiated hybrid composite (Figs. 4.21-4.24).

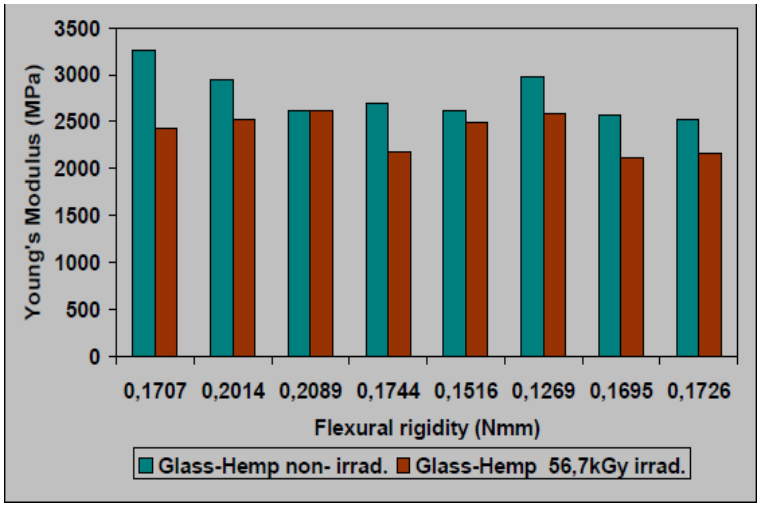

Figure 4.21. Comparison between Young's modulus distributions of both types of specimens non-irradiated and irradiated with 56.7 kGy doses

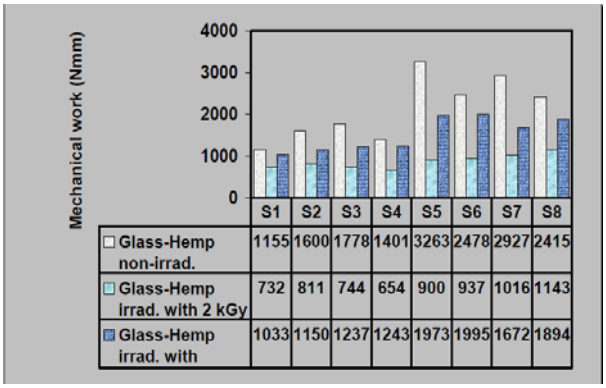

Figure 4.22. Mechanical work distribution compared on irradiated and non-irradiated composites

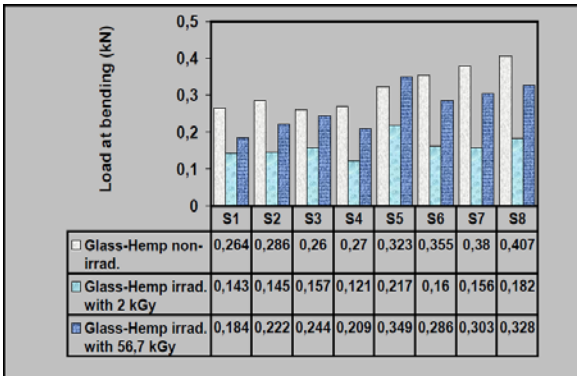

Figure 4.23. Load at bending distribution compared on irradiated and non-irradiated composites

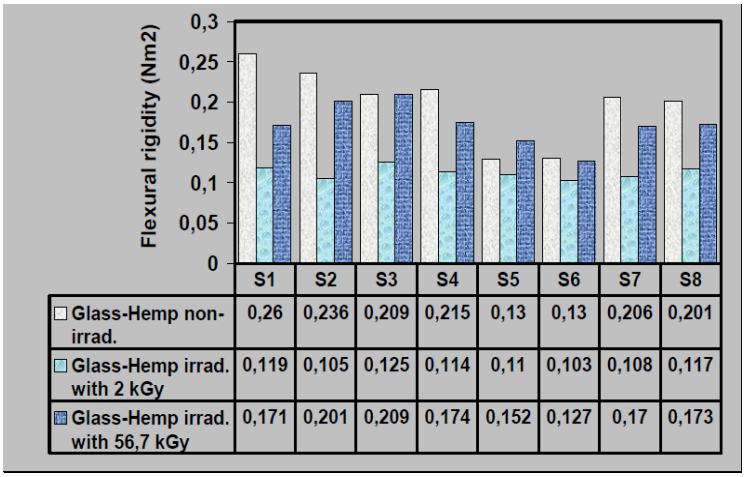

Figure 4.24. Rigidity at bending distribution: irradiated and non-irradiated glass-hemp composite

As shown from the above representations, the hybrid glass-hemp composite presents better mechanical properties at bending in case of irradiation with a higher dose (56.7 kGy) than in the case of irradiation with a lower dose (2kGy).

4.3. Radiation influence on micro-structural mechanics of an advanced hemp carbon hybrid composite

4.3.1. Introduction

The purpose of this paper is the development and analysis from the mechanical and micro-structural point of view a new biocomposite subjected to radiations, with applications in both nuclear industry and the accomplishment of parts in aerospace industry to reduce their weight and manufacturing costs. This new biocomposite improves the recycling degree meeting

at the same time the structural and passive protection performances. A composite material may be subjected to radiations since is a part of a constituent material which operates in an environment with radiations or may be intended to be subjected to radiations to obtain material's superior properties.

In this second sense, the challenge is to reach some increased static and dynamic structural properties carrying out composites with enhanced characteristics that put better in evidence the sandwich structure concept. Since the field of composites is an interdisciplinary one and more than a connection between stable disciplines such as chemistry, physics or engineering, the experience from these is essential to develop new materials with well-defined applications.

The idea of using composite materials do not lead only to replace metals or other composites but also using in a constructive way these materials, taking into account the outstanding properties and manufacturing possibilities to create innovative structures with new shapes that should be used for particular constructions. So, first, a material with increased strength, recyclable and easy to be manufactured is designed then is subjected to radiations seeking in this way the integration of this material in structures used in aerospace and especially in nuclear applications taking into account its properties.

In general, there is a special fascination for natural fibers reinforced composites and even more in the production of cars, composites prove to be competitive in terms of costs and replacing possibilities of traditional materials (metals, ceramics, glass, etc.) [HSC05], [SVL11b], [HTE11a] , [AMO13] .

Radiations represent physical phenomena by which energy is transmitted to one region of space to another. X and gamma rays are electromagnetic radiations being at the upper limit of the energy spectrum having the property to produce the phenomenon of ionization, through interaction with the atoms that travels the respective substance. X-rays with energy less than 100 keV are strongly absorbed by the substance while X-rays with energy grater than 200 keV and gamma rays may travel considerable thickness from the substance, their absorption being much lower. [BMI13] , [STE12] , [STE07] .

Under the action of ionizing radiations, polymers are subjected to profound chemical and structural transformations, their chemical composition, structure and all mechanical and physical-chemical properties are changing. Irradiation may affect the materials properties both in a negative way (case in which we are talking about damage by radiation) and in positive sense leading to an improvement of these properties. Physical properties of composite materials are significantly altered after irradiation due to the assigned energy of incident photons to elementary constituents of irradiated material.

The assigned energy dissipates gradually in material, spreading spatially and being transferred from photons to electrons and from electrons to atoms, molecules and hence to the entire structure. This added energy leads to chemically active compounds and changes or failures in the crystalline zone, failures that become active centers for further transformations and lead to changes in the properties of these bodies.

4.3.2. Material and method

Irradiation of samples for testing has been conducted on IRASM irradiator (www.irasm.ro) and absorbed dose has been measured with the ECB dosimeter. Irradiations have been performed in the 1-250 kGy range, covering the doses used in most applications of radiation technology, but very high doses also, in which the effects of degradation can be put into evidence with certainty. Thus, specimens made of composite materials based on thermosetting resin and hemp fibers have been irradiated some with a dose of 2 kGy and some with a dose of 56.7 kGy.

The new carbon-hemp fabric hybrid composite consists of four layers of thermosetting resin reinforced with carbon fibers having 40% fibers volume fraction and hemp fabric with the fibers volume fraction of 20 %. The process for producing the carbon-hemp fabric hybrid composite material consists that to form layers, hand lay-up technology has been used which provides the use of a roller to impregnate with resin both carbon fibers and hemp fabric. The mechanical characteristics of the thermosetting resin with hardener are: tensile stress at break: 86 MPa; Youn's modulus: 3200 MPa; resistance to impact: 40 kJ/m2.

The layered composite panel is made of a carbon layer with a thickness of 1.5 mm alternating with a second layer of hemp fabric with a thickness of 0.5 mm, this operation repeats until a composite panel is carried out formed of four layers. Finally, the thickness of layered composite panel is 4 mm (Fig. 4.25). The obtained panel has been kept at room temperature for two weeks after which eight specimens denoted C-Cnp have been cut, having the corresponding shape for bending test [SVL11b].

Figure 4.25 a. Hybrid carbon-hemp composite panel

Figure 4.25 b. Cross-section through hybrid carbon-hemp composite panel

The specimens cut from hybrid C-Cnp composite have been irradiated with a dose of 2 kGy respective 56.7 kGy after which they have been tested at bending on an LR5KPlus Lloyd Instruments material testing machine that provides a maximum force of 5 kN. The specimens have been subjected to three-point bending tests with a constant speed of 5 mm/min until break or until the stress (load) has reached a pre-determined value (Fig. 4.26).

Figure 4.26 a. Carbon-hemp specimen during three-point bending t*est*

Figure 4.26 b. Carbon-hemp specimens after bending tests

During tests, load and deflection have been measured. The dimensions of each specimen, their width and cross-section area have been also accurately measured. These dimensions have been introduced as input data in computer connected to the testing machine having Nexygen software. This software takes the experimental data from testing machine and process them statistically [CNI12].

4.3.3. Experimental results

In table 4.6, the main mechanical characteristics of hybrid carbon-hemp composite are presented.

Table 4.6. Main mechanical properties of hybrid carbon-hemp composite

Characteristics	Value
Stiffness (N/mm)	9465900
Stress at break (MPa)	157.12
Young's modulus of bending (MPa)	11832.0
Work to break (Nmm)	2203
Strain to break (-)	0.013697

After tests, a summary of experimental data have been carried out on non-irradiated and irradiated specimens with 2 kGy respective 56.7 kGy doses (tables 4.7-4.8).

Table 4.7. Young's modulus of bending of non-irradiated and irradiated carbon-hemp composite specimens

Specimen	Young's modulus of bending (MPa)		
	Non-irradiated specimens	2 kGy dosis irradiated specimens	56.7 kGy dosis irradiated specimens
1	3662.19	4701.09	3728.97
2	4455.91	3555.84	4323.13
3	4477.69	3852.03	3716.29
4	4160.15	4259.30	3817.76
5	4382.61	4185.66	2932.17
6	5036.92	5100.63	3707.38
7	2751.84	2387.86	3808.73
8	3272.22	3165.79	4625.06

Table 4.8. Tensile strength of non-irradiated and irradiated carbon-hemp composite specimens

Specimen	Tensile strength (MPa)		
	Non-irradiated specimens	2 kGy dosis irradiated specimens	56.7 kGy dosis irradiated specimens
1	53645.50	68863.74	36415.78
2	65272.12	52087.59	42218.13
3	65591.25	56426.33	36291.92
4	60939.78	62392.17	37282.86
5	64198.43	61313.43	28634.49
6	73783.09	74716.28	36204.93
7	40310.17	34978.50	37194.67
8	47933.01	46373.98	45166.66

Flexural rigidity, Young's modulus of bending, work to break and load-deflection distributions are shown in Figs. 4.27 – 4.31.

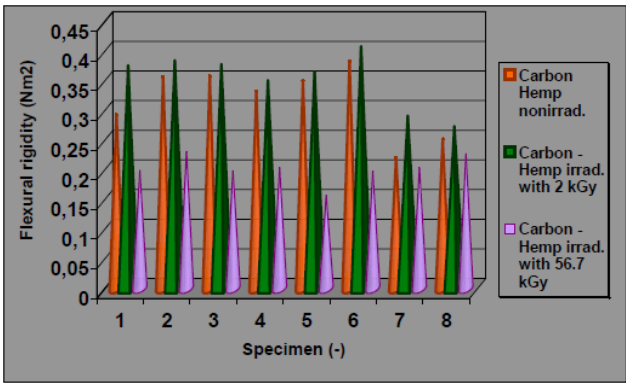

Figure 4.27. Flexural rigidity distributions of non-irradiated and irradiated carbon-hemp composite specimens

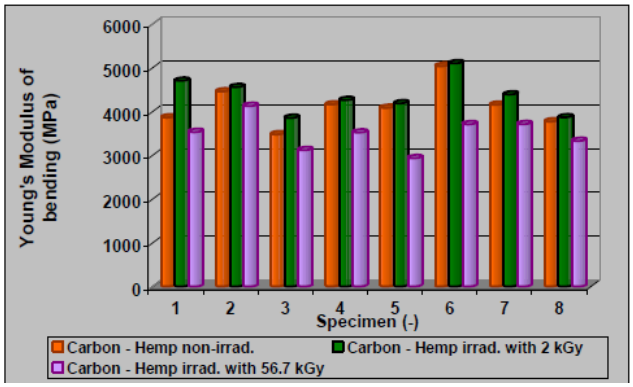

Figure 4.28. Young's modulus of bending distributions of non-irradiated and irradiated carbon-hemp composite specimens

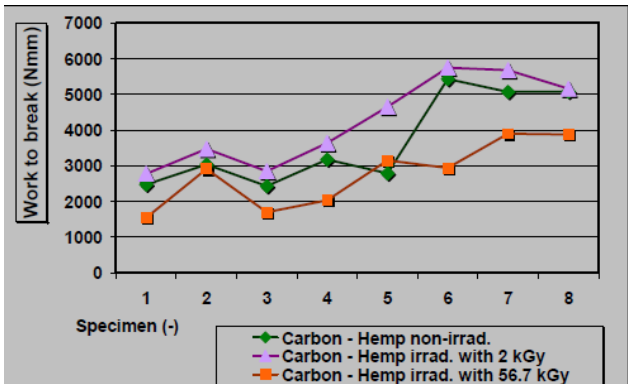

Figure 4.29. Work to break distributions of non irradiated and irradiated composite specimens

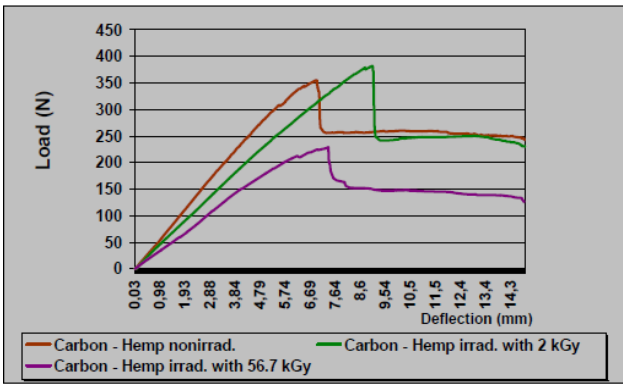

Figure 4.30. Load-deflection distributions of specimen no. 4

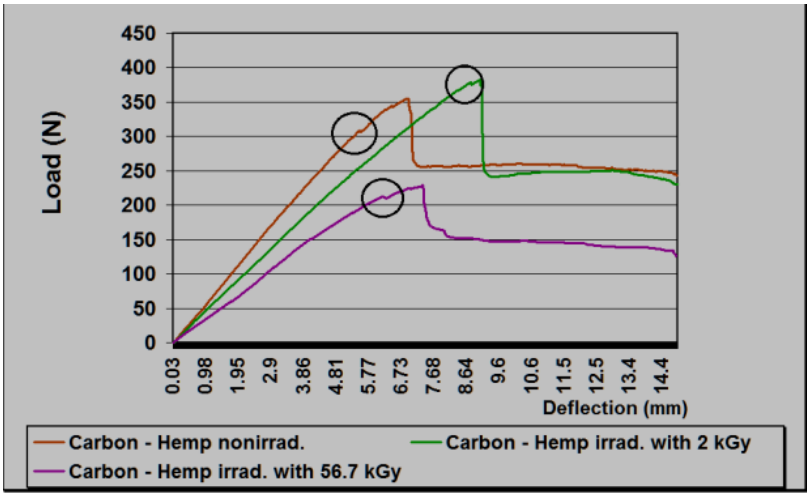

Figure 4.31 Load-deflection distributions of specimen no. 4 with registration of first failure

4.3.4. Discussion, results and conclusions

From the graphical representation of the main mechanical properties shown in Figs. 4.28-4.30 it is obvious that this new hybrid carbon-hemp composite behaves much better if is irradiated with a lower dosis than a high dosis of irradiation. This fact is positive taken into account that a large dosis of radiation can be harmful to human beings.

Considering specimen no. 4 as a characteristic specimen from the group of three types of eight specimens (non-irradiated, irradiated with a dosis of 2 kGy and 56.7 kGy) we have represented in Fig. 4.31 the force-deflection distribution highlighting the first failure zone. It can be noticed that in case of non-irradiated specimen, the first failure occurs at a load of 308.72 N. In case in which the specimen is irradiated with 2 kGy dosis, the first failure appears at a load of 371.89 N and irradiated with 56.7 kGy dosis, the load value decreases at 213.61 N at which the first failure can be recorded.

All these aspects reinforce the fact that the mechanical properties may be positive changed in case of a relatively small dosis of 2 kGy radiation but with the increase of radiation dosis, these properties decrease dramatically

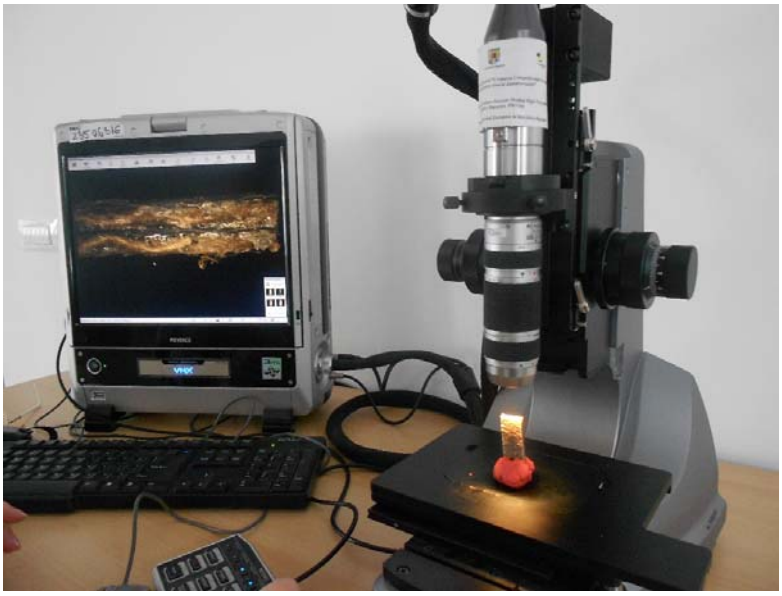

Figure 4.32a. The VHX digital microscope

The macroscopic analysis highlights and determines failures stages of manufacturing technology. The view in detail has been carried out with a powerful microscope that can magnify the studied area by 500 to 2000 times and images have been accomplished as clear as possible and even into material's depth. The results obtained with microscope have been both 2D and 3D noting how the whole structure of this material has been changed. Thus, in Fig. 4.32b, the cross-section of the new hybrid carbon-hemp composite structure is highlighted, i.e. carbon and hemp layers as well as the resin that in part has interfered with the hemp layer.

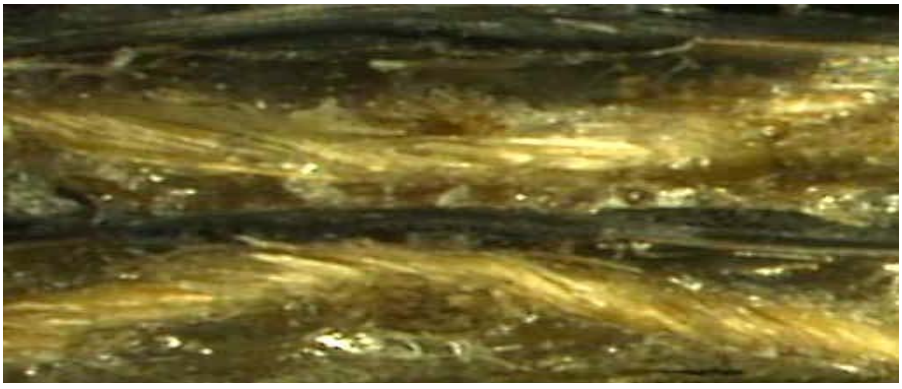

Figure 4.32b. Cross-section through the new non –irradiated carbon-hemp fabric based specimen (20X magnitude)

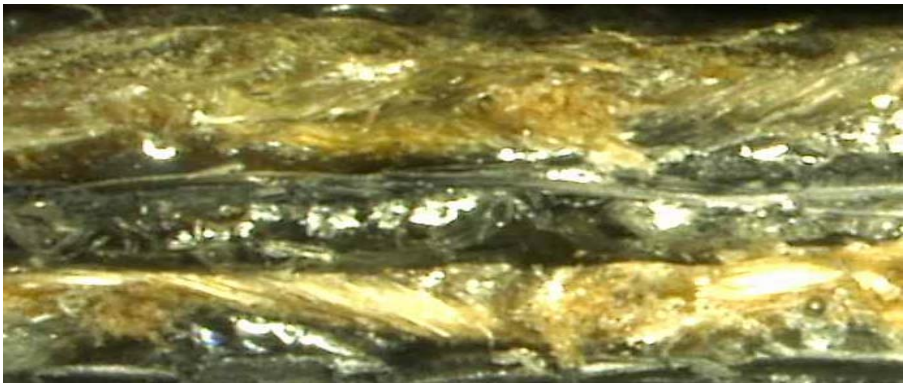

Figure 4.33a. Cross-section through the new 2 kGy irradiated carbon-hemp fabric based specimen (20X magnitude)

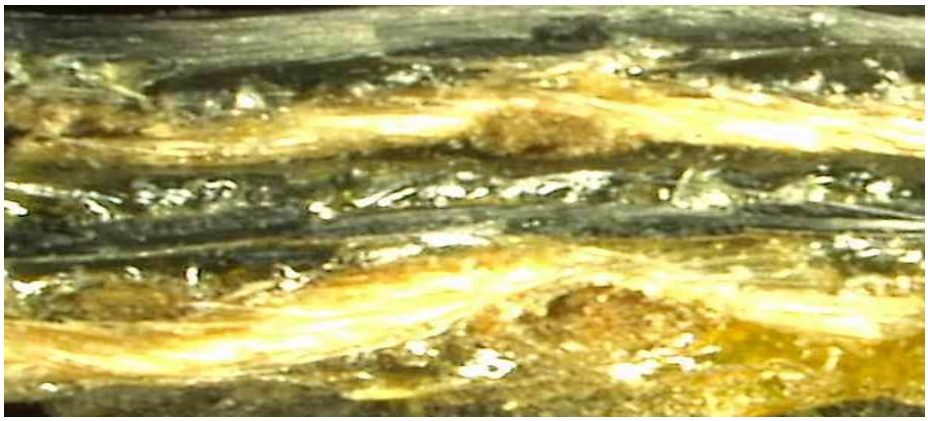

Figure 4.33b. Cross-section through the new 56.7 kGy irradiated carbon-hemp fabric based specimen (20X magnitude)

When the specimens have been irradiated with 2 kGy dosis (Fig. 4.33a), a "crystallization" of the resin layer occurs as well as an increase in the thickness of hemp and carbon fibers which led to an improvement of mechanical properties, as highlighted in Figs. 4.28-4.32. In contrast, increasing the irradiation dosis to 56.7 kGy a "crystallization" of both resin and carbon fibers occurs, the composite gaining a brittle appearance (Fig. 4.33b).

This fact is reflected obviously in graphical representation of the main mechanical properties (Figs. 4.27-4.31) where it can be easily seen a rather significant decrease of these properties if compared with those obtained on initial non-irradiated composite but also on small dosis irradiated composite.

Side and front views of macroscopic specimens' break area are visualized in Figs. 4.34-4.34.

Figure 4.34. Side view of carbon-hemp fabric based specimens' break area

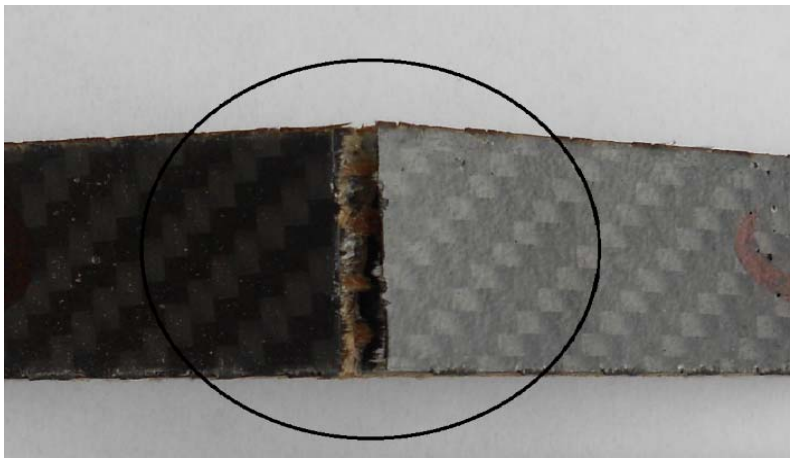

Figure 4.35. Front view of carbon-hemp fabric based specimens' break area

As general conclusions for metallographic analysis, we emphasize that macroscopic analysis has been carried out after a final control study performed on specially prepared surfaces. Conducting research on macroscopic composite specimens revealed also the layered and heterogeneous structure of the material. From the micrographs analysis conducted on studied specimens, the fibers distributions and orientation, the filler distributions as well as non-uniformities, material's failure, vacuoles and inclusions existing in resin matrix have been noticed.

The irradiation process revealed structural and morphological changes that affected the mechanical properties of new hybrid carbon-hemp composite however, the improvement of mechanical properties in case of a small 2 kGy irradiation dosis recommends this type of material for a wide range of applications in the automotive and aerospace industries.

(B-ii) The evolution and development plans for career development

1. The general framework of academic career development

Mechanical engineering is a key fits into a variety of employment opportunities: research design; Mechanical testing laboratories; production; transport; services (maintenance equipment, maintenance, production preparation, etc); sales export-import auto parts, parts of devices. It is still focused field study, design and computer modeling:

∗ the behavior of mechanical structures (vehicles, aircraft, construction, machinery, equipment, etc.), made from various materials under different stress conditions and environment;

∗ the impact of noise and vibration effects on the environment;

∗ the most modern methods of experimental analysis, measurement, testing, experimental results.

Also the main competencies can be grouped into:

∗ skills and abilities related to the calculation and design of mechanical deformable structures using computer programs;

∗ ability to realize the experimental researches of stress and strain of parts and mechanical structures;

∗ ability to test materials including composites materials and analysis of the test results

Accordingly, the teaching staff of the Department of Mechanical Engineering have a great responsibility primarily driven by the imperative of further development of specialized study programs and continuing affirmation of scientific research in the field of mechanical engineering.

In the context of current and future development of the field of mechanical engineering in Romania, we are in face with a major challenge. Indeed, as it is well known, in mechanical engineering market appeared numerous private operators, which slowly but surely developed continuously and, with it, increase the needs for training of the new generations of specialists.

2. Premises academic career development - previous achievements

I will stay involved in current activities so far, but I intend to develop and expand these. In this proposal of the academic career development I will show what I want to do in the future, based on what previously activities. In the following I will present:

I. The elements of success in my professional career earlier

II. The development of my future career in university

III. Building my career

I. The elements of success in my professional career earlier

I. 1. Studies

University:

1992 - 1997 - Transilvania University of Brasov-Faculty of Wood Industry - graduated with diploma exam score 9.84; I obtained Engineering Degree in Industrial Engineering

Graduated

1999 - 2006 - Transilvania University of Brasov - I obtained a Ph.D. degree in Industrial Engineering, with "Wood and wooden materials thermo insulation panels used in building construction", Scientific leader – Prof.PhD Ivan Cismaru

2006-2008 - Transilvania University of Brasov, Faculty of Mechanical Engineering - I obtained a Masters degree in Computational Mechanics

2009-2014 - Transilvania University of Brasov - I obtained a Ph.D. degree in Mechanical Engineering with "Contributions to the dynamics analyze of transmission used in small wind turbines" - Transilvania University of Brasov, Faculty of Mechanical Engineering, Department of Mechanical Engineering, Scientific leader – Prof.PhD Gheorghe Deliu

I. 2. Summary of activity

In the Department of Mechanical Engineering of the Faculty of Mechanical Engineering, Transilvania University of Brasov I activate from 1998, as: Assistent 1998-2002, 2002-2005 Assistent Professor, Lecturer in 2005, Associate Professor 2014-present

As lecturer I presented to the students the following courses taught in the licence and master curricula:

- Mechanics I
- Mechanics II
- Computational Mechanics
- Technical Mechanics

The concepts learned in the courses Mechanics I, Mechanics II are illustrated with examples from the field of mechanical engineering, acquiring the necessary knowledge for the design and calculation of mechanical systems used in industry, construction, aviation.

In previous years we have held seminars on Mechanics I, Mechanics II, Computational Mechanics.

I was in the Organising Committee of the International Conferences organised in the Faculty of Mechanical Engineering - COMAT2006, COMAT2008, COMAT2010, COMAT2012, COMEC2005, COMEC2007, COMEC2009, COMEC2011, COMEC2013, NT2F12.

Also, from September 2013 I am coordinator of a new program of licence.

I am a member in a professional association, EUROMECH.

My scientific relevance and impact of the results have disseminated in books and published papers.

In order to improve my teaching abilities I wrote one book as sole author and one book as first author with a total score of **22.92 points** at the Academic and professional criterium (DID). National minimum standards ask a score of **10 points**.

The papers published in journals and proceedings of scientific meetings prove my synthesis capacity, compliance with the scientific concept of the problem and demonstrate the level of the technical and scientific ability in research acquired. According to the same standards Scientific research (CDI) I must realise a minimum of 10 points. I realised a total score of **43.162** of which:

- 23 papers published in ISI indexed Proceedings volumes with a total of **2.3 points**
- 16 papers published in ISI ranked journals, with a total of **10.556 points**
- 15 papers cited in ISI ranked journals, with a total of **18.095 points**
- Three specialized monographs, with a total of **14.520 points**

Regarding the recognition and impact activities (RIA), whose minimum score is 10 points, I totalised a score of **32.105** of which **8.913 points** as project manager, according to the information presented in my files.

The concepts learned in the course of Mechanics ensure, through illustrative examples of mechanical engineering design and calculation acquire the necessary knowledge of mechanical systems used in industry, construction, aviation.

Regarding the ability to transfer knowledge and results to the economic or social or disseminate their scientific results I considered the following:

- I choose publishing houses accredited by the Romanian authority in research CNCSIS (as INFOMARKET, Matrix Rom Bucharest, Transylvania University Press);
- I choose especially ISI Thomson ranked journals for my papers (as Journal of Optoelectronics and Advanced Materials, Optoelectronics and Advanced Materials-Rapid Communications, Journal of Applied Mathematics, Romanian Journal of Physics);
- I participated in over 22 national and international conferences, of which 18 took place abroad.

My ability to work in teams and efficiency of scientific collaborations results from my activities in the past years, such as:

- The experience and ability to work in collaboration was gained in the research grants, since 2005 until now, as a collaborator or director;
- The topics of my researches covers a wide spectrum of subjects in mechanical engineering with an emphasis on dynamic analysis methods and mechanics of composite materials.

The research conducted in several grants demonstrates my ability to perform development.

Also in 2010-2013 I achieved a scholarship (as postdoc) with the title: *Determination of non-stationary dynamic response of structures of polymeric composite materials with application in the automotive and engineering - DINACOM.*

II. The development of my future career in university

Further development of academic career will be having as main directions both teaching and research. In addition, a very important aspect of future development is related to academic career as a doctoral leadership.

Teaching activity

Teaching activity will be focused on the continued development of teaching to meet the demands of a competitive education, quality standards, enabling graduates organized specializations within the department to acquire skills necessary to professional recognition and to labor market integration.

Main direction:

- Updating and upgrading of teaching syllabuses to ensure consistency of content and task specialization, skills set and adapt to dynamic trends of contemporary society;

- Implementation and development of modern technologies for teaching and learning in order to ensure adequate professional training practical realities; promoting methods of analysis, research methodologies, models of organizing activities with the participation of creative teaching; application of teaching methods based on information technology;

- Upgrading and equipping of laboratories for practical activities extend to subjects taught;

- Stimulating and supporting scientific research of the students;

- Analysis and evaluation of teaching.

The research activity

Developing research focuses as before on participation in specialized national and international events, publishing and disseminating the results of research and collaboration and development of new methods and results in field research projects.

More specifically, to increase the relevance and scientific impact my work I aim the following:

- Publication of a minimum of two (2) articles per year in scientific journals ranked by Thompson Reuters in mechanical engineering, especially in the journals that have a minimum impact factor of 0.5.

- Publication of a minimum of two (2) articles per year, indexed in databases other than Thompson Reuters, but recognized by CNATDCU.

- I will attend the conference, especially internationally, conducted both at home and abroad (minimum 2 per year). Participation in conferences provide, in addition to dissemination, the opportunity to exchange experiences and information with other institutions in the field, things that can lead not only to my development as a researcher, but also to the prestige of the department (ie faculty and university) in the field.

- Participation in national and international research networks.

Directions for future research will address the following areas:

1. Mechanics - engineering applications; mathematical and statistical methods used in the modelling and processing of experimentally measured data.

2. Dynamic Analysis of Mechanical Systems;

3. Analytical Mechanics;

4. Mechanics of composite materials.

Corelation between the research activity with the teaching activity

Research results will be reflected in future books and articles which I will publish as well as research projects which I will coordinate. In future projects will encourage master to participate in research and to disseminate the results through their participation in various conferences.

I will work actively to achieve a small library specialized in the department, namely the realization of a database, including books and journals owned by members of the department to use that anyone who needs the information contained .

III. Building my career

The career building that I propose is based on a set of values: feedback, transparency, openness to new, communication, teamwork. I am counting on the support of these values from the Department of Mechanical Engineering team and their promotion. I believe that my development of my career in the field of mechanical engineering and in related fields, are dependent on respect and support of these enumarated values.

I want to build an academic career and an excellent professional reputation that will ensure success and increased visibility of the Department of Mechanical Engineering and of the Faculty of Mechanical Engineering in Transilvania University of Brasov. The instruments used in carrying out the development plan will both maintain and increase standards of academic excellence and direct collaboration with colleagues and students.

(B-iii) Bibliography

REFERENCES

[ABB59] ABBOTT I.H., VON DOENHOFF A., Theory of wing sections. (Including a summary of airfoil data), General Publishing Company Ltd., Canada, Standard Book Number 486-60586-8, 1959.

[ALD87] ALDOSS T.K., OBEIDAT K.M.. Performance analysis of two Savonius rotors running side by side using the discrete vortex method. Wind Eng, 11-6, 265-276, 1987.

[AND06] SCHELLEKENS A.G., Brevet de Invenţie , UK, 2042647 F 03 D, 3/06.

[AMA96] AMASI L., Studiul adaptării la condiţiile de amplasament a pompelor eoliene, Referat doctorat nr.1, Universitatea Politehnica Timisoara, Catedra de Masini Hidraulice, 1996.

[AOS07] AOS Imaging Studio light Manual Version 2.5.2, 2007.

[ARN73] ARNOLD V.I., Ecuații diferențiale ordinare. Ed. Științifică și Enciclopedică, București, 1973.

[ARN80] ARNOLD V.I., Metodele matematice ale mecanicii clasice. Ed. Științifică și Enciclopedică, București, 1980.

[BAG83] Bagci C., Elastodynamic Response of Mechanical Systems using Matrix Exponential Mode Uncoupling and Incremental Forcing Techniques with Finite Element Method. Proceeding of the Sixth Word Congress on Theory of Machines and Mechanisms, India, p. 472 (1983).

[BAL07] BALINT D.I., Metode numerice de calcul al câmpurilor tridimensionale în distribuitorul şi rotorul turbinei Kaplan, 2007.

[BAH76] B. M. Bahgat and K. D. Willmert, "Finite element vibrational analysis of planar mechanisms,"Mechanism and Machine Theory, vol. 11, no. 1, pp. 47–71, 1976.

[BAN07] BANDOC G., DEGERATU M., Instalaţii şi echipamente pentru utilizarea energiei mecanice nepoluante . Utilizarea energiei vântului. Editura Matrix Rom, Bucureşti, 2007.

[BEN06] BENJANIRAT S., Computational studies of horizontal axis wind turbine in high wind speed condition using advanced turbulence models, Teză de doctorat, Georgia Institute of Technology, 2006.

[BER05] BERNAD I.S., Hidrodinamica echipamentelor de reglare pentru acţionări hidraulice, Editura Orizonturi Universitare, Timişoara, 2005.

[BIS09] BISWAS D.K., Report to the Indian Agricultural Research Institute, India,2009.

[BLA11] Blajer,W., Kołodziejczyk,K., Improved DAE formulation for inverse dynamics simulation of cranes, Multibody Syst Dyn 25, pp.131–143, 2011

[BOS07] BOSTAN I., DULGHERU V., Sisteme de conversie a energiilor regenerabile, Ed. Tehnică – Info., ISBN 978-955-63-076-4, 2007.

[BRA79] BRAG J.M. , SGHMIDT W.L., Performance Matching and Optimization of Wind Powered Water Pumping, Energy Conversion, vol 19, pp 33-39, Perjamon Press, Oxford, 1979.

[BUC90] BUCHER W., Performance report of a wind-electric pumping systems. World Energy Congress, Vol. 3, pp. 1584-1588, 23-28 Sept, 1990.

[BUR92] BURTON J.D., HIJAZIN M., Lift Rod Load Reduction for Wind Driven Pumps. 2nd World Renewable Energy Congress, vol. 3, pg. 1256-1533, Reading, September, 1992.

[BUR88] BURTON J.D., The mechanical coupling of wind turbines to low lift rotodynamic water pumps, Solar and Wind tehnology, vol.5, no. 3, p. 207-214, 1988.

[CAS96] CASTELLI M., BENINI E., BEDON G., Rotor of vertical-axis wind turbine, European Patent EP 2 696 066 A2.

[CHA89] CHAUVIN A., BENGHRIB D., Drag and lift coefficients evolution of a Savonius rotor. Exp.s in Fluids; 8:118-120, 1989.

[CLE81] Cleghorn W.L., Fenton R.G, and Tabarrok B, "Finite element analysis of high-speed flexible mechanisms," Mechanism and Machine Theory, vol. 16, no. 4, pp. 407–424, 1981.

[COS11] COȘGAREA R., COFARU C., ALEONTE M., SCUTARU M.L., JELENSCHI, S., An approach for modeling the valve train systemto control the homogeneous combustion in a compression ignition engine , 12th International Conference on Automation & Information (ICAI '11) Transilvania University of Brasov, ISBN 978-960-474-292-9, Aprilie 11-13, 2011.

[COS06] COȘOIU C. I., Modele integrate de proiectare a agregatelor eoliene, Referat de doctorat, 2006.

[COS08] COȘOIU C. I., The behavior of a nozzle placed in an uniform velocity field, Progrese in simularea echipamentelor si proceselor industriale. Solutii eficiente cu ANSYS si Fluent, 2008.

[DEL99a] DELIU GH., SECARĂ E., MACOVEI M., Regimul aerodinamic al palelor de turbină eoliană cu ax vertical, Buletinul Universității Petrol-Gaze Ploiești, Vol.LI, Nr.1, p335-338, ISSN 1221-9371, 1999.

[DEL99b] DELIU GH., SECARĂ E., MACOVEI M., Legea optimă de variație a unghiului de orientare a palelor la turbine eoliene verticale, Buletinul Universității Petrol-Gaze Ploiești, Vol.LI, Nr.1, p339-344, ISSN 1221-9371, 1999.

[DEL02] DELIU GH., COTOROS D., POPESCU R., Analysis and Synthesis of a Plane Mechanism used in Industrial Aplication, al VII-lea Simpozion național cu participare internațională PRASIC'02, Brașov, Vol.I, p.99-102, Editura Universității Transilvania, ISBN 973-635-064-9, 7-8 Noiembrie, 2002.

[DEL03a] DELIU GH., Mecanica. Ed. Albastra, Cluj-Napoca, 2003.

[DEL03b] DELIU GH., VLASE S., DELIU M., A Study and an Optimization of a Plane Mechanism used in Industrial Applications, International Conference on Adaptive Modelling &Simulation, ADMOS2003, p.152, Book of Abstracts, Goteborg, Sweden (see also Adaptive Modelling and Simulation by N-E.Wiberg and P.Diez, ISBN: 84-95999-30-7, 29 September – 1 October, 2003.

[DEL05] DELIU GH., VLASE S., Lanț cinematic închis prin inerție, Annals of the University of Oradea, pp 169-175, IMT Oradea, 26-27 mai 2005.

[DEL07a] DELIU M, DELIU GH., A simple Method to Estimate the Wind Potential oF a Region, RECENT, Vol.8, nr.2 (20), p.91-96, 2007.

[DEL07b] DELIU M, DELIU GH., On the Statistical Aspect of the Wind potential of a Land Zone, Proceeding of the 4th ICCEMS, RECENT, Vol.8., nr.3a (21a) November, p.277-280, 25-26 October 2007.

[DEU08] Deü J.-F., Galucio A.C., Ohayon R., Dynamic responses of flexible-link mechanisms with passive/active damping treatment. Computers & Structures, Volume 86, Issues 3–5, Pages 258–265, 2008,

[DOR14] DORA R.I., Designul si opimizarea turbinelor eoliene cu ax vertical, de mica putere, implementabile in mediul urban, Teză de doctorat, Universitatea TRANSILVANIA din Brașov, 2014.

[DUD89] DUDIȚĂ F., DIACONESCU D., Curs de mecanisme, Fascicula 1 Structura, Reprografia Universităţii din Braş, 1989.

[DUY80] NHUYEN D.V., Experimental Study for the Optimization of the Performance of the Filippini Vertical Axis Wind Rotor, Wind Engineering, Vol 4, No 1, pp. 43-47, 1980.

[DUN00] DUNQUE E.P.N., JOHNSON W., Numerical Predictions of Wind Turbine Power And Aerodynamic Loads For The NERL phase II Combined Experiment Rotor, AIIA Paper, 38, 2000.

[ERD72] Erdman,A.G., Sandor, G.N., and A. Oakberg, "A general method for kineto-elastodynamic analysis and synthesis of mechanisms," ASME Journal of Engineering for Industry, vol. 94, no. 4, p. 1193, 1972.

[FAN03] Fanghella P, Galletti C, and G. Torre, "An explicit independent-coordinate formulation for the equations of motion of flexible multibody systems," Mechanism and Machine Theory, vol. 38, no. 5, pp. 417–437, 2003.

[FRA75] FRAENKEL P., Food from windmills, Intermediate Technology Development Group, UK, 1975.

[FUJ88] FUJISAWA N., OGAWA Y., SHIRAI H., Power augmentation measurement and flow field visualisation for coupled Savonius rotors. Wind Eng.; 12-6: 322-331, 1988.

[FUJ96] FUJISAWA N., Velocity measurements and numerical calculations of flow fields in and around Savonius rotors. J. Wind Eng. Ind. Aero.; 59: 39-50, 1996.

[GHE11] GHEORGHE V., LIHTEȚCHI M.,, Scutaru M.L., Cofaru C., Vlase S., Test of steering boxes with change hydraulic reaction. The. 4th International Conference, "Computational Mechanics and Virtual Engineering"COMEC 2011, Brasov, ISBN 978-973-131-122-7, 20-22 Octombrie, 2011.

[GOD76] GODFRAY G.R., DAF Company report, Canada, 1976.

[GRA03] GRANT A., KELLY N., The Development of a ducted wind turbine simulation model Eighth International IBPSA Conference, Eindhoven, Netherlands, 11-14 August, 2003.

[GUX85] CHENG G.X., YAO R.S., Study of blades for Vertical Axis Wind Turbine. Solar and Wind Energy Application, International Conference, Beijing China, pp. 108-114, 3-6 August, 1985.

[GUX88] CHENG G.X., YAO R.S., CAIPING S., The study of reverse S-Shaped Vanes of Vertical Axis Wind Turbogenerators, Asian and Pacific Area Wind, Energy Conference, APWEC'88, Shanghai, China, pp. 397-400, 1-4 August, 1988.

[HAR61] Harris C.M., and Crede C.E.,, Shock and Vibration Handbook Volume 1, McGraw-Hill, New York, NY, USA, 1961.

[HSC05] H. Schürmann, Konstruiren mit Faser-Kunststoff-Verbunden, Springer (2005).

[HOU09] Hou W., Zhang X., 2009, Dynamic analysis of flexible linkage mechanisms under uniform temperature change. Journal of Sound and Vibration, Volume 319, Issues 1–2, Pages 570–592.

[IAC77] IACOB C., Mecanica teoretică, Ed. Didactică și Pedagogică, București, 1977.

[ILI84] ILIE V., ALMASI L., NEDELCU ŞT., BORZAŞI D., LUNCĂ GH., MARKE G., Utilizarea energiei vîntului, EdituraTehinică, 1984.

[ION04] IONESCU D.GH., Introducere în mecanica fluidelor, Editura Tehnică Bucureşti, 2004.

[IVA82] IVANOIU M., Aspecte critice ale construcției și calculului sistemelor inovative de conversie a energiei vântului. Primul Simpozion Național pentru Utilizarea Energiei Vântului, Brașov, 26-27 noiembrie, 1982.

[IVA84] IVANOIU M., Sinteză asupra modelelor de calcul elaborate pentru studiul instalațiilor de conversie a energiei vântului, raport personal, comunicat de Catedra de Mașini Hidraulice, Inst. Politehnic Timișoara, februarie 1984.

[IVA13] IVANOIU M., Turbine eoliene cu ax vertical (VAWT). Modele istorice ale transferului energetic, Editura Universității Transilvania din Brașov, 2013.

[KAW01] KAWAMURA T., Hayashi T., Miyashita K., Application of the domain decomposition method to the flow around the Savonius rotor, 12 th International Conference on Domain Decomposition Methods, T Chan, T Kako, H Kawarada and O Pironneau (Editors), 2001.

[KHA11] Khang, N.V., Kronecker product and a new matrix form of Lagrangian equations with multipliers for constrained multibody systems, Mechanics Research Communications, Volume 38, Issue 4, pp. 294-299 ,2011.

[KOS77] KOSLOWSKI H., Investigation of weather a Savonius rotor is a suitable prime mover. Intermediate Tehnology Development Group, UK, 1977.

[LAT05] LATES M., Aspects regarding the small power type windmills implementation in Romania, Proceedings of International Conference on Sustainable Energy, Braşov, România, ISBN 973 – 635 539 – X, 7 – 9 July 2005.

[LEG80] Le GOURIERES D. Énergie éolienne. Eyrolles, Paris, 1980.

[MAY96] Mayo J, Domínguez J., Geometrically non-linear formulation of flexible multibody systems in terms of beam elements: Geometric stiffness. Computers & Structures, Volume 59, Issue 6, Pages 1039–105, 1996

[MAL11] ALEONTE M., COFARU C., COȘGAREA R., SCUTARU M.L., JELENSCHI L., SANDU G., Experimental Researches of fulling systems and alcool blends on Combustions and emission in a two strocke si engine, 12th International Conference on Automation & Information (ICAI '11) Transilvania University of Brasov, ISBN 978-960-474-292-9, Aprilie 11-13, 2011.

[MAR11] MARINA V., Mecanica rațională, Vol.I, Editura Tehnica-Info, 2011.

[MAN72] MANOLESCU N., KOVACS FR., ORANESCU A., Teoria mecanismelor și mașinilor. Ed. Didactică și Pedagogică, București, 1972.

[MAS07] Massonet, C.H. et al., Computer Structures Calculus, Tehnică, Bucuresti, Romania, 1974.

[MEM01] MENET J.-L., MÉNART B., Une procédure de comparaison de quelques éoliennes classiques basée sur l'utilisation du critère L-sigma. Actes du 15è Congrès Français de Mécanique, 2001.

[MEN02] MENET J.-L., Local production of electricity with a small Savonius rotor, in Proceedings of the Global Wind Power Conference, 2002.

[MEN03] MENET J.-L., COTTIER F., Etude paramétrique du comportement aérodynamique d'une éolienne lente à axe vertical de type Savonius. Actes du 16è Congrès Français de Mécanique, 2003.

[MEN04] MENET J.-L., A double-step Savonius rotor for local production of electricity : a design study. Renewable Energy; 29:1843-1862, 2004.

[MEN08] MENTXAKA ROA A., MAITRE, T., AMET E., PELLONE C., 2D Numerical Moddelling of the Power Characteristics for Cross Flow Turbines Equi. Politehnica University of Timisoara, Transactions on Mechanics, Tom 53 (67), 2008.

[MEV01] MENET J.-L. VALDÈS L.-C. MÉNART B., A comparative calculation of the wind turbines capacities on the basis of the L-σ criterion. Renewable Energy, 22: 491-506, 2001.

[MIH11] MIHĂLCICĂ M., Contribuţii la identificarea persoanelor prin analiza mişcării, Teză de Doctorat, Universitatea Transilvania din Braşov, 2011.

[NAT80] Nath P.K., and A. Ghosh, "Kineto-elastodynamic analysis of mechanisms by finite element method,"Mechanism and Machine Theory, vol. 15, no. 3, pp. 179–197, 1980.

[NEG06] NEGREA I., VISA I., Conceperea si dezvoltarea centralelor eoliene de mica putere, Sesiunea de Comunicări Ştiintifice cu Participare Internaţională Terra Dacica - România Mileniului Trei, CD-ROM Proceedings, ISSN: 1453-0139, Academia Fortelor Aeriene Henri Coanda, Braşov, România, 5-6 Mai 2006.

[NET06] Neto M.A., Ambrósio J.A.C, Leal R.P., Composite materials in flexible multibody systems. Computer Methods in Applied Mechanics and Engineering, Volume 195, Issues 50–51, p. 6860–6873, 2006

[OBI90] OBIDNIAK L., Brevet de inventie US 4915580 F 03 1/04, 1990.

[PAR02] PARASCHIVOIU I., Wind Turbine Designe on Darrieus Cconcept, Ecole Polytechnique de Montreal, 2002.

[PAR08] PARVIZ E.H., Planar Multibody Dynamics: formulation, programming and applications, 2008.

[PEC13] PECHLIVANOGLOU, G., Passive and active flow control solutions for wind turbine blades, TU Berlin, PhD Thesis, 2013.

[PEL67] PELECUDI CH., Bazele analizei mecanismelor, Ed. Academiei, București, 1967.

[PEN09] Pennestri',E., de Falco,D., Vita,L., An Investigation of the Influence of Pseudoinverse Matrix Calculations on Multibody Dynamics by Means of the Udwadia-Kalaba Formulation, Journal of Aerospace Engineering, Volume 22, Issue 4, pp. 365–372 (2009).

[PIR05] Piras G., Cleghorn W.L., Mills J.K., Dynamic finite-element analysis of a planar high speed, high-precision parallel manipulator with flexible links. Mech. Mach. Theory, Volume 40, Issue 7, p. 849–862, 2005

[PSF12] FĂGĂRAȘ (HABA) P.S., SCUTARU M.L., BURCĂ I., MUNTEANU M.V., Mechanical models for the virtual analysis of the mechanical systems. Part II, 4th International Conference Advanced Composite Materials Engineerings COMAT, ISBN 978-973-131-164-7, 18-20 Oct., 2012.

[RAB96] RABAH K.V.O., OSAWA B.M., Design and field testing of Savonius wind pump in East Africa. Int. J. Amb. En.; 17-2:89-94, 1996.

[SAV31] SAVONIUS S. J., The S-rotor and its applications. Mech Eng.; 53-5: 333-337, 1931.

[SCU09] SCUTARU M.L., TEODORESCU-DRĂGHICESCU, VLASE S., Mecanica Tehnică, Editura Infomarket, 2009.

[SCU11] SCUTARU M.L., SECARĂ E., ENESCU I., PURCĂREA R., AMBRUȘ C., Finit element analisys of a shell element with a general tree-dimension motion, The. 4th International Conference, "Computational Mechanics and Virtual Engineering" COMEC , Brasov, ISBN 978-973-131-122-7, 20-22 Octombrie, 2011.

[SCU12a] SCUTARU M.L., DELIU GH.M., MOTOC D.L., Inertia Driven Reduced DOE Mechanism for Aeolian Pumps, 23rd International Congress of Theoretical and Applied Mechanics, ICTAM 2012, Beijing, China, 19-24 August 2012.

[SCU12b] SCUTARU M.L., Dynamic response of the multibody system in a symbolioc representation, 4th International Conference Advanced Composite Materials Engineerings COMAT 2012, Brasov, 2012 ISBN 978-973-131-164-7, 18-20 October, 2012.

[SCU12c] SCUTARU M.L., VLASE S., FĂGĂRAȘ (HABA) P.S., Mechanical models for the virtual analysis of the mechanical systems- Part I, 4th International Conference Advanced Composite Materials Engineerings COMAT 2012, Brasov, 2012 ISBN 978-973-131-164-7, 18-20 October 2012.

[SCUd12] SCUTARU M.L., VLASE S., Some Properties of Motion Equations Describing the Nonlinear Dynamical Response of a Multibody System with Flexible Elements, Journal of Applied Mathematics, Article Number: 628503 DOI: 10.1155/2012/628503, 2012.

[SCU13] SCUTARU M.L., Mecanica-Cinematica. Teorie și aplicații, Editura Universității Transilvania din Brașov, 2013.

[SCU14a] M. L. SCUTARU, M. Baritz, B. P. Galfi- Radiation influence on micro-structural mechanics of an advanced hemp carbon hybrid composit, Optoelectronics and Advanced Materials Volume: 8 Issue: 11-12 Pages: 1145-1149 Published: Nov. – Dec. 2014, FI=0,449

[SCU14b] M. L. SCUTARU**,**- Toward the use of irradiation for the composite materials properties improvemen, Journal of Optoelectronics and Advanced Materials Volume: 16 Issue: 9-10 Pages: 1165-1169 Published: September-Octomber 2014, FI=0,563.

[SCU14c] M. L. SCUTARU, M. Baba, M.I. Baritz – „ Irradiation influence on a new hybrid hemp bio-composite", Journal of Optoelectronics and Advanced Materials Volume: 16 Issue: 7-8 Pages: 887- 891 Published: July-August 2014, FI=0,563**.**

[SCU14d] M.L.SCUTARU, M.Baba – "Investigation of the Mechanical Properties of Hybrid Carbon-Hemp Laminated Composites Used as Thermal Insulation for Different Industrial Applications", Advances in Mechanical Engineering, Article Number: 829426 Published: 2014, FI=0,5

[SHI01] Shi Y.M., Li Z.F., Hua H.X., Fu Z.F., Liu T.X., The Modelling and Vibration Control of Beams with Active Constrained Layer Damping. Journal of Sound and Vibration, Volume 245, Issue 5, p. 785–800, 2001

[SNI11] SÎRBU N., LIHTEȚCHI I.,VLASE S., GHEORGHE V., NICOARĂ D., SCUTARU M.L., Influence of rolling conection rays of mechanical parts and manual rolling equipment, 3rd International Conference on Manufacturing Engineering, Quality and Production System (MEQAPS'11) , Transilvania University of Brasov, ISBN 978-960-474-249-3, 11-13 April, 2011.

[SUN86] Sung, C.K., An Experimental Study on the Nonlinear Elastic Dynamic Response of Linkage Mechanism. Mech. Mach. Theory, 21, p.121–133, 1986

[TEO10] TEODORESCU H., VLASE S., CHIRU A., ROȘU D., SCUTARU M.L., SECARĂ E., Simulation of elastic properties of sheet molding compounds, Harvard University, Cambridge, USA, January 27-29, ISBN 978-960-474-150-2, 2010.

[THO86] Thompson, B.S., Sung, C.K., A survey of Finite Element Techniques for Mechanism Design. Mech.Mach.Theory, 21, nr. 4, p. 351–359 ,1986.

[USI88] USHIYAMA, I., NAGAI, H. Optimum design configurations and performances of Savonius rotors. Wind Eng. ;12-1: 59-75, 1988.

[USP12] US_20120195757_A1, PAULIN D., Vertical wind power generator, 2012.

[USK12] US_20120243990_A1, KOSCH A. J., Vertical axis wind turbine, 2012 .

[USP85] US4508973 A, PAYNE J. M., Wind turbine electric generator, 1985.

[VÂL63] VÂLCOVOVICI, V., BĂLAN, ȘT., VOINEA, R., Mecanică teoretică. Ed. Tehnică, București, 1963.

[VAD01] VALDES L.-C., Raniriharinosy K. Low technical pumping of high efficiency., Ren. Energy; 24:275-30, 2001.

[VOI84] VOINEA, R., VOICULESCU, D., CEAUȘU, V., Mecanica. Ed. Did. și Ped., București, 1984.

[VLA05] VLASE S., Mecanica Computațională, vol.I, Editura Infomarket, 2005.

[VLA07] VLASE S., Mecanică.Cinematică, Editura Infomarket, 2007.

[VLA09] VLASE S., Mecanică.Dinamică, Editura Infomarket, 2009.

[VLA12] Vlase,S., Dynamical Response of a Multibody System with Flexible Elements with a General Three-Dimensional Motion. Romanian Journal of Physics, Volume 57, Number 3-4, 2012.

[VLA13a] VLASE S., TEODORESCU H., ITU C., SCUTARU M.L., Elasto-Dynamics of a solid with a general „rigid" motion using FEM model. Part II. Analysis of a Double Cardan Joint, Romania Journal of Physics, Vol. 58, Iss. 7-8, pp.882-892, 2013.

[VLA13b] VLASE, S., TEODORESCU,P.P., Elasto-dynamics of a solid with a general "rigid" motion using FEM model. Part I.Rom. Journ. Phys., Vol. 58, Nos. 7–8, P. 872-881, Bucharest, 2013.

[VLA14a] VLASE S., DĂNĂȘEL C., SCUTARU M.L., MIHĂLCICĂ M., Finite Element Analysis of a two-dimensional linear elastic system with a plane "rigide motion" , Romanian Journal of Physics,Vol.59, Iss.5-6, pp.476-487, 2014.

[VLA14b] VLASE, S., Eigenvalues and Eigenmodes of an Inclined Homogeneous Truss in a Rotational Field. Rom. Journ. Phys., 59, 699-714 , 2014.

[VLA87a] VLASE,S., A Method of Eliminating Lagrangian Multipliers from the Equation of Motion of Interconnected Mechanical Systems. Journal of Applied Mechanics, ASME Transactions, Vol.54,p.235,1887.

[VLA87b] Vlase,S., A Method of Eliminating Lagrangean Multipliers from the Equations of Motion of Interconnected Mechanical Systems. Journal of applied Mechanics, ASME Transactions, vol. 54, nr. 1 (1987a).

[WIL74] WILSON R.E., LISSAMAN P.B.S., Applied Aerodynamics of wind power machines, Research Applied to National Needs, GI-41840; Oregon State University, 1974.

[WOH11] WO_2012069905_A2, HASSENFLU J.F., A wind turbine, 2011.

[WOE12]WO_2012177111_A2, ENNAJI M., SAADI J., Eolienne a axe vertical, convertible, autoregule, combinant une savonius et un darrieus, a aubage compose, 2012.

[ZHA07] Zhang X., Lu J., Shen Y., Simultaneous optimal structure and control design of flexible linkage mechanism for noise attenuation. Journal of Sound and Vibration, Volume 299, Issues 4–5, p. 1124–1133, 2007

[ZHA01] Zhang X., and A. G. Erdman, "Dynamic responses of flexible linkage mechanisms with viscoelastic constrained layer damping treatment," Computers and Structures, vol. 79, no. 13, pp. 1265–1274, 2001.

[XIA07] Xianmin, Z., Jianwei,L., and S. Yunwen, "Simultaneous optimal structure and control design of flexible linkage mechanism for noise attenuation," Journal of Sound and Vibration, vol. 299, no. 4-5, pp. 1124–1133, 2007.

INTERNET

[***1] American Wind Energy Association (AWEA) (2004), Global market report 2004, Washington, D.C.(http://www.awea.org/pubs/documents/globalmarket2004.pdf)

[***2] www.builditsolar.com

[***3] Cartea Albastră Rowea. Un punct de vedere al asociaţiei române pentru energia vântului, privind posobilitatea dezvoltării energiei eoliene în Romania în anii 1991-2010. Octombria 1990 – Bucuresti

[***4] Construction plans for 10 m diameter sail windmill, TOOL Fundation, Netherlands

[***5] International Energy Agency (IEA) (2003), Key world energy statistics, Paris, France. (http://library.iea.org/dbtw-wpd/Textbase/nppdf/free/2003/key2003.pdf)

[***6] http://www.didactic.ro/files/4/determinare_caracteristici_vant.pdf

[***7] Note on 6 m diameter sail windmill, Sarvodaya Educational Development Institute, Sri Lanka

[***8] Plans for 25 foot diameter sail windmill, Windworks, USA

[***9] Performance data for 25 foot diameter sail windmill, Brace Research Institute, CANADA

[***10] http://www.diebrennstoffzelle.de/alternativen/wind/index.shtml

[***11] http://www.ewea.org/index.php?id=1665

[***12]www.gruppen.greenpeace.de/aachen/energie-windrad.jpgcopyright: Langrock / Greenpeace

[***13] http://www.ironmanwindmill.com/how-windmills-work.htm

[***14] www. instant-trips.blogspot.com

[***15] www.jbengs.de/galerie/pages/bild279.htm

[***16] www.mistereledunarii.wordpress.com

[***17] http://www.olympia.nl/home1-5/griekenland/kos/pages-kos/atmz/beziensw-antimachia-kos.html

[***18] http://www.sizilien-sicily-sicilia.de/Energie-uk.htm

[***19] http://www.solar-and-wind-power-source.com/vertical-axis-wind-turbines.html

[***20] http://www.windpower.org/en/tour/design/horver.htm

[***21] www.windmission.dk